Acta Universitatis Agriculturae Sueciae

SLU
SWEDISH UNIVERSITY
OF AGRICULTURAL
SCIENCES

Modification of forest trees by genetic engineering

From design to the field

Evgeniy Donev

Doctoral thesis No 2021:67

Faculty of Forest Sciences

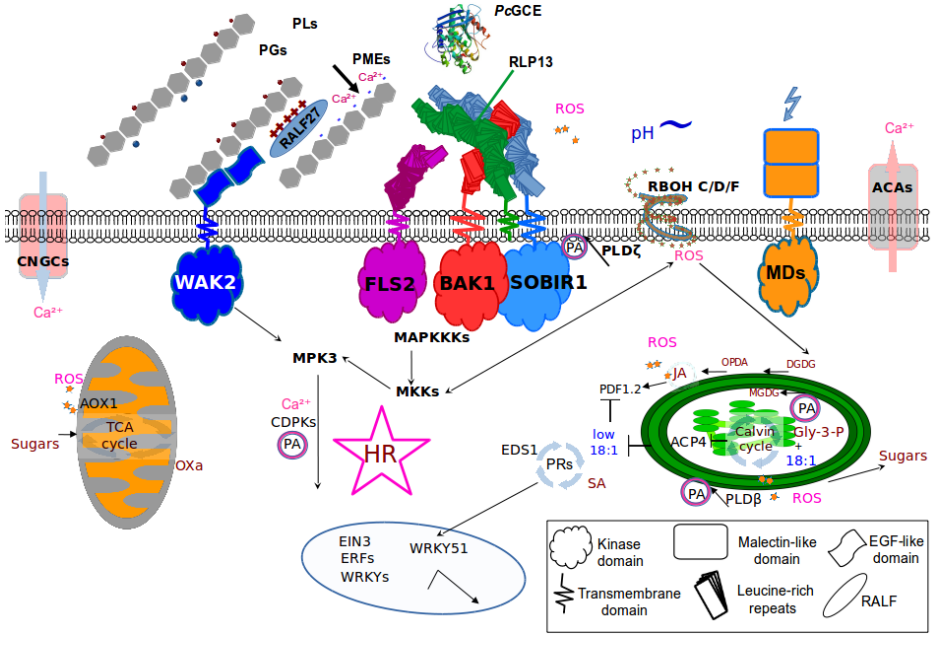

Modification of forest trees by genetic engineering

From design to the field

Evgeniy Donev
Faculty of Forest Sciences
Department of Forest Genetics and Plant Physiology
Umeå

SLU
SWEDISH UNIVERSITY
OF AGRICULTURAL
SCIENCES

DOCTORAL THESIS
Umeå 2021

Acta Universitatis Agriculturae Sueciae
2021:67

Cover: **Fungal enzyme *Pc*GCE is used in genetically modified aspen to reduce recalcitrance of its woody biomass. The diagram shows a proposed model for *Pc*GCE perception in aspen cells.** *Pc*GCE protein is suggested to be recognized in the apoplastic space by a pattern recognition receptor complex involving SOBIR1, BAK1 and RLP 13 homologous proteins. The assembled co-receptors transphosphorylate each-other and initiate pattern triggered immunity (PTI), which activates a broad range of cellular responses in the cytosol, chloroplasts and mitochondria.

ISSN 1652-6880
ISBN (print version) 978-91-7760-811-0
ISBN (electronic version) 978-91-7760-812-7

Print: Original Tryckeri Umeå, 2021

Abstract

Developing viable genetic engineering methods for cell wall modification in trees is important to improve in a timely manner the properties of lignocellulose for biorefinery applications. New wood cell wall functionalities can be introduced by altered expression of native enzymes or by expressing microbial enzymes *in planta*. However, cell wall-modified plants could exhibit altered growth or other off-target effects. Understanding mechanisms of such effects will help to design better strategies for cell wall modification in woody crops dedicated to biorefinery.

Hybrid aspen (*Populus tremula* L. x *tremuloides* Michx.) constitutively expressing glucuronoyl esterase from *Phanerochaete carnosa* Burt (*Pc*GCE) has improved cellulose-to-glucose conversion but exhibits premature leaf senescence and immune defence reactions. Here I show that the observed untargeted effects are triggered by perception of *Pc*GCE protein as a pathogen-associated molecular pattern (PAMP), and that these effects are avoided when *Pc*GCE expression is limited to developing xylem cells by the wood-specific promoter. The findings stress importance of testing different microbial enzymes and using tissue-specific strategies of cell wall modification.

Wood cell wall modification itself can trigger off-target effects by perception of damage-associated molecular patterns (DAMPs). This prompted a genome-wide identification and expression analysis of *Populus* malectin/malectin-like domain-containing proteins, which include candidate receptors involved in secondary cell wall damage perception. Co-expression network analysis was used to identify their putative partners participating in cell wall damage signaling in developing wood. This knowledge will be important to develop strategies of wood cell wall modification, which will disarm the DAMP signaling pathway.

Field conditions expose plants to multitude of biotic and abiotic stresses, revealing off-target phenotypes of genetically modified plants, which are not easily detected in greenhouse experiments. We have carried out two five-year trials with transgenic and intragenic hybrid aspen. The first one reports effects of reducing xylan acetylation using different methods. The second one describes growth and saccharification of lines having altered expression of xylogenesis-related genes, selected by large-scale greenhouse screenings. We found that reducing acetylation and avoiding off-target effects is possible with a right strategy. Further, tree growth was affected more by some genetic minipulations in the field than in the greenhouse. Saccharification analyses revealed that tree productivity plays most important role in determining glucose (Glc) yields per stem. The findings will help to design future biotechnological approaches to optimize trees for biorefinery.

Keywords: transgenic trees, hybrid aspen, secondary cell wall, xylan, fungal enzymes, saccharification, field trial

Author's address: Evgeniy Donev, Swedish University of Agricultural Sciences, Department of Forest Genetics and Plant Physiology, SE-901-83, Umeå, Sweden

Abstrakt

Att utveckla biotekniska metoder för cellväggsmodifiering av träd är en lovande strategi för förbättring av the lignocellulosa egenskaper för bioraffinaderier.

Nya växtcellväggsfunktioner kan introduceras genom förändrat uttryck av nativa enzymer eller genom expression av mikrobiella enzymer. Emellertid kan cellväggsmodifierade växter visa förändrade tillväxtprestanda eller uppvisa icket önskvärda fenotypeffekter. Studier på hybridasp (*Populus tremula* L. x *tremuloides* Michx.) som uttrycker på ett konstitutivt sätt, glucuronoyl esterase from *Phanerochaete carnos*a Burt (*Pc*GCE) har lett till förbättrat cellulosa-till-glukosomvandling, dock växterna har visat tidig åldring av löv och starkt aktiverande av immunförsvarsreaktioner. Här visar jag att de observerade icket önskvärda effekterna utlöses av växt igenkänning av *Pc*GCE protein som ett patogenassocierat molekylärt mönster (PAMP). Ektopisk expression av enzymatiskt inaktiv *Pc*GCE^{S217A} resulterade i samma oönskade effekter, vilket indikerar att *Pc*GCE har en PAMP elicitor aktivitet. *Pc*GCE uttryck, kontrollerad av träspecifik promotorn (WP) undvek alla oönskade effekter, vilket betonade vikten av att använda vävnadsspecifika modifieringsstrategier för att ändra egenskaper hos cellväggen.

Modifiering av växtcellsvägg kan också utlösa off-target-effekter genom uppfattning av skadeassocierade molekylära mönsters (DAMP). Detta föranledde en analys av *Populus* Malectin/Malectin-Like Domain-innehållande (PtMD) proteiner, som inkluderar receptorkandidater som är aktiverade efter uppfattningen av skador på den sekundära cellväggen. Co-expression nätverksanalys användes för att identifiera co-expression partnörer av xylogenes-relaterade *PtMD*-gener.

Till skillnad från växthuset, i fältförhållanden utsätts växter för både biotiska och abiotiska påfrestningar, vilket kan avslöja icket önskade växtfenotyper. I ett femårigt fältförsök undersökte vi hybridaspväxter med reducerad xylanacetylering som inducerades antingen genom att lägre uttryck av asp-nativa REDUCED WALL ACETYLATION (RWA) gener eller genom att uttrycka gener som kodar för svampacetylxylanesteraser (AXE) från *Aspergillus niger* (*An*AXE1) och *Hypocrea jecorina* (*Hj*AXE). Vi jämförde också effekterna av att använda allmänna och vävnadsspecifika promotorer. I ytterligare en femårig fältstudie undersökte vi fältprestandan av hybridaspens intrageniska linjer, med förändrat uttryck för gener som är involverade i sekundärväggbildning. Asplinjerna valdes ut baserat på tillväxt och biomassa i storskalig växthus screening. Våra resultat visar att träproduktivitetsegenskaper har den viktigaste rollen för glukos (Glc) utvinning per stam, antingen med eller utan förbehandling. Resultaten ökade vår förståelse av de viktigaste bestämningsfaktorerna för sackarifieringsutbyten från träd som odlas i fältförhållanden, vilket kommer att bidra till att utforma framtida biotekniska metoder för att optimera träd för bioraffinaderi.

Keywords: transgenic trees, hybrid aspen, secondary cell wall, xylan, fungal enzymes, saccharification, field trial

Author's address: Evgeniy Donev, Swedish University of Agricultural Sciences, Department of Forest Genetics and Plant Physiology, SE-901-83, Umeå, Sweden

Contents

List of publications

This thesis is based on the work contained in the following papers, referred to by Roman numerals in the text:

I. **Evgeniy N. Donev**, Marta Derba-Maceluch, Xiao-Kun Liu, Henri Colyn Bwanika, Izabela Dobrowolska, Mohit Thapa, Joanna Leśniewska, Jan Šimura, Alex Yi-Lin Tsai, Dan Boström, Leszek A. Kleczkowski, Maria E. Eriksson, Karin Ljung, Emma R. Master, Ewa J. Mellerowicz. *Pc*GCE is a potent elicitor of defense responses in aspen. (Manuscript; pre-print is available at BioRiv, https://doi.org/10.1101/2021.09.23.460629

II. Vikash Kumar, **Evgeniy N. Donev**, Félix R. Barbut, Sunita Kushwah, Chanaka Mannapperuma, János Urbancsok, Ewa J. Mellerowicz (2020). Genome-wide identification of *Populus* malectin/malectin-like domain-containing proteins and expression analyses reveal novel candidates for signaling and regulation of wood development. *Frontiers in Plant Science*, **11**, 588846. doi: 10.3389/fpls.2020.588846

III. Derba-Maceluch, Fariba Amini, **Evgeniy N. Donev**, Prashant Mohan-Anupama Pawar, Lisa Michaud, Ulf Johansson, Benedicte R. Albrectsen, Ewa J. Mellerowicz (2020). Cell wall acetylation in hybrid aspen affects field performance, foliar phenolic composition and resistance to biological stress factors in a construct-dependent fashion.

Frontiers in Plant Science, **11**, 651. doi: 10.3389/fpls.2020.00651

IV. Pia Guadalupe Dominguez, **Evgeniy Donev**, Marta Derba-Maceluch, Anne Bünder, Mattias Hedenström, Ivana Tomášková, Ewa J. Mellerowicz, Totte Niittylä. (2021). Sucrose synthase determines carbon allocation in developing wood and alters carbon flow at the whole tree level in aspen. *The New Phytologist*, **229**, 186–198. doi: 10.1111/nph.16721

V. **Evgeniy N. Donev**, Marta Derba-Maceluch, Zakiya Yassin, Madhavi Latha Gandla, Pramod Sivan, Gerhard Scheepers, Francisco Vilaplana, Ulf Johansson, Magnus Hertzberg, Björn Sundberg, Leif J. Jönsson, Ewa J. Mellerowicz. Field testing of transgenic aspen from large greenhouse screening identifies unexpected winners. (Manuscript).

Papers II, III, IV are reproduced with the permission of the publishers.

The contribution of Evgeniy Donev to the papers included in this thesis was as follows:

I. Performed majority of experiments and data analysis (transcriptomics, metabolomics, grafting experiment, phenotyping, ROS analysis). Contributed to study design. Major part in experimental design and writing the manuscript.

II. Analyzed expression of *Pt*MD genes in hybrid aspen by RNA sequencing, identifyied conserved regions of *Pt*MD proteins, and peformened *in silico* gene expression analysis in different organs.

III. Participated in the field work, sample preparation and data analysis.

IV. Analyzed growth data and performed RNA expression analysis (qPCR) of SUS1 gene in transgenic lines grown in the field.

V. Analyzed expression analysis (qPCR) of the targeted genes in all lines grown in the field experiment. Analyzed data analysis from majority of experiments and played major role in writing the manuscript.

Additional publication from the author which is not part of thesis:

Evgeniy Donev, Madhavi Latha Gandla, Leif J. Jönsson and Ewa J. Mellerowicz. (2018). Engineering non-cellulosic polysaccharides of wood for the biorefinery. *Frontiers in Plant Science*, **9**, 1537. doi: 10.3389/fpls.2018.01537

Abbreviations

4CL	4-COUMARATE:COENZYME A LIGASE
2OGD	2OXOGLUTARATE-DEPENDENT DIOXYGENASE
AA	Auxiliary Activity enzymes
ABA	ABscisic Acid
ACA	AUTO-INHIBITED Ca^{2+} ATPASE
ACP	ACYL CARRIER PROTEIN
AG-II	ArabinoGalactan type II
AGPase	ADP-GLC PYROPHOSPHORYLASE
ANX1	ANXUR1
AOX	ALTERNATIVE OXIDASE
AP2	APETALA2
Ara	Arabinose
ARF	ADP-RIBOSYLATION FACTOR
AXE	ACETYL XYLAN ESTERASE
AXY	ALTERED XYLOGLUCAN
BAK1	BRI1-ASSOCIATED RECEPTOR KINASE
BRI1	BRASSINOSTEROID INSENSITIVE 1
C3′H	*p*-COUMAROYL QUINATE/SHIKIMATE 3′-HYDROXYLASE
C4H	CINNAMATE 4-HYDROXYLASE
CAD	CINNAMYL ALCOHOL DEHYDROGENASE
CA-RE	CAmbium-Radial Expansion zone
CAZymes	Carbohydrate-Active enZymes
CBM	Carbohydrate-Binding Module
CDPK	CALCIUM-DEPENDENT PROTEIN KINASE

CE	Carbohydrate Esterase
CNGC	CYCLIC NUCLEOTIDE-GATED ION CHANNEL
COMT	CAFFEATE/5-HYDROXY-FERULATE *O*-METHYLTRANSFERASE
DA	Degree of Acetylation
DAMP	Damage-Associated Molecular Pattern
EDS1	ENHANCED DISEASE SUSCEPTIBILITY 1
EIX	ETHYLENE-INDUCING XYLANASE
ERF	ETHYLENE RESPONSIVE FACTOR
ETI	Effector Triggered Immunity
FAE	FERULIC ACID ESTERASE
FER	FERONIA
F5H	FERULATE-5-HYDROXYLASE
FLS2	FLAGELLIN SENSITIVE 2
Fru	Fructose
FT-IR	Fourier Transform Infrared Spectroscopy
Gal	Galactose
GalA	Galacturonic Acid
GC-MS	Gas Chromatography–Mass Spectrometry
GCE	GLUCURONOYL ESTERASE
GH	Glycoside Hydrolases
G-layer	Gelatinous layer
Glc	Glucose
Gly	Glycerol
Gly-3-P	Glycerol-3-Phosphate
GolS	GALACTINOL SYNTHASE
GT	Glycosyl Transferase
GUX	GLUCURONIC ACID SUBSTITUTION OF XYLAN
GXMT	GLUCURONOXYLAN METHYLTRANSFERASE
HG	HomoGalacturonan
HR	Hypersensitive Response
INV	INVERTASE
IRX	IRregular Xylem
JA	Jasmonic Acid
Kin	Kinesin domain
LCC	Lignin-Carbohydrate Complex

LRR	Leucine-Rich Repeat
LYK	LYSM-CONTAINING RECEPTOR-LIKE KINASE
Man	Mannose
MAT	METHIONINE ADENOSYLTRANSFERASE
MAPK	MITOGEN-ACTIVATED PROTEIN KINASE
MD	Malectin Domain
ML	Middle Lamella
MLD	Malectin-Like Domain
MLO	Mildew Resistance Locus O
MGDG/DGDG	Mono/Di-GalactosylDiacylGlycerol
MYB	MYELOBLASTOSIS
MYBL	MYB-LIKE
NLR	Nucleotide-binding Leucine-rich Repeat
NST	NAC SECONDARY WALL THICKENING PROMOTING FACTOR
OG	OligoGalacturonides
OPDA	12-OxoPhytoDienoic Acid
OXa	Oxalic acid
PA	Phosphatidic Acid
PAMP	Pathogen-Associated Molecular Pattern
PCD	Programmed Cell Death
PCW	Primary Cell Wall
PDF	PLANT DEFENSIN
PAE	PECTIN ACETYLESTERASE
Phe	Phenylalanine
PG	POLYGALACTURONASE
PL	POLYSACCHARIDE LYASE
PLC	PHOSPHOLIPASES C
PLD	PHOSPHOLIPASES D
PME	PECTIN METHYLESTERASE
PMR	POWDERY MILDEW RESISTANT
PK	Protein Kinase
PR	PATHOGENESIS-RELATED
PRR	Pattern Recognition Receptors
PSKR1	PHYTOSULFOKINE RECEPTOR 1
PTI	PAMP-Triggered Immunity

RALF	RAPID ALKALINIZATION FACTOR
RBOHD	RESPIRATORY BURST OXIDASE HOMOLOG PROTEIN D
RES	Reducing End Sequence
RG-I	RhamnoGalacturonan type I
RG-II	RhamnoGalacturonan type II
RLCK	RECEPTOR-LIKE CYTOPLASMIC KINASE
RLK	RECEPTOR-LIKE KINASE
RLP	RECEPTOR-LIKE PROTEIN
Rha	Rhamnose
ROS	Reactive Oxygen Species
RWA	REDUCED WALL ACETYLATION
SA	Salicylic Acid
SAR	Systematic Acquired Resistance
SCW	Secondary Cell Wall
SND	SECONDARY WALL ASSOCIATED NAC DOMAIN PROTEIN
SOBIR1	SUPPRESSOR OF BIR1
SPP	SUCROSE PHOSPHATE PHOSPHATASE
SPS	SUCROSE PHOSPHATE SYNTHASE
SS	STARCH SYNTHASE
Suc	Sucrose
SuSy	SUCROSE SYNTHASE
TBL	TRICHOME BIREFRINGENCE-LIKE
TMD	TransMembrane Domain
THE1	THESEUS1
TF	Transcription Factor
UAP	UDP-N-ACETYLGLUCOSAMINE PYROPHOSPHORYLASE
UPD-Glc	Uridine Diphosphate Glucose
VND	VASCULAR-RELATED NAC-DOMAIN
WAK	WALL ASSOCIATED KINASE
WP	Wood-specific Promoter

1. Introduction

1.1 Need for biotechnology in crops

Plant biomass is the most abundant, naturally degradable and renewable carbon resource on Earth (Bar-On et al., 2018), which is mainly composed of structurally diverse plant cell walls, as well as minor part of non-structural carbohydrates, proteins, lipids, and secondary metabolites. Terrestrial plants store approximately 50 billion tons of carbon each year (Field et al., 1998), and represent an important source of industrial raw material (Pauly and Keegstra, 2008). Growing population on Earth and extensive use of fossil hydrocarbons, contribute to release of pollutants, distortions of ecosystems, and loss of biodiversity (Wheeler and Watts, 2018; He and Silliman, 2019; Tollefson, 2021). The efforts for transition from fossil-fuel driven to carbon-neutral economy, increase the demand of renewable and compostable resources by modern industries (Fenning and Gershenzon, 2002). Wood biomass is a sustainable source with unexplored potential for production of biofuels, chemicals, plastics and lignocellulosic bioproducts (Philp, 2018). The focus on this work is to evaluate the benefits, risks and productivity potential of transgenic modification of the eudicot tree *Populus* (Jansson and Douglas, 2007), which is widespread in the northern hemisphere (Rogers et al., 2020). The aim of this modification is to improve the properties of lignocellulose for biorefinery applications. Hardwood tree species such as *Populus* sp. are characterized by a lower content of resins and lignins in the wood, compared to softwood trees (Rowell et. al., 2012), and are therefore well suited for production of biofuels, pulp, and other biobased products (Hinchee, et al., 2009).

1.2 Wood cell wall as renewable source

The composition of plant cell walls varies between species, cell type and developmental stage (Alberts et al., 2015), and exhibits remarkable variability in the different cell wall layers, which is defining their identity (Mellerowicz and Gorshkova, 2012).

1.2.1 Primary Cell Wall

Primary cell wall (PCW) mediates cell expansion and is important for plant morphogenesis (Fry, 2011; Alberts et al., 2015; Bidhendi and Geitmann, 2016). Cellulose is synthesized at the plasma membrane by protein complexes made of CesA proteins, which adopt a six lobed rosette shape (Delmer, 1999; Alberts et al., 2015). Cellulose microfibrils make the foundation of the PCW "skeleton", which is further impregnated with non-cellulosic polysaccharides and, in some cell types, lignin (Fry, 2011; Alberts et al., 2015).

1.2.2 Secondary Cell Wall

Secondary cell wall (SCW) deposition enhances the rigidity of the plant cell wall and provides mechanical support to the individual cells and to the whole tissue (Fry, 2011; Meents et. al., 2018). The secondary wall layers include the outer layer (S1), middle layer (S2), and inner layer (S3) (Xu et al., 2006), the thickest of which is S2.

1.2.3 Main compounds of xylem cell wall

1.2.3.1 Cellulose

Cellulose is responsible for 40-45% of wood dry weight (Rowell et al., 2012). It is a linear homopolymer, which consists of β-1,4 linked glucan chains, organized as frameworks that contribute to the mechanical strength of cell wall (Ghaffar and Fan, 2015). The glucan chains are held together via hydrogen bonds and van der Waals forces, which creates sheets stacked cellulose microfibrils (Li et al., 2014a). The microfibrils have crystalline interiors surrounded by semi-crystalline layers (Fernandes et al., 2011; Zhao et al., 2012). The abundance and the structure of the cellulose varies between plant species and cell wall layers (Brown, 2004).

Microfibrils in PCW enable cell expansion in specific direction. The orientation of the cellulose microfibrils in cambial fusiform initials is random or longitudinal allowing radial cell expansion (Mellerowicz et al., 2001). Cellulose microfibrils found in S1 secondary wall layer form dense and almost horizontally aligned arrays, which limits radial expansion of the growing xylem cell. The thicker S2 layer is characterized by longitudinally arranged cellulose microfibrils, having low microfibril angle, while the microfibrils of the S3 layer are horizontally arranged, similarly to S1 layer. Cortical microtubules orientation is an important factor for the control of cellulose microfibrils orientation, with impact on cell wall patterning (Paredez et al., 2006).

1.2.3.2 Pectins

Pectins correspond to ca 5% of wood dry weight (Voragen et al., 2009). They are complex acidic polysaccharides, mainly found in middle lamella (ML) and PCW. Pectins are synthesized in the Golgi apparatus and exported with help of vesicles to the apoplastic space, where they diffuse into the cell wall (Mohnen, 2008; Meents et al., 2018). Depending on structure, the pectin family is divided into three main classes: homogalacturonan (HG), rhamnogalacturonan I (RG-I) and rhamnogalacturonan II (RG-II). The most abundant pectin is HG, which is a homopolymer composed of α-(1,4)-linked GalA. RG-I has a backbone composed of linked disaccharide repeat [α-D-GalA-(1,2)-α-L-Rha-(1,4)-]$_n$, decorated with α-1,5-linked L -arabinose (Ara) side chains or with β-1,4-linked D-galactose (Gal) side chains that can be further branched with arabinan forming type I arabinogalactan (Mohnen, 2008; Harholt et al., 2010). Hardwood tension wood and softwood compression wood, jointly named reaction wood, contain high levels of β-1,4-galactans and type I arabinogalactan (Donev et al., 2018), assumed to be associated with RG-I backbone (Gorshkova et al., 2015). RG-II is the most structurally complex pectin, which has α-(1,4)-linked GalA backbone to which different oligosaccharide side chains are attached with varying sugar composition (Mohnen, 2008; Harholt et al., 2010).

1.2.3.3 Hemicelluloses

Hemicelluloses constitute ca 15-25% of the wood dry weight (Rowell et al., 2012). They are heterogeneous polysaccharides with branched, cross-linked structure, which are found in both PCW and SCW. Hemicelluloses show

varying content and structure between different species and tissues within a species, and cell wall layers in the cells of a tissue (Scheller and Ulvskov, 2010). They interact with other cell wall compounds by various ways. For example, they form hydrogen bonds with cellulose, and covalent ether or ester bonds with lignin and hydroxycinnamic acids (Peng et al., 2009).

Hemicelluloses are made in the Golgi apparatus and transported to the apoplastic space with help of vesicles, which fuse to the plasma membrane (Meents et al., 2018). When hemicelluloses are deposited to the cell wall, they are further modified by various cell wall located enzymes (Voiniciuc et al., 2018).

1.2.3.3.1 Xyloglucan

Xyloglucan is the predominant hemicellulosic polysaccharide in PCW of dicotyledonous angiosperms where it is partially associated with cellulose by H-bonding (Hsieh and Harris, 2012; Zheng, et al., 2018). Its backbone is made up of linear chains of β-(1,4)-linked D-glucopyranose, to which xylose (Xyl) chains are bound and Gal, fucose (Fuc) or Ara, could be further linked to the Xyl residues with some variability among species (Hayashi, 1989; Pauly et al., 1999; Pauly and Keegstra, 2016).

1.2.3.3.2 Xylan

Xylans are found in both PCW and SCW layers. Xylan is a heterogeneous β-(1,4)-linked D-xylopyranosyl polymer divided into arabinoxylans, glucurono(arabino)xylan and (4-*O*-Methyl)-glucuronoxylans (Ebringerová and Heinze, 2000). The PCW of dicots contains small amounts of xylan, where glucuronoarabinoxylan constitutes approximately 5% (Darvil et al., 1980). PCW xylan is characterized with GlcA substitution at every sixth Xyl residue, where GlcA is decorated with a 2-linked pentose instead of 4-*O*-methyl group (Mortimer, et al., 2015). Glucuronoxylan found in SCW of woody species includes the acetylated-glucuronoxylan of hardwoods and the non-acetylated glucurono(arabino)xylan of softwoods, both types characterized by a 4-*O*-methyl-α-D-glucuronic acid substitution (Busse-Wicher et al., 2016), which mediates ester bonds with lignin (Bååth et al., 2016; Giummarella et al., 2019). It has been estimated that half of the xylosyl residues are *O*-acetylated at C-2 or C-3 or at both these positions (Chong et al., 2014: Busse-Wicher et al., 2014). Xylan decorations influence the

interactions of xylan with other cell compounds and with itself. For example, evenly spaced substitution with GlcA residues at every eight Xyl residue in SCW is associated with so-called xylan major domain, while randomly spaced GlcA decorations characterize xylan minor domain (Bromley et al., 2013). It has been proposed that xylan major domain forms two-screw confirmation, which allows H-bonds mediated interaction with cellulose microfibrils (Grantham et al., 2017).

1.2.3.3.3 Mannan

Mannans are a ubiquitous class of hemicelluloses abundant in the SCW of both hardwoods and softwoods, though with higher amount in softwood species, where galactoglucomannans make up to 18% of the dry cell wall mass (Rowell et al., 2012). Galactoglucomannans constitute ca 9% of softwood compression wood. Small amounts of mannan are also found in PCW (Melton et al., 2009). Glucomannan backbone is composed of β-(1,4)-linked D-mannose (Man) and D-Glc, and Gal residues are occasionally linked to Man via α-(1,6)-glycosidic bond (Rowell et al., 2012).

1.2.3.4 Arabinogalactan proteins

Arabinogalactan proteins are found in small amount in plants cell walls, though in larch wood they represent ca 10-20% of the of the dry cell wall mass (Fengel and Wegener, 1984; Donev et al., 2018). They are also highly abundant in tension wood (Gorshkova et el., 2015). The arabinogalactan proteins are heavily glycosylated with type II arabinogalactan (AG-II) chains built by β-(1,3) and β-(1,6) linked Gal units, decorated with arabinose, rhamnose, and 4-*O*-methyl-α-D-glucuronic acid (Donev et al., 2018). It has been shown that AG-II is very abundant in G-layer of tension wood (Gorshkova et al., 2015; Guedes et al., 2017). AGP could be also attached to the arabinose residue of arabinoxylan (Tan et al., 2013).

1.2.3.5 Callose

Callose is composed of Glc units, linked with β-(1,3)-glycosidic bond, with occasional β-1,6-branches, synthesized by plasma membrane callose syntheses (Chen and Kim, 2009). Callose is deposited in response to pathogen attacks, and accumulates shortly after a mechanical, chemical or abiotic stress between cell wall and plasmamembrane. It is also abundantly

accumulated at the plasmodesmata, at the cell plate during cytokinesis, and deposited as plugs in the pollen tubes.

1.2.3.6 Lignin

Lignin is an impregnating phenolic polymer, characterized by an amorphous, three-dimensional structure (Rowell et al., 2012; Börcsök and Pásztory, 2021). Lignification of SCW is considered a final step of the wood cell wall formation (Meents et al., 2018), and it starts from the pectin rich ML and PCW (Westermark, 1985; Christiernin, et al., 2005). The biosynthesis of lignin monomers starts via the general phenylpropanoid and then monolignol-specific pathways, where *p*-coumaryl alcohol, coniferyl alcohol and sinapyl alcohol are synthesized from phenylalanine (Phe) (Boerjan et al., 2003, Vanholme et al., 2010; Li et al., 2014b). *p*-hydroxyphenyl (H), guaiacyl (G) and syringyl (S) monolignol units are exported from the cytosol to the cell wall and are integrated in the lignin polymer via dehydrogenative radical polymerization, assisted by peroxidases, laccases, polyphenol oxidases, and coniferyl alcohol oxidases. During its deposition lignin displaces water, which creates a hydrophobic environment. Lignin S and G units are the main building blocks of hardwoods lignins, while G lignin is the main type in grasses and in softwoods (Vanholme et al., 2010; Li et al., 2014b). Lignin provides strength and stiffness to the cell wall and strongly contributes to the wood recalcitrance, by hindering polysaccharides from hydrolytic enzymes (Yang et al., 2013). Lignin biosynthesis could be triggered by various biotic and abiotic stresses, such as pathogen attacks, wounding, metabolic stress, and cell wall perturbations (Caño-Delgado et al., 2003; Tronchet et al., 2010).

1.2.3.7 Other cell wall proteins

More than 1000 water-soluble and insoluble cell wall proteins have been identified in *A. thalina* (Albenne et al., 2014). Studying plant cell wall proteomes is a challenging procedure. During extraction, some of the soluble proteins are lost, while insoluble cross-linked proteins could remain strongly attached to the plant cell wall. Cell wall proteins are regulating various properties of cell walls, and are classified into several classes, such as acting on/or interacting with polysaccharides (hydrolases, esterases, lyases, expansins, lectins), oxidoreductases (peroxidases, oxidases, blue copper

binding proteins), proteases, lipid metabolism proteins (lipases, lipid transfer proteins), signaling proteins, arabinogalactan proteins (discussed above) and structural proteins (extensins, glycine-rich proteins). There are still many cell wall proteins with yet unknown function.

1.2.4 Interactions between main polysaccharides of wood

As discussed above, non-cellulosic matrix polysaccharides interact with lignin matrix, cellulose microfibrils and with themselves. Cell wall compounds are bound via a plethora of covalent, ionic, and hydrophobic chemical interactions, and thereby determine the wood cell wall architecture (Cosgrove, 2005; Peng et al., 2009; Scheller and Ulvskov, 2010; Park and Cosgrove, 2015). In lignified cell walls, non-cellulosic polysaccharides, such as hemicelluloses and pectins are bonded by ester, ether and glycosidic bond linkages with phenylpropane subunits of lignin and form lignin-carbohydrate complexes (LCC) (Jeffries, 1990; Giummarella et al., 2019).

Wood cell wall nanostructure and anatomical traits determine the properties and extractability of the lignocellulosic biomass. Improved knowledge about these traits would contribute for design of efficient technologies for wood extraction (Donev et al., 2018; Brandon and Scheller, 2020).

1.3 Main tools for cell wall modification in forest trees

1.3.1 Model species

Most of the studies of genetically modified plant species are based on experiments conducted on *Arabidopsis thaliana*, which is extensively used model organism in plant science. Even though secondary growth is present in *A. thaliana* it does not produce much wood and is an annual plant, which makes it less suitable for studying essential developmental and seasonal features associated with tree species (Woodward and Bartel, 2018). Also, its small mass can make it challenging to extract metabolites present in limited amounts. Most of *A. thaliana* gene families are found in other flowering plants, such as poplar trees, grain crops or rice (Woodward and Bartel, 2018). *Populus* includes fast-growing species, having relatively small genome size, which are easily transformed and vegetatively propagated (Jansson and

Douglas, 2007; Sannigrahi et al., 2010; Straus et al., 2016). The sequenced genome of *Populus trichocarpa* makes it a suitable model organism for exploration of a great set of biological processes and seasonal growth in woody species (Tuskan et al., 2006). Nowadays, it is possible to identify common ancestral DNA sequences of different model organisms and *Populus,* which helps predicting function of unknown genes (Pinard et al., 2015; Kumar et al., 2019, 2020). The genomes of several eudicots (Myburg et al., 2014; Salojärvi et al., 2017) and conifer species have also been published (Birol et al., 2013; Nystedt et al., 2013; De La Torre et al., 2014), and the list is constantly growing, which expands the catalogue of possible tree model organisms, available for testing biotechnological tree improvement strategies.

1.3.2 Cisgenesis, intragenesis and transgenesis

The insertion of a gene with its own introns and regulatory elements, into a recipient genome is called cisgenesis (Devi et al., 2013). It is a way to produce genetically modified plants by introduction of unchanged DNA fragment originating from the same or cross-compatible species. Plant phenotypes derived by cisgenesis, could also be obtained via conventional breeding, though the procedure takes longer time. An important benefit of using cisgenesis, compared to conventional cross breeding, is that the desired gene is inserted without unwanted adjacent sequences (linkage drag) (Haverkort et al., 2008). Intragenesis is similar to cisgenesis, though it allows the insertion of artificially synthesized chimeric gene into the recipient genome, by combination of promoters, coding regions and terminator sequences. In difference to cisgenesis, intragenesis cannot be achieved by conventional breeding (Devi et al., 2013). The transgenesis deploys DNA sequences originating from other species, such as microbes (Devi et al., 2013; Gandla et al., 2015; Derba-Maceluch et al., 2020; Reem et al., 2020).

1.3.3 Regulation of cell wall biosynthesis in xylem cells

Plant cell walls are made of several different layers. Xylem cell wall comprises ML, PCW, SCW and sometimes tertiary wall, which are deposited in a highly controlled manner (Mellerowicz and Gorshkova, 2012). Each layer is a complex polymeric biocomposite with distinct characteristics

(Mellerowicz et al., 2001; Sarkar et al., 2009; Mellerowicz and Gorshkova, 2012). Regulation of xylem cell wall biosynthesis consists of a multi-leveled system (Taylor-Teeples et al., 2015) that ultimately determines the growth of the cell, its final shape and volume, and provides adaptation to various biotic and abiotic stress conditions.

VASCULAR-RELATED NAC-DOMAINS 1-7 (VND) (Kubo et. al., 2005; Yamaguchi et al., 2008) and NAC SECONDARY WALL THICKENING PROMOTING FACTORS (NSTs) (Mitsuda et. al., 2005, 2007) also known as SECONDARY WALL ASSOCIATED NAC DOMAIN PROTEINS (SNDs), (Zhong et al., 2007). are among the most important TFs in *A. thaliana*, associated with SCW development. Among them is the SND1/NST3 regulates SCW formation in xylem fibers. SND2, considered to be an indirect target of SND1, has impact on secondary cell wall thickness of *Eucalyptus* fibers (Hussey et al., 2011). Other TFs regulating secondary cell wall formation belong to MYELOBLASTOMOSIS (MYB) transcription factor family. Among them, there are the master switches MYB46 and MYB83 (Zhong et al., 2007; McCarthy et al., 2009), which act as the second level regulators controlled by SND1. These key regulators of SCW formation can be deployed for designing plants with unique physicochemical and ultrastructural cell wall features. For example, *A. thaliana nst1 nst3* double knockout mutants, have severely suppressed secondary wall thickening in interfascicular fibers and secondary xylem (Mitsuda et al., 2007). Expression of ERF035, which belongs to the APETALA2/ET responsive factor (AP2/ERF) family, in *nst1 nst3* mutant has resulted in restored thickness of the cell wall, though with PCW characteristics (Sakamoto et al., 2018).

1.3.4 Carbon allocation in plants

Photosynthesis, which occurs in the chloroplasts, fixes carbon from CO_2 by the Calvin cycle (Bar-Peled and O'Neill, 2011; Obata, 2019). First, triose phosphate (triose-P) is produced, which is transported to the cytosol by a triose-P/phosphate translocator. In the cytosol, two triose-P molecules produce one fructose-1,6-bisphosphate (Fru-1,6-BP), from which fructose-6-phosphate (Fru-6-P) and glucose-6-phosphate (Glc-6-P) are formed. PHOSPHOGLUCOMUTASE (PGM) converts Glc-6-P into glucose-1-phosphate (Glc-1-P), which is further converted into ADP-Glc, by ADP-

GLC PYROPHOSPHORYLASE (AGPase) (Seifert, 2004; Bar-Peled and O'Neill, 2011; Yu et al., 2015; Temple et al., 2016; Obata, 2019). Furthermore, UGPase mediates the reversible reaction between UTP and Glc-1-P to produce UDP-Glc, while UDP-N-ACETYLGLUCOSAMINE PYROPHOSPHORYLASE (UAP) is capable to convert UDP-Glc back to UTP and Glc-1-P (Xiao et al., 2017). SUCROSE PHOSPHATE SYNTHASE (SPS) from family GT4 catalyzes the reaction between UDP-Glc and Fru-6-P to produce Sucrose 6-phosphate (Suc-6-P), which is further modified by SUCROSE PHOSPHATE PHOSPHATASE (SPP) to form sucrose (Suc) (Ruan, 2014). Suc is transported from the source photosynthetic tissues to non-photosynthetic tissues (sink tissues) via phloem, where it provides energy and fixed carbon to produce amino acids, nucleotides, lipids, secondary metabolites and complex carbohydrate structures. SUCROSE SYNTHASE (SuSy) from family GT4, is involved in the cytosolic sugar metabolism in mainly sink tissues, where it catalyzes the reversible reaction of Suc into Fru and UDP-Glc (Stein and Granot, 2019). Invertases from family GH32 are also capable to cleave Suc in sink tissues to yield Glc and Fru (Ruan, 2014). UDP-Glc is a substrate for cellulose and callose biosynthesis and for biosynthesis of other sugar nucleotides needed for the biosynthesis of pectins and hemicelluloses (Seifert, 2004; Bar-Peled and O'Neill, 2011; Stein and Granot, 2019). Cytosolic nucleotide sugars could be imported via nucleotide sugar transporters to the Golgi apparatus, where hemicellulosic and pectic polysaccharides are synthesized (Temple et al., 2016). Regulation of carbon flux is an important route to be exploited in biotechnology of woody species (Gerber et al., 2014; Dominguez et al., 2020).

1.3.5 Carbohydrate-active enzymes

Carbohydrate-active enzymes (CAZymes) are involved in the biosynthesis and the modification of carbohydrates and thus are the key enzymes for wood cell wall biosynthesis and modification (Mellerowicz and Sundberg, 2008). CAZymes are divided into five main families: glycoside hydrolases (GH), glycosyl transferases (GT), polysaccharide lyases (PL), carbohydrate esterases (CE) and auxiliary activity enzymes (AA), and they also include other proteins with carbohydrate-binding modules (CBM) (Coutinho et al., 2003; Lombard et al., 2014; Pinard et al., 2015; Kumar et al., 2019).

Generating knowledge about CAZymes in woody species is important for the development of tree breeding programs and for biotechnology of trees based on genetic engineering since it allows the deployment of these proteins for modification of plant cell wall compounds, which potentially could lead to more efficient conversion of cell wall polysaccharides for biorefinery. For example, improved biomass deconstruction was achieved by overexpression of β-(1,3)-glucan synthase gene *PMR4* (*POWDERY MILDEW RESISTANT4*) from family GT48, which resulted in elevated callose content in silvergrass (*Miscanthus x giganteus* J.M.Greef , Deuter ex Hodk., Renvoize) and improved saccharification yields (Falter et al., 2015).

1.3.6 Choice of promoters

Ectopic expression of a gene can be controlled by highly expressing constitutive promoters, such as the *35S* promoter derived from cauliflower mosaic virus (CaMV), or promoters of actin and ubiquitin genes (de Buanafina et al., 2008). However, the expression from such promoters is not always stable. For example, *35S*-driven transgene induction could vary in response to heat (Boyko et al., 2010) or aging (Kiselev et al., 2021). Moreover, the biosynthesis and differentiation of the plant cell wall of living cells is continuously adapting to developmental and environmental cues. Thus, ectopic expression of cell wall biosynthetic and modifying genes could interfere with the regulation of biosynthesis, potentially leading to off-target effects (Tomassetti et al., 2015). A strategy to limit such negative impacts is the use of tissues-specific or inducible promoters, which limits the expression of heterologous enzyme to certain part of the plant or at certain developmental stage. Promoters of genes expressed only during senescence (Weaver et al., 1998; Noh and Amasino, 1999), heat-shock (de Buanafina et al., 2008; 2010; 2012), or SCW formation (Ratke, et al., 2015) have been tested and shown to prevent off-target effects. For example, abundant expression of a fungal *POLYGALACTURONASE* (*PG*), GH28 (*Aspergillus niger* van Thieghem) in *A. thaliana* controlled by β-estradiol inducible promoter, leads to negative effects on growth. Expression of this enzyme under the control of the promoter of a gene, which is expressed at the onset of senescence has avoided all the negative effects on growth (Tomassetti et al., 2015). Furthermore, using *GT43B/AtIRX9* promoter allows xylem cell-specific chemical modifications (Ratke et al., 2015; Pawar et. al, 2017a;

2017b), which avoid possible undesirable responses in transgenic trees dedicated for biorefinery (Derba-Maceluch et al., 2020).

1.3.7 Targeting of enzymes to different cellular compartments

Targeted expression of a heterologous enzyme to specific subcellular compartment, such as apoplastic space, endoplasmic reticulum or Golgi is a strategy to increase enzyme yield locally in the cell, and thus ensure its proper function (de Buanafina et al., 2008; 2010; 2012; Pogorelko et al., 2011). A construct can be designed by addition of a short target peptide at the N-terminus or C-terminus of the synthesized protein. Signal peptides and retention signals direct the synthesized protein for secretion to the apoplast or to a specific organelle (Park et al., 2016). After protein delivery to its destination, the signal peptide could be cleaved off by a signal peptidase. Targeted protein delivery ensures the matching enzyme properties with the chemical environment of the compartment (e.g. pH, availability of substrates and co-factors). Using vacuolar-targeting also allows the sequestering of the enzyme until plant cell death, thus avoiding possible untargeted effects associated with the development of the plant.

1.4 Status of plant cell wall modification for biorefinery

1.4.1 Reduction of biomass recalcitrance-general strategies

The recalcitrance of plant biomass hampers its biochemical conversion. Therefore, harsh pretreatments are required which increases industrial costs, and complicates fermentation processes (Li et al., 2014b). This motivates efforts to design crops characterized with efficient polysaccharide isolation. Numerous efforts have been made during the last 15-20 years to design plants characterized by low biomass recalcitrance, by changing the quality and the composition of the cell wall compounds (Donev et al., 2018; Brandon and Scheller, 2020). Reduced wood recalcitrance has been achieved by altered expression of native genes responsible for lignin biosynthesis and for biosynthesis and modification of matrix polysaccharides (Chen and Dixon, 2007; Lee et al., 2009; Xu et al., 2011; Cook et al., 2012; Mansfield et al., 2012; Petersen et al., 2012; Van Acker et al., 2013; Yang et al. 2013; Biswal et al., 2014, 2015). Another strategy for engineering plants for biorefinery is

a post-synthetic modification of cell wall compounds by expressing microbial enzymes and targeting them to cell wall (de Buanafina et al., 2008; 2010; Pogorelko et al., 2011; Tsai et al., 2012; Gandla et al., 2015; Pawar et al. 2016; Derba-Maceluch et al., 2020; Reem et al., 2020).

1.4.2 Modification of lignin for enhanced bioconversion by modifying expression of native genes

Much knowledge on lignin biosynthetic pathway has been generated by studying phenylpropanoid pathway mutants in Arabidopsis (Boerjan et al., 2003; Vanholme et al., 2010; Li et al., 2014b). Typically, these mutants had reduced lignin content or altered lignin composition, which was frequently associated with red-colored wood, stunted growth, developmental defects and the so-called *irregular xylem* (*irx*) phenotype when vessel elements were collapsed or had irregular shape (Marita et al., 1999; Franke et al., 2002a; 2000b; Hoffmann et al., 2004; Schilmiller et al., 2009). Mutants in *CINNAMATE-4-HYDROXYLASE* (*C4H*), which is an enzyme converting *t*-cinnamic acid to *p*-coumaric acid in early phenylpropanoid pathway, had reduced lateral rooting and increased hypocotyl adventitious rooting (Schilmiller et al., 2009; El Houari et al., 2021). The mutant accumulated *c*-cinnamic acid, which coincided with polar auxin transport inhibition, suggesting that perturbation of lignin biosynthesis could cause accumulation of bioactive intermediates associated with negative impact on growth.

Studies of natural variant populations of *P. trichocarpa* revealed relationship between saccharification and lignin content and composition (Studer et al., 2011). Samples with S/G ratio < 2.0 exhibited a clear negative correlation between sugar release with pretreatment and lignin content. Furthermore, enzymatic hydrolysis without pretreatment was improved in samples with lignin content below 20%, independently of the S/G ratio. Also, certain samples with average lignin content and S/G ratios have shown very high sugar release. These observations underline the complex relation between lignin content and sugar release and indicate that factors other than lignin and S/G ratio also influence the wood recalcitrance.

In four-year field trial, transgenic hybrid poplar (*P. tremula* × *P. alba* var. *glandulosa*) with reduced expression levels of *CINNAMYL ALCOHOL DEHYDROGENASE* (*CAD*) or *CAFFEATE/5-HYDROXY-FERULATE O-METHYLTRANSFERASE* (*COMT*), exhibited normal growth and no differences in plant pathogen interactions compared to WT (Pilate et al.,

2002). The downregulation of *CAD*, which is involved in the biosynthesis of all lignin monomers (Boerjan et al., 2003; Vanholme et al., 2010; Li et al., 2014b), led to easier delignification and improved characteristics in kraft pulping of tree trunks. In contrast, suppression of *COMT*, which is responsible for S lignin biosynthesis (Boerjan et al., 2003; Vanholme et al., 2010; Li et al., 2014b), did not improve chemical pulping, compared to WT plants (Pilate et al., 2002). Another field trial study (Sykes et al., 2015) has investigated hybrid eucalyptus (*Eucalyptus urophylla* Blake × *Eucalyptus grandis* Hill ex Maiden Stand) with reduced expression of *C4H* and *P-COUMAROYL QUINATE/SHIKIMATE 3'-HYDROXYLASE* (*C3'H*). Both these genes are active at early steps of the monolignol biosynthetic pathway (Boerjan et al., 2003; Vanholme et al., 2010; Li et al., 2014b). *Eucalyptus* lines with reduced *C4H* and *C3'H* levels displayed lower lignin content, reduced recalcitrance to saccharification after hot water pretreatment and altered S/G/H ratios, compared to WT (Sykes et al., 2015).

1.4.3 Modification of pectin for enhanced bioconversion with native genes

Even though pectins are minor wood compounds, they have impact on wood properties and recalcitrance (Donev et al., 2018). Overexpression of *PECTATE LYASE* from PL family 1 (PL1) in hybrid aspen, has resulted in improved xylan and xyloglucan solubility (Biswal et al., 2014). These results indicate that HG influences the recovery of other non-cellulosic polysaccharides. Downregulation of *GALACTURONOSYLTRANSFERASE 4* and *12* (*GAUT4* and *GAUT12*) genes, which are involved in the biosynthesis of pectin and xylan, respectively (Mohnen, 2008), improved sugar release and growth in switchgrass, rice and eastern cottonwood (Biswal et al., 2015; 2018). Modification of pectin integrity typically leads to off-target effects. For example, overexpression of *POLYGALCTURONASE 1* (*PG1*) in apple trees resulted in silvery colored leaves, early leaf shedding, altered stomata function and defect in cell adhesion (Atkinson et al., 2002).

1.4.4 Engineering xylan for enhanced bioconversion with native genes

Improved understanding of the xylan structure and chemical interaction with other cell wall polymers, contributes to improved design for engineering plants with enhanced bioconversion (Bura et al., 2009; De Martini et al.,

2013; Busse-Wicher et al., 2014; 2016). Reducing the length of xylan backbone, glucuronosylation, acetylation and glucuronosyl methylation are considered promising approaches for modifying xylan structure for biorefinery applications (Donev et al., 2018).

Xylan content in *A. thaliana* are reduced in mutants of genes encoding either xylan synthase complex or enzymes associated with the synthesis of xylan reducing end sequence (RES) (Smith et al., 2017). The mutants usually display *irx* phenotype and stunted growth. Genetically engineered poplar plants with reduced xylan content were obtained by downregulating *Populus* homologous genes (Lee et al., 2009; Li et al., 2011; Biswal et al., 2015; Ratke et al., 2018). Improved conversion of biomass to sugars was usually observed with no growth defects, although plants sometimes exhibited reduced cell wall thickness and, in one case, increased lignification (Li et al., 2011). Occasionally, increased growth was reported for xylan-reduced lines (Biswal et al., 2015; Derba-Maceluch et al., 2015; Ratke et al., 2018)

Biosynthesis of glucuronic acid decoration of xylan backbone in *A. thaliana* is mediated by *GLUCURONIC ACID SUBSTITUTION OF XYLAN* (*GUX*) genes from family GT8 (Mortimer et al., 2010; Lee et al., 2012). *gux1 gux2* mutants exhibited increase by 30% in glucose yield and by 700% in xylose yields during saccharification and no negative effects on growth (Lyczakowski et al., 2017). Positive effects on xylan release were also observed in *glucuronoxylan methyltransferase 1* (*gxmt1*) mutant with reduced levels of 4-*O*-methylation of glucuronic acid side chain (Urbanowicz et al., 2012). In poplar, suppressing glucuronoxylan methyl transferase *DUF579-3/GXM3* resulted in reduction of xylan GlcA side chains and GlcA methylation, which led to accelerated xylan and cellulose conversion but not to higher saccharification yields (Song et al., 2016). However, the trees had reduced mechanical strength of the stem and reduced growth

Acetylation of xylan is important for plant growth, development and lignocellulose properties (Pawar et al., 2013; Pauly and Ramírez, 2018; Brandon and Scheller, 2020). Increased acetylation of wood obtained in laboratory has successfully prevented attacks against brown, white and soft rot fungi, showing that high degree of acetylation (DA) improves wood resistance to biological degradation (Larsson-Brelid et al., 2000). Even though high DA is a desirable property for solid woods products, it reduces the saccharification efficiency and the subsequent fermentation of woody

biomass (Helle et al., 2003). Acetic acid is considered a main inhibitor of fermenting microorganisms (Jönsson et al., 2013), therefore reduced acetylation in wood plants is beneficial for both sugar and ethanol yields. Lower xylan DA possibly enhance accessibility to microbial enzymes, such as endoxylanases, which could result in better wood hydrolysis (Pawar et al., 2016; 2017b).

Three gene families, involved in *O*- acetylation of xylan have been identified in *A. thaliana*; *REDUCED WALL ACETYLATION* (*RWA*), *TRICHOME BIREFRINGENCE-LIKE* (*TBL*), and *ALTERED XYLOGLUCAN* (*AXY*) (Gille and Pauly, 2012; Schultink et al., 2015). *O*-acetyl groups decorate every other xylosyl backbone units at positions 2 and 3 or both (Busse-Wicher et al., 2014; Chong et al., 2014). Severe deacetylation of xylan could cause, xylem cell collapse and strongly reduced growth (Lee et al., 2011; Manabe et al., 2013; Xiong et al., 2013; Yuan et al., 2013). In hybrid aspen, downregulation of RWA clades under control of wood-specific promoter, has resulted in moderate (15–25%) reduction of acetylation (Ratke et al., 2015; Pawar et al., 2017a), with positive effects on saccharification and without alteration of growth and development.

1.5 Deployment of microbial enzymes for cell wall modification for biorefinery

Saprophytic and pathogenic microbes living on lignocellulose, use an impressive enzymatic repertoire for decomposing lignocellulose, which has been explored *in vitro* (Sindhu et al., 2016). These enzymes could also be exploited *in planta*. One strategy is the post-synthetic modification of plant cell wall to make it less recalcitrant by expressing microbial CAZymes and other enzymes. This has been shown to generate plants with improved cell wall traits, such as increased carbohydrate content, reduced lignin content and reduced biomass recalcitrance, compared to control plants (Park et al., 2004; Kaida et al., 2009; de Buanafina et al., 2010; Lionetti et al., 2010; Pogorelko et al., 2011; Tsai et al., 2012; Gandla et al., 2015; Tomassetti et al., 2015; Pawar et al., 2016; 2017b; Hao et al., 2021). Another strategy is the production of enzymes important in saccharification process *in planta*.

1.5.1 Production of microbial thermostable cell wall-degrading enzymes in plants

Plants can be deployed for production of commercially applicable thermostable cell wall-degrading enzymes, which are active only at high temperatures and do not interfere with the cell wall biosynthesis during plant growth and development (Mir et al., 2014; Damm et al., 2016; Park et al., 2016). For example, heat-stable codon-optimized xylanases from *Clostridium thermocellum* Ozkan and *Dictyoglomus thermophilum* Saiki thermophilic bacteria were expressed in tobacco (*Nicotiana tabacum* L.) (Chatterjee et al., 2010) and *A. thaliana* (Borkhardt et al., 2010), respectively. Deleterious effects were not observed in the transgenic plants compared to WT. Interestingly, the xylanase produced in transgenic tobacco was resistant to both endogenous plant proteases and to heat denaturation (Chatterjee et al., 2010), while the xylanase produced in *A. thaliana* was not degraded during stem senescence (Borkhardt et al., 2010).

1.5.2 Modification of cell wall xylan structure by microbial enzymes expressed *in planta*

1.5.2.1 Reduction of xylan acetylation

Acetyl xylan esterases (AXEs) found in wood degrading fungi and bacteria, are involved in hydrolysis of acetyl groups present on xylan chain (Pawar et al., 2013). Reduced xylan acetylation has been achieved in *A. thaliana* by expression of an AXE from *A. niger* (*An*AXE1) from family CE1, without any negative impact on plant growth in the greenhouse (Pogorelko et al., 2013; Pawar et al., 2016). However, it has led to the activation of several defense-related genes leading to increased resistance to necrotrophic fungi (Pogorelko et al., 2013) and biotrophic pathogens (Pawar et al., 2016). The strategy of expressing AXE for post-synthetic reduction of xylan acetylation has been tested also in hybrid aspen. Ectopic expression of *An*AXE1 (Pawar et al., 2017b) and wood-specific expression of *Hypocrea jecorina* Berkeley & Broome AXE (*Hj*AXE) from family CE5 (Wang et al., 2020) were well tolerated by plants in greenhouse experiments, and their lignocellulose yielded 20-30 % more Glc in saccharification without pretreatment, compared to WT.

1.5.2.2 Disruption of lignin-xylan bonds by expressing fungal glucuronoyl esterase

Covalent bonds between lignin and xylan are considered a crucial recalcitrance factor for woody species. Use of microbial glucuronoyl esterase (GCE) from family CE15, which can hydrolyze the ester bond between lignin and 4-*O*-methyl-α-D-glucuronic acid (Spániková et al., 2006; Biely et al., 2015; Bååth et al., 2016), has a potential to decrease lignocellulose recalcitrance. When GCE from the white-rot basidiomycete *Phanerochaete carnosa* Burt (*Pc*GCE) was expressed in *A. thaliana,* the interfascicular fiber walls had reduced lignin cross-linking and Xyl recovery was increased by 15 % (Tsai et al., 2012). However, cell wall thickness in the interfascicular fibers was severely reduced and the plants exhibited smaller leaf size, shorter height, delayed flowering, and early leaf senescence compared to the WT. Despite the severe morphological changes observed in the transgenics, the results indicate that *Pc*GCE could alter the extent of cross-linked lignin, within plant cell walls.

When *Pc*GCE was expressed in hybrid aspen, under control of *35S* promoter, and the protein was targeted to cell walls, the wood composition was altered and the saccharification efficiency improved (Gandla et al., 2015). Glc conversion in saccharification after acid pretreatment was improved by 12%, most likely as a result of reduced cross-links between xylan and lignin. Monosaccharide composition analysis have showed a reduction of 4-*O*-Me-glucuronic acid and no alteration in Xyl content. The performed Fourier Transform Infrared Spectroscopy (FT-IR) and pyrolysis - gas chromatography/mass spectrometry (Py-GC/MS) analyses of wood samples obtained from the transgenic plants showed an increase in lignin and a decrease in carbohydrate content. *35S:PcGCE* plants have also exhibited highly increased Klason lignin levels and reduced extractives levels. These changes were accompanied by reduced growth and accelerated leaf senescence.

1.6 Damage- and pathogen-associated molecular patterns activate immune responses

Any modification of cell wall or any exposure to a microbial enzyme could be perceived as a microbial attack leading to activation of defense reactions

in plants. Cell wall integrity signaling is also expected when modifying cell walls. Indeed, there is increasing evidence that the modification of cell wall affects growth and survival (Franke et al., 2002a; 2002b; Voelker et al., 2011a; 2011b; Van Acker et al., 2013; Klose et al., 2015; Gandla et al., 2015; Reem et al., 2020). Therefore, a thorough understanding of molecular mechanisms involved in early perception of wall damage or in perception of foreign proteins is essential for development of successful biotechnological strategies of plant cell wall modification.

1.6.1 Damage-associated molecular patterns

Fragments of cell wall polymers, cutin monomers or extracellular nucleotides could act as elicitors perceived by the plant cell as damage-associated molecular patterns (DAMPs), which could activate defense responses (Hou et al., 2019). Example of plant cell wall related DAMPs are oligogalacturonides (OGs) (Legendre et al., 1993; Norman et al., 1999; D'Ovidio et al., 2004), cellooligomers (Souza et al., 2017) or xyloglucan oligosaccharides (Claverie et al., 2018).

1.6.2 Pathogen-associated molecular patterns

The presence of microbial compounds, known as microbe or pathogen-associated molecular patterns (MAMP/PAMP) (Boller and Felix, 2009; Raaymakers and Van den Ackerveken, 2016; Yu et al., 2017) could also be recognized by the plant. For example, the fungal cell wall homopolymer chitin shared among various classes of pathogens is perceived as foreign compound (Felix et al., 1998). The 22-amino-acids N-terminal peptide of flagellin (flg22), originating from gram-negative bacteria acts also as PAMP elicitor (Felix et al., 1999). Microbial proteins could also show PAMP activity. For example, the fungal ethylene-inducing xylanase (EIX) from *Trichoderma viride* Pers. triggers defense response in tobacco (*Nicotiana tabacum* L.) and tomato plants (*Solanum lycopersicum* L.) (Bailey et al., 1990; Avni et al., 1994; Sussholz et al., 2020), independently of its xylan degradation activity (Enkerli et al., 1999; Rotblat et al., 2002).

1.6.3 Initiation of plant immune and CWI responses

DAMPs and PAMPs interact with cell surface-localized receptor proteins called pattern recognition receptors (PRRs) (Couto and Zipfel, 2016; He et al., 2018), the stimulation of which activates the pattern-triggered immunity (PTI) (Yu et al., 2017).

Modification of plant cell wall could also influence its mechanical properties, which are likely sensed by plants. Moreover, plant cell wall structure and biosynthesis need to be regulated and adapted to various environmental queues perceived by the plant. Molecular pathways, commonly named cell wall integrity (CWI) signaling have been proposed to maintain a feedback link between the plant cell wall and the protoplasts (Hématy et al., 2007; Wolf and Höfte, 2014; Hamann, 2015; Voxeur and Höfte, 2016; Wolf, 2017; Rui and Dinneny, 2020).

The ectodomains of plasma membrane-localized sensors mediate signals derived from the extracellular space (Gish and Clark, 2011; Engelsdorf and Hamann, 2014) and activate responses (Böhm et al., 2014; Albert et al., 2015; Yu et al., 2017; He et al., 2018; Kanyuka and Rudd, 2019). Receptor-like kinases (RLKs) and receptor-like proteins (RLPs) are sensors which perceive either exogenous derived signal, or endogenous signal originating from larger polymers or compartments inside the cell (Boller and Felix, 2009; Duran-Flores and Heil, 2016).

Approximately 600 members belonging to RLK/Pelle kinase family, have been identified in *A. thaliana* (Shiu and Bleecker, 2001; 2003). Besides RLKs, this family comprises also receptor-like cytoplasmic kinases (RLCKs) without transmembrane domain (TMD), which are involved in intracellular signal transduction (Xi et al., 2019). Leucine-rich repeat (LRR) domain proteins LRR-RLKs or LRR-RLPs, represent the biggest subfamily of RLKs and RLPs receptors. More than 200 LRR-RLKs and LRR-RLPs are identified in *A. thaliana* (Shiu and Bleecker, 2001). Another group of RLKs, belonging to the class of *Catharanthus roseus* receptor-like kinase 1-like proteins (*Cr*RLK1Ls) are considered major players in mediating CWI signals (Wolf and Höfte, 2014; Li et al., 2016; Franck et al., 2018). Apart from the transmembrane helix and the C-terminal intracellular Ser and Thr kinase domain, the *Cr*RLK1Ls are characterized with two malectin ectodomains (MDs), which form a malectin-like domain (MLD). The first characterized MD gene associated with CWI is *THESEUS1* (*THE1*). THE1 is activated as

a result of altered cellulose biosynthesis, which in turn induces lignification (Hématy et al., 2007; Merz et al., 2017).

Besides CWI signaling, *Cr*RLK1L proteins could be involved in mediation of PTI. For example, FERONIA (FER) protein regulates positively PTI by formation of hetero-dimerized co-receptor complexes composed of BAK1-FLS2-FER or BAK1-EFR-FER (Stegmann et al., 2017). Also, it has been shown that *Cr*RLK1L protein ANXUR1 (ANX1) influence PTI antagonistically (Mang et al., 2017).

Activation of plant immune and CWI responses are associated with altered hormonal profiles. For example, elevated levels of SA, JA, and ET accompany responses to many biotic and abiotic stresses (Oñate-Sánchez and Singh, 2002; Turner et al., 2002; Mur et al., 2006). Each hormonal pathway contributes to the complex regulatory network, adapted to specific type of developmental stage, environmental condition, or pathogen attack. In some cases, a second class of perception is initiated by the activation of cytoplasmic intracellular receptors, called plant disease resistance (R) proteins, that recognize pathogen virulence effectors. Their activation initiates a rapid host response called effector-triggered immunity (ETI) (Jones and Dangl, 2006; Cui et al., 2015) associated with calcium ion spikes propagation, accumulation of reactive oxygen species (ROS), production of pathogenesis-related (PR) proteins and activation of programmed cell death (PCD) (Hammond-Kosack and Jones, 1996; Chisholm et al., 2006; Gururani et al., 2012; Balint-Kurti, 2019).

1.7 Need for field trial experiments for evaluation of genetically modified trees

1.7.1 Genetic modification concerns

There are certain drawbacks associated with cisgenesis, intragenesis and transgenesis. For example, the presence of an extra copy of a gene in the recipient genome, could lead to altered regulation or silencing of the gene family (Devi et al., 2013). A random insertion of a gene into the genome could disrupt an important genome function or affect the expression of an nearby present native gene. This so-called positional effect could be avoided using CRISPR/Cas9 technique, which is considered the most precise site-specific genome editing method used to delete, insert or replace gene

sequences (Xie and Yang, 2013). However, regardless of method, any genetic manipulation can lead to unpredicted metabolic and physiological effects and requires thorough testing.

Perennial, long-lived trees, such as poplar species reproduce vegetatively and sexually. The movement of pollen and seeds, as well as spread of sprouts could cause gene flow far beyond the area of plantings, which is a major concern in field trials with genetically modified trees. It has been predicted that fertility is a main factor for gene flow (DiFazio et al., 2012), whereas vegetative spread, such as shoots initiation from roots or rooting of fallen branches (Klocko et al., 2018) is of a lesser concern as it can be more easily controlled.

The risk of gene flow into wild populations complicates the permission procedures for field trials of genetically modified trees (Klocko et al., 2018). This leads to shortage of field data, which could assess the ecological and the commercial impact of genetically modified trees, compared to control plants (Strauss et al., 2017). Initial laboratory and greenhouse trials seldom match the results obtained from field trails (Voelker et al., 2011a; 2011b; Viswanath et al., 2012), while in permitted field trails, the plants must be removed before reaching maturity. Juvenile trees though, could show different wood characteristics, compared to adult trees (Zobel and Sprague, 1998).

Possible strategies to avoid the problem with gene flow, is selecting non-flowering or fruitless individuals, or to produce sterile individuals (Ranney, 2004) by modifying genes, which control flowering and fertility. (Vining et al., 2012).

1.7.2 Need for evaluation of transgenics plants in field conditions

In field conditions, plants are exposed to both biotic and abiotic stresses, which could result in altered growth performance, compared to greenhouse (Strauss, 2003; Strauss et al., 2016). For example, constructs with overexpressed gibberellic acid biosynthetic genes, which have impact on biomass deposition, have shown highly variable correlation of growth rate between greenhouse and field experiments (Viswanath et al., 2011). Also, transgenic poplar lines, having antisense downregulation of lignin biosynthetic gene from the *4-COUMARATE:COENZYME A LIGASE* family (*4CL*) have shown normal growth in the greenhouse (Hu et al., 1999) and disappointing performance in field conditions (Voelker et al., 2010; 2011a;

2011b). These observations demonstrate the need for field trails early in a research project, particularly when the transgenes have impact on plant structure and physiology.

There are examples, where modification of plant cell wall, could alter traits associated with biotic and abiotic stress tolerance. For example, knock out of *PECTIN ACETYLESTERASE 9* (*AtPAE9*) in *A. thaliana* has led to increased RGI and HG acetylation compared to control plants (De Souza et al., 2014) and decreased concentrations of stress responses associated phytohormones JA, SA, ABA, and auxin (Kloth et al., 2019), while constitutive expression of *Aspergillus nidulans* Eidam *PECTIN METHYLESTERASE* (*An*PME) in *A. thaliana* has generated plants with reduced sensitivity to osmotic stress (Reem et al., 2020). Altered traits associated with biotic and abiotic stress tolerance, could affect crop performance in the field. Therefore, is important to investigate the disease resistance to one or more pathogens and to evaluate the general performance of genetically improved plants in their real cultivation conditions (Purrington, 2000; Brown, 2002).

2. Objectives

In ***Paper* I**, we addressed problem of activation of DAMP/PAMP signaling when modifying cell walls for biorefinery. Our aim was:

- To elucidate the cause for the observed untargeted effects in hybrid aspen with constitutive expression of *Pc*GCE. We tested if the observed off-target effects are triggered by DAMPs or by perception of *Pc*GCE protein as a PAMP.

- To develop strategy for expression of *Pc*GCE avoiding negative off-target effects. We tested if driving the expression from WP is a promising strategy for avoiding the negative effects in the leaves.

Using tissue-specific promoters for driving expression of target genes or transgenes will not avoid possible activation of DAMP signaling. Moreover, any change in cell wall could be perceived by CWI perception mechanism in wood cells. This prompted us to identify main *Populus* players associated with CWI or DAMP perception. Main objectives of ***Paper* II** were:

- To carry out genome-wide identification of MD/MLD receptor candidates in *Populus*, and identify those that are active during SCW biosynthesis. Also, we aimed at identifying putative partners of the xylogenesis-related *PtMD*s, by co-expression analysis.

Previous greenhouse analyses identified several types of transgenic aspen lines with reduced acetylation of xylan and superior saccharification properties. The objectives of ***Paper* III** were:

- To test the field performance of transgenic hybrid aspen plants with reduced xylan acetylation

- To compare in the field conditions different strategies of xylan deacetylation, biosynthetic deacetylation in the Golgi, or post-synthetically in the cell wall, deacetylation using two different CE CAZymes (CE1 and CE5) in the apoplastic space, and deacetylation using either *35S* or wood-specific promoters.

In ***Paper* IV** and ***Paper* V** we investigated the field performance of hybrid aspen intragenic lines that were selected as having improved traits in large-scale greenhouse screening. The main aims were:

- To functionally analyze selected genes,
- To investigate stability of expression of target genes and stability of phenotypes
- To identify off-target phenotypes
- To evaluate constructs with regard to saccharification, growth and wood quality traits
- To elucidate the relationships between productivity, cell wall properties, wood anatomy and quality traits and saccharification efficiency.

3. Results and Discussion

3.1 Is glucuronoyl esterase a promising enzyme for wood improvement? (***Paper* I**)

Despite the promising results on Glc conversion, it is difficult to ignore the secondary morphological effects observed in the transgenic plants expressing *Pc*GCE, such as reduced growth and premature leaf senescence. Transcriptomics study, performed on *A. thaliana* plants with constitutive expression of *Pc*GCE (Tsai et al., 2017) has led to the identification of upregulated genes associated with oxidative stress and immune responses. Tsai et al., (2017) suggested three main causes for the observed results: (1) metabolites or intermediates generated by the activity of the enzyme could induce the observed responses, (2) the enzyme activity could alter the plant cell wall structure affecting the integrity of the cell wall, resulting in activation of defense responses, and (3) some domain of the introduced enzyme might be recognized by the plant as a PAMP pathogenic epitope. In ***Paper* I**, we carried out detailed analysis of *Pc*GCE overexpressing hybrid aspen lines to elucidate molecular mechanism of *Pc*GCE off-target action. We provide evidence that *Pc*GCE act as a PAMP elicitor. Moreover, we show an alternative strategy of deployment of this enzyme that avoids off-target effects caused by the enzyme.

3.1.1 Hormonal, metabolic and transcriptome changes in *35S:PcGCE* mature leaves indicate activation of immune defense responses

Global transcript profiling in mature and young developing leaves revealed that genes involved in biotic and abiotic stresses were most affected gene categories in transgenic plants (***Paper* I**; Fig. 3B, Tab. S8**).** Hormonomics analysis of mature leaves of *35S:PcGCE* plants expressing the active enzyme (***Paper* I**; Fig. 3C**)**, showed increased levels of JA, SA, ABA, auxin and altered profile of cytokinins products, which correlated with the formation of leaf necrotic spots. Transcripts related to signaling by these hormones and ET were also significantly altered (***Paper* I**; Table S3). Elevated levels of SA, JA, and ET are associated with disease resistance signal transduction (Oñate-Sánchez and Singh, 2002; Turner et al., 2002; Mur et al., 2006).

Although oversimplified, it has been suggested that SA and JA-ET trigger antagonistic defense responses against pathogens with different host interaction (Mur et al., 2006; Koornneef and Pieterse, 2008). SA is dominant in the response against biotrophic pathogens, whereas JA and ET are associated with defense against necrotrophs (Niki et al., 1998; Thomma et al., 2001; Kunkel and Brooks, 2002; Rojo et al., 2003; Glazebrook, 2005; Lorenzo and Solano, 2005; van Loon et al., 2006). ABA is involved in the regulation of plant growth, development and drought stress (Tuteja, 2007), and is also a strong modulator of JA-induced defenses (Proietti et al., 2018). Moreover, there is a significant evidence that activation of biotic and abiotic stress hormonal pathways is age - and organ - dependent (Kus et al., 2002; Zeier, 2005). For example, in *A. thaliana* SA and ABA balance the trade-offs between biotic and abiotic stress responses, in leaf-age dependent mode (Berens et al., 2019). Furthermore, it has been suggested that cytokinins act as a hub, for defense responses mediated by other hormones (Choi et al., 2011), which could explain their altered profile in the leaves of *35S:PcGCE* plants.

Metabolomic analysis of the leaves of *35S:PcGCE* plants revealed relatively small changes but they were consistent between leaf 21 and 23 (***Paper* I**; Fig. 3D). Mevalonate (H3MG), which is a precursor of many essential isoprenoid compounds and mediates the induction of nuclear-associated calcium spikes (Venkateshwaran et al., 2015), triggered by wounding or treatment with pathogen elicitors (Oba et al., 1985; Stermer and Bostock, 1987; Yang et al., 1991; Choi et al., 1992) increased in transgenic lines.

Different stresses induce local increase in soluble sugars (Gómez-Ariza et al., 2007, Bolouri Moghaddam and Van den Eden, 2012; Morkunas and Ratajczak, 2014). Raffinose, and galactinol, which are suggested to act as signal molecules in biotic and abiotic stress responses (Sengupta et al., 2015) were increased in transgenic plants. In the transcriptomics data of mature leaves (leaf 21 and leaf 23) in two *35S:PcGCE* transgenic lines (***Paper* I**; Tab. S3), we found that the raffinose pathway was highly upregulated, including galactinol synthase genes. Overexpression of a cucumber *GALACTINOL SYNTHASE* (*CsGolS1*) from family GT8 in tobacco (*Nicotiana tabacum* L.) resulted in an increased resistance to necrotrophic fungus *Botrytis cinerea* Pers (Kim et al., 2008). Cell wall invertases (cwINVs) from family GH32, which cleave Suc to Fru and Glc were also

upregulated in both young and mature leaves of *35S:PcGCE* plants (***Paper* I**; Tab. S3, S7) and Suc and Fru levels were increased in mature leaves (***Paper* I**; Fig. 3D). It has been shown that cwINVs are induced during pathogen attacks, creating a sink at the PAMP perception site (Fotopoulos et al., 2003; Sutton et al., 2007; Essmann et al., 2008; Kühn and Grof, 2010; Morkunas and Ratajczak, 2014).

Furthermore, *myo*-inositol levels were increased in transgenic leaves (***Paper* I**; Fig. 3D). Inositol derived molecules are important secondary messengers for the adaption of plants to both abiotic and biotic stress (Gillaspy, 2011). Lipids and phosphates are added or removed from inositol derived molecules (Michell, 2011). For example, in response to extracellular signal, PHOSPHOLIPASE C (PLC) could hydrolyze phosphatidylinositol-(4,5)P2 (PtdInsP2) from the cell membranes or vesicles to produce the secondary messenger molecules, diacylglycerol and inositol-(1,4,5)-P3 (Gillaspy, 2011). Transcriptomics data showed (***Paper* I**; Tab. S7) that a number of PLCs were significantly upregulated already in young expanding leaf of *35S:PcGCE* line 10. The movement of information from the membrane to the cytosol, via the inositol signaling has impact on plant growth, development, physiology (Mueller-Roeber and Pical, 2002; Gillaspy, 2011), and the regulation of auxin (Tan et al., 2007) and JA receptors (Sheard et al., 2010).

Gly-3-P, which was another elevated compound in the mature leaves of *35S:PcGCE* lines (***Paper* I**; Fig. 3D), is a regulator of plant defense signaling (Venugopal et al., 2009) and mobile inducer of systematic acquired resistance (SAR) (Chanda et al., 2008; Mandal et al., 2011). Gly-3-P plays a central role in energy-producing reactions, such as glycerolipid biosynthesis and glycolysis (Kachroo and Kachroo, 2009), and is a main acetyl-CoA supplier to the TCA cycle (Fernie et al., 2004). In the chloroplasts, Gly-3-P enters glycerolipid biosynthesis by acylation with oleic acid to form lyso-phosphatidic acid (lyso-PA), which is precursor of phosphatidic acid (PA) (Kunst et al., 1988). Free fatty acid analysis (***Paper* I**; Fig. S1), showed that oleic acid was significantly downregulated in young and mature leaves of *35S:PcGCE* line 10. Low levels of oleic acid triggers SA-driven responses (Kachroo et al., 2001) via upregulation of transcription factors WRKY50/51 (Gao et al., 2011). Transcriptomics data (***Paper* I**; Tab. S3, S7) and qPCR (***Paper* I**; Fig. 4C) analysis showed significantly elevated levels of WRKY51 in all investigated leaves of *35S:PcGCE* lines. Furthermore, PA is an

important intermediate in lipid biosynthesis, which is accumulated in response to pathogen infection, drought, salinity, wounding and cold (Testerink and Munnik, 2011). PA is also capable to activate calcium-dependent protein kinases (CDPKs) (Farmer and Choi, 1999; Szczegielniak et al., 2005), and is involved in the regulation of ET signaling (Testerink et al., 2008). PA could be produced by direct hydrolysis of phospholipids by phospholipases D (PLDs) (Van der Luit et al., 2000), members of which were consistently upregulated in the transcriptomics data of all leaves investigated in our study (***Paper* I**; Tab. S3, S7).

Overall, the omics results of *35S:PcGCE* leaves revealed altered metabolic profile and activation of biotic stress responses.

3.1.2 Gradual progress of immune defenses in developing leaves of *35S:PcGCE* plants

We investigated the expression levels of *Pc*GCE (***Paper* I**; Fig. 4A) and ROS content (***Paper* I**; Fig. 4B) in sequential leaf samples from the apical bud to mature necrotic leaves in *35S:PcGCE* plants. These leaf series showed a progressive increase of ROS, and an exponential accumulation of *PcGCE* transcripts from the younger to older leaves (***Paper* I**; Fig. 4A). In order to understand the transcriptional changes in the leaf series of transgenic plants, we investigated the expression levels of four stress response marker genes (***Paper* I**; Fig. 4C). We followed the expression pattern of a *JAZ1* homologous gene, which a marker for JA signaling (Chini et al., 2007; Thines et al., 2007; Chung et al., 2008). *JAZ1* levels increased exponentially from young fully expanded leaves to necrosis affected leaves, following the path of *PcGCE* transcripts (***Paper* I**; Fig. 4C). Furthermore, we followed the expression of homolog of *RESPIRATORY BURST OXIDASE HOMOLOG PROTEIN D* (*RBOHD*). The activity of RBOH causes a rapid H_2O_2 accumulation in the extracellular space, required for the propagation of the SAR signal, and the onset of hypersensitive response (HR) (Lew et al., 2020; Li et al., 2021). It has been shown that PAMP-induced ROS burst is compromised in *rbohD* mutants, thus RBOHD is the major enzyme involved in ROS production during pathogen responses (Nühse et al., 2007). *RBOHD* homolog was upregulated only in older leaves, correlating with necrosis progression(***Paper* I**; Fig. 4C). We investigated also expression of HR marker genes such as homologs of *ENHANCED DISEASE SUSCEPTIBILITY 1* (*EDS1)* and *WRKY51*, which antagonize the JA

mediated signaling and enhance the defense responses in a SA dependent manner, inducing PR proteins (Gao et al., 2011; Zhang et al., 2018). Homologs of both *EDS1* and *WRKY51* were highly induced in older leaves (***Paper* I**; Fig. 4C). Homolog of *WRKY51* was highly upregulated already in young, expanded leaves, suggesting that long distance signaling, and SAR were activated in very young leaves of transgenic plants. Taken together, the analysis revealed two main stages of *Pc*GCE induced stress responses, including early JA dominated phase and late SAR response, associated with HR.

3.1.3 *Pc*GCE mRNA is not mobile

Since transcriptomics, hormonomics, metabolomics and sequential leaf analysis revealed upregulation JA, SA, ET signaling, as well as ROS accumulation in *35S:PcGCE*, we wanted to distinguish between local and non-cell autonomous responses induced by *Pc*GCE. For that purpose, we performed a grafting experiment (***Paper* I**; Fig. 5A), where scions of five-week-old transgenic and WT plants were grafted onto the transgenic or WT rootstocks. *Pc*GCE transcripts were not detected in the leaves of WT parts of the grafted plants, but only in the leaves of transgenic scions and rootstocks (***Paper* I**; Fig. 5B). This indicates that the *PcGCE* mRNA is not mobile, and any immune responses in non-transgenic parts must be induced by *Pc*GCE at a distance.

To monitor activation of immune responses in grafted plants, we analyzed ROS accumulation and expression of *JAZ1* and *RBOHD* homologs in the leaves. Indeed, there was an increase in ROS and in *JAZ1* and *RBOHD* homologs transcript levels in WT scions grafted on transgenic rootstocks, and in WT rootstocks carrying transgenic scions, as compared to WT/WT grafts (***Paper* I**; Fig. 5, CD). In the WT scions grafted on transgenic rootstocks, the levels of *JAZ1* and *RBOHD* transcripts were higher when the leaves were present on the rootstocks (***Paper* I**; Fig. 5D), while increase in ROS was not dependent on the presence or removal of the leaves (***Paper* I**; Fig. 5C). This indicates that JA (as evidenced by *JAZ1*) and SAR (as evidenced by *RBOHD* and ROS) responses are induced at a distance from *Pc*GCE perception site and their induction is enhanced by old leaves.

Moreover, grafting a *35S:PcGCE* scion on WT rootstock did not avoid activation of immune responses in the scion (***Paper* I**; Fig. 5D). This indicate that transgenic roots are not required for activation of defense responses. It

further shows that the grafting cannot be used as a strategy to rescue off-target phenotypes in transgenic scions. Also, it was clear that *35S:PcGCE* has to be locally present in the leaves for the induction of strong immune responses (***Paper* I**; Fig. 5B).

3.1.4 *Pc*GCE is perceived as PAMP

To investigate if the observed off-target effects of *Pc*GCE were triggered by the enzymatic activity of *Pc*GCE or by the perception of the enzyme as a PAMP, we expressed enzymatically inactive *Pc*GCE^{S217A} in hybrid aspen plants, under control of 35S promoter. Similarly, as the active *Pc*GCE, the mutated *Pc*GCE^{S217A} induced growth penalties, leaf necrosis and premature senescence, and the expression levels of the enzyme correlated positively with the symptoms (***Paper* I**; Fig. 9A-E**)**. This indicates that *Pc*GCE is perceived as PAMP in aspen leaves.

3.1.5 Expressing of *Pc*GCE from wood-specific promoter

The grafting experiment demonstrated that the *PcGCE* transcripts were not mobile (***Paper* I**; Fig. 5B), which suggests that expressing the protein in a tissue that lacks *Pc*GCE perceiving mechanism, would avoid stress-related symptoms. We tested if limiting the expression of *Pc*GCE to developing wood using the wood-specific promoter of aspen *GT43B* gene (Ratke et al., 2015) could rescue the phenotype.

WP:PcGCE lines did not show premature leaf senescence (***Paper* I**; Fig. 6A), and had slightly thicker stems and increased stem height, compared to WT (***Paper* I**; Fig. 6, CD). Interestingly, ROS concentrations in leaves of *WP:PcGCE* lines, were slightly higher compared to WT (***Paper* I**; Fig. 6, GH). The levels of ROS though, remained stable at different developmental stages in *WP:PcGCE* plants , which was in difference to the progressive ROS increase in the leaves of *35S:PcGCE* lines (***Paper* I**; Fig. 4B).

Hormonomics analysis in *WP:PcGCE* lines revealed slight downregulation of active auxin precursors, ABA, SA and degradation products of cytokinins, while jasmonates products were not affected (***Paper* I**; Tab. S5). These results indicate that hormonal profiles of *WP:PcGCE* lines were different compared to *35S:PcGCE* lines (***Paper* I**; Fig. 3C).

Similarly to *35S:PcGCE* plants (***Paper* I**; Fig. 3D), *WP:PcGCE* plants revealed elevation of certain soluble sugars (***Paper* I**; Tab. S6), though with

less distinct fold changes. Metabolites related to the TCA cycle, were not altered in *WP:PcGCE* plants (***Paper* I**; Tab. S6). Transcriptomic analysis of the mature leaves of *WP:PcGCE* lines revealed only three DE genes commonly affected in two lines investigated (***Paper* I**; Fig. 6I). *PtCEL9B3* from family GH9 encoding extracellular cellulase involved in cell expansion (Takahashi et al., 2009) was upregulated, while a homolog of *PHYTOSULFOKINE RECEPTOR 1* (*PSKR1*) and a homolog of *MILDEW RESISTANCE LOCUS O 5* (*MLO5*), were downregulated (***Paper* I**; Tab. S6). Both downregulated genes are involved in calcium signaling, associated with developmental and biotic stress responses (Mosher et al., 2013; Hartmann et al., 2014; Meng et al., 2020). These results suggest that the expression of the transgene under control of *WP* promoter avoids the severe growth inhibition and immune defense-related symptoms observed in *35S:PcGCE* lines.

3.1.6 Early immune response activation genes in *35S:PcGCE* leaves

Phenotypes of *WP:PcGCE* lines and grafting experiments excluded developing xylem and roots as a site of *Pc*GCE perception and a source of systemic signals, leaving leaves as a likely place. This was supported by the positive impact of leaves on the immune marker gene activation response. To reveal candidates for the perception of *Pc*GCE, we performed transcript profiling of leaves at earliest stages of development, which should be less affected by secondary *Pc*GCE effects than the mature leaves studied before. We investigated the first unfolded leaf (Leaf 8) and young expanding leaf (Leaf 11) of *35S:PcGCE* line 10 (***Paper* I**; Fig. 7; Tab. S7, S8), but still finding over 1500 genes affected by *Pc*GCE at the youngest leaf developmental stage. To narrow down this list, we excluded those DE genes that were active in developing wood tissues (***Paper* I**; Tab. S9). This gene list, including approx. 450 genes, was analyzed in detail.

Besides the activation of genes associated with JA, SA and ET signaling, we observed upregulation of genes encoding cell surface immune receptors and transmembrane calcium transporters. Several genes encoding RLKs, RLPs, MDs, *CYCLIC NUCLEOTIDE GATED ION CHANNELS* (*CNGC*s), calcium-transporting *AUTOINHIBITED* Ca^{2+}*/ATPases* (*ACA*s) and *WALL ASSOCIATED KINASES* (*WAK*s) showed higher expression levels, compared to WT plants. Based on the data (***Paper* I**; Tab. S9) we propose that *Pc*GCE perception at the cell surface likely involves tightly coordinated

crosstalk between RLPs, RLKs and MDs proteins, which form hetero-dimerized co-receptor complexes (Böhm et al., 2014; Albert et al., 2015; Couto and Zipfel, 2016; Yu et al., 2017; He et al., 2018; Kanyuka and Rudd, 2019). Plant stress response signaling is known to be associated with rapid trans-phosphorylation between members of the PRR complexes (Schulze et al., 2010; Schwessinger et al., 2011) that induces early PAMP response associated with transient generation of ROS in the apoplastic space. ROS act as a toxin barrier and reinforce the cell wall *via* cross-linking of cell wall glycoproteins (Torres et al., 2006). ROS also modulate specific defense responses, phytohormone signaling and gene expression reprogramming (Scheler et al., 2013). Activation of receptor complexes and ROS production in *PcGCE* expressing leaves could activate MITOGEN-ACTIVATED PROTEIN KINASES (MAPKs) (Kovtun et al., 2000; Asai et al., 2002; Gao et al., 2008; Meng and Zhang, 2013; Xu and Zhang, 2015) and CDPKs (Boudsocq et al., 2010), which creates a crosstalk between Ca, ROS and MAPKs signaling.

Beside several receptors and MAPKs, we also found upregulation of many genes associated with pectin modification, such as genes encoding *PECTIN METHYL ESTERASES* (*PME*s) from family CE8, *POLYGALACTURONASES* (*PG*s) from family GH28 and *PECTATE LYASES* (*PL*s) from family PL1(***Paper* I**; Tab. S7). Pectins remodeling and release of OGs has impact on a wide range of defense responses (Norman et al., 1999; Bellincampi et al., 2000; Galletti et al., 2008; 2011; Ferrari et al., 2008). Negatively charged pectins could attract cationic compounds, such as Ca^{+2} (Celus et al., 2018) and RAPID ALKALINIZATION FACTORS (RALFs). RALFs encode hormone peptides associated with stress responses and development and interacting with *Cr*RLK1Ls (Campbell and Turner, 2017; Doblas et al., 2018; Kumar et al., 2020), with impact on calcium signaling and extracellular pH levels (Bedinger et al., 2010; Wu et al., 2007). Two homologs to *RALF27* were upregulated in the first unfolded leaf of *35S:PcGCE* line 10 (***Paper* I**; Tab. S9). Interestingly, *RALF27* homologs were found in the genomes of two poplar fungal pathogens: *Sphaerulina musiva* (Peck) Quaedvlieg, Verkley & Crous and *Septoria populicola* Peck (Thynne et al., 2017), suggesting a lateral gene transfer between host and pathogens. WAKs serve as OGs receptors responsive to pectin methylesterification status (Kohorn, 2016; Decreux and Messiaen, 2005). We found two upregulated *WAK2* homologs in the first unfolded leaf and

young expanding leaf of *35S:PcGCE* line 10 (***Paper* I**; Tab. S9). WAK2 mediates pathogen and stress responses, via activation of MITOGEN-ACTIVATED PROTEIN KINASE 6 (MPK6) (Kohorn et al., 2009), which further modulate ET and ROS signaling (Joo et al., 2008; Han et al., 2010; Li et al., 2012). These series of networks could fine-tune a broad range of cellular responses, such as phytohormones crosstalk, ROS balance, activation of intracellular R genes and ETI activation (Zhao et al., 2005; Dodds and Rathjen, 2010; Tsuda and Katagiri, 2010; Kazan and Lyons, 2014). Based on these results, we propose a model for *Pc*GCE perception and immune response propagation shown in Figure 1.

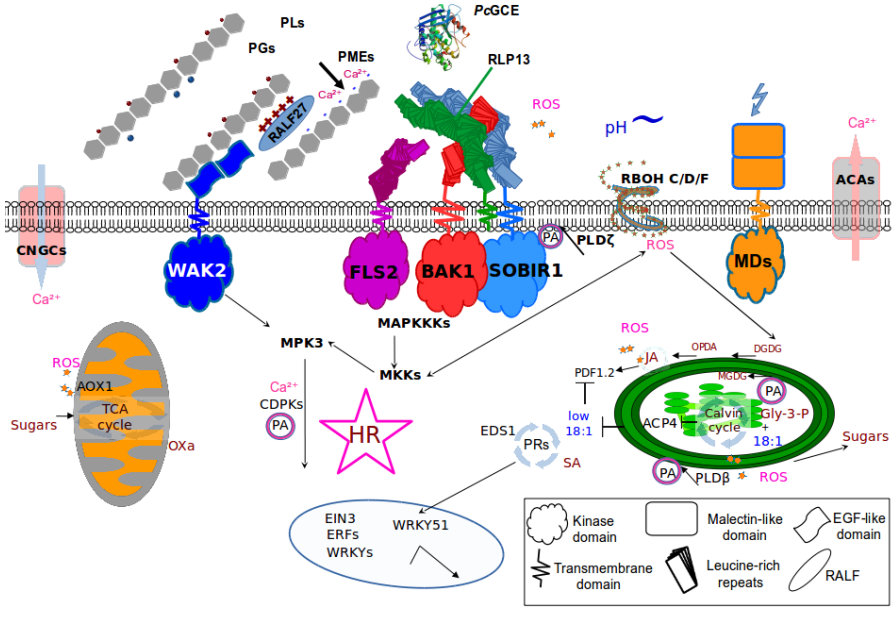

Figure 1. Proposed model for *Pc*GCE perception and immune response propagation. *Pc*GCE protein is recognized in the apoplastic space, which drives the formation of co-receptor PRR complexes between cell surface RLPs and RLKs. The assembled co-receptor complexes transphosphorylate each-other and initiate PTI, which activates a broad range of cellular responses in the cytosol, chloroplasts and mitochondria. This leads to the activation of ROS, increase in cytosolic sugars and phytohormones signaling, followed by transcriptional reprogramming and MAPKs cascades propagation. Upregulation of PMEs, PGs, PLs leads to homogalacturonan degradation and resulting OGs are sensed by WAK2, which further stimulates MAPK

cascades. PLDs fine-tune the cellular responses by direct PA hydrolysis from the membrane phospholipids. Inside the cell CDPKs, lipids, ET, JA and SA signaling defines the severity of the stress response. Immune responses are multiplied by the activation of intracellular PR-proteins, which ultimately leads to ETI and HR, accompanied by a pronounced elevation of ROS levels.

Abbreviations: ACAs – AUTO-INHIBITED CALCIUM ATPASEs, AOX1 – ALTERNATIVE OXIDASE 1, ACP4 – ACYL CARRIER PROTEIN 4, BAK1 – BRI1-ASSOCIATED RECEPTOR KINASE 1, BRI1 – BRASSINOSTEROID INSENSITIVE 1, CDPKs –CALCIUM-DEPENDENT PROTEIN KINASEs, EDS1 – ENHANCED DISEASE SUSCEPTIBILITY 1, EIN3 – ETHYLENE INSENSITIVE 3, ERFs – ETHYLENE RESPONSIVE FACTORs, ETI – effector triggered immunity, CDPKs – CA-DEPENDENT PROTEIN KINASEs, CNGCs – CYCLIC NUCLEOTIDE-GATED ION CHANNELs, FLS2 – FLAGELLIN SENSITIVE 2, Gly-3-P – glycerol-3-phosphate, MGDG/DGDG – mono/di-galactosyldiacylglycerol, JA – jasmonic acid, MPKs – MITOGEN-ACTIVATED PROTEIN KINASEs, MKKs – MITOGEN-ACTIVATED PROTEIN KINASE KINASEs, MAPKKKs – MITOGEN-ACTIVATED PROTEIN KINASE KINASE KINASEs, MDs – malectin domain proteins, OPDA – 12-oxophytodienoic acid, OXa – oxalic acid, PA – phosphatidic acid, PDF1.2 – PLANT DEFENSIN 1.2, PGs – POLYGALACTURONASEs, PLs – PECTATE LYASEs, PLDs – PHOSPHOLIPASEs D, PMEs – PECTIN METHYL ESTERASEs, PRs – pathogenesis-related proteins, PRRs – pattern recognition receptors, PTI – pattern triggered immunity, RALF27 – RAPID ALKALINIZATION FACTOR 27, RLKs – RECEPTOR-LIKE KINASEs, RLPs – RECEPTOR LIKE PROTEINs, ROS – reactive oxygen species, SA – salicylic acid, SOBIR1 – SUPPRESSOR OF BIR1, WAK2 – WALL-ASSOCIATED KINASE 2.

3.1.7 *WP:PcGCE* plants - resilient trees with enhanced bioconversion?

As transcriptomic analysis of the leaves of *WP:PcGCE* plants, showed downregulation of a homologs of *MLO5* and *PSKR1* it is possible that these plants have altered biotic resistance. It has been shown that loss of function *mlo* mutation in barley improved resistance against powdery mildew *Blumeria graminis* f. sp. *hordei* Marchal (Büschges et al., 1997) and necrotrophic fungus *Bipolaris sorokiniana* (Shoemaker) (Kumar et al., 2000). However, barley *mlo* mutants are more susceptible to the hemibiotrophic rice blast fungus, *Magnaporthe grisea* Saccardo (Jarosch et al., 1999). Another side effect of *mlo* mutants is an increase of necrotic leaf spot formation, which results in reduced yield (Bjørnstad and Aastveit, 1990; Kjær et al., 1990; Jørgensen, 1992).

A. thaliana pskr1 knockout mutant is more resistant to oomycete *Hyaloperonospora arabidopsidis* Pers and the root-knot nematode *Meloidogyne incognita* Kofoid & White, which are evolutionarily distant

pathogens (Rodiuc et al., 2016). However, the mutant is more susceptible to the necrotrophic fungus *Alternaria brassicicola* Wiltshire (Mosher et al., 2013).

In the greenhouse, *WP:PcGCE* plants did not show any negative effects on growth or necrosis of the leaves, despite the downregulation of *MLO5* and *PSKR1* homologous genes. But negative effects on growth are not always obvious in greenhouse experiments (Strauss et al., 2016). It has been shown that, in field conditions the activation of defense responses and R genes negatively affects yield (Purrington, 2000; Brown, 2002; Silva et al., 2019). Testing *WP:PcGCE* lines in the field would be necessary before the construct could be dedicated for biorefinery. It will be interesting to follow if the *WP:PcGCE* lines will be influenced by changing environmental conditions or will keep its excellent greenhouse performance. Also, it is important to evaluate the general plant-pathogen performance of these plants. Under the pressure of future climate change, forest industry would require trees with improved survival rate, characterized with resilience to broad range of pathogens (Morin et al., 2018; Burdon and Zhan, 2020).

3.2 Identification of malectin domain-containing genes expressed in the wood (***Paper* II**)

The biorefinery-targeted biomass improvement most frequently affects chemistry and/or structure of secondary walls. This could be linked to off-target effects triggered by perception of defects in cell wall integrity. The main aim of the study (***Paper* II)** was to identify receptor candidates involved in cell wall integrity signaling, which are active during secondary cell wall formation in *Populus*.

We performed a genome-wide identification of malectin/malectin-like domain-containing (MD) genes and identified 146 *MD* genes in *P. trichocarpa*. Phylogenic analysis grouped the *PtMD* genes into five superclades characterized by the following domain patterns: 1) LRR-MD-PK, 2) MLD-LRR-PK 3) MLD-PK (*Cr*RLK1L), 4) MLD-LRR (RLPs) and 5) MD-Kin (***Paper* II**; Fig. 1).

Expression of these 146 *PtMD* genes was studied in developing leaves and developing wood tissues by RNA sequencing (***Paper* II**; Fig. 5). The analysis revealed that the majority of *PtMD*s had highest expression in

mature leaves. 13 *PtMD* genes revealed maximum expression in developing xylem, though many of them showed also high levels in the leaves. The high leaf expression levels of the *PtMD* genes suggested that they could be involved in foliar defenses. This prompted us to investigate transcriptomics datasets available for various tissues and organs of plants subjected to different stresses, in either greenhouse or field conditions (***Paper* II**; Fig. 6). This confirmed high expression of large sets of *PtMD* genes during abiotic/biotic stresses in the leaves. Interestingly, transcriptomic analysis of young expanded, young fully expanded and mature leaves of *35S:PcGCE* plants, showed a progressive upregulation of MD genes during leaf development (***Paper* I**; Tab. S2, S7, S8), confirming their role in foliar defenses.

We used AspWood database (Sundell et al., 2017), to display with high-spatial-resolution *PtMD* transcript abundance in developing secondary vascular tissues of aspen (***Paper* II**; Fig. 7). 89 *PtMD* genes (61%) were found expressed (***Paper* II**; Tab. S7), but most of them had maximum expression in the phloem and in the cambium-radial expansion zone (CA-RE) (***Paper* II**; Fig. 7). The majority of *PtMD*s with high expression in the phloem (***Paper* II**; Fig. 7 and Tab. S7) belong to the LRR-MD-PK superclade. Genes with high expression during CA-RE zone were represented of variety of domain structures, such as MD-Kin, LRR-MD-PK, MLD-LRR, and MLD-PK (*Cr*RLK1L). *PtMD* genes which exhibited high levels of expression under the transition between primary and secondary wall deposition, were mostly represented by MLD-PKs structure, typical of *Cr*RLK1L family.

Co-expression network analysis identified putative partners of xylogenesis-related *Pt*MD proteins. Ten *PtMD* genes, with expression peak in the cambium-radial expansion zone and primary to secondary transition zone (CA-RE/PW-SW) and eight genes with expression peak in the primary-to-secondary wall transition and secondary wall (PW-SW/SW), acted as a baits for co-expression partners in these zones. (***Paper* II**; Fig. 7 and Tab. S7).

The *PtMD* baits, which were expressed in CA-RE/PW-SW zones formed five unique networks, the biggest of which included the *At*FER ortholog *PtMD126*, and several genes associated with signaling by phosphorylation relay, ROS signaling and cell wall development (***Paper* II**; Fig. 8A and Tab. S8). The second biggest co-expression network associated with the *At*THE1

ortholog *PtMD98* (***Paper* II**; Fig. 8A, Tab. 1 and Tab. S8), comprised IAA and GA signaling-related genes, and xylogenesis regulation players. A network, which was associated with *PtMD94*, included genes related to stress signaling and development, such as homologs of *AtRALFL31* (Campbell and Turner, 2017), *ABA INSENSITIVE 1* (*AtABI1*) (Kong et al., 2015), *BRASSINOSTEROID INSENSITIVE 1* (*AtBRI1*) (Zhou et al., 2018), *LYSM-CONTAINING RECEPTOR-LIKE KINASE 5* (*AtLYK5*) (Liao et al., 2017), and *FLAGELLIN-SENSITIVE 2* (*AtFLS2*) (Liu et al., 2012) (***Paper* II**; Fig. 8A, Tab1 and S8). Furthermore, genes *PtMD88* and *PtMD145*, which are expressed during early secondary wall biosynthesis, formed two small networks (***Paper* II**; Fig. 8A, Tab. 1 and Tab. S8).

The baits with expression peak in late secondary wall, formed five networks (Fig. 8B, Tab. 1 and Tab. S9). The largest of these was associated with *PtMD129* (related to *AtANX1* and *AtANX2*), and *PtMD137*, which encode LRR-RLK. In this network, there were genes associated with calcium and ROS signaling, and transcriptional regulators involved in the activation of secondary wall program, such as *AtMYB46* and *AtMYB83* (Zhong et al., 2007; McCarthy et al., 2009). The results reveal promising candidates for mediation of secondary wall integrity signaling, coordinated with cell division and secondary wall formation in developing wood.

3.3 Importance of field trials for evaluating transgenes (*Paper* III, *Paper* IV, *Paper* V)

Biomass formation and accumulation depends on the plant metabolism, which adapts rapidly and flexibly to environmental conditions in response to various queues (Lamers et al., 2020). In two different field trial experiments, we tested the performance of (i) hybrid aspen lines with reduced xylan acetylation (***Paper* III)** and (ii) investigated the effects of altered expression of genes which are highly expressed during secondary wall formation (***Paper* IV, *Paper* V)**. In both cases, the lines were selected considering different traits based on extensive experiments in the greenhouse.

3.3.1 Field performance of hybrid aspen with reduced xylan acetylation (***Paper* III**)

In this five-year field trial, we tested transgenic constructs that either suppressed process of acetylation in the Golgi by reducing expression of RWA genes, or that induced post-synthetic deacetylation of xylan in cell wall by expressing fungal xylan acetyl esterases *An*AXE1 and *Hj*AXE. Thus, we could compare the impacts of reducing xylan acetylation biosynthetically in the Golgi or post-synthetically in the cell wall. In the case of post-synthetic xylan modification, we could compare performance of two different AXEs belonging to two different CE families: *An*AXE1 from family CE1 and *Hj*AXE from family CE5. Moreover, transgenes were controlled by either constitutive *35S* promoter or by wood-specific *WP* promoter (Ratke et al., 2015).

In the previous greenhouse experiments, all these constructs showed reduced xylan acetylation, improved saccharification without pretreatment and normal growth (Pawar et al., 2017a; 2017b; Wang et al., 2020; Pramod et al., 2021). However, in the field, there was a high incidence of random dwarfism; 17% of all acetyl reduced lines became dwarf after the first year in the field (***Paper* III**; Fig. 1B), which in one case was associated with variegation (***Paper* III**; Fig. 1C). This result suggests a possible link between acetyl homeostasis and chromatin state regulation (Cai and Tu, 2012; Etchegaray and Mostoslavsky, 2016) that could affect activity of transposons (Kaeppler et al., 2000). Other lines grew normally throughout the five-year trial period, suggesting that dwarfism is induced during a narrow window between planting and the second growth season in some lines, after which the lines have stable phenotypes. AXE-expressing lines controlled by *35S* promoter showed reduction in growth compared to wild type, while lines with *WP* did not show any negative effects on growth (***Paper* III**; Fig. 2, ABC). Poor field growth performance in *35S* lines could be caused by increased susceptibility to herbivores since AXE activity decreases leaf pH by formation of acetic acid. To test that, we investigated leaf chewing damage, salicinoid phenolic glucosides (SPGs), and condensed tannins (CTs) (***Paper* III**; Fig. 5BC¸ Tab. 2), since altered foliar concentrations of these classes of compounds could indicate activation of defense responses to herbivory and other biotic and abiotic stresses (Bandau et al., 2015; Lindroth and Madritch, 2015) Indeed, *35S*-AXE lines displayed altered profiles of CT,

SPGs, and a higher incidence of foliar arthropod chewing (***Paper* III**; Fig. 5B). Construct *35S:AnAXE1* showed an increase by 187% in chewing symptoms compared to WT and construct *35S:HjAXE* - by 44%, while *35S:RWA-CD* trees were not affected (***Paper* III**; Fig. 5B). Thus, it is AXE activity rather than xylan acetylation status in the leaves that mediates an increase in chewing. Interestingly, the CT levels were altered in opposite directions in *35S:AnAXE1* and *35S:HjAXE* constructs. Construct *35S:AnAXE1* showed higher levels of foliar CT concentrations, compared to WT, while *35S:HjAXE* construct showed lower CT levels (***Paper* III**; Fig. 5C) highlighting the fact that the correlation between CT levels and herbivory is not simple and can be influenced by other factors. *35S:HjAXE* construct displayed also increased foliar necrosis (***Paper* III**; Fig. 5A), suggesting that *Hj*AXE could either be recognized by the plant as PAMP inducer, similar to *Pc*GCE (***Paper* I**), or that it could lead to stress signaling via DAMP or other pathway. Moreover, leaf weight and chlorophyll content were lower for *35S:HjAXE* plants (***Paper* III**; Fig. 3, AB). Thus, the performance of *WP:AXE1* and *35S:RWA-CD* plants was the best considering growth and resistance to natural stresses encountered during the five-year field trial. Our results demonstrate the advantages of deploying *WP* (*GT43B)* promoter for genetic modification of woody tissues.

3.3.2 Field performance of hybrid aspen constructs targeting genes involved in wood formation (***Paper* IV, *Paper* V**)

In ***Paper* IV** and ***Paper* V** we investigated field performance of 32 genetically engineered hybrid aspen lines. The lines represented seven constructs that modified expression of genes, which are active during wood formation (***Paper* V**, Fig. 1A). The lines were selected from a large collection of lines based on better wood quality, growth or saccharification as found in experiments in the greenhouse.

3.3.2.1 Stability of expression of target genes does not guarantee the stability of phenotypes

We analyzed RNA expression of targeted genes in developing wood tissues of all 32 lines and identified those with most altered expression levels as compared to WT (***Paper* V**, Fig. 1; Table S1). In case of two constructs, the expression levels were opposite than expected based on the construct used,

but since we did not have data on their greenhouse expression, we cannot assume that this change was field specific. Lines with previous greenhouse expression data (*C4H* and *SuSy*), exhibited similar reduction in transcripts in the field as observed in the greenhouse (Bjurhager et al., 2010; Gerber et al., 2014). These results indicate stability of targeted gene expression in genetically engineered trees over several years of field cultivation, as we also observed in case of *GUS* gene expression (***Paper* III**, Fig. 4) and confirming results from other studies (Strauss et al., 2016; Pramod et al., 2021). In stark contrast with the maintenance of targeted gene expression, the phenotypes in the field could not be predicted from greenhouse experiment, as illustrated by lack of correlation between field and greenhouse height (***Paper* V,** Fig. S1). Interestingly, the main line reshuffling occurred between the first and the second year in the field (***Paper* V,** Fig. 3B) suggesting that the overwintering may be a critical test for the intragenic line performance.

3.3.2.2 Functional analysis of genes based on strong phenotypes in the field

The phenotypes of lines with altered expression of genes that are highly expressed during wood development (***Paper* V**, Fig. 1A) provided clues about their function in natural conditions. Aspen *SUS1* gene (*SuSy*) encoding sucrose synthase predicted to function in primary metabolism reactions providing UDP-Glc, and thus all other precursors for cell wall polysaccharides as well as other glycosylation reactions (Seifert, 2004; Coleman et al., 2009; Bar-Peled and O'Neill, 2011; Wei et al., 2015; Yu et al., 2015; Temple et al., 2016; Obata, 2019; Stein and Granot, 2019). Previously, it has been shown that reduced *SuSy* expression in hybrid aspen led to reduced cell wall polymer mass per volume (including cellulose, hemicellulose, and lignin) and decreased wood density, but the growth of the plants was not affected (Gerber et al., 2014). This suggested that UDP-Glc needed for biosynthesis of these cell wall components can be largely satisfied by alternative pathways, such as *via* invertases that cleave Suc in sink tissues to yield Glc and Fru (Stein and Granot, 2019). This hypothesis was supported by significant increase of acid invertase activity, and no change in neutral invertase activity in the greenhouse grown *SuSy*-suppressed lines (***Paper* IV,** Fig. 6). Our analysis of the same lines in the field indicated that compensation for the reduced sucrose synthase activity is not effective in these conditions. Field-grown *SuSy* lines showed consistent stem height reduction from the third season (***Paper* IV**, Fig. 5A). After five years in the

field these lines showed several defects in wood anatomy, density and several wood quality traits (***Paper* V**, Figs. 2-5). In other species, defects in growth caused by suppression of sucrose synthase were exacerbated under stress conditions (Ricard et al., 1998; Wang et al., 2014; Takehara et al., 2018). Furthermore, sucrose synthase activity in the outer trunk wood in poplar (*Populus* × *canadensis* Moench ‹*robusta* ›) has strong seasonal oscillation (Schrader and Sauter, 2002), which suggests that it is involved in C allocation during activity-dormancy cycles. Taken together, results obtained from the field trial reported in ***Paper* IV** and **Paper V**, show that SuSy affects C allocation and metabolism in developing wood, and is a central player in plant growth and development in natural conditions.

C4H encodes an enzyme involved in the conversion of *t*-cinnamic acid to *p*-coumaric acid, that could also act on the next step converting *p*-coumaric acid to caffeic acid (Boerjan et al., 2003; Vanholme et al., 2010; Li et al., 2014b). Reduction of *C4H* influences the biosynthesis of lignin and has negative impact on growth and development in *A. thaliana* causing proliferation of adventitious roots and reduction of apical dominance (Schilmiller et al., 2009). These developmental alterations were recently shown to be induced by *c*-cinnamic acid accumulation that is a bioactive compound interfering with polar auxin transport (El Houari et al., 2021). Aspen *C4H* RNAi construct exhibited severe dwarfism in the field that depended on the level of *C4H* suppression, and was accompanied by reduction in cell wall thickness, wood density, and lignin content, and by accumulation of phenolics (***Paper* V**, Fig. 2-6), supporting C4H role in phenylpropanoid pathway.

A. thaliana ZAC encodes a protein regulating GTPase activity in ARABINOSYLATION FACTOR 1 and 3 (ARF1 and ARF3) involved in vesicle transport between ER and Golgi (Jensen et al., 2000). The phenotypes of field-grown aspen Z*AC* overexpressing lines were characterized by severe dwarfism, altered wood anatomy but normal wood chemistry (***Paper* V**, Fig. 2-6), indicating that ZAC homeostasis is needed for stem elongation and secondary growth including cell division, radial cell expansion and secondary wall thickening.

S-adenosylmethionine Synthase (SAM) provides universal methyl group donor, S-adenosylmethionine, to various transmethylation reactions including biosynthesis of lignin and ET (Jin et al., 2017). Effects of *SAM*

downregulation in aspen depended on the level of its suppression. Strong downregulation, down to less than 10% of WT expression, inhibited height and diameter growth, but a milder downregulation, to approx. 25 % of WT level, had growth-promoting effect (***Paper* V**, Fig. 2). Since there were no changes in lignin content in transgenic lines, *SAM* does not appear to limit lignin biosynthesis.

2OGD is a member of a large family of 2-oxoglutarate-dependent dioxygenases (2ODDs) which oxidize a large spectrum of substrates. (Kawai et al., 2014), and its closest neighbors are involved in biosynthesis of gibberellins, flavonoids and ethylene, but orthologous genes have not yet been functionally characterized in any species. Suppression of *2OGD* in aspen tended to stimulate stem height growth and significantly increased stem diameter and biomass in the most suppressed line (***Paper* V**, Fig. 2). Sugar composition of transgenic lines (***Paper* V**, Fig. S3) suggested higher cellulose and lower matrix contents. The data suggest that activity of *2OGD* inhibits stem primary and secondary growth, and cellulose biosynthesis.

MYB-like (MYBL) belongs to a large group of MYB-related transcription factors with one MYB domain (Katiyar et al., 2012). The aspen *MYBL* was broadly expressed with upregulation during secondary wall formation and further upregulation in mature xylem, where only ray cells are viable. This indicates its ubiquitous expression. *MYBL* suppression in the cambium resulted in a mild decrease in carbohydrate and increase in S and total lignin contents (***Paper* V**, Fig. 6). This suggests that MYBL is a positive regulator of cell wall carbohydrate biosynthesis, and/or a negative regulator of cell wall lignin biosynthesis.

3.3.2.3 Evaluation of different constructs with regard to saccharification and growth (***Paper* V**)

Four constructs showed improvement in saccharification properties of lignocellulose (***Paper* V**, Fig. 7). *C4H* downregulated lines had by far most improved Glc yields per wood weight in saccharification without pretreatment (NP) but their dwarf phenotype influenced their Glc yields per stem, which were strongly decreased compared to WT. A moderately suppressed *SAM* line (*SAM-B*) was the only line with improved Glc yield in NP per wood weight as well as per stem.

Glc yield per wood weight in saccharification after acid pretreatment (PT) was most strongly improved in *2OGD* construct, followed by SuSy and SAM constructs. Since *SuSy* lines suffered from poor growth, only *2OGD* and

SAM-B lines had nominally higher yields per stem. Thus, the line *SAM-B* and the construct *2OGD* were two unexpected winners of the trial with most improved Glc yield per stem in PT and the same *SAM-B* line was most improved in Glc yield in NP from all tested lines. This result shows a power of blind screening of genes without knowing their function.

3.3.2.4 Relationships between growth, biomass traits, cell wall properties and saccharification efficiency (***Paper* V**)

Analysis of 49 traits associated with growth, wood anatomy, wood quality and biomass chemical and physical properties in constructs with improved saccharification properties let us to enquire which of these traits are associated with improved saccharification parameters (***Paper* V**, Fig. 8). Using multivariate OPLS modeling of four different types of Glc yields: per wood weight in NP and PT, and per stem in NP and PT, we found that only few variables were significantly contributing to models predicting these yields.

Glc yield per wood weight in NP was expectedly positively related to tension wood, carbohydrate and phenolics contents, and negatively to lignin contents. Strong negative correlation between the Glc yield and growth parameters was also apparent, which could be related to the contribution of *C4H* phenotypes to the model as shown in a OPLS scatter plot (***Paper* V**, Fig. 8 A). The same biomass-related but not growth-related variables, contributed to Glc yield per wood weight in PT but affecting the yield in opposite ways (***Paper* V**, Fig. 8 B).

In case of Glc yields per tree, whether in NP or in PT, same variables turned out to be most important. These variables reflected growth and wood density, whereas lignocellulose traits having positive impact yields per wood weight, which are usually the only type of yields reported in saccharification studies, were in fact negatively influencing yields per stem (**Paper V**, Fig. 8 CD).

These results suggest that in the field conditions, there might be a negative genetic correlation between biomass yield and lignocellulose saccharification yield. Similar conclusion was voiced based on data on acetylation-reduced lines grown in the field (Pramod et al., 2021). The relationship between Glc yield per wood weight in PT and growth should be investigated with larger collections of genotypes than used here to determine how universal it is. Based on the currently available results it can be said that

that improving biomass yields per stem is a good strategy for tree improvement for biorefinery.

Conclusions

This thesis addressed several problems important for developing viable strategies of biotechnological improvement of trees for biorefinery-adapted feedstocks.

***Paper* I** investigated the problem of activation of PAMP signaling when modifying cell walls by expressing *in planta* microbial genes from wood decaying organisms. We showed that ectopically expressing GCE from the wood decaying fungus *P. carnosa* (*Pc*GCE) induced premature leaf senescence and immune defence responses in the leaves. Plants expressing enzymatically inactive *Pc*GCE^{S217A} exhibited the same off-target effects, which proved that *Pc*GCE has PAMP elicitor activity. Omics analyses of transgenic plants identified genes encoding candidate proteins participating in *Pc*GCE perception and signaling. Wood-specific expression of *PcGCE* was shown to be a good strategy to avoid all off-target effects. This agrees with the perception candidates not being expressed in developing wood, and *PcGCE* transcripts not being cell-to-cell mobile.

***Paper* II** addressed the problem of possible activation of cell wall integrity signalling when modifying wood cell walls for biorefinery. Any change in cell wall could lead to activation of cell wall integrity perception mechanism in wood cells, but proteins involved in such activity in wood cells have not been so far identified. As a first step to identify them, we carried out genome-wide analysis of MD/MLD proteins, which resulted in 146 receptor candidates in *Populus*. Among these genes, we identified those that are active during secondary cell wall biosynthesis, and we also identified their putative partners by co-expression analysis.

***Papers* III, IV** and **V** addressed problem of transferring results from the greenhouse to the field.

In ***Paper* III**, the performance of transgenic and intragenic lines with reduced xylan acetylation was tested in field conditions for five seasons. This identified a possible problem concerning 17% of transgenic lines which showed random dwarfism after the first cultivation year in the field, suggesting a link between acetyl metabolism and transposon activity. Other lines with either biosynthetic reduction of acetylation in the Golgi or post-synthetic deacetylation in cell walls grew well. For transgenic lines, a better growth was detected when using wood specific promoter compared to 35S promoter, since the latter lead to higher foliar insect herbivory and changes in condensed tannins and phenylpropanoid glucosides. Differences in performance of two tested fungal xylan acetyl esterases were also revealed. None of these phenotypes were seen in the greenhouse conditions.

In ***Paper* IV** and ***Paper* V** we investigated field performance of hybrid aspen intragenic lines selected for growth and biomass traits in large-scale greenhouse screening. We demonstrated severe dwarfism and anomalies in wood development in lines with suppressed *SUS1* gene encoding sucrose synthase, implying an essential role for this enzyme in the field conditions, possibly related to C metabolism during activity-dormancy cycles. Analysis of other constructs provided insights into role of several genes of unknown function, including *2OGD*, *MYBL* and *SAM*, in wood formation. Suppression of *2OGD* and moderate suppression of *SAM* proved most beneficial for improving saccharification yields on a per stem basis. Influence of growth, wood anatomy, biomass chemical and physical traits on Glc yields per wood weight is different between saccharification without and with pretreatment. For Glc yields per stem basis either with or without pretreatment, wood productivity traits play most important role. The results increased our understanding of main determinants of saccharification yields from trees grown in the field conditions, which will help to design future biotechnological approaches to optimize trees for biorefinery.

Popular science summary

The demand for renewable energy motivates efforts for development of new methods for biofuel production. Biofuels could be sustainably produced from plant biomass. For that, the biomass should be decomposed to simple sugars, which can be further fermented to ethanol. However, the process of conversion is costly and requires hash pretreatments using chemicals and energy. This can be reduced if the plants could be improved for the use in bioconversion. With modern genetic engineering techniques it is possible to design plants having biomass characterized by more easily extractable cell wall components that are better suited for bioconversion. Hybrid aspen is a fast-growing tree amenable to genetic engineering techniques that could be used to try different strategies of biomass improvement. This thesis addressed several problems important for developing trees for biorefinery. One problem is to devise strategy that induces changes in the biomass that are required but does not interfere with plant growth and development. It is not simple because plants can detect induced modification and react to a change in a similar way as they react to stresses. In this thesis, I tested several approaches to developed a strategy of deployment of a microbial enzyme that reduces biomass cross linking without off-target effects.

Developing improved variants in the laboratory must be followed by their testing in a setting which represents their usual cultivation conditions. In many cases, genetically modified plants grow well in the greenhouse but show undesirable off-target effects in the field conditions. To evaluate the performance of promising genetically improved plants, it is important to test them in the field where they must cope with multitude of biotic and abiotic stresses, which could induce undesirable reactions. In this thesis we analyzed growth and biotic stress tolerance data from two field trials and we evaluated the field grown woody biomass for its improved bioprocessing characteristics. We identified best engineering strategies based on field results and best transgenic modifications that could be used in trees improved for bioprocessing in biorefinery.

The findings contribute to a broader understanding of the mechanisms responsible for plant development, stress responses and wood biosynthesis.

Populär vetenskaplig sammanfattning

Efterfrågan på förnybar energi motiverar ansträngningar för utveckling av nya metoder för produktion av biobränslen. Biobränslen kan produceras hållbart från växtbiomassa. För detta bör biomassan sönderdelas till enkla sockerarter, för att producera etanol. Omvandlingsprocessen är dock kostsam och kräver förbehandlingar med kemikalier och energi. Detta kan minskas om plantorna skulle kunna förbättras för användning vid bioomvandling. Med moderna gentekniker är det möjligt att konstruera växter med biomassa som kännetecknas av cellväggskomponenter som är lättare att extrahera. Hybridasp är ett snabbt växande träd som är mottagligt för gentekniska tekniker som kan användas för att testa olika strategier för förbättring av biomassa. Denna avhandling behandlade flera problem som är viktiga för att utveckla träd för bioraffinaderi. Ett problem är att utforma en strategi som inducerar förändringar i biomassan, utan at störa växtens tillväxt och utveckling. Det är inte enkelt eftersom växter kan upptäcka inducerad modifiering och reagera på en förändring på ett liknande sätt som de reagerar på naturliga påfrestningar. I denna avhandling testade jag flera metoder för att utveckla en strategi för introduktion av ett mikrobiellt enzym som minskar tvärbindning av biomassa utan inducerade negativa effekter.

Utveckling av förbättrade varianter i laboratoriet måste följas i en miljö som representerar deras vanliga odlingsförhållanden. I många fall växer genetiskt modifierade växter bra i växthuset men visar oönskade effekter i naturliga fältförhållanden. För att utvärdera prestanda för lovande genetiskt förbättrade växter är det viktigt att testa dem i en miljö där de måste hantera många biotiska och abiotiska påfrestningar, vilket kan orsaka oönskade reaktioner. I denna avhandling analyserade vi tillväxt och biotisk stresstolerans data från två fältförsök och utvärderade fältodlad träbiomassa för dess förbättrade bioprocessegenskaper. Vi identifierade de bästa tekniska strategierna baserade på fältresultat och bästa transgena modifieringar som kan användas i träd dedikerade för bioraffinaderi.

Resultaten bidrar till en bredare förståelse av de mekanismer som är ansvariga för växtutveckling, växtstress och träbiosyntes.

Acknowledgements

First, I would like to express my sincere thanks to my PhD supervisor **Professor Ewa Mellerowicz** for the given opportunity to pursue a PhD. During the last four years, in her company I found a space where scientific ideas could be born, questioned and developed. She was always behind me during the project and encouraged me even in difficult moments.

I would like to express my thanks to all previous and current group members in the group of Professor Ewa Mellerowicz, which I met during my PhD studies. Thank you to; **Marta Derba-Maceluch, Vikash Kummar, Sunnita, Kummar, János Urbancsok, Pramod Sivan, Zulema Lorenzo, Felix Barbut**.

In particularly, I would like to thank to **Marta Derba-Maceluch**, which introduced me to the scientific projects and supported me every time I encountered obstacles in my work. Marta introduced me to common lab practices and contributed strongly to the development of my analytical skills.

I would like to thank to **Felix Barbut**, which helped me frequently during lab and greenhouse work. He was a person with whom I could discuss novel ideas, during the project.

One important part of my PhD project has been analysis of big data sets. The bioinformatic core at UPSC has always been supportive during my bioinformatic projects. I am particularly thankful to **Nicolas Delhomme** and **Nathaniel Street**; teachers and inspirational source of mine. Thanks to them, I met my PhD supervisor Ewa Mellerowicz.

I would like to thank Swedish Metabolomics Centre for meeting the questionaries of my projects and suggesting suitable methods for metabolomic analysis. Thank you, **Annika Johansson**, **Hans Stenlund** and the rest of the metabolomics team.

I would like to express my gratitude to all other labs and facilities with which I have been cooperated with. Thank you; **Maria Eriksson**, **Leszek Kleczkowski**, **Zakiya Yassin, Gerhard Scheepers, Björn Sundberg, Leif J. Jönsson, Madhavi Latha Gandla**, **Cheng Lee**.

Finally, I would like to express my sincere gratitude to all colleagues which I have had the chance to meet, during my work at Umeå Plant Science Centre (UPSC). This department is filled with tolerance, flexibility, open-mindedness and professionalism. Every one of you have inspired and influenced me in a positive way. I have been proud to be part of this department.

References

Albenne, C., Canut, H., Hoffmann, L. and Jamet, E. (2014). Plant cell wall proteins: a large body of data, but what about runaways?. *Proteomes*, **2**, 224–242.

Albert, I., Böhm, H., Albert, M., Feiler, C.E., Imkampe, J. and Nürnberger, T. (2015). An RLP23-SOBIR1-BAK1 complex mediates NLP-triggered immunity. *Nat. Plants*, **1**, 15140.

Alberts, B., Johnson, A., Lewis, J., Morgan, D., Raff, M., Roberts, K. and Walter, P. (2015). *Molecular biology of the cell*. 6th ed. New York: Garland Science. 1081–1089.

Asai, T., Tena, G., Plotnikova, J., Willmann, M.R., Chiu, W.L., Gomez-Gomez, L., et al. (2002). MAP kinase signalling cascade in Arabidopsis innate immunity. *Nature*, **415**, 977–983.

Atkinson, R.G., Schröder, R., Hallett, I.C., Cohen, D. and MacRae, E.A. (2002). Overexpression of polygalacturonase in transgenic apple trees leads to a range of novel phenotypes involving changes in cell adhesion. *Plant Physiol*. **129**, 122–133.

Avni, A., Bailey, B.A., Mattoo, A.K. and Anderson, J.D. (1994). Induction of ethylene biosynthesis in *Nicotiana tabacum* by a *Trichoderma viride* xylanase is correlated to the accumulation of 1-aminocyclopropane-1-carboxylic acid (ACC) synthase and ACC oxidase transcripts. *Plant Physiol.* **106**, 1049–1055.

Bååth, J., Giummarella, N., Klaubauf, S., Lawoko, M. and Olsson, L. (2016). A glucuronoyl esterase from *Acremonium alcalophilum* cleaves native lignin-carbohydrate ester bonds. *FEBS Lett.* **590**, 2611–2618.

Bailey, B.A., Dean, J.F.D. and Anderson, J.D. (1990) An ethylene biosynthesis-inducing endoxylanase elicits electrolyte leakage and necrosis in *Nicotiana tabacum cv* xanthi leaves. *Plant Physiol*. **94**, 1849–1854.

Balint-Kurti, P. (2019). The plant hypersensitive response: concepts, control and consequences. *Mol. Plant Pathol*. **20**, 1163–1178.

Bandau, F., Decker, V.H., Gundale, M.J., and Albrectsen, B.R. (2015). Genotypic tannin levels in *Populus tremula* impact the way nitrogen enrichment affects growth and allocation responses for some traits and not for others. *PLoS One*. **10**, e0140971.

Bar-On, Y. M., Phillips, R. and Milo, R. (2018). The biomass distribution on Earth. *Proc. Natl. Acad. Sci. USA*. **15**, 6506–6511.

Bar-Peled, M. and O'Neill, M.A. (2011). Plant nucleotide sugar formation, interconversion, and salvage by sugar recycling. *Ann. Rev. Plant Biol.* **62**, 127–155.

Bedinger, P.A., Pearce, G. and Covey, P.A. (2010). RALFs: peptide regulators of plant growth. *Plant Signal. Behav.* **5**, 1342–1346.

Bellincampi, D., Dipierro, N., Salvi, G., Cervone, F. and De Lorenzo, G. (2000). Extracellular H(2)O(2) induced by oligogalacturonides is not involved in the inhibition of the auxin-regulated rolB gene expression in tobacco leaf explants. *Plant Physiol*. **122**, 1379–1385.

Berens, M.L., Wolinska, K. W., Spaepen, S., Ziegler, J., Nobori, T., Nair, A., Krüler, V., et al. (2019). Balancing trade-offs between biotic and abiotic stress responses through leaf age-dependent variation in stress hormone cross-talk. *Proc. Natl. Acad. Sci. USA.* **116**, 2364–2373.

Bidhendi, A.J. and Geitmann, A. (2016). Relating the mechanics of the primary plant cell wall to morphogenesis. *J. Exp. Bot*. **67**, 449–461.

Biely, P., Malovíková, A., Uhliariková, I., Li, X.L. and Wong, D.W. (2015). Glucuronoyl esterases are active on the polymeric substrate methyl esterified glucuronoxylan. *Febs Lett.* **589**, 2334–2339.

Birol I., Raymond A., Jackman S.D., Pleasance S., Coope R., Taylor G.A., et al. (2013). Assembling the 20 Gb white spruce (*Picea glauca*) genome from whole-genome shotgun sequencing data. *Bioinformatics*, **29**, 1492–1497.

Biswal, A.K., Atmodjo, M. A., Li, M., Baxter, H. L., Yoo, C.G., Pu, Y., et al. (2018). Sugar release and growth of biofuel crops are improved by downregulation of pectin biosynthesis. *Nat. Biotechnol*. **36**, 249–257.

Biswal, A.K., Hao, Z., Pattathil, S., Yang, X., Winkeler, K., Collins, C., et al. (2015). Downregulation of GAUT12 in *Populus deltoides* by RNA silencing results in reduced recalcitrance, increased growth and reduced xylan and pectin in a woody biofuel feedstock. *Biotechnol. Biofuels*, **8**, 41.

Biswal, A.K., Soeno, K., Gandla, M.L., Immerzeel, P., Pattathil, S., Lucenius, J., et al. (2014). Aspen pectate lyase PtxtPL1-27 mobilizes matrix polysaccharides from woody tissues and improves saccharification yield. *Biotechnol Biofuels*. **7**, 11.

Bjørnstad, A. and Aastveit, K. (1990). Pleiotropic effects on the ml-o mildew resistance gene in barley in different genetical backgrounds. *Euphytica,* **46**, 217–26.

Bjurhager, I., Olsson, A.M., Zhang, B., Gerber, L., Kumar, M., Berglund, L.A., et al. (2010). Ultrastructure and mechanical properties of *Populus* wood with reduced lignin content caused by transgenic down-regulation of cinnamate 4-hydroxylase. *Biomacromolecules*, **11**, 2359–2365.

Boerjan, W., Ralph, J. and Baucher, M. (2003). Lignin biosynthesis. *Annu. Rev. Plant Biol.* **54**, 519–546.

Böhm, H., Albert, I., Fan, L., Reinhard, A. and Nürnberger, T. (2014). Immune receptor complexes at the plant cell surface. *Curr. Opin. Plant. Biol*. **20**, 47–54.

Boller, T. and Felix, G. (2009). A renaissance of elicitors: perception of microbe-associated molecular patterns and danger signals by pattern-recognition receptors. *Annu. Rev. Plant Biol*. **60**, 379–406.

Bolouri Moghaddam, M.R. and Van den Eden, W. (2012). Sugars and plant innate immunity. *J. Exp. Bot.* **63**, 3989–3998.

Börcsök, Z. and Pásztory, Z. (2021). The role of lignin in wood working processes using elevated temperatures: an abbreviated literature survey. *Eur. J. Wood Prod.* **79,** 511–526.

Borkhardt, B., Harholt, J., Ulvskov, P., Ahring, B. K., Jørgensen, B. and Brinch-Pedersen, H. (2010). Autohydrolysis of plant xylans by apoplastic expression of thermophilic bacterial endo-xylanases. *Plant Biotechnol. J.* **8**, 363–374.

Boudsocq, M., Willmann, M.R., McCormack, M., Lee, H., Shan, L., He, P., et al. (2010). Differential innate immune signalling via $Ca^{(2+)}$ sensor protein kinases. *Nature*, **464**, 418–422.

Boyko, A., Molinier, J., Chatter, W., Laroche, A. and Kovalchuk, I. (2010). Acute but not chronic exposure to abiotic stress results in transient reduction of expression levels of the transgene driven by the 35S promoter. *New Biotechnol*. **27**, 70–77.

Brandon, A.G., and Scheller, H.V. (2020). Engineering of bioenergy crops: dominant genetic approaches to improve polysaccharide properties and composition in biomass. *Front. Plant Sci.* **11**, 282.

Bromley, J.R., Busse-Wicher, M., Tryfona, T., Mortimer, J.C., Zhang, Z., Brown, D.M., et al. (2013). GUX1 and GUX2 glucuronyltransferases decorate distinct domains of glucuronoxylan with different substitution patterns. *Plant J.* **74**, 423–434.

Brown J. K. (2002). Yield penalties of disease resistance in crops. *Curr. Opin. Plant Biol.* **5**, 339–344.

Brown, R.M. (2004). Cellulose structure and biosynthesis: What is in store for the 21st century? *J. Polym. Sci., Part A: Polym. Chem*. **42**, 487-495.

Bura, R., Chandra, R. and Saddler, J. (2009). Influence of xylan on the enzymatic hydrolysis of steam-pretreated corn stover and hybrid poplar. *Biotechnol. Prog.* **25**, 315-322.

Burdon, J.J. and Zhan, J. (2020). Climate change and disease in plant communities. *PLoS Biol.* **18**, e3000949.

Büschges, R., Hollricher, K., Panstruga, R., Simons, G., Wolter, M., Frijters, A., et al. (1997). The barley Mlo gene: a novel control element of plant pathogen resistance. *Cell*, **88**, 695–705.

Busse-Wicher, M., Gomes, T.C., Tryfona, T., Nikolovski, N., Stott, K., Grantham, N.J., et al. (2014). The pattern of xylan acetylation suggests xylan may interact with cellulose microfibrils as a twofold helical screw in the secondary plant cell wall of *Arabidopsis thaliana*. *The Plant J.* **79**, 492–506.

Busse-Wicher, M., Li, A., Silveira, R.L., Pereira, C.S., Tryfona, T., Gomes, T.C., et al. (2016). Evolution of xylan substitution patterns in gymnosperms and angiosperms: implications for xylan interaction with cellulose. *Plant Physiol*. **171**, 2418–2431.

Cai, L. and Tu, B.P. (2012). Driving the cell cycle through metabolism. *Annu. Rev. Cell Dev. Biol.* **28**, 59–87.

Campbell, L. and Turner, S.R. (2017). A comprehensive analysis of RALF proteins in green plants suggests there are two distinct functional groups. *Front. Plant Sci*. **8** ,37.

Caño-Delgado, A., Penfield, S., Smith, C., Catley, M.and Bevan, M. (2003). Reduced cellulose synthesis invokes lignification and defense responses in *Arabidopsis thaliana*. *Plant J.* **34**, 351–362.

Celus, M., Kyomugasho, C., Van Loey, A.M., Grauwet, T. and Hendrickx, M.E. (2018). Influence of pectin structural properties on interactions with divalent cations and its associated functionalities. *Compr. Rev. Food Sci. Food Saf.* **17**, 1576–1594.

Chanda, B., Venugopal, S.C., Kulshrestha, K., Navarre, D., Downie, B., Kachroo, A., et al. (2008). Glycerol-3-phosphate levels are associated with basal resistance to the hemibiotrophic fungus *Colletotrichim higgin-sianum* in Arabidopsis. *Plant Physiol*. **140,** 2017–2029.

Chatterjee, A., Das, N.C., Raha, S., Babbit, R. , Huang, Q.W. , Zaitlin, D. and Maiti, I.B. (2010) Production of xylanase in transgenic tobacco for industrial use in bioenergy and biofuel applications. *In Vitro Cell. Dev. Biol. Plant*, **46**, 198–209.

Chen, F. and Dixon, R.A. (2007). Lignin modification improves fermentable sugar yields for biofuel production. *Nat. Biotechnol.*, **25**, 759–761.

Chen, X. and Kim, J. (2009). Callose synthesis in higher plants. *Plant Signal. Behav*. **4**, 489–492.

Chini A., Fonseca S., Fernández G., Adie B., Chico J.M., Lorenzo O., et al. (2007). The JAZ family of repressors is the missing link in jasmonate signalling. *Nature*, **448**, 666–671.

Chisholm, S.T., Coaker, G., Day, B. and Staskawicz, B.J. (2006). Host-microbe interactions: shaping the evolution of the plantimmune response. *Cell*, **124**, 803-814.

Choi, D., Ward, B.L and Bostock, R.M. (1992). Differential induction and suppression of potato 3-hydroxy-3-methylglutaryl coenzyme. A reductase genes in response to *Phytophthora infestans* and to its elicitor arachidonic acid. *Plant Cell*, **4**, 1333–1344.

Choi, J., Choi, D., Lee, S., Ryu, C.M. and Hwang, I. (2011). Cytokinins and plant immunity: old foes or new friends? *Trends Plant Sci*. **16**, 388-394.

Chong, S.L., Virkki, L., Maaheimo, H., Juvonen, M., Derba-Maceluch, M., Koutaniemi, S., et al. (2014). O-acetylation of glucuronoxylan in Arabidopsis thaliana wild type and its change in xylan biosynthesis mutants. *Glycobiology*, **24**, 494–506.

Christiernin, M., Ohlsson, A.B., Berglund, T. and Henriksson, G. (2005). Lignin isolated from primary walls of hybrid aspen cell cultures indicates significant differences in lignin structure between primary and secondary cell wall. *Plant Physiol. Biochem.* **43**, 777–785.

Chung, H.S., Koo, A. J., Gao, X., Jayanty, S., Thines, B., Jones, A.D. and Howe, G.A. (2008). Regulation and function of Arabidopsis JASMONATE ZIM-domain genes in response to wounding and herbivory. *Plant Physiol*. **146**, 952–964.

Claverie, J., Balacey, S., Lemaître-Guillier, C., Brulé, D., Chiltz, A., Granet, L., et al. (2018). The cell wall-derived xyloglucan is a new DAMP triggering plant immunity in *Vitis vinifera* and Arabidopsis thaliana. *Front. Plant Sci.* **9**, 1725.

Coleman, H.D., Yan, J. and Mansfield, S.D. (2009). Sucrose synthase affects carbon partitioning to increase cellulose production and altered cell wall ultrastructure. *Proc. Natl. Acad. Sci. USA*. **106**, 13118–13123.

Cook, C.M., Daudi, A., Millar, D.J., Bindschedler, L.V., Khan, S., Bolwell, G.P., et al. (2012). Transcriptional changes related to secondary wall formation in xylem of transgenic lines of tobacco altered for lignin or xylan content which show improved saccharification. *Phytochemistry*, *74*, 79–89.

Cosgrove, D.J. (2005). Growth of the plant cell wall. *Nat. Rev. Mol. Cell Biol*. **6**, 850-861.

Coutinho, P.M., Deleury, E. and Henrissat, B. (2003). The families of carbohydrate-active enzymes in the genomic era. *J. Appl. Glycosci.* **50**, 241– 244.

Couto, D. and Zipfel, C. (2016). Regulation of pattern recognition receptor signalling in plants. *Nat. Rev. Immunol*. **16**, 537–552.

Cui, H., Tsuda, K. and Parker, J.E. (2015). Effector-triggered immunity: from pathogen perception to robust defense. *Annu. Rev. Plant Biol.* **66**, 487–511.

D'Ovidio, R., Mattei, B., Roberti, S. and Bellincampi, D. (2004). Polygalacturonases, polygalacturonase-inhibiting proteins and pectic oligomers in plant-pathogen interactions. *Biochim. Biophys. Acta.* **1696**, 237–244.

Damm, T., Commandeur, U., Fischer, R. and Usadel, B. (2016). Improving the utilization of lignocellulosic biomass by polysaccharide modification. *Process Biochem*. **51**, 288–296.

Darvill, A.G., McNeil, M., Darvil, A.G. and Albersheim, P. (1980). Structure of plant cell walls. *Plant Physiol.* **66**, 1135–1139.

De La Torre, A.R., Birol, I., Bousquet, J., Ingvarsson, P.K., Jansson, S., Jones, S.J.M., et al. (2014). Insights into conifer giga-genomes. *Plant Physiol*. **166**, 1724–32.

De Martini, J.D., Pattathil, S., Miller, J.S., Li, H., Hahncde, M.G. and Wyman, C.E. (2013). Investigating plant cell wall components that affect biomass recalcitrance in poplar and switchgrass. *Energy Environ. Sci*. **6**, 898.

de Buanafina, M.M, Langdon, T., Hauck, B., Dalton, S. and Morris, P. (2008). Expression of a fungal ferulic acid esterase increases cell wall digestibility of tall fescue (*Festuca arundinacea*). *Plant Biotechnol.J*. **6,** 264–280.

de Buanafina, M.M. and Fescemyer, H.W. (2012). Modification of esterified cell wall phenolics increases vulnerability of tall fescue to herbivory by the fall armyworm. P*lanta*, **236**, 513–523.

de Buanafina, M.M., Langdon, T., Hauck, B., Dalton, S., Timms-Taravella, E. and Morris, P. (2010). Targeting expression of a fungal ferulic acid esterase to the apoplast, endoplasmic reticulum or golgi can disrupt feruloylation of the growing cell wall and increase the biodegradability of tall fescue (*Festuca arundinacea*). *Plant Biotechnol. J.* **8**, 316–331.

De Souza, A., Hull, P.A., Gille, S. and Pauly, M. (2014). Identification and functional characterization of the distinct plant pectin esterases PAE8 and PAE9 and their deletion mutants. *Planta*, **240**, 1123–1138.

Decreux, A. and Messiaen, J. (2005). Wall-associated kinase WAK1 interacts with cell wall pectins in a calcium-induced conformation. *Plant Cell Physiol.* **46**, 268–278.

Delmer D. P. (1999). CELLULOSE BIOSYNTHESIS: Exciting times for a difficult field of study. *Annu. Rev. Plant Physiol. Plant Mol. Biol.* **50**, 245–276.

Derba-Maceluch, M., Amini, F., Donev, E.N., Pawar, P.M., Michaud, L., Johansson, U., et al. (2020). Cell wall acetylation in hybrid aspen affects field performance, foliar phenolic composition and resistance to biological stress factors in a construct-dependent fashion. *Front. Plant Sci.* **11**, 651.

Derba-Maceluch, M., Awano, T., Takahashi, J., Lucenius, J., Ratke, C., Kontro, I., et al. (2015). Suppression of xylan endotransglycosylase PtxtXyn10A

affects cellulose microfibril angle in secondary wall in aspen wood. *New Phytol*. **205**, 666-681.

Devi, E.L., Chongtham S.K., Holeyachi, P., Kousar, N., Singh, M., Chandana Behera, C., et al. (2013) Cisgenesis and intragenesis: twin sisters for crop improvement. *Res. J. Agric. For Sci.* **1**, 22–26.

DiFazio, S.P., Leonardi, S., Slavov, G.T., Garman, S. L., Adams, W.T. and Strauss, S.H. (2012). Gene flow and simulation of transgene dispersal from hybrid poplar plantations. *New Phytol.* **193**, 903–915.

Doblas, V.G., Gonneau, M. and Höfte, H. (2018). Cell wall integrity signaling in plants: Malectin-domain kinases and lessons from other kingdoms. *Cell Surf. (Amsterdam, Netherlands)*, **3**, 1–11.

Dodds, P. N. and Rathjen, J. P. (2010). Plant immunity: towards an integrated view of plant-pathogen interactions. *Nat. Rev. Genet.* **11**, 539–548.

Dominguez, P.G., Donev, E., Derba-Maceluch, M., Bünder, A., Hedenström, M., Tomášková, I., et al. (2020). Sucrose synthase determines carbon allocation in developing wood and alters carbon flow at the whole tree level in aspen. *The New phytologist*, **229**, 186–198.

Donev, E., Gandla, M.L., Jönsson, L.J. and Mellerowicz, E.J. (2018). Engineering non-cellulosic polysaccharides of wood for the biorefinery. *Front. Plant Sci.* **9**, 1537.

Duran-Flores, D. and Heil, M. (2016). Sources of specificity in plant damaged-self recognition. *Curr. Opin. Plant Biol.* **32**, 77–87.

Ebringerová, A. and Heinze, T. (2000). Xylan and xylan derivatives - Biopolymers with valuable properties. Naturally occurring xylans structures, isolation procedures and properties. *Macromol. Rapid Commun.* **21**, 542–556.

El Houari, I., Van Beirs, C., Arents, H.E., Han, H., Chanoca, A., Opdenacker, D., et al. (2021). Seedling developmental defects upon blocking CINNAMATE-4-HYDROXYLASE are caused by perturbations in auxin transport. *New Phytol*. **230**, 2275–2291.

Engelsdorf, T. and Hamann, T. (2014). An update on receptor-like kinase involvement in the maintenance of plant cell wall integrity. *Ann. Bot*. **114**, 1339–1347.

Enkerli, J., Felix, G. and Boller, T. (1999). The enzymatic activity of fungal xylanase is not necessary for its elicitor activity. *Plant Physiol.* **121**, 391–397.

Essmann., J., Schmitz-Thom, I., Schon, H., Sonnewald, S., Weis, E. and Scharte, J. (2008). RNA interference-mediated repression of cell wall invertase impairs defense in source leaves of tobacco. *Plant Physiol*. **147**, 1288–1299.

Etchegaray, J.P. and Mostoslavsky, R. (2016). Interplay between metabolism and epigenetics: a nuclear adaptation to environmental changes. *Mol. Cell*, **62**, 695–711.

Falter, C., Zwikowics, C., Eggert, D., Blümke, A., Naumann, M., Wolff, K., et al. (2015). Glucanocellulosic ethanol: the undiscovered biofuel potential in energy crops and marine biomass. *Sci. Rep.* **5**, 13722.

Farmer, P.K. and Choi, J.H. (1999). Calcium and phospholipid activation of a recombinant calcium-dependent protein kinase (DcCPK1) from carrot (*Daucus carota* L.). *Biochim Biophys. Acta*, **1434**, 6–17.

Felix, G., Baureithel, K. and Boller, T. (1998). Desensitization of the perception system for chitin fragments in tomato cells. *Plant Physiol*. **117**, 643–650.

Felix, G., Duran, J.D., Volko, S. and Boller, T. (1999). Plants have a sensitive perception system for the most conserved domain of bacterial flagellin. *Plant J*. **18**, 265–276.

Fengel, D. and Wegener, G. (1984). Wood: Chemistry, Ultrastructure, Reactions. Berlin–New York: Walter de Gruyter. pp. 124-125.

Fenning, T.M. and Gershenzon, J. (2002). Where will the wood come from? Plantation forests and the role of biotechnology. *Trends Biotechnol.* **20**, 291–296.

Fernandes, A.N., Thomas, L.H., Altaner, C.M., Callow, P., Forsyth, V.T., Apperley, D.C., et al. (2011). Nanostructure of cellulose microfibrils in spruce wood. *Proc. Natl. Acad. Sci. USA.* **108**, E1195-E1203.

Fernie, A.R., Carrari, F. and Sweetlove, L.J. (2004). Respiratory metabolism: glycolysis, the TCA cycle and mitochondrial electron transport. *Curr Opin Plant Biol.* **7**, 254–261.

Ferrari, S., Galletti, R., Pontiggia, D., Manfredini, C., Lionetti, V., Bellincampi, D., et al. (2008). Transgenic expression of a fungal endo-polygalacturonase increases plant resistance to pathogens and reduces auxin sensitivity. *Plant Physiol.*, **146**, 669–681.

Field, C.B., Behrenfeld, M.J., Randerson, J.T. and Falkowski, P. (1998). Primary production of the biosphere: integrating terrestrial and oceanic components. *Science*, **281**, 237–240.

Fotopoulos, V., Gilbert, M.J., Pittman, J.K., Marvier, A.C., Buchanan, A.J., Sauer, N., et al. (2003). The monosaccharide transporter gene, AtSTP4, and the cell-wall invertase, Atbetafruct1, are induced in Arabidopsis during infection with the fungal biotroph *Erysiphe cichoracearum*. *Plant Physiol*. **132**, 821–829.

Franck, C.M., Westermann, J. and Boisson-Dernier, A. (2018). Plant malectin-like receptor kinases: from cell wall integrity to immunity and beyond. *Ann.Rev. Plant Biol*. **69**, 301–328.

Franke, R., Hemm, M.R., Denault, J.W., Ruegger, M.O., Humphreys, J.M. and Chapple, C. (2002a). Changes in secondary metabolism and deposition of an unusual lignin in the ref8 mutant of Arabidopsis. *Plant J.* **30**, 47–59.

Franke, R., Humphreys, J.M., Hemm, M.R., Denault, J.W., Ruegger, M.O., Cusumano, J.C., et al. (2002b). The Arabidopsis REF8 gene encodes the 3-hydroxylase of phenylpropanoid metabolism. *Plant J.* **30**, 33–45.

Fry, S. (2011). Cell wall polysaccharide composition and covalent crosslinking. In: Ulvskov, P. (Ed.) Plant Polysaccharides: Biosynthesis and Bioengineering. Wiley-Blackwell. *Annu. Plant Rev*. **41**, 1-42.

Galletti, R., Denoux, C., Gambetta, S., Dewdney, J., Ausubel, F.M., De Lorenzo, G., et al. (2008). The AtrbohD-mediated oxidative burst elicited by oligogalacturonides in Arabidopsis is dispensable for the activation of defense responses effective against *Botrytis cinerea*. *Plant Physiol*. **148**, 1695–1706.

Galletti, R., Ferrari, S. and De Lorenzo, G. (2011). Arabidopsis MPK3 and MPK6 play different roles in basal and oligogalacturonide- or flagellin-induced resistance against *Botrytis cinerea*. *Plant Physiol.* **157**, 804–814.

Gandla, M., Derba-Maceluch, M., Liu, X., Gerber, L., Master, E.R., Mellerowicz, E.J. and Jönsson, L.J. (2015). Expression of a fungal glucuronoyl esterase in *Populus*: effects on wood properties and saccharification efficiency. *Phytochemistry*, **112**, 210–220.

Gao, M., Liu, J., Bi, D., Zhang, Z., Cheng, F., Chen, S., et al (2008). MEKK1, MKK1/MKK2 and MPK4 function together in a mitogen-activated protein kinase cascade to regulate innate immunity in plants. *Cell Res*. **18**, 1190-1198.

Gao, Q.M., Venugopal, S., Navarre, D. and Kachroo, A. (2011). Low oleic acid-derived repression of jasmonic acid-inducible defense responses requires the WRKY50 and WRKY51 proteins. *Plant Physiol.* **155**, 464–476.

Gerber, L., Zhang, B., Roach, M., Rende, U., Gorzsás, A., Kumar, M., et al. (2014). Deficient sucrose synthase activity in developing wood does not specifically affect cellulose biosynthesis, but causes an overall decrease in cell wall polymers. N*ew Phytol.* **203**, 1220–1230.

Ghaffar, S.H. and Fan, M. (2015). Revealing the morphology and chemical distribution of nodes in wheat straw. *Biomass and Bioenergy*, **77**, 123–134.

Gillaspy, G.E. (2011). The cellular language of myo-inositol signaling. *The New Phytol.* **192**, 823–839.

Gille, S. and Pauly, M. (2012). O-acetylation of plant cell wall polysaccharides. *Front. Plant Sci.* **3**, 12.

Gish, L.A. and Clark, S.E. (2011). The RLK/Pelle family of kinases. *Plant J.* **66**, 117–127.

Giummarella, N., Balakshin, M., Koutaniemi, S., Kärkönen, A. and Lawoko, M. (2019). Nativity of lignin carbohydrate bonds substantiated by biomimetic synthesis. *J Exp. Bot.* **70**, 5591–5601.

Glazebrook, J. (2005). Contrasting mechanisms of defense against biotrophic and necrotrophic pathogens. *Annu. Rev. Phytopathol*. 43, 205–27.

Gómez-Ariza, J., Campo, S., Rufat, M., Estopà, M., Messeguer, J., San Segundo, B., et al. (2007). Sucrose-mediated priming of plant defense responses and broad-spectrum disease resistance by overexpression of the maize pathogenesis-related PRms protein in rice plants. *Mol. Plant Microbe. Interact*. **20**, 832–842.

Gorshkova, T., Mokshina, N., Chernova, T., Ibragimova, N., Salnikov, V., Mikshina, P., et al. (2015). Aspen tension wood fibers contain β-(1-> 4)-galactans and acidic arabinogalactans retained by cellulose microfibrils in gelatinous walls. *Plant Physiol.* **169**, 2048–2063.

Grantham, N.J., Wurman-Rodrich, J., Terrett, O.M., Lyczakowski, J.J., Stott, K., Iuga, D., et al. (2017). An even pattern of xylan substitution is critical for interaction with cellulose in plant cell walls. *Nat. Plants*, **3**, 859–865.

Guedes, F., Laurans, F., Quemener, B., Assor, C., Lainé-Prade, V., Boizot, N., et al. (2017). Non-cellulosic polysaccharide distribution during G-layer formation in poplar tension wood fibers: abundance of rhamnogalacturonan I and arabinogalactan proteins but no evidence of xyloglucan. *Planta*, **246**, 857–878.

Gururani, M.A., Venkatesh, J., Upadhyaya, C.P., Nookaraju, A., Pandey, S.K. and Park, S.W. (2012). Plant disease resistance genes: Current status and future directions. *Physiol. Mol. Plant Pathol*. **78**, 51–65.

Hamann, T. (2015). The plant cell wall integrity maintenance mechanism - A case study of a cell wall plasma membrane signaling network. *Phytochemistry*, **112**, 100–109.

Hammond-Kosack, K.E. and Jones, J.D. (1996). Resistance gene-dependent plant defense responses. *Plant Cell*, **8**,1773–1791.

Han, L., Li, G.J., Yang, K.Y., Mao, G., Wang, R., Liu, Y., et al. (2010). Mitogen-activated protein kinase 3 and 6 regulate *Botrytis cinerea*-induced ethylene production in Arabidopsis. *Plant J.* **64**, 114–127.

Hao, Z., Yogiswara, S., Wei, T., Benites, V.T., Sinha, A., Wang, G., et al. (2021). Expression of a bacterial 3-dehydroshikimate dehydratase (QsuB) reduces lignin and improves biomass saccharification efficiency in switchgrass (*Panicum virgatum* L.). *BMC Plant Biol.* **21**, 56.

Harholt, J., Suttangkakul, A. and Vibe Scheller, H. (2010). Biosynthesis of pectin. *Plant Physiol.* **153**, 384–395.

Hartmann, J., Fischer, C., Dietrich, P. and Sauter, M. (2014). Kinase activity and calmodulin binding are essential for growth signaling by the phytosulfokine receptor PSKR1. *Plant J.* **78**,192–202.

Haverkort A.J., Boonekamp P.M., Hutten R., Jacobsen L., Lotz, A.P. Kessel G., et al. (2008). Societal costs of late blight in potato and prospects of durable resistance through cisgenic modification. *Potato Res*. **51**, 47- 57.

Hayashi, T. (1989). Xyloglucans in the primary-cell wall. *Annu. Rev. Plant Physiol. Plant Mol. Biol*. **40**, 139–168.

He, Q. and Silliman, B.R. (2019). Climate Change, Human Impacts, and Coastal Ecosystems in the Anthropocene. *Curr. Biol.* **29**, R1021–R1035.

He, Y., Zhou, J., Shan, L. and Meng, X. (2018). Plant cell surface receptor-mediated signaling - a common theme amid diversity. *J. Cell Sci*. **131**, jcs209353.

Helle, S., Cameron, D., Lam, J., White, B. and Duff, S. (2003). Effect of inhibitory compounds found in biomass hydrolysates on growth and xylose fermentation by a genetically engineered strain of *S.cerevisiae*. *Enzyme Microb. Technol.* **33**, 786–792.

Hématy, K., Sado, P.E., Van Tuinen, A., Rochange, S., Desnos, T., Balzergue, S., et al. (2007). A receptor-like kinase mediates the response of Arabidopsis cells to the inhibition of cellulose synthesis. *Curr. Biol.* **17**, 922–931.

Hinchee, M., Rottmann, W., Mullinax, L., Zhang, C., Chang, S., Cunningham, M., et al. (2009). Short-rotation woody crops for bioenergy and biofuels applications. *In Vitro Cell Dev. Biol. Plant*, **45**, 619–629.

Hoffmann, L., Besseau, S., Geoffroy, P., Ritzenthaler, C., Meyer, D., Lapierre, C., et al. (2004). Silencing of hydroxycinnamoyl-coenzyme A shikimate/quinate hydroxycinnamoyltransferase affects phenylpropanoid biosynthesis. *Plant Cell*, **16**, 1446–1465.

Hou, S., Liu, Z., Shen, H. and Wu, D. (2019). Damage-associated molecular pattern-triggered immunity in plants. *Front. Plant Sci*. **10**, 646.

Hsieh, Y.S. and Harris, P.J. (2012). Structures of xyloglucans in primary cell walls of gymnosperms, monilophytes (ferns *sensu lato*) and lycophytes. *Phytochemistry*, **79,** 87–101.

Hu, W.J., Harding, S.A., Lung, J., Popko, J.L., Ralph, J., Stokke, D.D., et al. (1999). Repression of lignin biosynthesis promotes cellulose accumulation and growth in transgenic trees. *Nat. Biotech*. **17**, 808–812.

Hussey, S.G., Mizrachi, E., Spokevicius, A.V., Bossinger, G., Berger, D.K. and Myburg, A.A. (2011). SND2, a NAC transcription factor gene, regulates genes involved in secondary cell wall development in Arabidopsis fibres and increases fibre cell area in *Eucalyptus*. *BMC plant biology*, **11**, 173.

Jansson, S. and Douglas, C.J. (2007). *Populus*: a model system for plant biology. *Annu. Rev. Plant Biol*. **58**, 435–458.

Jarosch, B., Kogel, K.H. and Schaffrath, U. (1999). The ambivalence of the Barley Mlo locus: Mutations conferring resistance against powdery mildew (*Blumeria graminis* f. sp. *hordei*) enhance susceptibility to the rice blast fungus *Magnaporthe grisea*. *Mol. Plant. Microbe. Interact*. **12**, 508–514.

Jeffries, T.W. (1990). Biodegradation of lignin-carbohydrate complexes. *Biodegradation*, **1**, 163–176.

Jensen, R.B., Lykke-Andersen, K., Frandsen, G.I., Nielsen, H.B., Haseloff, J., Jespersen, H.M., Mundy, J. and Skriver, K. (2000). Promiscuous and specific phospholipid binding by domains in ZAC, a membrane-associated Arabidopsis protein with an ARF GAP zinc finger and a C2 domain. *Plant molecular biology*, **44**, 799–814.

Jin, Y., Ye, N., Zhu, F., Li, H., Wang, J. and Jiang, L. (2017). Calcium-dependent protein kinase CPK28 targets the methionine adenosyltransferases for degradation by the 26S proteasome and affects ethylene biosynthesis and lignin deposition in Arabidopsis. *Plant J*. **90**, 304–318.

Jones, J.D.G. and Dangl, J.L. (2006). The plant immune system. *Nature,* **444**, 323–329.

Jönsson, L.J., Alriksson, B. and Nilvebrant, N.O. (2013). Bioconversion of lignocellulose: inhibitors and detoxification. *Biotechnol. Biofuels*, **6**, 16.

Joo, S., Liu, Y., Lueth, A. and Zhang, S. (2008). MAPK phosphorylation-induced stabilization of ACS6 protein is mediated by the non-catalytic C-terminal domain, which also contains the cis-determinant for rapid degradation by the 26S proteasome pathway. *Plant J.* **54**, 129–140.

Jørgensen, I.H. (1992). Discovery, characterization and exploitation of Mlo *powdery mildew* resistance in *barley*. *Euphytica* **63,** 141–152.

Kachroo, A. and Kachroo, P. (2009). Fatty acid derived signals in plant defense. *Annu. Rev. Phytopathol*. **47**, 153–176.

Kachroo, P., Shanklin, J., Shah, J., Whittle, E.J. and Klessig, D.F.A. (2001). Fatty acid desaturase modulates the activation of defense signaling pathways in Plants. *Proc. Natl. Acad. Sci. USA.* **98**, 9448-53.

Kaeppler S.M., Kaeppler H.F. and Rhee Y. (2000). Epigenetic aspects of somaclonal variation in plants. *Plant Mol. Biol.* **43**, 179–18810.

Kaida, R., Kaku, T., Baba, K., Oyadomari, M., Watanabe, T. and Hayashi, T. (2009). Loosening xyloglucan accelerates the enzymatic degradation of cellulose in wood. *Mol. Plant*, **2**, 904–909.

Kanyuka, K. and Rudd, J.J. (2019). Cell surface immune receptors: the guardians of the plant's extracellular spaces. *Curr. Opin. Plant Biol*. **50**, 1–8.

Katiyar, A., Smita, S., Lenka, S.K., Rajwanshi, R., Chinnusamy, V. and Bansal, K.C. (2012). Genome-wide classification and expression analysis of MYB

transcription factor families in rice and Arabidopsis. *BMC Genomics*, **13,** 544.

Kawai, Y., Ono, E. and Mizutani, M. (2014). Evolution and diversity of the 2-oxoglutarate-dependent dioxygenase superfamily in plants. *Plant J*, **78**, 328–343.

Kazan, K. and Lyons, R. (2014). Intervention of phytohormone pathways by pathogen effectors. *Plant cell*, **26**, 2285–2309.

Kim, M.S., Cho, S.M., Kang, E.Y., Im, Y.J., Hwangbo, H., Kim, Y.C., et al. (2008). Galactinol is a signaling component of the induced systemic resistance caused by *Pseudomonas chlororaphis* O6 root colonization. *Mol. Plant. Microbe. Interact.* **21**, 1643–1653.

Kiselev, K.V., Aleynova, O.A., Ogneva, Z.V., Suprun, A.R. and Dubrovina, A.S. (2021). 35S promoter-driven transgenes are variably expressed in different organs of Arabidopsis thaliana and in response to abiotic stress. *Mol. Biol. Rep*. **48**, 2235–2241.

Kjær, B., Jensen, H.P., Jensen, J. and Jørgensen, J.H. (1990). Associations between 3 ml-o *powdery mildew* resistance genes and agronomic traits in barley. *Euphytica,* **46**, 185–93.

Klocko, A.L., Lu, H., Magnuson, A., Brunner, A.M., Ma, C. and Strauss, S.H. (2018). Phenotypic expression and stability in a large-scale field study of genetically engineered poplars containing sexual containment transgenes. *Front. Bioeng. Biotechnol.* **6**, 100.

Klose, H., Günl, M., Usadel, B., Fischer, R. and Commandeur, U. (2015). Cell wall modification in tobacco by differential targeting of recombinant endoglucanase from *Trichoderma reesei*. *BMC Plant Biol.* **15**, 54.

Kloth, K.J., Abreu, I.N., Delhomme, N., Petřík, I., Villard, C., Ström, C., et al. (2019). PECTIN ACETYLESTERASE9 Affects the transcriptome and metabolome and delays aphid feeding. *Plant Physiol.* **181**, 1704–1720.

Kohorn, B.D. (2016). Cell wall-associated kinases and pectin perception. *J. Exp. Bot.* **67**, 489–494.

Kohorn, B.D., Johansen, S., Shishido, A., Todorova, T., Martinez, R., Defeo, E., et al. (2009). Pectin activation of MAP kinase and gene expression is WAK2 dependent. *Plant J.* **60**, 974–982.

Kong, L., Cheng, J., Zhu, Y., Ding, Y., Meng, J., Chen, Z., et al. (2015). Degradation of the ABA co-receptor ABI1 by PUB12/13 U-box E3 ligases. *Nat. Commun*. **6**, 8630.

Koornneef, A. and Pieterse, C.M.J. (2008). Cross talk in defense signaling. *Plant Physiol.* **146**, 839–844.

Kovtun, Y., Chiu, W.L., Tena, G. and Sheen, J. (2000). Functional analysis of oxidative stress-activated mitogen-activated protein kinase cascade in plants. *Proc. Natl. Acad. Sci. USA.* **97**, 2940–2945.

Kubo, M., Udagawa, M., Nishikubo, N., Horiguchi, G., Yamaguchi, M., Ito, J., et al. (2005). Transcription switches for protoxylem and metaxylem vessel formation. *Genes Dev.* **19**, 1855–1860.

Kühn, C. and Grof, C.P. (2010). Sucrose transporters of higher plants. *Curr. Opin. Plant Biol.* **13**, 288–298.

Kumar, J., Hückelhoven, R., Beckhove, U., Nagarajan, S. and Kogel, K.H. (2000). A compromised Mlo pathway affects the response of Barley to the necrotrophic fungus *Bipolaris sorokiniana* (Teleomorph: *Cochliobolus sativus*) and its toxins. *Phytopathology*, **91**, 127–33.

Kumar, V., Donev, E.N., Barbut, F.R., Kushwah, S., Mannapperuma, C., Urbancsok, J. et al. (2020). Genome-wide identification of *Populus* malectin/malectin-like domain-containing proteins and expression analyses reveal novel candidates for signaling and regulation of wood development. *Front. Plant Sci*. **11**, 588846.

Kumar, V., Hainaut, M., Delhomme, N., Mannapperuma, C., Immerzeel, P., Street, N.R., et al. (2019). Poplar carbohydrate-active enzymes: whole-genome annotation and functional analyses based on RNA expression data. *Plant J.* **99**, 589–609.

Kunkel, B.N. and Brooks, D.M. (2002). Cross talk between signaling pathways in pathogen defense. *Curr. Opin. Plant Biol.* **5**, 325–331.

Kunst, L., Browse, J. and Somerville, C. (1988). Altered regulation of lipid biosynthesis in a mutant of Arabidopsis deficient in chloroplast glycerol-3-phosphate acyltransferase activity. *Proc. Natl. Acad. Sci. USA*. **85**, 4143–4147.

Kus, J.V., Zaton, K., Sarkar, R. and Cameron, R.K. (2002). Age-related resistance in Arabidopsis is a developmentally regulated defense response to *Pseudomonas syringae*. *Plant Cell*, **14**, 479–490.

Lamers, J., van der Meer, T. and Testerink, C. (2020). How plants sense and respond to stressful environments. *Plant Physiol.* **182**, 1624–1635.

Larsson-Brelid, P., Simonson, R., Bergman, Ö. and Nilsson, T. (2000). Resistance of acetylated wood to biological degradation. *Holz. Roh. Werkst*. **58**, 331–337.

Lee, C., Teng, Q., Huang, W., Zhong, R. and Ye, Z.H. (2009). Down-regulation of PoGT47C expression in poplar results in a reduced glucuronoxylan content and an increased wood digestibility by cellulase. *Plant Cell Physiol.* **50**, 1075–1089.

Lee, C., Teng, Q., Zhong, R. and Ye, Z.H. (2011). The four Arabidopsis reduced wall acetylation genes are expressed in secondary wall-containing cells and required for the acetylation of xylan. *Plant Cell Physiol.* **52**, 1289–1301.

Lee, C., Teng, Q., Zhong, R. and Ye, Z.H. (2012). Arabidopsis GUX proteins are glucuronyltransferases responsible for the addition of glucuronic acid side chains onto xylan. *Plant Cell Physiol*. **53**, 1204–1216.

Lefebvre, V., Fortabat, M.N., Ducamp, A., North, H.M., Maia-Grondard, A., Trouverie, J., et al. (2011). ESKIMO1 disruption in Arabidopsis alters vascular tissue and impairs water transport. *PLoS ONE*, **6**, e16645.

Legendre, L., Rueter, S., Heinstein, P.F. and Low, P.S. (1993). Characterization of the oligogalacturonide-induced oxidative burst in cultured soybean (*Glycine max*) Cells. *Plant Physiol.* **102**, 233–240.

Lew, T., Koman, V.B., Silmore, K.S., Seo, J.S., Gordiichuk, P., Strano, M.S., et al. (2020). Real-time detection of wound-induced H2O2 signalling waves in plants with optical nanosensors. *Nat. Plants*, **6**, 404–415.

Li, C., Wu, H.M. and Cheung, A.Y. (2016). FERONIA and her pals: functions and mechanisms. *Plant Physiol*. **171**, 2379–2392.

Li, G., Meng, X., Wang, R., Mao, G., Han, L., Liu, Y., et al. (2012). Dual-level regulation of ACC synthase activity by MPK3/MPK6 cascade and its downstream WRKY transcription factor during ethylene induction in Arabidopsis. *PLoS Genet*. **8**, e1002767.

Li, P., Zhao, L., Qi, F., Htwe, N., Li, Q., Zhang, et al. (2021). The receptor-like cytoplasmic kinase RIPK regulates broad-spectrum ROS signaling in multiple layers of plant immune system. *Mol. Plant*, **S1674-2052,** 00222-7.

Li, Q., Min, D., Wang, J.P., Peszlen, I., Horvath, L., Horvath, B., et al. (2011). Down-regulation of glycosyltransferase 8D genes in *Populus trichocarpa* caused reduced mechanical strength and xylan content in wood. *Tree Physiol*. **31**, 226–236.

Li, Q., Song, J., Peng, S., Wang, J.P., Qu, G.Z., Sederoff, R.R., et al. (2014b). Plant biotechnology for lignocellulosic biofuel production. *Plant Biotechnol. J.* **12**, 1174–1192.

Li, S., Bashline, L., Lei, L. and Gu, Y. (2014a). Cellulose synthesis and its regulation. *Arabidopsis Book*, **12**, e0169.

Liao, D., Cao, Y., Sun, X., Espinoza, C., Nguyen, C.T., Liang, Y., et al. (2017). Arabidopsis E3 ubiquitin ligase PLANT U-BOX13 (PUB13) regulates chitin receptor LYSIN MOTIF RECEPTOR KINASE5 (LYK5) protein abundance. *New Phytol.* 214, 1646–1656.

Lindroth, R.L. and Madritch, M.D. (2015). Condensed tannins increase nitrogen recovery by trees following insect defoliation. *New Phytol.* **208**, 410–420.

Lionetti, V., Francocci, F., Ferrari, S., Volpi, C., Bellincampi, D., Galletti, R., et al. (2010). Engineering the cell wall by reducing de-methyl-esterified homogalacturonan improves saccharification of plant tissues for bioconversion. *Proc. Natl. Acad. Sci USA*. **107,** 616–621.

Liu, J., Li, W., Ning, Y., Shirsekar, G., Cai, Y., Wang, X., et al. (2012). The U-Box E3 ligase SPL11/PUB13 is a convergence point of defense and flowering signaling in plants. *Plant physiology*, **160**, 28–37.

Lombard, V., Golaconda Ramulu, H., Drula, E., Coutinho, P.M. and Henrissat, B. (2014). The carbohydrate-active enzymes database (CAZy) in 2013. *Nucleic Acids Res.* **42**, D490–D495.

Lorenzo, O. and Solano, R. (2005). Molecular players regulating the jasmonate signalling network. *Curr. Opin. Plant Biol.* **8**, 532–540.

Lyczakowski, J.J., Wicher, K.B., Terrett, O.M., Faria-Blanc, N., Yu, X., Brown, D., et al. (2017). Removal of glucuronic acid from xylan is a strategy to improve the conversion of plant biomass to sugars for bioenergy. *Biotech. Biofuels*, **10**, 224.

Manabe, Y., Verhertbruggen, Y., Gille, S., Harholt, J., Chong, S.L., Pawar, P.M., et al. (2013). Reduced wall acetylation proteins play vital and distinct roles in cell wall O-acetylation in Arabidopsis. *Plant Physiol.* **163**, 1107–1117.

Mandal, M.K., Chanda, B., Xia, Y., Yu, K., Sekine, K.T., Gao, Q.M., et al. (2011). Glycerol-3-phosphate and systemic immunity. *Plant Signal. Behav.* **6**, 1871–1874.

Mang, H., Feng, B., Hu, Z., Boisson-Dernier, A., Franck, C.M., Meng, X., et al. (2017). Differential regulation of two-tiered plant immunity and sexual reproduction by ANXUR receptor-like kinases. *Plant Cell*, **29**, 3140–3156.

Mansfield, S.D., Kang, K.Y. and Chapple, C. (2012). Designed for deconstruction--poplar trees altered in cell wall lignification improve the efficacy of bioethanol production. *New Phytol.* **194**, 91–101.

Marita, J.M., Ralph, J., Hatfield, R.D. and Chapple, C. (1999). NMR characterization of lignins in Arabidopsis altered in the activity of ferulate-5-hydroxylase. *Proc. Natl. Acad. Sci. USA*. **96**, 12328-12332.

McCarthy, R.L., Zhong, R. and Ye, Z.H. (2009). MYB83 is a direct target of SND1 and acts redundantly with MYB46 in the regulation of secondary cell wall biosynthesis in Arabidopsis. *Plant Cell Physiol.* **50**, 1950–1964.

Meents, M.J., Watanabe, Y. and Samuels, A.L. (2018). The cell biology of secondary cell wall biosynthesis. *Ann. Bot.* **121**, 1107–1125.

Mellerowicz, E.J. and Gorshkova TA. (2012). Tensional stress generation in gelatinous fibres: A review and possible mechanism based on cell-wall structure and composition. *J Exp. Bot.* **63**, 551–65.

Mellerowicz, E.J. and Sundberg, B. (2008). Wood cell walls: biosynthesis, developmental dynamics and their implications for wood properties. *Curr. Opin. Plant Biol.* **11**, 293– 300.

Mellerowicz, E.J., Baucher, M., Sundberg, B. and Boerjan, W. (2001). Unravelling cell wall formation in the woody dicot stem. *Plant Mol. Biol.* **47**, 239–274.

Melton, L.D., Smith, B.G., Ibrahim. R. and Schröder, R. (2009). Mannans in primary and secondary plant cell walls. *N.Z.J. For Sci.* **39**, 153–160.

Meng, J.G., Liang, L., Jia, P.F., Wang, Y.C., Li, H.J. and Yang, W.C. (2020). Integration of ovular signals and exocytosis of a Ca^{2+}channel by MLOs in pollen tube guidance. *Nat. Plants.* **6**, 143–153.

Meng, X. and Zhang, S. (2013). MAPK cascades in plant disease resistance signaling. *Annu. Rev. Phytopathol.* **51**, 245-266.

Merz, D., Richter, J., Gonneau, M., Sanchez-Rodriguez, C., Eder, T., Sormani, R., et al. (2017). T-DNA alleles of the receptor kinase THESEUS1 with opposing effects on cell wall integrity signaling. *J. Exper. Bot*. **68**, 4583–4593.

Michell, R.H. (2011). Inositol and its derivatives: their evolution and functions. *Adv. Enzym. Regul*. **51**, 84–90.

Mir, B.A., Mewalal, R., Mizrachi, E., Myburg, A.A. and Cowan, D.A. (2014). Recombinant hyperthermophilic enzyme expression in plants: a novel approach for lignocellulose digestion. *Trends Biotechnol.* **32**, 281–289.

Mitsuda, N., Iwase, A., Yamamoto, H., Yoshida, M., Seki, M., Shinozaki, K., et al. (2007). NAC transcription factors, NST1 and NST3, are key regulators of the formation of secondary walls in woody tissues of Arabidopsis. *Plant cell*, **19**, 270–280.

Mitsuda, N., Seki, M., Shinozaki, K. and Ohme-Takagi, M. (2005). The NAC transcription factors NST1 and NST2 of Arabidopsis regulate secondary wall thickenings and are required for anther dehiscence. *Plant cell*, **17**, 2993–3006.

Mohnen, D. (2008). Pectin structure and biosynthesis. *Curr. Opin. Plant Biol*. **11**, 266–277.

Morin, X., Fahse, L., Jactel, H., Scherer-Lorenzen, M., García-Valdés, R. and Bugmann, H. (2018). Long-term response of forest productivity to climate change is mostly driven by change in tree species composition. *Sci. Rep.* **8**, 5627.

Morkunas, I. and Ratajczak, L. (2014). The role of sugar signaling in plant defense responses against fungal pathogens. *Acta Physiol. Plant*, **36**, 1607–1619.

Mortimer, J.C., Faria-Blanc, N., Yu, X., Tryfona, T., Sorieul, M., Ng, Y. Z., et al. (2015). An unusual xylan in Arabidopsis primary cell walls is synthesised by GUX3, IRX9L, IRX10L and IRX14. *Plant J.* **83**, 413–426.

Mortimer, J.C., Miles, G.P., Brown, D.M., Zhang,Z., Segura, M.P., Weimar, T., et al. (2010). Absence of branches from xylan in Arabidopsis gux mutants reveals potential for simplification of lignocellulosic biomass. *Proc. Natl. Acad. Sci. USA*. **107**, 17409–17414.

Mosher, S., Seybold, H., Rodriguez, P., Stahl, M., Davies, K.A., Kemmerling, B., et al. (2013). The tyrosine-sulfated peptide receptors PSKR1 and PSY1R modify the immunity of Arabidopsis to biotrophic and necrotrophic pathogens in an antagonistic manner. *Plant J.* **73**, 469–482.

Mueller-Roeber, B. and Pical, C. (2002). Inositol phospholipid metabolism in Arabidopsis. Characterized and putative isoforms of inositol phospholipid kinase and phosphoinositide-specific phospholipase C. *Plant Physiol.* **130**, 22–46.

Mur, L.A., Kenton, P., Atzorn, R., Miersch, O. and Wasternack, C. (2006). The outcomes of concentration-specific interactions between salicylate and jasmonate signaling include synergy, antagonism, and oxidative stress leading to cell death. *Plant Physiol.* **140**, 249–262.

Myburg, A.A., Grattapaglia, D., Tuskan, G.A., Hellsten, U., Hayes, R.D., Grimwood, J., et al. (2014). The genome of *Eucalyptus grandis*. *Nature*, **510**, 356–362.

Niki, T., Mitsuhara, I., Seo, S., Ohtsubo, N. and Ohashi, Y. (1998) Antagonistic effect of salicylic acid and jasmonic acid on the expression of pathogenesis-related (PR) protein genes in wounded mature tobacco leaves. *Plant Cell Physiol.* **39**, 500–7.

Noh, Y.S., Amasino, R.M., 1999. Identification of a promoter region responsible for the senescence-specific expression of SAG12. *Plant Mol. Biol*. **41,** 181–194.

Norman, C., Vidal, S. and Palva, E.T. (1999). Oligogalacturonide-mediated induction of a gene involved in jasmonic acid synthesis in response to the cell-wall-degrading enzymes of the plant pathogen *Erwinia carotovora*. *Mol. Plant Microbe Interact.* **12**, 640–644.

Nühse, T.S., Bottrill, A.R., Jones, A.M. and Peck, S.C. (2007). Quantitative phosphoproteomic analysis of plasma membrane proteins reveals regulatory mechanisms of plant innate immune responses. *Plant J*. **51**, 931–940.

Nystedt, B., Street N., Wetterbom, A., Zuccolo, A., Lin, Y.C., Scofield, D.G., et al. (2013). The Norway spruce genome sequence and conifer genome evolution. *Nature*, **497**, 579–584.

Oba, K., Kondo, K., Doke, N. and Uritani, I. (1985). Induction of 3-hydroxy-3-methylglutaryl coenzyme A reductase in potato tubers after slicing, fungal

infection or chemical treatment and some properties of the enzyme. *Plant Cell Physiol*. **26**, 873–880.

Obata, T. (2019). Metabolons in plant primary and secondary metabolism. *Phytochem Rev.* **18**, 1483–1507.

Oñate-Sánchez, L. and Singh, K.B. (2002). Identification of Arabidopsis ethylene-responsive element binding factors with distinct induction kinetics after pathogen infection. *Plant Physiol.* **128**, 1313–1322.

Paredez, A.R., Somerville, C.R. and Ehrhardt, D.W. (2006). Visualization of cellulose synthase demonstrates functional association with microtubules. *Science,* **312**, 1491–1495.

Park, S.H., Ong, R.G. and Sticklen, M. (2016). Strategies for the production of cell wall-deconstructing enzymes in lignocellulosic biomass and their utilization for biofuel production. *Plant Biotech. J.* **14**, 1329–1344.

Park, Y.B. and Cosgrove, D.J. (2015). Xyloglucan and its interactions with other components of the growing cell wall. *Plant Cell Physiol.* **56**, 180–194.

Park, Y.W., Baba, K., Furuta, Y., Iida, I., Sameshima, K., Arai, M., et al. (2004). Enhancement of growth and cellulose native cellulose accumulation by overexpression of xyloglucanase in poplar. *FEBS Lett.* **564**, 183–187.

Pauly, M. and Keegstra, K. (2008). Cell-wall carbohydrates and their modification as a resource for biofuels. *Plant J.* **54**, 559–568.

Pauly, M. and Keegstra, K. (2016). Biosynthesis of the plant cell wall matrix polysaccharide xyloglucan. *Annu. Rev. Plant Biol.* **67**, 235–259.

Pauly, M. and Ramírez, V. (2018). New insights into wall polysaccharide O-acetylation. *Front. Plant Sci*. **9,** 1210.

Pauly, M., Albersheim, P., Darvill, A. and York, W.S. (1999). Molecular domains of the cellulose/xyloglucan network in the cell walls of higher plants. *Plant J*. **20**, 629-639.

Pawar P.M.A., Derba-Maceluch, M., Chong, S.L., Gómez, L.D., Miedes, E., Banasiak, A., et al. (2016). Expression of fungal acetyl xylan esterase in *Arabidopsis thaliana* improves saccharification of stem lignocellulose. *Plant Biotechnol. J*. **14**, 387-397.

Pawar, P.M.A., Derba-Maceluch, M., Chong, S.L., Gandla, M.L., Bashar. S.S., Sparrman, T., et al. (2017b). In muro deacetylation of xylan affects lignin properties and improves saccharification of aspen wood. *Biotechnol. Biofuels*, **10**, 1-11.

Pawar, P.M.A., Koutaniemi, S., Tenkanen, M. and Mellerowicz, E.J. (2013). Acetylation of woody lignocellulose: significance and regulation. *Front. Plant. Sci.* **4**, 118.

Pawar, P.M.A., Ratke, C., Balasubramanian, V.K., Chong, S.L., Gandla, M.L., Adriasola, M., et al. (2017a). Downregulation of RWA genes in hybrid

aspen affects xylan acetylation and wood saccharification. *New Phytol*. **214**, 1491-1505.

Peng, F., Ren, J.L., Xu, F., Bian, J., Peng, P. and Sun, R.C. (2009). Comparative study of hemicelluloses obtained by graded ethanol precipitation from sugarcane bagasse. *J. Agric. Food Chem*. **57**, 6305–6317.

Petersen, P.D., Lau, J., Ebert, B., Yang, F., Verhertbruggen, Y., Kim, J.S., et al. (2012). Engineering of plants with improved properties as biofuels feedstocks by vessel-specific complementation of xylan biosynthesis mutants. *Biotechnol. Biofuels*, **5**, 84.

Philp, J. (2018). The bioeconomy, the challenge of the century for policy makers. *New Biotech.* **40**, 11–19.

Pilate, G., Guiney, E., Holt, K., Petit-Conil, M., Lapierre, C., Leplé, J.C., et al. (2002). Field and pulping performances of transgenic trees with altered lignification. *Nature Biotechnol.* **20**, 607–612.

Pinard, D., Mizrachi, E., Hefer, C.A., Kersting, A.R., Joubert, F., Douglas, C.J., et al. (2015). Comparative analysis of plant carbohydrate active enZymes and their role in xylogenesis. *BMC genomics,* **16**, 402.

Pogorelko, G., Fursova, O., Lin, M., Pyle, E., Jass, J. and Zabotina, O.A. (2011). Post-synthetic modification of plant cell walls by expression of microbial hydrolases in the apoplast. *Plant Mol. Biol.* **77**, 433–445.

Pogorelko, G., Lionetti, V., Fursova, O., Sundaram, R.M., Qi, M., Whitham, S.A., Bogdanove, A.J., et al. (2013). Arabidopsis and *Brachypodium distachyon* transgenic plants expressing *Aspergillus nidulans* acetylesterases have decreased degree of polysaccharide acetylation and increased resistance to pathogens. *Plant Physiol.* **162**, 9–23.

Pramod, S., Gandla, M.L., Derba-Maceluch, M., Jönsson, L.J., Mellerowicz, E.J. and Winestrand, S. (2021). Saccharification Potential of Transgenic Greenhouse- and Field-Grown Aspen Engineered for Reduced Xylan Acetylation. *Front. Plant Sci.* **12**, 704960.

Proietti, S., Caarls, L., Coolen, S., Van Pelt, J.A., Van Wees, S. and Pieterse, C. (2018). Genome-wide association study reveals novel players in defense hormone crosstalk in Arabidopsis. *Plant Cell Environ.* **41**, 2342–2356.

Purrington, C.B. (2000). Costs of resistance. *Curr. Opin. Plant Biol.* **3**, 305–308.

Raaymakers, T.M. and Van den Ackerveken, G. (2016). Extracellular recognition of oomycetes during biotrophic infection of plants. *Front Plant Sci*. **7**, 906.

Ranney, T.G. (2004). Population control: developing non-invasive nursery crops. *Proc. Intern. Plant Propag. Soc*. **54**, 604–607.

Ratke, C., Pawar, P.M., Balasubramanian, V.K., Naumann, M., Duncranz, M.L., Derba-Maceluch, M., et al. (2015). Populus GT43 family members group into distinct sets required for primary and secondary wall xylan

biosynthesis and include useful promoters for wood modification. *Plant Biotech. J.* **13**, 26–37.

Ratke, C., Terebieniec, B.K., Winestrand, S., Derba-Maceluch, M., Grahn, T., Schiffthaler, B., et al. (2018). Downregulating aspen xylan biosynthetic GT43 genes in developing wood stimulates growth via reprograming of the transcriptome. *New Phytol.* **219**, 230–245.

Reem, N.T., Chambers, L., Zhang, N., Abdullah, S.F., Chen, Y., Feng, G., et al. (2020). Post-synthetic reduction of pectin methylesterification causes morphological abnormalities and alterations to stress response in *Arabidopsis thaliana. Plants*, **9**, 1558.

Ricard, B., Toai, T.V., Chourey, P. and Saglio, P. (1998). Evidence for the critical role of sucrose synthase for anoxic tolerance of maize roots using a double mutant. *Plant Physiol.* **116**, 1323–1331.

Rodiuc, N., Barlet, X., Hok, S., Perfus-Barbeoch, L., Allasia, V., Engler, G., et al. (2016). Evolutionarily distant pathogens require the Arabidopsis phytosulfokine signalling pathway to establish disease. *Plant Cell Environ.* **39**, 1396–1407.

Rogers, P.C., Pinno, B.D, Šebesta, J., Albrectsen, B.R., Li, G., Ivanova, N., et al. (2020). A global view of aspen: Conservation science for widespread keystone systems. *Glob. Ecol. Conserv.* **21**, 1–35.

Rojo, E., Solano, R. and Sánchez-Serrano, J.J. (2003). Interactions between signaling compounds involved in plant defense. *J. Plant Growth Regul.* **22,** 82–98.

Rotblat, B., Enshell-Seijffers, D., Gershoni, J.M., Schuster, S. and Avni, A. (2002). Identification of an essential component of the elicitation active site of the EIX protein elicitor. *Plant J.* **32**, 1049–1055.

Rowell, R.M., Pettersen, Rowell, J.S. and Tshabalala, M.A. (2012). Cell wall chemistry. In R.M. Rowell (Ed.), Handbook of wood chemistry and wood composites, Boca Raton, FL: *CRC Presss*, 33–72.

Ruan, Y.L. (2014). Sucrose metabolism: gateway to diverse carbon use and sugar signaling. *Annu. Rev. Plant Biol.* **65**, 33–67.

Rui, Y. and Dinneny, J.R. (2020). A wall with integrity: surveillance and maintenance of the plant cell wall under stress. *New Phytol*. **225**, 1428–1439.

Sakamoto, S., Somssich, M., Nakata, M.T., Unda, F., Atsuzawa, K., Kaneko, Y., et al. (2018). Complete substitution of a secondary cell wall with a primary cell wall in Arabidopsis. *Nat. Plants*, **4**, 777–783.

Salojärvi, J., Smolander, O.P., Nieminen, K., Rajaraman, S., Safronov, O., Safdari, P., et al. (2017). Genome sequencing and population genomic analyses

provide insights into the adaptive landscape of silver birch. N*ature Genet*. **49**, 904–912.

Sannigrahi, P., Ragauskas, A.J. and Tuskan, G.A. (2010). Poplar as a feedstock for biofuels: a review of compositional characteristics. *Biofuel. Bioprod. Biorefin.* **4**, 209–226.

Sarkar, P., Bosneaga, E. and Auer, M. (2009). Plant cell walls throughout evolution: towards a molecular understanding of their design principles. *J. Exp. Bot.* **60**, 3615–3635.

Scheler, C., Durner, J. and Astier, J. (2013). Nitric oxide and reactive oxygen species in plant biotic interactions. *Curr. Opin. Plant Biol*. **1**, 534–39.

Scheller, H.V. and Ulvskov, P. (2010). Hemicelluloses. *Annu. Rev. Plant Biol*. **61**, 263–289.

Schilmiller, A.L., Stout, J., Weng, J.K., Humphreys, J., Ruegger, M.O. and Chapple, C. (2009). Mutations in the cinnamate 4-hydroxylase gene impact metabolism, growth and development in Arabidopsis. *Plant J.* **60**, 771–782.

Schrader, S. and Sauter, J.J. 2002. Seasonal changes of sucrose-phosphate synthase and sucrose synthase activities in poplar wood (*Populus x canadensis* Moench *'robusta'*) and their possible role in carbohydrate metabolism. *J. Plant Physiol.* **159**, 833–843.

Schultink, A., Naylor, D., Dama, M. and Pauly, M. (2015). The role of the plant-specific ALTERED XYLOGLUCAN9 protein in Arabidopsis cell wall polysaccharide O-acetylation. *Plant physiol.* **167**, 1271–1283.

Schulze, B., Mentzel, T., Jehle, A.K., Mueller, K., Beeler, S., Boller, T., et al. (2010). Rapid heteromerization and phosphorylation of ligand-activated plant transmembrane receptors and their associated kinase BAK1. *J. Biol. Chem.* **285**, 9444–9451.

Schwessinger, B., Roux, M., Kadota, Y., Ntoukakis, V., Sklenar, J., Jones, A., et al. (2011). Phosphorylation-dependent differential regulation of plant growth, cell death, and innate immunity by the regulatory receptor-like kinase BAK1. *PLoS Genet.* **7**, e1002046.

Seifert, G.J. (2004). Nucleotide sugar interconversions and cell wall biosynthesis: how to bring the inside to the outside. *Curr. Opin. Plant Biol.* **7**, 277–284.

Sengupta, S., Mukherjee, S., Basak, P. and Majumder, A.L. (2015). Significance of galactinol and raffinose family oligosaccharide synthesis in plants. *Front. Plant Sci.* **6**, 656.

Sheard, L.B., Tan, X., Mao, H., Withers, J., Ben-Nissan, G., Hinds, T.R., et al. 2010. Jasmonate perception by inositol-phosphate-potentiated COI1-JAZ co-receptor. *Nature,* **468**, 400–405.

Shiu, S.H. and Bleecker, A.B. (2001). Receptor-like kinases from Arabidopsis form a monophyletic gene family related to animal receptor kinases. *Proc. Natl. Acad. Sci. USA*. **98**, 10763–10768.

Shiu, S.H., and Bleecker, A.B. (2003). Expansion of the receptor-like kinase/Pelle gene family and receptor-like proteins in Arabidopsis. *Plant Physiol*. **132**, 530–543.

Silva, A.C., Lima, M.D, Eloy, N.B., Thiebaut, F., Montessoro, P., Hemerly, A.S., et al. (2019). The Yin and Yang in plant breeding: the trade-off between plant growth yield and tolerance to stresses. *Biotech. Res. Innov.* **3**, 73–79.

Sindhu, R., Binod, P. and Pandey, A. (2016). Biological pretreatment of lignocellulosic biomass--An overview. *Bioresource Technol.* **199**, 76–82.

Smith, P.J., Wang, H.T., York, W.S., Peña, M.J. and Urbanowicz, B.R. (2017). Designer biomass for next-generation biorefineries: leveraging recent insights into xylan structure and biosynthesis. Biotechnol. Biofuels, 10, 286.

Song, D., Gui, J., Liu, C., Sun, J. and Li, L. (2016). Suppression of PtrDUF579-3 Expression Causes Structural Changes of the Glucuronoxylan in Populus. *Front Plant. Sci.* **7**, 493.

Souza, C.A., Li, S., Lin, A.Z., Boutrot, F., Grossmann, G., Zipfel, C., et al. (2017). Cellulose-derived oligomers act as damage-associated molecular patterns and trigger defense-like responses. *Plant Physiol.* **173**, 2383–2398.

Spániková, S. and Biely, P. (2006). Glucuronoyl esterase--novel carbohydrate esterase produced by *Schizophyllum commune*. *FEBS Lett.*, **580**, 4597–4601.

Stegmann, M., Monaghan, J., Smakowska-Luzan, E., Rovenich, H., Lehner, A., Holton, N., et al. (2017). The receptor kinase FER is a RALF-regulated scaffold controlling plant immune signaling. *Science,* **355**, 287–289.

Stein, O. and Granot, D. (2019). An overview of sucrose synthases in plants. *Front. Plant Sci.* **10**, 95.

Stermer, B.A. and Bostock, R.M. (1987). Involvement of 3-hydroxy-3-methylglutaryl coenzyme A reductase in the regulation of sesquiterpenoid phytoalexin synthesis in potato. *Plant Physiol.*, **84**, 404–408.

Strauss, S.H. (2003). Genomics, genetic engineering, and domestication of crops. *Science*, **300**, 61–62.

Strauss, S.H., Jones, K.N., Lu, H., Petit, J.D., Klocko, A.L., Betts, M.G, et al. (2017). Reproductive modification in forest plantations: impacts on biodiversity and society. *New Phytol.* **213**, 1000–1021.

Strauss, S.H., Ma, C., Ault K. and Klocko A.L. (2016). Lessons from two decades of field trials with genetically modified trees in the USA: Biology and

regulatory compliance. In: Vettori C. et al. (eds) Biosafety of Forest Transgenic Trees. *Forestry Sciences*, **82**. Springer, Dordrecht.

Studer, M.H., DeMartini, J.D., Davis, M.F., Sykes, R.W., Davison, B., Keller, M., et al. (2011). Lignin content in natural *Populus* variants affects sugar release. *Proc. Natl. Acad. Sci. USA*. **108**, 6300–6305.

Sundell, D., Street, N.R., Kumar, M., Mellerowicz, E.J., Kucukoglu, M., Johnsson, C., et al. (2017). AspWood: high-spatial-resolution transcriptome profiles reveal uncharacterized modularity of wood formation in *Populus tremula*. *Plant Cell*, 29, 1585–1604.

Sussholz, O., Pizarro, L., Schuster, S. and Avni, A. (2020). SlRLK-like is a malectin-like domain protein affecting localization and abundance of LeEIX2 receptor resulting in suppression of EIX-induced immune responses. *Plant J*. **104**, 1369–1381.

Sutton, P., Gilbert, M., Williams, L. and Hall, J.L. (2007). Powdery mildew infection of wheat leaves changes host solute transport and invertase activity. *Physiol. Plant,* **129**, 787–795.

Sykes, R.W., Gjersing, E.L., Foutz, K., Rottmann, W.H., Kuhn, S.A., Foster, C.E., et al. (2015). Down-regulation of p-coumaroyl quinate/shikimate 3'-hydroxylase (C3'H) and cinnamate 4-hydroxylase (C4H) genes in the lignin biosynthetic pathway of *Eucalyptus urophylla* × *E. grandis* leads to improved sugar release. *Biotechnol. Biofuels*, 8, 128.

Szczegielniak, J., Klimecka, M., Liwosz, A., Ciesielski, A., Kaczanowski, S., Dobrowolska, G., et al. (2005). A wound-responsive and phospholipid-regulated maize calcium-dependent protein kinase. *Plant Physiol.* **139**, 1970– 1983.

Takahashi, J., Rudsander, U.J., Hedenström, M., Banasiak, A., Harholt, J. and Mellerowicz, E.J. (2009). KORRIGAN1 and its aspen homolog PttCel9A1 decrease cellulose crystallinity in Arabidopsis stems. *Plant Cell Physiol.* **50**, 1099 –1115.

Takehara, K., Murata, K., Yamaguchi, T., Yamaguchi, K., Chaya, G., Kido, S., et al. (2018). Thermo-responsive allele of sucrose synthase 3 (Sus3) provides high-temperature tolerance during the ripening stage in rice (*Oryza sativa* L.). *Breed. Sci.* **68**, 336–342.

Tan, L., Eberhard, S., Pattathil, S., Warder, C., Glushka, J., Yuan, C., et al. (2013). An Arabidopsis cell wall proteoglycan consists of pectin and arabinoxylan covalently linked to an arabinogalactan protein. *Plant Cell*, **25**, 270–287.

Tan, X., Calderon-Villalobos, L.I., Sharon, M., Zheng, C., Robinson, C.V., Estelle, M., et al. (2007). Mechanism of auxin perception by the TIR1 ubiquitin ligase. *Nature*, **446**, 640–645.

Taylor-Teeples, M., Lin, L., de Lucas, M., Turco, G., Toal, T.W., Gaudinier, A., et al. (2015). An Arabidopsis gene regulatory network for secondary cell wall synthesis. *Nature*, **517**, 571–575.

Temple, H., Saez-Aguayo, S., Reyes, F.C. and Orellana, A. (2016). The inside and outside: topological issues in plant cell wall biosynthesis and the roles of nucleotide sugar transporters. *Glycobiology*, **26**, 913–925.

Testerink, C. and Munnik, T. (2011). Molecular, cellular, and physiological responses to phosphatidic acid formation in plants. *J. Exp. Bot*. 62, 2349–2361.

Testerink, C., Larsen, P.B., McLoughlin, F., van der Does, D., van Himbergen, J.A. and Munnik, T. (2008). PA, a stress-induced short cut to switch-on ethylene signalling by switching-off CTR1? *Plant Sign. Behav.* **3**, 681–683.

Thines B., Katsir L., Melotto M., Niu Y., Mandaokar A., Liu G., et al. (2007). JAZ repressor proteins are targets of the SCF(COI1) complex during jasmonate signalling. *Nature*, **448**, 661–665.

Thomma, B.P., Penninckx, I.A., Broekaert, W.F. and Cammue, B.P. (2001). The complexity of disease signaling in Arabidopsis. *Current opinion in immunology*, **13**, 63–68.

Thynne, E., Saur, I., Simbaqueba, J., Ogilvie, H.A., Gonzalez-Cendales, Y., Mead, O., et al. (2017). Fungal phytopathogens encode functional homologues of plant rapid alkalinization factor (RALF) peptides. *Mol. Plant Pathol.*, **18**, 811–824.

Tollefson J. (2021). IPCC climate report: Earth is warmer than it's been in 125,000 years. *Nature*, **596**, 171–172.

Tomassetti, S., Pontiggia, D., Verrascina, I., Reca, I.B., Francocci, F., Salvi, G., et al. (2015). Controlled expression of pectic enzymes in Arabidopsis thaliana enhances biomass conversion without adverse effectson growth. P*hytochemistry,* 112, 221–230.

Torres, M.A., Jones, J.D. and Dangl, J.L. (2006). Reactive oxygen species signaling in response to pathogens. *Plant Physiol*. **141**, 373–78.

Tronchet, M., Balagué, C., Kroj, T., Jouanin, L. and Roby, D. (2010). Cinnamyl alcohol dehydrogenases C and D, key enzymes in lignin biosynthesis, play an essential role in disease resistance in Arabidopsis. *Mol. Plant Pathol.* **11**, 83–92.

Tsai, A.Y., Canam, T., Gorzsás, A., Mellerowicz, E.J., Campbell, M.M. and Master, E.R. (2012). Constitutive expression of a fungal glucuronoyl esterase in Arabidopsis reveals altered cell wall composition and structure. *Plant Biotechnol. J.* **10**, 1077–1087.

Tsai, A.Y., Chan, K., Ho, C.Y., Canam, T., Capron, R., Master, E.R., et al. (2017). Transgenic expression of fungal accessory hemicellulases in Arabidopsis

thaliana triggers transcriptional patterns related to biotic stress and defense response. *PloS One*, **12**, e0173094.

Tsuda, K. and Katagiri, F. (2010). Comparing signaling mechanisms engaged in pattern-triggered and effector-triggered immunity. *Curr. Opin. Biotechnol.* **13**, 459–465.

Turner, J.G., Ellis, C. and Devoto, A. (2002). The jasmonate signal pathway. *Plant Cell*, **14** *Suppl*. S153–S164.

Tuskan G., Difazio S., Jansson S., Bohlmann J., Grigoriev I., Hellsten U., et al. (2006). The genome of black cottonwood, *Populus trichocarpa* (Torr. & Gray). *Science (New York, N.Y.)*, **313**, 1596–1604.

Tuteja, N. (2007). Abscisic acid and abiotic stress signaling. *Plant Signal. Behav.* **2**, 135–138.

Urbanowicz, B.R., Peña, M.J., Ratnaparkhe, S., Avci, U., Backe, J., Steet, H.F., et al. (2012). 4-O-methylation of glucuronic acid in Arabidopsis glucuronoxylan is catalyzed by a domain of unknown function family 579 protein. *Proc. Natl. Acad. Sci*. **109**, 14253–14258.

Van Acker, R., Vanholme, R., Storme, V., Mortimer, J.C., Dupree, P. and Boerjan, W. (2013). Lignin biosynthesis perturbations affect secondary cell wall composition and saccharification yield in *Arabidopsis thaliana*. *Biotech. Biofuels*, **6**, 46.

Van der Luit, A.H., Piatti, T., Van Doorn, A., Musgrave, A., Felix G, Boller, T., et al. (2000). Elicitation of suspension-cultured tomato cells triggers the formation of phosphatidic acid and diacylglycerol pyrophosphate. *Plant Physiol*. **123**, 1507–1516.

van Loon, L.C., Geraats, B.P. and Linthorst, H.J. (2006). Ethylene as a modulator of disease resistance in plants. *Trends Plant Sci.* **11**, 184–191.

Vanholme, R., Demedts, B., Morreel, K., Ralph, J. and Boerjan, W. (2010). Lignin biosynthesis and structure. *Plant Physiol*. **153**, 895-905.

Venkateshwaran, M., Jayaraman, D., Chabaud, M., Genre, A., Balloon, A.J., Maeda, J., et al. (2015). A role for the mevalonate pathway in early plant symbiotic signaling. *Proc. Natl. Acad. Sci. USA.* **112**, 9781–9786.

Venugopal, S.C., Chanda, B., Vaillancourt, L., Kachroo, A. and Kachroo, P. (2009). The common metabolite glycerol-3-phosphate is a novel regulator of plant defense signaling. *Plant Signal Behav*. **4**, 746–749.

Vining, K.V., Contreras, R.N., Ranik, M. and Strauss, S.H. (2012). Genetic methods for mitigating invasiveness of woody ornamental plants: research needs and opportunities. *HortScience*, **47**, 1210–1216.

Viswanath, V., Albrectsen, B.R. and Strauss, S.H. (2012). Global regulatory burden for field testing of genetically modified trees. *Tree Genet. Genomes*, **8**, 221–226.

Viswanath, V., Ma, C., Etherington, E., Dharmawardhana, P., Pearce, D.W., Rood, S.B., et al. (2011). Greenhouse and field evaluation of transgenic poplars with modified gibberellin metabolism and signaling genes. *BMC Proc*. **5**, O22.

Voelker, S.L., Lachenbruch, B., Meinzer, F.C. and Strauss, S. H. (2011b). Reduced wood stiffness and strength, and altered stem form, in young antisense 4CL transgenic poplars with reduced lignin contents. *New Phytol*. **189**, 1096–1109.

Voelker, S.L., Lachenbruch, B., Meinzer, F.C., Jourdes, M., Ki, C., Patten, A.M., et al. (2010). Antisense down-regulation of 4CL expression alters lignification, tree growth, and saccharification potential of field-grown poplar. *Plant Physiol*. **154**, 874–886.

Voelker, S.L., Lachenbruch, B., Meinzer, F.C., Kitin, P. and Strauss, S.H. (2011a). Transgenic poplars with reduced lignin show impaired xylem conductivity, growth efficiency and survival. *Plant Cell Environ.* **34**, 655–668.

Voiniciuc, C., Pauly, M. and Usadel, B. (2018). Monitoring polysaccharide dynamics in the plant cell wall. *Plant Physiol.* **176**, 2590–2600.

Voragen, A.G.J., Coenen, GJ., Verhoef, R.P and Schols, H.A. (2009). Pectin, a versatile polysaccharide present in plant cell walls. *Struct. Chem*. **20**, 263-275.

Voxeur, A. and Höfte, H. (2016). Cell wall integrity signaling in plants: "To grow or not to grow that's the question". *Glycobiology*, **26**, 950–960.

Wang, H., Sui, X., Guo, J., Wang, Z., Cheng, J., Ma, S., et al. (2014). Antisense suppression of cucumber (*Cucumis sativus* L.) sucrose synthase 3 (CsSUS3) reduces hypoxic stress tolerance. *Plant, Cell Environ.* **37**, 795–810.

Wang, Z., Pawar, P.M., Derba-Maceluch, M., Hedenström, M., Chong, S.L. and Mellerowicz, E.J. (2020). Hybrid aspen expressing a carbohydrate esterase family 5 acetyl xylan esterase under control of a wood-specific promoter shows improved saccharification. *Front Plant. Sci.* **11**, 380.

Weaver, L.M., Gan, S., Quirino, B., Amasino, R.M., 1998. A comparison of the expression patterns of several senescence-associated genes in response to stress and hormone treatment. *Plant Mol. Biol*. **37**, 455–469.

Wei, Z., Qu, Z., Zhang, L., Zhao, S., Bi, Z., Ji, X., Wang, X. and Wei, H. (2015). Overexpression of poplar xylem sucrose synthase in tobacco leads to a thickened cell wall and increased height. *PloS One.* **10**, e0120669.

Westermark, U. (1985). The occurrence of p-hydroxyphenylpropane units in the middle-lamella lignin of spruce (*Picea abies*) *Wood Sci. Technol*. **19**, 223–32.

Wheeler, N. and Watts, N. (2018). Climate change: From science to practice. *Curr. Environ. Health Rep.* **5**, 170–178.

Wilson, I.B.H. (2002). Glycosylation of proteins in plants and invertebrates. *Curr. Opin. Struct. Biol.* **12**, 569– 577.

Wolf, S. (2017). Plant cell wall signalling and receptor-like kinases. *Biochem. J*. **474**, 471–492.

Wolf, S. and Höfte, H. (2014). Growth control: a saga of cell walls, ROS, and peptide receptors. *Plant Cell*, **26**, 1848–1856.

Woodward, A.W. and Bartel, B. (2018). Biology in bloom: A primer on the *Arabidopsis thaliana* model system. *Genetics*, **208**, 1337–1349.

Wu, J., Kurten, E.L., Monshausen, G., Hummel, G.M., Gilroy, S. and Baldwin, I.T. (2007). NaRALF, a peptide signal essential for the regulation of root hair tip apoplastic pH in *Nicotiana attenuata*, is required for root hair development and plant growth in native soils. *Plant J.* **52**, 877–890.

Xi, L., Wu, X.N., Gilbert, M. and Schulze, W.X. (2019). Classification and interactions of LRR receptors and co-receptors within the Arabidopsis plasma membrane - an overview. *Front. Plant Sci.* **10**, 472.

Xiao, G., Zhou, J., Lu, X., Huang, R. and Zhang, H. (2017). Excessive UDPG resulting from the mutation of UAP1 causes programmed cell death by triggering reactive oxygen species accumulation and caspase-like activity in rice. *New Phytol*. **217**, 332–343.

Xie, K. and Yang, Y. (2013). RNA-guided genome editing in plants using a CRISPR-Cas system. *Mol. Plant*, 6, 1975–1983.

Xiong, G., Cheng, K. and Pauly, M. (2013). Xylan O-acetylation impacts xylem development and enzymatic recalcitrance as indicated by the Arabidopsis mutant tbl29. *Mol. Plant*, **6**, 1373–1375.

Xu, B., Escamilla-Treviño, L.L., Sathitsuksanoh, N., Shen, Z., Shen, H., Zhang, Y. H., et al. (2011). Silencing of 4-coumarate:coenzyme A ligase in switchgrass leads to reduced lignin content and improved fermentable sugar yields for biofuel production. *New Phytol.* **192**, 611–625.

Xu, F., Zhong, X.C., Sun, R.C. and Lu, Q. (2006). Anatomy, ultrastructure and lignin distribution in cell wall of Caragana Korshinskii. *Ind. Crops Prod*. **24**, 186–193.

Xu, J. and Zhang, S. (2015). Mitogen-activated protein kinase cascades in signaling plant growth and development. *Trends Plant Sci.* **20**, 56–64.

Yamaguchi, M., Kubo, M., Fukuda, H. and Demura, T. (2008). Vascular-related NAC-DOMAIN7 is involved in the differentiation of all types of xylem vessels in Arabidopsis roots and shoots. *Plant J.* **55**, 652–664.

Yang, F., Mitra, P., Zhang, L., Prak, L., Verhertbruggen, Y., Kim, J.S., et al. (2013). Engineering secondary cell wall deposition in plants. *Plant Biotech. J.*, **11**, 325–335.

Yang, Z., Park, H., Lacy, G.H. and Cramer, C.L. (1991). Differential activation of potato 3-hydroxy-3-methylglutaryl coenzyme A reductase genes by wounding and pathogen challenge. *Plant Cell*, **3**, 397–405.

Yu, S.M., Lo, S.F. and Ho, T.D. (2015). Source-sink communication: Regulated by hormone, nutrient, and stress cross-cignaling. *Trends Plant Sci.* **20**, 844–857.

Yu, X., Feng, B., He, P. and Shan, L. (2017). From chaos to harmony: responses and signaling upon microbial pattern recognition. *Annu. Rev. Phytopathol.* **55**, 109–137.

Yuan, Y., Teng, Q., Zhong, R. and Ye, Z.H. (2013). The Arabidopsis DUF231 domain-containing protein ESK1 mediates 2-O- and 3-O-acetylation of xylosyl residues in xylan. *Plant Cell Physiol.* **54**, 1186–1199.

Zeier, J. (2005). Age-dependent variations of local and systemic defence responses in Arabidopsis leaves towards an avirulent strain of Pseudomonas syringae. *Physiol. Mol. Plant Pathol.* **66**, 30–39.

Zhang, W., Zhao, F., Jiang, L., Chen, C., Wu, L. and Liu, Z. (2018). Different pathogen defense strategies in Arabidopsis: More than pathogen recognition. *Cells*, **7,** 252.

Zhao, J., Davis, L.C. and Verpoorte, R. (2005). Elicitor signal transduction leading to production of plant secondary metabolites. *Biotechnol. Adv.* **23**, 283–333.

Zhao, X.B., Zhang, L.H. and Liu, D.H. (2012). Biomass recalcitrance. Part I: the chemical compositions and physical structures affecting the enzymatic hydrolysis of lignocellulose. *Biofuels, Bioprod. Biorefining*, **6**, 465-482.

Zheng, Y., Wang, X., Chen, Y., Wagner, E. and Cosgrove, D.J. (2018). Xyloglucan in the primary cell wall: assessment by FESEM, selective enzyme digestions and nanogold affinity tags. *Plant J.* **93**, 211–226.

Zhong, R., Richardson, E.A. and Ye, Z.H. (2007). The MYB46 transcription factor is a direct target of SND1 and regulates secondary wall biosynthesis in Arabidopsis. *Plant Cell*, **19**, 2776–2792.

Zhou, J., Liu, D., Wang, P., Ma, X., Lin, W., Chen, S., et al. (2018). Regulation of Arabidopsis brassinosteroid receptor BRI1 endocytosis and degradation by plant U-box PUB12/PUB13-mediated ubiquitination. *Proc. Natl. Acad. Sci. USA*. **115**, E1906–E1915.

Zobel, B.J. and Sprague, J.R. (1998). "Characteristics of Juvenile Wood," in *Juvenile Wood in Forest Trees*, ed T. E. Timell (Heidelberg: Springer-Verlag), 21–55.

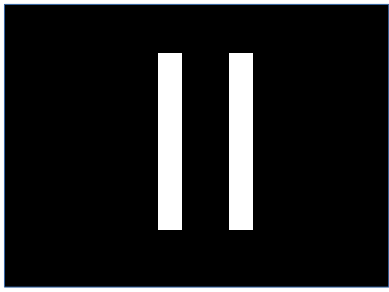

frontiers in Plant Science

ORIGINAL RESEARCH
published: 22 December 2020
doi: 10.3389/fpls.2020.588846

Genome-Wide Identification of *Populus* Malectin/Malectin-Like Domain-Containing Proteins and Expression Analyses Reveal Novel Candidates for Signaling and Regulation of Wood Development

Vikash Kumar[1], Evgeniy N. Donev[1], Félix R. Barbut[1], Sunita Kushwah[1], Chanaka Mannapperuma[2], János Urbancsok[1] and Ewa J. Mellerowicz[1]*

[1] Department of Forest Genetics and Plant Physiology, Umeå Plant Science Centre, Swedish University of Agricultural Sciences, Umeå, Sweden, [2] Department of Plant Physiology, Umeå Plant Science Centre, Umeå University, Umeå, Sweden

OPEN ACCESS

Edited by:
Seonghoe Jang, World Vegetable Center Korea, South Korea

Reviewed by:
Hanyao Zhang, Southwest Forestry University, China
Melis Kucukoglu, University of Helsinki, Finland
Nathalie Leblanc-Fournier, Université Clermont Auvergne, France

***Correspondence:**
János Urbancsok
janos.urbancsok@slu.se

Specialty section:
This article was submitted to Plant Development and EvoDevo, a section of the journal Frontiers in Plant Science

Received: *11 August 2020*
Accepted: *18 November 2020*
Published: *22 December 2020*

Citation:
Kumar V, Donev EN, Barbut FR, Kushwah S, Mannapperuma C, Urbancsok J and Mellerowicz EJ (2020) Genome-Wide Identification of Populus Malectin/Malectin-Like Domain-Containing Proteins and Expression Analyses Reveal Novel Candidates for Signaling and Regulation of Wood Development. Front. Plant Sci. 11:588846. doi: 10.3389/fpls.2020.588846

Malectin domain (MD) is a ligand-binding protein motif of pro- and eukaryotes. It is particularly abundant in Viridiplantae, where it occurs as either a single (MD, PF11721) or tandemly duplicated domain (PF12819) called malectin-like domain (MLD). In herbaceous plants, MD- or MLD-containing proteins (MD proteins) are known to regulate development, reproduction, and resistance to various stresses. However, their functions in woody plants have not yet been studied. To unravel their potential role in wood development, we carried out genome-wide identification of MD proteins in the model tree species black cottonwood (*Populus trichocarpa*), and analyzed their expression and co-expression networks. *P. trichocarpa* had 146 *MD* genes assigned to 14 different clades, two of which were specific to the genus *Populus*. 87% of these genes were located on chromosomes, the rest being associated with scaffolds. Based on their protein domain organization, and in agreement with the exon-intron structures, the *MD* genes identified here could be classified into five superclades having the following domains: leucine-rich repeat (LRR)-MD-protein kinase (PK), MLD-LRR-PK, MLD-PK (*Cr*RLK1L), MLD-LRR, and MD-Kinesin. Whereas the majority of *MD* genes were highly expressed in leaves, particularly under stress conditions, eighteen showed a peak of expression during secondary wall formation in the xylem and their co-expression networks suggested signaling functions in cell wall integrity, pathogen-associated molecular patterns, calcium, ROS, and hormone pathways. Thus, *P. trichocarpa MD* genes having different domain organizations comprise many genes with putative foliar defense functions, some of which could be specific to *Populus* and related species, as well as genes with potential involvement in signaling pathways in other tissues including developing wood.

Keywords: *Populus*, cell wall integrity, malectin domain, malectin-like domain, CBM57, receptor-like protein kinases, *Cr*RLK1L

INTRODUCTION

Plant cells are surrounded by cell walls made of cellulose, hemicelluloses, pectins and structural proteins, with lignin being present in cell types specialized for mechanical support (sclerenchyma) and water transport (xylem). Cell wall biosynthesis needs to be regulated so that its mechanical properties can be adapted to different circumstances according to the signals perceived. It is becoming generally accepted that there is constant feedback from the wall to the protoplast, mediated by different molecular pathways commonly termed cell wall integrity (CWI) signaling (Hématy et al., 2007; reviewed by Wolf and Höfte, 2014; Hamann, 2015; Voxeur and Höfte, 2016; Wolf, 2017; Rui and Dinneny, 2020). Perception of signals external to the protoplast is usually mediated by plasmalemma-localized proteins with various ectodomains. One large group of ectodomain-containing proteins is the receptor-like kinases (RLKs) that allow the plant cells to perceive external cues and transduce them, using a phosphorylation relay, into signals to initiate cellular responses (Gish and Clark, 2011; Engelsdorf and Hamann, 2014). Plant RLKs belong to the RLK/Pelle kinase family, one of the largest gene families in plants with more than 600 members in *Arabidopsis* (Shiu and Bleecker, 2001, 2003). It comprises both RLKs and receptor-like cytoplasmic kinases (RLCKs), and has been divided into 45 subfamilies, including wall-associated kinases, extensin-like RLKs, lectin RLKs, and leucine-rich repeat RLKs. RLCKs are cytoplasmic kinases without a transmembrane domain (TMD) and they recognize signaling molecules intracellularly. The RLKs usually function as heterodimers: one subunit with a large extracellular domain interacts with a ligand, and the other, which has a smaller extracellular domain, stabilizes this interaction and enhances signal transduction (Xi et al., 2019).

Among the different clades of plant RLKs, the *Catharanthus roseus* receptor-like kinase 1-like proteins (*Cr*RLK1Ls) have received significant attention as mediators of CWI (reviewed by Wolf and Höfte, 2014; Li et al., 2016; Franck et al., 2018). The family is conserved in all Streptophytes analyzed so far, including moss and liverwort, indicating its ancient origin (Galindo-Trigo et al., 2016). *Cr*RLK1Ls are characterized by two malectin ectodomains (MDs) forming a malectin-like domain (MLD), a transmembrane helix and a C-terminal intracellular Ser and Thr kinase domain. The *Arabidopsis* genome contains 17 *Cr*RLK1L genes and the majority of them have been functionally analyzed. THESEUS1 (THE1) was the first member to be identified as a mediator of dwarfism and ectopic lignification induced by defects in cellulose biosynthesis (Hématy et al., 2007; Merz et al., 2017). Other members of *Cr*RLK1L family including CURVY1 (CVY1), FERONIA (FER) and ANXUR1 (ANX1) are required for polar cell growth in different cell types. FER, ANX1/2 and BUDDHA'S PAPER SEAL1 and 2 (BUPS1 and 2) participate in sexual reproduction. FER mediates signaling by reactive oxygen species (ROS) and Ca^{2+} during pollen tube reception at the filiform apparatus (Escobar-Restrepo et al., 2007), whereas ANX1/2 together with BUPS1/2 form a receptor complex for RAPID ALKALINIZATION FACTOR (RALF) 4 or 19 in the growing tip of pollen tube and regulate ROS and Ca^{2+} gradients essential for its growth and CWI (Ge et al., 2017). In addition, *Cr*RLK1L proteins are involved in immune responses. FER positively regulates pathogen-associated molecular pattern (PAMP)-triggered immunity (PTI) by facilitating the formation of a receptor complex composed of BAK1-FLS2-FER or BAK1-EFR-FER (Stegmann et al., 2017), whereas ANX1 functions antagonistically in PTI and inhibits effector-triggered immunity (ETI) (Mang et al., 2017). The downstream responses of *Cr*RLK1Ls are diverse and include Rho-GTPases activating NADPH oxidases involved in the production of apoplastic ROS (Foreman et al., 2003; Duan et al., 2010; Denness et al., 2011; Boisson-Dernier et al., 2013), RLCKs (Boisson-Dernier et al., 2015; Du et al., 2016), inhibition of the proton pump AHA1 (Haruta et al., 2014), Ca^{2+} signaling mediated by MLO proteins (Kessler et al., 2010; Meng et al., 2020), as yet unknown Ca^{2+} channels and a signaling cascade via intracellular kinases that eventually activate or repress gene transcription (Franck et al., 2018).

The MLD, which is characteristic of *Cr*RLK1L proteins, and the MD are also found in other types of plant RLKs (Zhang et al., 2016; Bellande et al., 2017). The MD was first identified in the protein called malectin residing in the endoplasmic reticulum of *Xenopus laevis* and other animals, where it monitors protein glycosylation by binding diglucose motifs with α-1,4-, α-1,3- and α-1,2-linkage in glycosylated proteins (Schallus et al., 2008, 2010). However, the crystal structure of MLD in ANX1, ANX2, and FER indicated an absence of the aromatic residues that interact with diglucosides in animal MDs, and suggested different ligand specificities and/or functions of the MLDs in these proteins (Du et al., 2018; Moussu et al., 2018; Xiao et al., 2019). Several peptides from the RALF family have been demonstrated to bind to ectodomains of *Cr*RLK1L proteins in *Arabidopsis*: RALF34 to THE1 (Gonneau et al., 2018), RALF1/17/23/32/33 to FER (Haruta et al., 2014; Stegmann et al., 2017), and RALF4/19 to the ANX1/2-BUPS1/2 receptor complex (Ge et al., 2017). Recently it has been shown that the binding of RALF23 to FER is stabilized by interaction with LORELEI-like-GPI-ANCHORED PROTEINS (LLGs) and the formation of such a heterocomplex is required for PTI signaling (Xiao et al., 2019). Moreover, the ectodomain of FER has been shown to bind to the leucine-rich repeat (LRR) domain of LRR-extensin 1 (LRX1) (Dünser et al., 2019) and to pectin (Feng et al., 2018).

Malectin domain is classified as CBM57 in the CAZy database[1]. Interestingly, the CBM57 family is greatly expanded in the model tree species *Populus trichocarpa* compared to the herbaceous model plant *Arabidopsis thaliana* (Kumar et al., 2019). Moreover, transcript of the CBM57 family members are highly upregulated in developing wood tissues of *Populus tremula* (Kumar et al., 2019) and *Eucalyptus grandis* (Pinard et al., 2015). These data suggest that MD/MLD-containing proteins (subsequently called MD proteins) have important functions in trees. We hypothesize that MD proteins are involved in the regulation of cell wall formation during secondary growth via pathways analogous to those reported for primary growth (Wolf and Höfte, 2014; Hamann, 2015; Li et al., 2016; Wolf, 2017), and that they participate in signaling cascades related to stress responses and developmental processes in trees. To

[1] http://www.cazy.org/

find candidates for receptors active during secondary growth, we first carried out genome-wide identification of *P. trichocarpa* genes with predicted MD and MLD. Second, we used expression datasets from different organs (Sundell et al., 2015; Immanen et al., 2016) and high-resolution expression data for wood developmental zones in *P. tremula* (Sundell et al., 2017) to identify those MD proteins that are expressed during wood biosynthesis, and to classify them according to expression at specific stages of xylogenesis. Finally, we identified co-expression networks for the MD proteins expressed during secondary wall deposition, which include their putative interactors. Our analyses provide a framework to identify CWI monitoring, stress response, and other signaling pathways operating during wood development.

MATERIALS AND METHODS

Identification of *P. trichocarpa* Proteins With Malectin and Malectin-Like Domains

The MD proteins of black cottonwood (*P. trichocarpa* Torr. and A. Gray) were identified by Basic Local Alignment Search Tool (BLAST) (Altschul et al., 1990) searches in the genome browser of the PopGenIE database[2] containing *P. trichocarpa* genome assembly v3.0, using as baits the *P. trichocarpa* proteins containing Pfam domains 11721 and 12819, corresponding to MD and MLD, respectively, retrieved from the Pfam database[3] (El-Gebali et al., 2019). The same approach was applied to *A. thaliana* using the TAIR database (v10.0) for BLAST searches[4]. The BLASTP tool of a high-performance sequence aligner DIAMOND was used in –unal 0, –evalue 1e-05, –max-target-seqs 4000, and –more-sensitive mode, other parameters were kept as default (Buchfink et al., 2015). All other web-based tools were used in default mode as per developers' recommendations. The presence of MDs/MLDs in the proteins selected for both *P. trichocarpa* and *A. thaliana* was confirmed using the CDvist web tool[5] (Adebali et al., 2015), which also served to identify other conserved domains in these proteins. The amino acid sequence lengths, molecular weights, isoelectric points and indices of protein stability of the putative proteins were calculated using the ProtParam tool provided on the ExPASy website[6]. The presence of signal peptides and subcellular localization were predicted with the SignalP 4.1 server[7] (Petersen et al., 2011) and DeepLoc-1.0 server[8] (Armenteros et al., 2017), respectively. The exon-intron organization of the *PtMD* genes was determined using the PopGenIE GBrowse tool[9] and their localization was mapped to *P. trichocarpa* chromosomes using the chromosome-diagram tool[10]. Assignment of a gene to a gene cluster on each chromosome was based on the definition of Holub (2001).

Phylogenetic Analysis and Classification of the MD Proteins of *P. trichocarpa*

All *Pt*MD proteins identified were classified into clades based on phylogenetic analysis with *A. thaliana*. The amino acid sequences were aligned by MUSCLE[11] and phylogenetic trees were constructed using the neighbor-joining (NJ) method in the MEGA7 software package with a bootstrap test with 1000 replicates (Kumar et al., 2016).

To identify the conserved residues in MD and MLD regions of poplar MD proteins, these regions were aligned with reference sequences using Jalview Version 2 (Waterhouse et al., 2009) with the MAFFT option (Katoh et al., 2005).

To evaluate evolutionary conservation of *MD* genes across tree species, we have extracted protein sequences for *Eucalyptus grandis* v2.0, *Malus domestica* v1.0, *Salix purpurea* v1.0, *Theobroma cacao* v2.1, *Citrus sinensis* v1.1, *Prunus persica* v1.0 and *Betula pendula* v1.0 from Phytozome genome portal[12] using BLAST (with same parameters as stated in the section above) and *Pt*MDs as query sequences. The protein sequences of resulting hits and the MD proteins of *P. trichocarpa* and *A. thaliana* were used to generate a phylogenetic tree using one click method described in https://ngphylogeny.fr (Lemoine et al., 2019). The phylogenetic tree and other detailed method descriptions can be found at ftp://plantgenie.org/Publications/Kumar2020/Phylogeny.

Expression Analysis of *PtMDs* in Developing Leaves and Wood

Developing leaves (leaf number 8, 11, 21 and 23) and developing wood including cambium/phloem and xylem depositing secondary walls were collected from 10 weeks old hybrid aspen (*Populus tremula* L. *x tremuloides* Michx.) grown in the greenhouse. The cultivation conditions and RNA extraction protocols were as described in Ratke et al. (2018). Between five and ten biological replicates of each sample were sequenced using Illumina HiSeq-PE150 platforms of Novogene Bioinformatics Technology Co., Ltd. (Beijing). Quality control and mapping to *P. trichocarpa* transcriptome v3.0 of leaf 8 and 11 samples were performed by Novogene. Other samples had RNA-Seq raw data filtered using FastQC (v0.10.1[13]). rRNA reads were removed using SortMeRNA v1.8 (Kopylova et al., 2012). Low-quality reads were removed using Trimmomatic v0.27 (Lohse et al., 2012) with a sliding window of 5 bp, minimum quality score of 20, minimum read length of 50 bp, minimum leading read quality of 20 and a custom clipping file containing all Illumina adapters. The preprocessed reads were mapped to v3.0 of the *P. trichocarpa* transcriptome (retrieved from PopGenIE see

[2]http://popgenie.org
[3]https://pfam.xfam.org
[4]http://www.arabidopsis.org/
[5]http://cdvist.zhulinlab.org
[6]https://web.expasy.org/protparam/
[7]http:// www.cbs.dtu.dk/services/SignalP/
[8]http://www.cbs.dtu.dk/services/DeepLoc/
[9]http://popgenie.org/gbrowse
[10]http://popgenie.org/chromosome-diagram
[11]http://phylogeny.lirmm.fr/phylo_cgi/index.cgi
[12]https://genome.jgi.doe.gov/portal/pages/dynamicOrganismDownload.jsf?organism=Phytozome
[13]www.bioinformatics.babraham.ac.uk/projects/fastqc/

footnote 2) using Kallisto (v0.43.1) with default parameters (Bray et al., 2016). The raw counts were normalized separately for each experiment using Variance Stabilizing Transformation (VST) in R (v3.4.0; R Core Team, 2014) using the Bioconductor (v3.4; Gentleman et al., 2004) DESeq2 package (v1.16.1; Love et al., 2014). Then the VST data were merged together using a sample-based median centering approach as described by Kumar et al. (2019; the R scripts are available at https://github.com/UPSCb/UPSCb/tree/master/manuscripts/Kumar2018). Mean VST data for *PtMD*s were displayed using ComplexHeatmap with default parameters and using the tissue with a peak of expression for each gene as a categorical variable for clustering (Gu et al., 2016). The tissue/organ specificity score *tau* - a score ranging from 0 (ubiquitous expression) to 1 (tissue/organ specific expression), as detailed in Yanai et al. (2005) was calculated for each *PtMD* gene. The customized R scripts used to calculate *tau* are available at https://github.com/UPSCb/UPSCb/tree/master/manuscripts/Kumar2018. The raw RNA-Seq data for this study have been deposited in the European Nucleotide Archive (ENA) at EMBL-EBI under accession number PRJEB41170[14].

Expression of *PtMDs* in Different Organs of *Populus*

RNA-Seq datasets of expression values in different tissues/organs of outdoor and greenhouse grown aspen (*P. tremula* L.) and hybrid aspen (*P. tremula* L. x *tremuloides* Michx., clone T89) are available from the PlantGenIE website (Sundell et al., 2015). Data for secondary tissues of greenhouse grown T89 hybrid aspen are detailed by Immanen et al. (2016). Raw data for all biological replicates of each sample (min. = 3) were preprocessed as described in the section above except that the reads were aligned to the *Populus trichocarpa* genome using STAR and quantified using HTSeq. Other steps of quality assessment and filtering are explained above and available at: http://www.epigenesys.eu/en/protocols/bio-informatics/1283-guidelines-for-rna-seq-data-analysis. The VST values were median-centered for each sample, and means for all biological replicates were used for hierarchical clustering and calculating the *tau* tissue/organ specificity score, as described above.

PtMDs Involved in Wood Biosynthesis

The AspWood high-spatial-resolution RNA-Seq dataset (Sundell et al., 2017) was used for analysis of expression of *PtMDs* during wood biosynthesis. The database provides VST expression values for four trees. Identity of wood developmental zones was based on the expression of marker genes (Sundell et al., 2017). A heatmap of *PtMD* expression in wood developmental zones was constructed for one representative tree (tree 1) using the AspWood server[15].

Co-expression Analysis

PtMD genes from the selected expression clusters were used as 'Guide Genes' to obtain co-expression networks for developing secondary tissues, using the AspWood program (see text footnote 14). The AspWood calculates co-expression networks utilizing mutual information and context likelihood of relatedness as explained by Sundell et al. (2017). The corresponding GraphML files were generated using the ExNet tool[16] with a Z-score threshold of 5.0, and visualized using Cytoscape 3.4.0 (Shannon et al., 2003).

RESULTS AND DISCUSSION

Identification of MD Proteins in *P. trichocarpa* and Their Classification

Searches of the *P. trichocarpa* and *A. thaliana* genomes for MD proteins resulted in the identification of 146 and 87 gene models, respectively (**Supplementary Tables 1**, **2**). Previous analyses identified 62 *MD* genes in strawberry (Zhang et al., 2016), 74 in *A. thaliana* (Bellande et al., 2017; Sultana et al., 2020), and 84 in rice (Jing et al., 2020).

The *P. trichocarpa* proteins identified were analyzed for sequence similarity using protein sequence alignment and phylogenetic analysis, revealing the presence of 12 clades supported by at least 87 % of bootstrap replicates, and three ungrouped sequences, two of which had orthologous sequences in *A. thaliana*, and were therefore considered to be two single member clades III and XI (**Figures 1**, **2**). The sequences were numbered *PtMD1* to *PtMD146* according to their sequential appearance in the intraspecific phylogenetic tree (**Figure 1**). The predicted protein properties and probable subcellular localizations of *Pt*MD proteins are listed in **Supplementary Table 1**. The deduced sequence lengths ranged from 274 to 1192 amino acids, and isoelectric points (pIs) ranged from 4.55 to 9.49. Seventy-six out of the 146 *Pt*MD proteins had a signal peptide (SP) cleavage site. The SP was not found in any members of clades I and XIV. Thirteen of the *Pt*MDs were predicted to be soluble proteins, with the predicted localization of six of them being extracellular, six - including all members of clade XIV - being cytoplasmic and one being peroxisomal. Out of 133 membrane proteins, one was predicted to localize in the endoplasmic reticulum.

Domain analysis (**Figure 1** and **Supplementary Table 1**) revealed the presence of two major groups, one with MD (clades I–VIII, and XIV) and the other with MLD (clades IX to XIII). There was relatively little conservation in the amino acid sequence between the two domains (**Figure 3**), and in many cases, the proteins having MLD were not classified as members of the CBM57 family (**Supplementary Table 1**; Kumar et al., 2019). Nevertheless, similarity between MD and each of the two sub-domains of MLD has previously been shown by comparisons of their 3D structures (Moussu et al., 2018). Among the conserved residues of MD, which were proposed to interact with diglucose in *Xenopus laevis* malectin (Y67, Y89, Y116, F117, and D186) (Schallus et al., 2008, 2010), only Y67 and F117 were conserved in poplar MD (**Figure 3** and **Supplementary Figure 1**). In contrast, the residues proposed to interact with ligands in the MLD of ANX1, Y77, R102, E150, E182, R215, L232, and R234 (Moussu et al., 2018) were to a large

[14]https://www.ebi.ac.uk/ena/browser/view/PRJEB41170

[15]http://aspwood.popgenie.org/aspwood-v3.0/

[16]http://popgenie.org/exnet

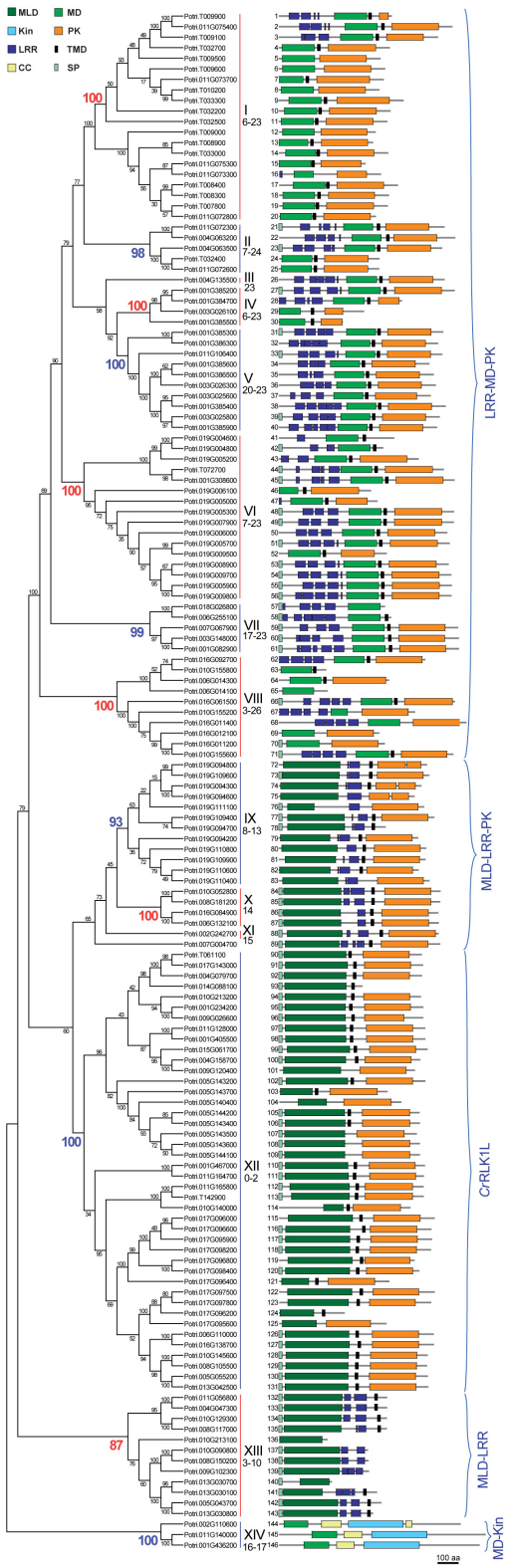

FIGURE 1 | Phylogenetic tree of poplar malectin/malectin-like domain-containing proteins (*Pt*MDs) showing their domain structures. The tree was constructed from MUSCLE-aligned amino acid sequences using the *(Continued)*

FIGURE 1 | Continued
neighbor-joining method in MEGA 7.0 with 1000 bootstrap replicates and bootstrap support is displayed beside the nodes as percentages. *Pt*MDs are identified by the number shown next to each protein structure. Domain abbreviations are: CC, coiled coil; Kin, kinesin; LRR, leucine-rich repeat; MD, malectin domain; MLD, malectin-like domain; PK, protein kinase; SP, signal peptide; TMD, transmembrane domain. Main clades are numbered with Roman numerals and their corresponding bootstrap values are colored in the phylogenetic tree. Numbers below the Roman numerals correspond to the number of introns observed within a clade. Five groups containing clades with similar protein domain structures are identified by the blue brackets: LRR-MD-PK (also known as poplar LRR-RLK XIII; Zan et al., 2013), MLD-LRR-PK (known as poplar LRR-RLK I; Zan et al., 2013), *Cr*RLK1L, MLD-LRR, and MD-Kin.

extent conserved in poplar MLD (**Figure 3** and **Supplementary Figures 2A,B**).

Clades I-XII had MD or MLD followed by a transmembrane helix preceding the protein kinase domain, in agreement with the typical topology of RLKs (**Figure 1** and **Supplementary Table 1**). Protein kinase domains were frequently of the Tyr kinase type. Some MD proteins with a kinase domain had extracellular localization predicted for this domain (**Supplementary Table 1**). Clade V was the only one in which all kinase domains were predicted to be intracellular. Extracellular kinase domains were also predicted for the majority of G- and L-type lectin RLKs in poplar (Yang et al., 2016) but experimental validation of such predictions is currently lacking.

In all clades but XII and XIV, several LRR domains were found in tandem repeats. The LRR domain forms a horseshoe-like structure that functions in protein-protein or protein-ligand interactions (Bella et al., 2008). LRRs are known to occur in LRR-RLKs, receptor-like proteins (RLPs), resistance (R) proteins, LRR extensins (LRX), and other families (Wang et al., 2008; Draeger et al., 2015; Choi et al., 2016; Song et al., 2018). Poplar MD proteins had various types of LRR domains, most frequently LRR_4 and LRR_8 (**Supplementary Table 1**). The proteins from clade XIII had unique combinations of LRR domains; *Pt*MD134 and *Pt*MD135 had the sd00031 LRR domain, *Pt*MD141 had the LRR_1 domain, and *Pt*MD137, -138, and -139 had the LRRNT2 domain. The LRR domains found in the poplar MD family either preceded MD (clades I-VIII) or followed MLD (clades IX-XI and XIII) (**Figure 1**). Thus, the placement of LRR domains correlated with the presence of either MD or MLD. In clades with members containing LRRs, there were also several members devoid of any LRRs. This probably indicates domain loss due to unequal crossing over. A previous study on poplar LRR-RLKs (Zan et al., 2013) identified and classified some of the MD proteins studied here; MD clades I-VIII were previously classified as LRR-RLK group XIII, and MD clades IX-XI as LRR-RLK group I (**Supplementary Table 1**).

Clade XI and clade XII members exhibited an unusual TMD, CD12087, which is typical of epidermal growth factor receptors of animals where it functions in receptor dimerization (Mineev et al., 2010). Whether it can carry out such a function in plant MD proteins remains to be investigated.

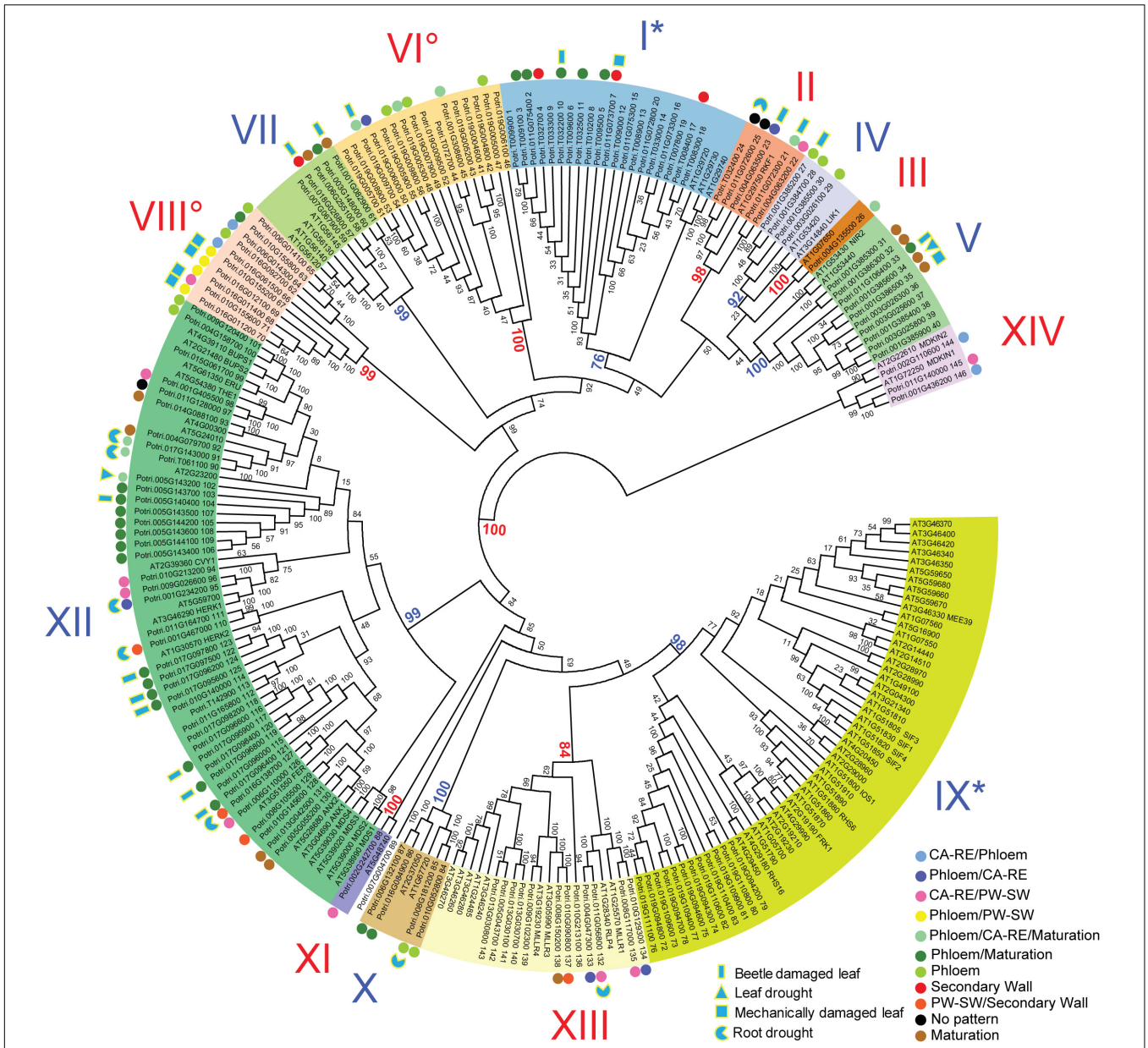

FIGURE 2 | Phylogenetic tree of malectin/malectin-like domain-containing proteins in *P. trichocarpa* and *A. thaliana*. Each protein ID is followed by the name (*A. thaliana*) or *Pt*MD protein number (*P. trichocarpa*). The phylogenetic tree was constructed based on MUSCLE-aligned amino acid sequences using the neighbor-joining method in MEGA 7.0 using 1000 bootstrap replicates, and the bootstrap support is displayed in percentages. Main clades are numbered with Roman numerals, and their supporting bootstrap values are shown in color. Colored dots beside *PtMDs* identify genes expressed in secondary vascular tissues based on the AspWood (http://aspwood.popgenie.org/aspwood-v3.0/) database and showing maximum expression in different developmental zones as indicated by colors. CA-RE, cambium-radial expansion zone; PW-SW, primary to secondary wall transition zone. Blue shapes with yellow outlines show stress-related expression based on the aspen expression atlas available at http://popgenie.org. Degree symbols and asterisks beside Roman numerals indicate clades that are represented by only one species or are significantly expanded in one species (χ^2-test, $P \leq 0.05$), respectively.

Clade XIV domain structure and topology was unique in having a kinesin domain (Kin) along with an N-terminal MD (**Figure 1**). This clade has not been previously included in the surveys of *MD* genes in *A. thaliana* (Bellande et al., 2017) or rice (Jing et al., 2020). Recently, one of the *A. thaliana* clade XIV members, MDKIN2, was found to function in pollen and seed development (Galindo-Trigo et al., 2020). Orthologs of the clade XIV genes could be identified in many species of Viridiplantae, including moss, lower vascular plants, dicots and monocots.

Based on domain composition and domain order, poplar MD gene clades could be grouped into a higher order organization with five superclades characterized by the following domain patterns: 1) LRR-MD-PK (LRR-RLK group XIII, Zan et al., 2013),

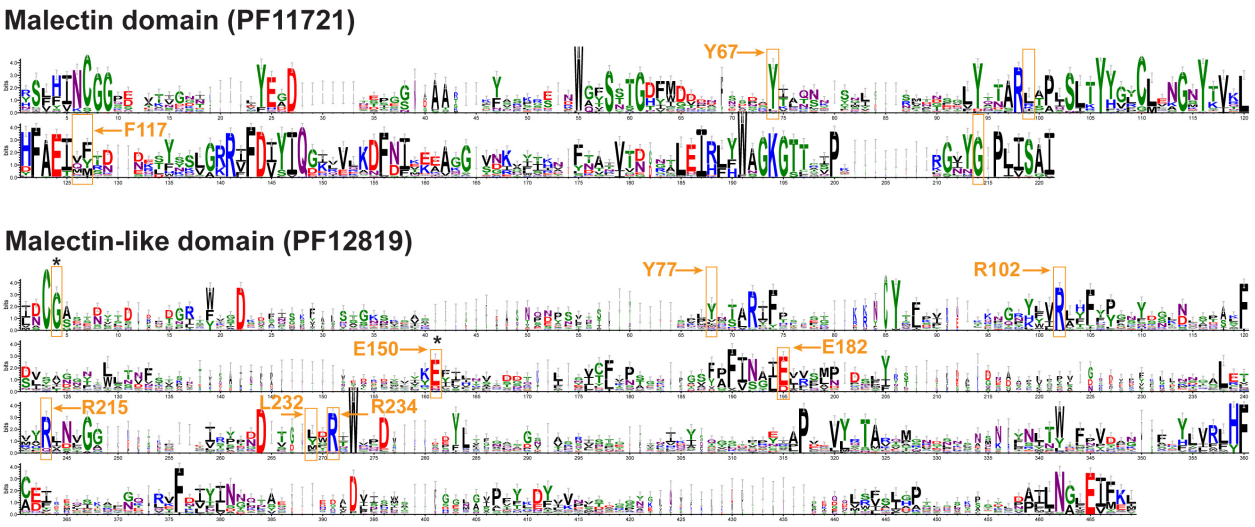

FIGURE 3 | Conserved motifs in malectin (top) and malectin-like (bottom) domains of *P. trichocarpa*. The residues involved in interaction with ligands according to Schallus et al. (2008) and Moussu et al. (2018) are shown in orange boxes. The amino acids conserved in *P. trichocarpa* are marked by arrows. The mutated residues in the THE1 protein in the *the1* mutants studied (Hématy et al., 2007) are indicated by black asterisks. The logos were created based on *P. trichocarpa* MD/MLD amino acid sequence alignments by using the WebLogo 3.7.4 online tool (http://weblogo.threeplusone.com, Crooks et al., 2004). The conservation of amino acid residues is represented in bits and residues are colored according to chemical properties. The associated multiple sequence alignments are shown in **Supplementary Figures 1**, **2**.

2) MLD-LRR-PK (LRR-RLK group I, Zan et al., 2013), 3) MLD-PK (*Cr*RLK1L), 4) MLD-LRR (RLPs) and 5) MD-Kin (**Figure 1**).

Chromosomal Distribution of *MD* Genes in *P. trichocarpa*

127 out of the 146 poplar *MD* gene models were mapped to chromosomes, while 19 gene models were located on five different scaffolds (**Figure 4**). The majority of chromosomal genes (79) were present in clusters comprising between two and eleven genes (**Figure 4** and **Supplementary Table 3**). Clusters were also present on the scaffolds. The clusters consisted of tandem repeats having the same or reverse orientations. This large number of tandem duplications strongly suggests that the main mechanism of MD family expansion in *P. trichocarpa* is via local gene duplication, rather than whole genome duplications. Gene multiplication at a given locus could occur via an unequal crossing over mechanism, which after multiple rounds would result in large numbers of tandemly repeated sequences. Such a mechanism was proposed as featuring particularly in various *LRR* gene families (Schaper and Anisimova, 2015) including *LRR-RLK* (Shiu and Bleecker, 2001; Zan et al., 2013; Zulawski et al., 2014; Zhang et al., 2016; Wang et al., 2019) and *R* genes (Choi et al., 2016). Indeed, 11 out of our16 clusters of *PtMD* genes had members with LRR domain(s) (**Supplementary Table 3**).

Tandem duplications allow rapid gene family expansion and the creation of novel alleles are thought to be particularly important for the co-evolution of *R* and *Avr* genes in hosts and their parasites (Holub, 2001; Choi et al., 2016). Partial duplications with omission of some domains form a key mechanism for neofunctionalization. Such a process apparently characterized the poplar MD family, since there were seven out of 16 clusters that included genes with LRR and kinase domains along with closely related members without LRR domains (**Figure 4** and **Supplementary Table 3**).

Analysis of Exon-Intron Structures of *PtMD* Genes

Exon-intron structure reflects the evolutionary history of genes; hence we analyzed the exon-intron organization of *PtMDs*. Although the majority of clades displayed very diverse numbers of introns (**Supplementary Table 4** and **Figure 1**), the maximum number of introns for clades within a superclade was similar. The superclade LRR-MD-PK, comprising clades I-VIII, had genes with very large numbers of introns (maximum between 23 and 26); superclade MLD-LRR-PK (clades IX-XI) had at most 15 introns; superclade MLD-PK (clade XII or the *Cr*RLK1L group) contained genes with up to two, but typically without any introns; and superclades MLD-LRR (clade XIII) and MD-Kin (clade XIV) had at most 10 and 17 introns, respectively (**Supplementary Table 4** and **Figure 1**). Lack, or low frequency, of introns in *Cr*RLK1L genes has also been observed in other species including strawberry, *Arabidopsis* and rice (Zhang et al., 2016; Bellande et al., 2017; Jing et al., 2020). Thus, the exon-intron organization of poplar *MD* genes supported their grouping into superclades, which represent ancestral diversification of plant *MD* genes.

Comparison of *P. trichocarpa* and *A. thaliana* MD Proteins

The phylogenetic tree of MD proteins was generally consistent between *P. trichocarpa* and *A. thaliana* with bootstrap values of greater than 76 % for the main clades (**Figure 2**). Three exceptions were noted, however: one orphan protein *Pt*MD89,

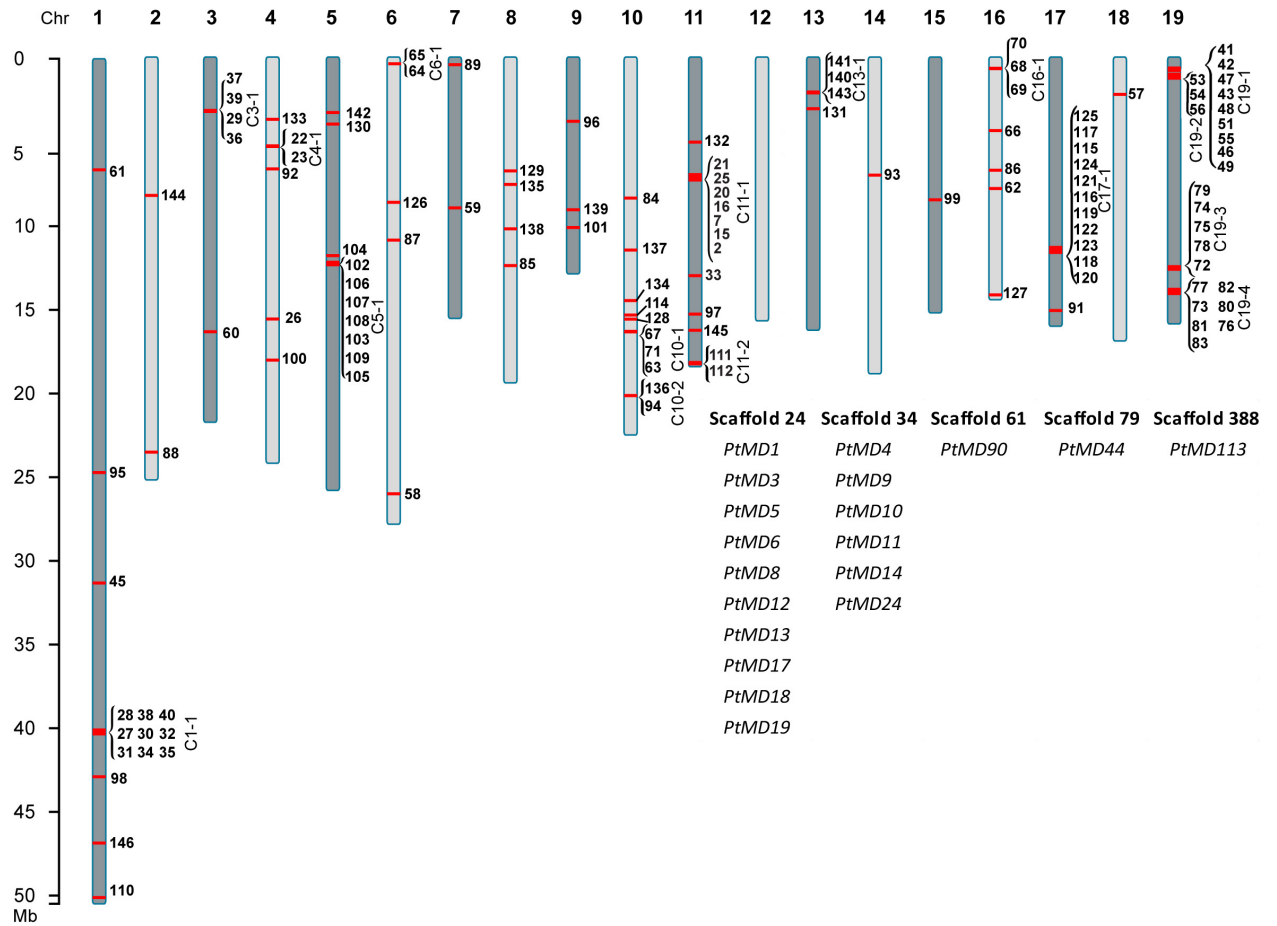

FIGURE 4 | Chromosomal localization of the *PtMD* genes. The *PtMD* ID numbers are indicated beside chromosomes. Several *PtMDs* are found in clusters, shown by parentheses and labeled with a letter "C" followed by the chromosome number and the cluster number. Some *PtMDs* are on scaffolds, shown below the chromosomes.

clade VI that included *Pt*MD41-*Pt*MD56, and clade VIII with *Pt*MD62-*Pt*MD71. These poplar genes apparently did not have orthologs in *A. thaliana*. To address a hypothesis that these genes represent tree-specific functions, we analyzed the MD gene families in other tree species with the whole genome data available (**Supplementary Figure 3**). Close homologs to *PtMD89* were found in other tree species including *Salix purpurea*, *Eucalyptus grandis*, *Theobroma cacao*, *Malus domestica*, *Prunus persica*, and *Citrus sinensis* (**Supplementary Figure 3**). Each of these species had only one putative *PtMD89* ortholog indicating that *PtMD89* function is conserved in angiosperm trees belonging to different families. Clades VI and VIII include tandemly repeated genes and were not well resolved by the phylogenetic analysis (**Figure 4** and **Supplementary Table 3**). The clear homologs to *P. trichocarpa* tandemly replicated genes of clade VI were present in *Salix purpurea* although we cannot exclude that genes with less supported association to clade VI are present in *Prunus persica*, *Malus domestica*, *Theobroma cacao* and *Betula pendula* (**Supplementary Figure 3**). Clade VIII included only *P. trichocarpa* and *Salix purpurea* genes, but this clade had a weak bootstrap support (**Supplementary Figure 3**). Thus, the genes of clades VI and VIII had undergone recent tandem duplication in the *P. trichocarpa* lineage after its separation from that of *A. thaliana* that could be conserved in other members of Salicaceae. It is therefore possible that they represent specialized genes, such as *R* genes important for immunity, that co-evolved with poplar symbionts and/or pathogens of the Salicaceae family (Holub, 2001).

Besides identifying clades not represented in *Arabidopsis*, we found that the relative clade sizes (number of genes per clade relative to genome size) show some differences between the two species (**Figure 2**). Clade IX was expanded in *A. thaliana*, whereas clade I was expanded in *P. trichocarpa* (χ^2-test at $P \leq 0.05$). The phylogenetic analysis of *MD* genes including different tree species confirmed the expansion of clade IX in *A. thaliana* and clade I in *P. trichocarpa* (**Supplementary Figure 3**).

Domain composition and organization were consistent between *P. trichocarpa* and *A. thaliana* in clades present in both species (**Supplementary Tables 1**, **2**). Previous studies in *A. thaliana* classified LRR-RLKs (Shiu and Bleecker, 2001) and

assigned them putative receptor or co-receptor functions based on the sizes of ectodomains (Xi et al., 2019). Many MD proteins identified in the current study were among the previously classified LRR-RLKs (**Supplementary Table 2**). The group of clades I-VIII, except for clades VI and VIII, which were not represented in *A. thaliana*, have been classified as being of the LRR-VIII-2 class (Shiu and Bleecker, 2001). This group had large ectodomains including several LRR motifs followed by MD, TMD and internal kinase domains (LRR-MD-PK) (**Supplementary Table 2** and **Figure 1**). *A. thaliana* proteins of clades IX-XI belong to class LRR-I (Shiu and Bleecker, 2001), having a large MLD ectodomain terminated with a short LRR repeat, TMD, and an internal protein kinase domain (MLD-LRR-PK), as was observed for poplar (**Supplementary Table 2** and **Figure 1**). *A. thaliana* clade XII proteins correspond to the *Cr*RLK1L group, which is characterized by a large MLD ectodomain followed by TMD and the internal protein kinase domain, whereas clade XIII in *A. thaliana*, as in *P. trichocarpa*, was characterized by a large ectodomain including MLD and LRR domains. Such proteins are classified as RLPs (Wang et al., 2008).

Only four out of the 14 clades identified contained members that have been functionally analyzed in *A. thaliana*. In addition to clade XII (*Cr*RLK1L), which has been the most extensively studied, with members involved in CWI sensing, polar growth, fertilization, and immune responses (Franck et al., 2018), the members of clades IV, V, and IX have been functionally characterized. Clade IV includes LYSM RLK1-INTERACTING KINASE 1 (LIK1), an RLK interacting with the chitin receptor formed by the CERK1-LYSM RLK1 complex, which signals the presence of chitin and activates PTI (Le et al., 2014). Clade IX includes several RLKs involved in both immunity and development. For example, IMPAIRED OOMYCETE SUSCEPTIBILITY 1 (IOS1) acts as a co-receptor of flagellin, EF-Tu and chitin, interacting with FLS2, EFR, and CERK1, respectively (Yeh et al., 2016). STRESS INDUCED FACTORs 1-4 (SIF1, SIF2, SIF3 and SIF4) have been characterized as RLKs involved in biotic and abiotic stress responses (Yuan et al., 2018). SIF2 was found to interact with BAK1 and mediate PTI during pathogen attack. *FLG22-INDUCED RECEPTOR-LIKE KINASE 1* (*FRK1*) is known to be an early-induced PTI gene (Asai et al., 2002). *ROOT HAIR SPECIFIC 6* and *16* (*RHS6* and *RHS16*) were found to be specifically expressed in root hairs and *RHS16* overexpression dramatically altered root hair morphology, indicating an important function in root hair growth (Won et al., 2009), whereas MATERNAL EFFECT EMBRYO ARREST 39 (MEE39) was found to be essential for embryo development based on the mutant phenotype (Pagnussat et al., 2005).

Expression of *PtMDs* in Different Organs of *Populus*

RNA sequencing strategy was adopted to examine the expression of 146 *PtMD* genes in developing leaves and wood tissues (**Figure 5** and **Supplementary Table 5**). Datasets were centered by median expression in each sample and the variance-stabilized transformation (VST) expression values were clustered considering the tissue with maximum expression as a covariate. Majority of *PtMD* genes had the highest expression in the leaves, especially the fully mature ones (leaf 23). Relatively large number of *PtMD* genes was highly expressed in expanding leaves (leaf 8), and many of these genes were also highly expressed in the cambium. There were 12 and 13 *PtMD* genes with maximum expression in the cambium-phloem and developing xylem tissues, respectively. Majority of these genes showed generally high expression in leaves.

High expression in mature leaves suggests function in foliar defenses and homeostasis for majority of the *PtMD* genes. To investigate it, we also examined the RNA sequencing datasets available for different organs and tissues subjected to variety of stress and growth conditions in the greenhouse and in the field, and calculated VST expression values (**Figure 6** and **Supplementary Table 6**) using the same approach as used for our leaf and wood developmental series. Considering all datasets examined (**Figures 5**, **6** and **Supplementary Tables 5**, **6**), out of the 146 genes, 145 were expressed at least in one of the organs and tissues tested. Similar to our datasets, the majority of *PtMD* genes (99) showed maximum expression in leaves, especially the mature ones. Moreover, many of them (51) showed the highest expression in leaves exposed to abiotic/biotic stress, such as beetle, drought or mechanical damage. The genes highly expressed in mature and stress-exposed leaves usually exhibited high expression specificity as determined by the *tau* specificity score (**Supplementary Table 6**). Interestingly, genes belonging to the clades missing in *Arabidopsis* (VI and VIII) were found expressed, indicating that they are functional, and many of them showed a peak of expression in the mature and beetle or mechanically damaged leaves (**Figure 2** and **Supplementary Tables 5**, **6**) pointing to their involvement in stress responses. These observations support an important role of the leaf-expressed *PtMD* genes in foliar defense responses, some of which could be species-specific, as suggested by the phylogenetic analyses revealing differences in the presence and size of certain clades of *MD* genes (**Figure 2** and **Supplementary Figure 3**) as well as by the expression analyses in different species. For example, almost all *MD* genes of strawberry (*Fragaria vesca*) were upregulated upon exposure to low temperature or drought stress (Zhang et al., 2016), whereas in rice (*Oryza sativa*), the expression levels of many *MD* genes greatly increased upon salt and drought stress, but not in response to low temperature (Jing et al., 2020).

Twenty *PtMD* genes were most highly expressed in roots of which nine showed highest expression in roots exposed to drought. Genes with maximal expression values detected in stressed organs were distributed among clades I, II, IV, V, VI, VII, VIII, X, XII, and XIII (**Figure 2**), suggesting stress response functions for these clades. Interestingly, no gene that was maximally expressed in stressed organs was found in clades III, IX, XI or XIV, suggesting their involvement in other types of signaling. Several *PtMD* genes were most highly expressed in the vegetative growing organs: young roots or leaves (**Figures 5**, **6** and **Supplementary Tables 5**, **6**). Eight genes, all from clades XII and XIII, were most highly expressed in female flowers at various developmental stages, and four in mature seeds. The genes highly expressed in expanding female flower buds or in mature seeds

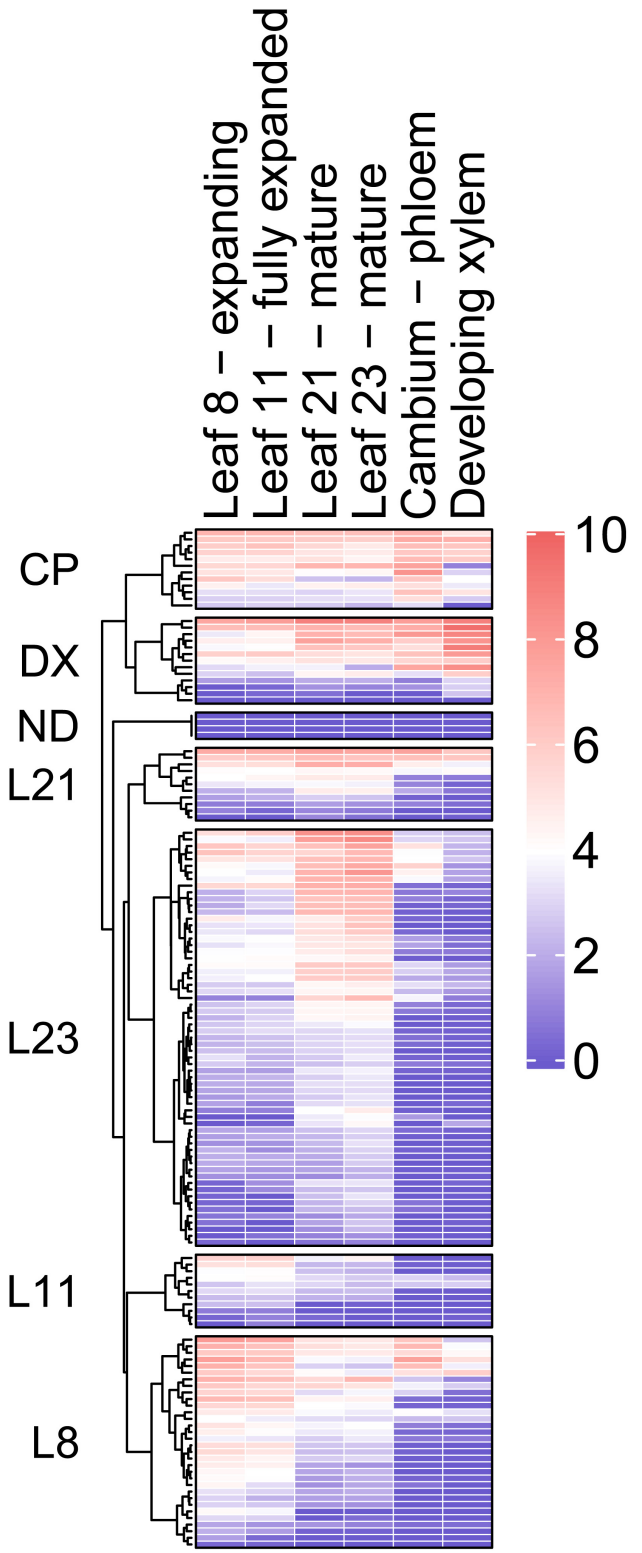

FIGURE 5 | Heatmap of *PtMD* gene expression patterns in developing leaves and wood of hybrid aspen based on RNA sequencing. Details about the expression of each *PtMD* gene in the different tissues are listed in **Supplementary Table 5**. CP, cambium-phloem; DX, developing xylem; ND, not detected.

were in many cases also highly expressed in developing secondary tissues, vascular cambium or developing secondary xylem and phloem (**Figure 6** and **Supplementary Table 6**).

PtMDs Involved in Wood Biosynthesis

Since many *PtMD* genes were found expressed in developing wood (**Figure 5** and **Supplementary Table 5**), we wanted to determine at which wood developmental stage these genes are active. For that, we used the AspWood database (see text footnote 14), which provides data on high-spatial-resolution transcript abundance in developing secondary xylem and phloem tissues of aspen (Sundell et al., 2017). Only 89 *PtMD*s (61%) were found to be expressed in developing secondary vascular tissues (**Supplementary Table 7**), with the majority exhibiting distinct patterns of expression, clustering in ten expression groups (**Supplementary Table 7** and **Figure 7**). This clustering indicates that certain sets of *PtMD*s have specific functions at certain stages of secondary vascular development. Some of the *PtMD* genes expressed in secondary vascular tissue also exhibited high expression under diverse stress conditions in leaves or roots (**Supplementary Table 6** and **Figure 2**).

The largest group of *PtMD* genes (50) that were expressed in secondary vascular tissue showed a peak of expression in the phloem (**Supplementary Table 7** and **Figure 7**). These genes were mostly from superclades LRR-MD-PK including many members of clade VI and VIII without orthologs in *Arabidopsis*, MLD-PK (*Cr*RLK1L), and MLD-LRR-PK. Cambium and radial expansion zones were the zones characterized by the greatest variety of *Pt*MD transcripts including members of superclades MD-Kin, LRR-MD-PK, MLD-LRR, and MLD-PK (*Cr*RLK1L). In contrast, *PtMD* genes having a peak of expression at the transition between primary and secondary wall deposition were mostly from the MLD-PK (*Cr*RLK1L) group. Intriguingly, the genes with maximum expression during secondary wall deposition were expressed at relatively low levels and many of them belonged to clade I of *Pt*MDs, which lacks LRR. *PtMD* genes with the highest expression in the maturation zone were mostly from clades V and XII.

Networks of Xylogenesis-Related *PtMD* Genes

To find putative partners involved in signaling pathways together with the xylogenesis-related *PtMD* genes, we analyzed co-expression networks of *PtMD* genes identified as being expressed during xylogenesis. Ten *PtMD* genes forming two clusters with a peak of expression in the cambium-radial expansion zone and primary to secondary transition zone (CA-RE/PW-SW), and eight genes from clusters PW-SW/Secondary Wall and Secondary Wall (**Figure 7** and **Supplementary Table 7**), representing, respectively, the early and main stages of secondary wall deposition were used as baits for network analyses.

The baits for the CA-RE/PW-SW zones formed five separate networks (**Figure 8A** and **Supplementary Table 8**), the largest being that of *PtMD126* -one of the two poplar orthologs of *AtFER*. It included several candidates for functioning in signaling by phosphorylation relay and ROS, and for regulation of cell

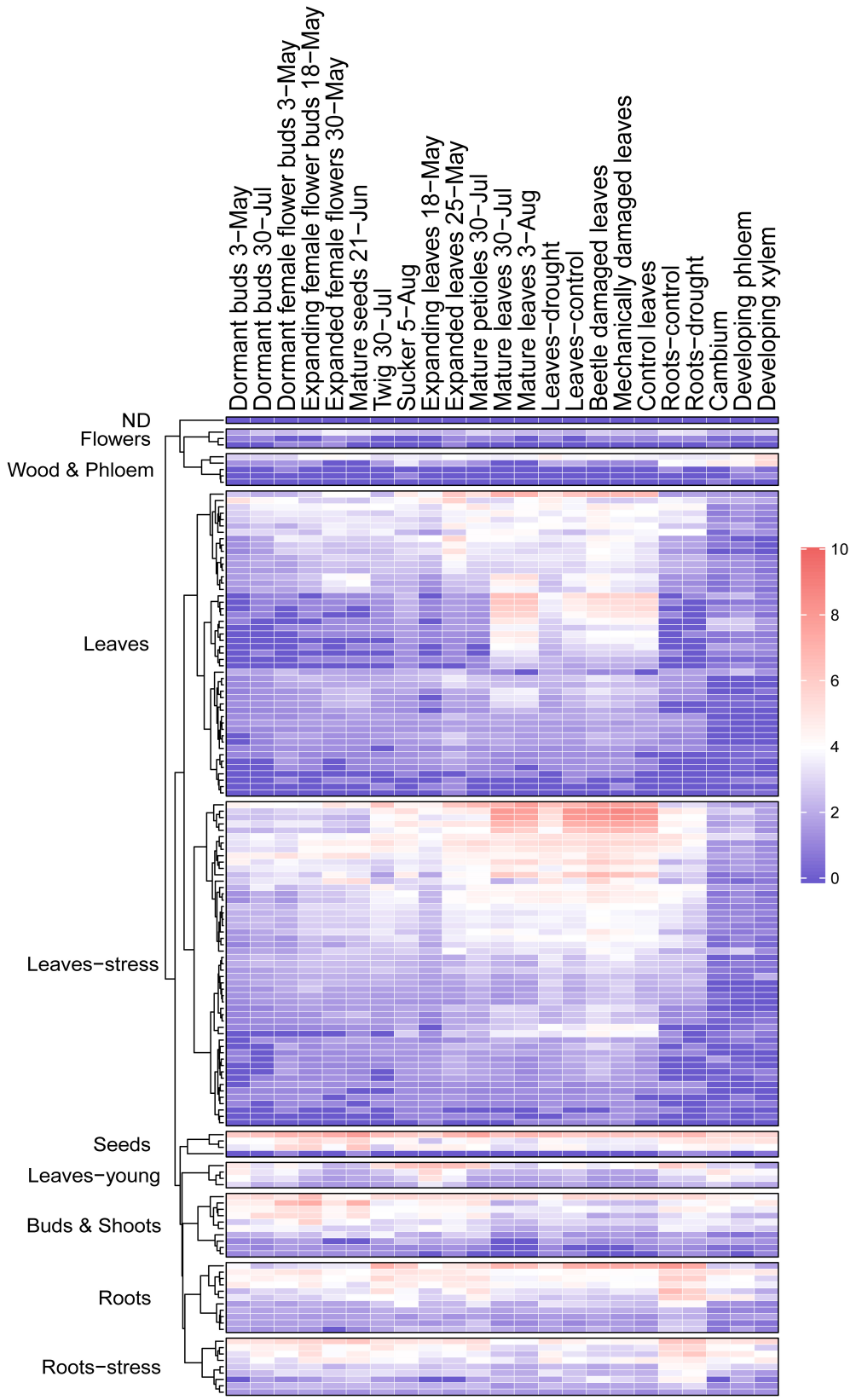

FIGURE 6 | Heatmap of *PtMD* gene expression patterns in different organs of aspen. Data were retrieved from repositories described by Sundell et al. (2015) and Immanen et al. (2016), and normalized expression values are listed in **Supplementary Table 6**.

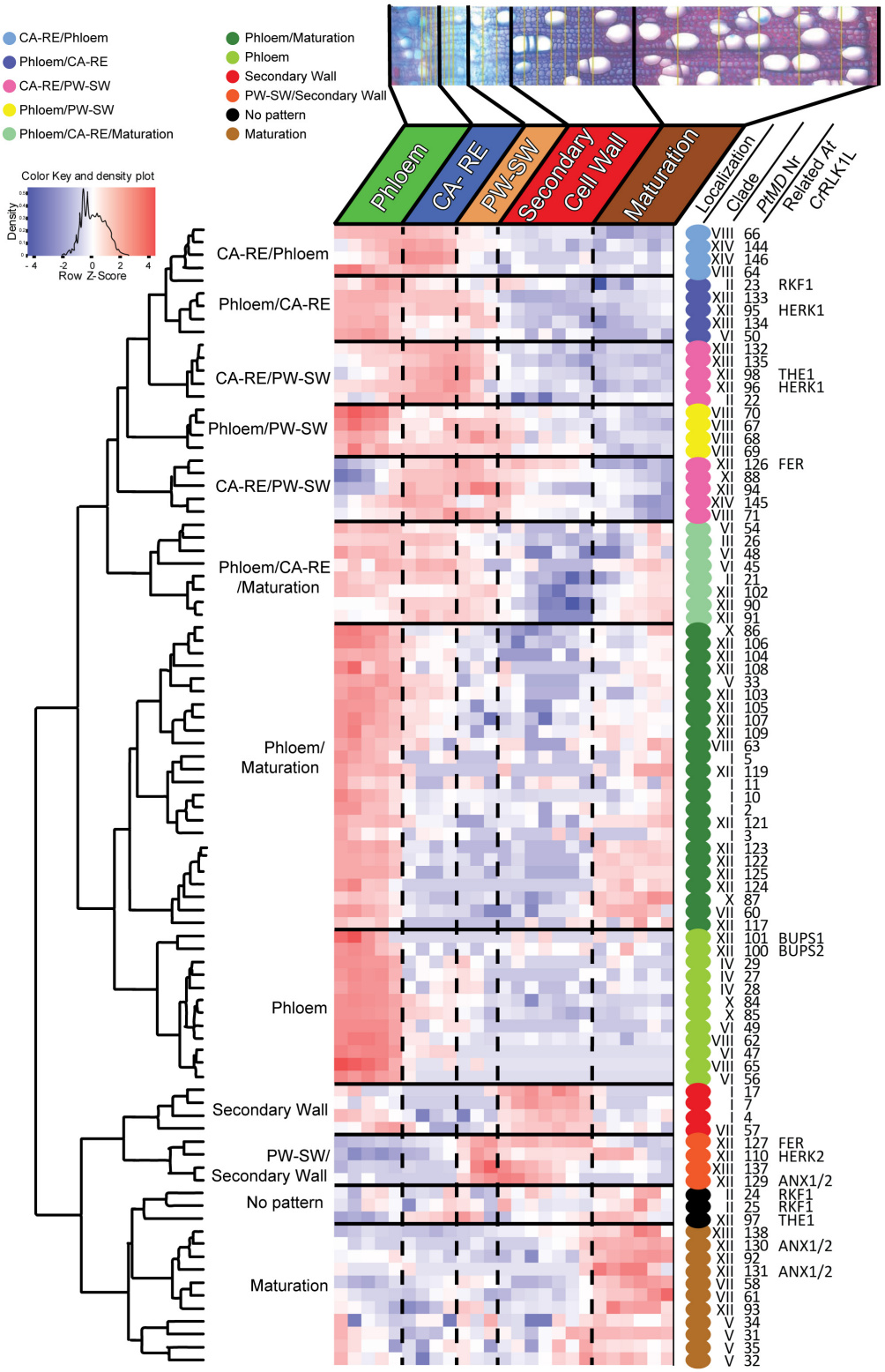

FIGURE 7 | Heatmap of scaled *PtMD* expression patterns in developing secondary vascular tissues based on the AspWood database (http://aspwood.popgenie.org/aspwood-v3.0/). The majority of *PtMD* genes show maximum expression in the phloem and in the cambium-radial expansion zone (CA-RE). Smaller clusters of genes are expressed in the developing xylem including the secondary wall formation zone, the transition between the primary and secondary wall zone (PW-SW), or the maturation zone. Specific wood developmental stages are defined based on the patterns of expression of marker genes (Sundell et al., 2017). Colored dots beside *PtMDs* identify groups with maximum expression in different developmental zones.

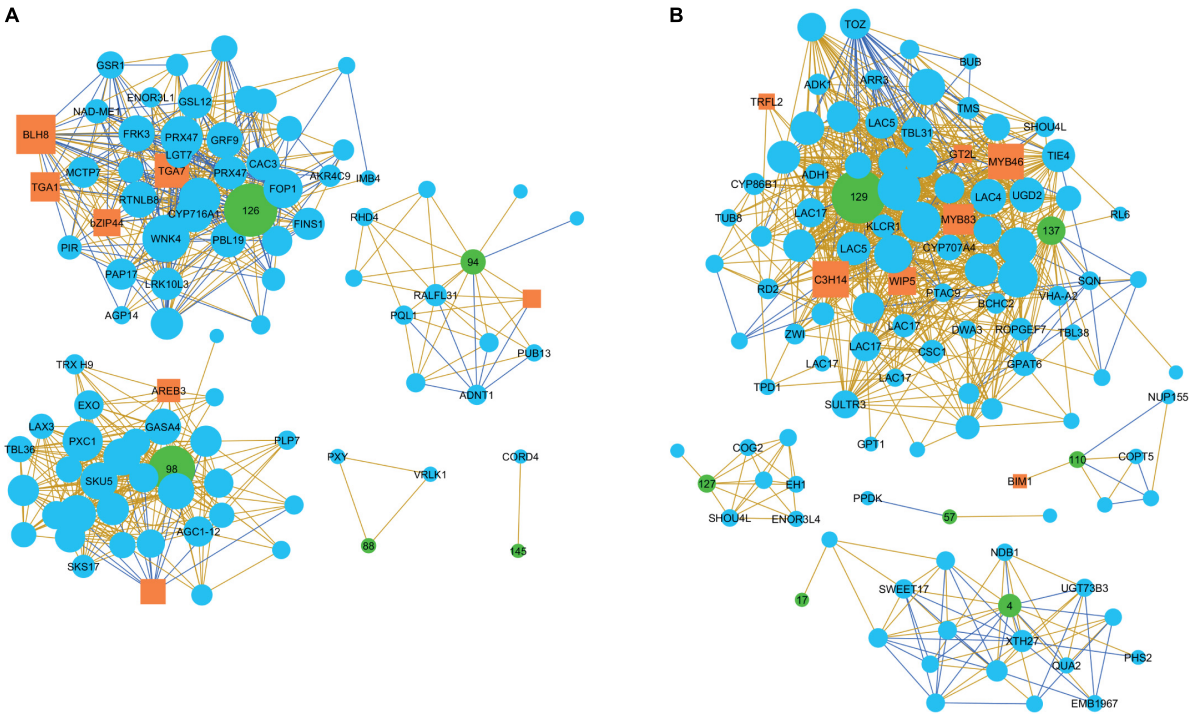

FIGURE 8 | Co-expression networks of *PtMD*s in developing wood of aspen. The networks of genes expressed during the early **(A)** and main **(B)** stages of secondary wall deposition. The co-expressed genes were selected with threshold = 5 from the AspWood database (http://aspwood.popgenie.org/aspwood-v3.0/) and visualized in Cytoscape v 3.4.0. The transcription factors are marked by orange rectangles and the *PtMD* genes, used as baits, by green circles with *PtMD* ID numbers. *PtMD7, 22, 71, 96, 132* and *135* did not have any co-expressed genes (not shown). The corresponding *Arabidopsis* gene names are used in the figures. Positive and negative correlations are shown by beige and blue lines, respectively. The size of each marker corresponds to the number of correlations associated with it.

wall development. Apoplastic ROS in wood forming tissues could have a double role, in signaling and in regulation of lignin polymerization. Thus, the *PtMD126* network included a homolog of *PBS1-LIKE 19* (*AtPBL19*), encoding a RLCK of subfamily VII-4, which signals a response to chitin perceived by CHITIN ELICITOR RECEPTOR KINASE 1 (*At*CERK1) through a phosphorylation relay (Bi et al., 2018), and ROS production (Rao et al., 2018). Homologs of *AtTGA1* and *AtTGA7*, which encode basic leucine zipper transcription factors involved in oxidative stress-mediated responses to biotrophic and necrotrophic pathogens (reviewed by Gatz, 2013), were, respectively, positively and negatively correlated with *PtMD126* (**Figure 8A** and **Table 1**). The oxidation state of *At*TGA1 is regulated by a glutaredoxin, *At*ROXY19 (Li et al., 2019), the homolog of which has been found to respond to altered secondary wall xylan in aspen (Ratke et al., 2018), suggesting that the *PtMD126* network might include candidates for sensing secondary wall integrity. *At*TGA1 interacts with the BLADE-ON-PETIOLE 1 and 2 (*At*BOP1/2) transcription factors (Wang et al., 2019), which are known to regulate xylem fiber differentiation (Liebsch et al., 2014). Moreover, the network includes a homolog of the BEL1-LIKE HOMEODOMAIN 8 (*At*BLH8*)* transcription factor, which controls expression of BOP1 (Khan et al., 2015; **Figure 8A** and **Table 1**). The network also includes a homolog of the gene encoding GROWTH-REGULATING FACTOR 9 (*At*GRF9), a 14-3-3 protein that regulates developmental programs and stress signaling by binding phosphoproteins and regulating their activities (Mayfield et al., 2007; Liu et al., 2014; Omidbakhshfard et al., 2018). The presence of a homolog of IMPORTIN-BETA 4 (*At*IMB4), which is required to transport GRF-INTERACTING FACTOR 1 (*At*GIF1) to the nucleus (Liu et al., 2019; **Figure 8A** and **Table 1**) further supports the involvement of *GRF/14-3-3* genes in the *PtMD126* network.

A separate large network was formed by neighbors of *PtMD98* -one of the two poplar orthologs of *AtTHE1* (**Figure 8A**, **Table 1** and **Supplementary Table 8**). This network comprised genes related to hormonal signaling by IAA and GA, and to the regulation of xylogenesis. One example is a homolog of *AtLAX3*, which encodes an auxin influx carrier (Swarup et al., 2008). Another is a homolog of *AtAGC1-12*, encoding a kinase phosphorylating the auxin efflux carrier *At*PIN1 (Haga et al., 2018). We have also identified a homolog of *AtGASA4* involved in GA responses and redox regulation (Rubinovich and Weiss, 2010). It is noteworthy that GA responses and *GASA* genes were also found to be upregulated in response to a secondary wall xylan defect in aspen (Ratke et al., 2018). Moreover, the co-expression network included an LRR-RLK homologous to *At*PXY-CORRELATED 1 (*At*PXC1), which is required for secondary wall deposition (Wang et al., 2013).

TABLE 1 | Genes co-regulated with poplar *MD* genes expressed during secondary wall formation that were discussed in the text.

First neighbors	Poplar name	Best BLAST AGI codes	Ath-names	Baits							Ath short description	Pathway/process
				MD126 (Potri.006G110000)	MD94 (Potri.010G213200)	MD98 (Potri.001G405500)	MD88 (Potri.002G242700)	MD129 (Potri.008G105500)	MD137 (Potri.010G090800)	MD110 (Potri.001G467000)		
Potri.014G052700		AT5G47070	PBL19	+							PBS1-LIKE 19 - a RLCK phosphorylating MAPKKK5 and MEKK1 in response to chitin	PAMP, ROS, P, JA, and BR signaling, BOP1/2
Potri.002G090700		AT5G65210	TGA1	+							TGA-BINDING 1 - a bZIP TF, a redox-controlled regulator of SAR and development	PAMP, ROS, P, JA, and BR signaling, BOP1/2
Potri.005G170500		AT1G77920	TGA7	–							TGA-BINDING 7 - a bZIP TF, a redox-controlled regulator of SAR and development	PAMP, ROS, P, JA, and BR signaling, BOP1/2
Potri.004G213300		AT2G27990	BLH8	+							BEL1-like TF, regulating BOP1 and integrating stress signaling via JA	PAMP, ROS, P, JA, and BR signaling, BOP1/2
Potri.001G392200		AT2G42590	GRF9	+							GROWTH-REGULATING FACTOR 9, 14-3-3 gene. Binds Ca^{2+} and regulates development.	$Ca^{2+}$and P signaling and regulation
Potri.010G169800		AT4G27640	IMB4	+							IMPORTIN-BETA 4 transporting GRF-interacting factor 1 (GIF1) to nucleus	$Ca^{2+}$and P signaling and regulation
Potri.009G029600		AT3G46510	PUB13		+						PLANT U-BOX 13, an E3 ubiquitin ligase involved in ubiquitination of receptor FLS2.	PAMP signaling
Potri.005G100500		AT3G51460	RHD4		+						ROOT HAIR DEFECTIVE4, a phosphatidylinositol-4-P phosphatase required by root hairs	P signaling and regulation
Potri.015G108700		AT5G61820			+						Stress up-regulated Nod 19 protein;	$Ca^{2+}$and P signaling and regulation
Potri.017G059500		AT4G13950	RALFL31		+						RAPID ALKALINIZATION FACTOR LIKE 31 - peptide hormone	*Cr*RLK1L -mediated signaling
Potri.005G174000		AT1G77690	LAX3			+					Auxin influx carrier LAX3 (Like Aux1)	Auxin signaling
Potri.010G236200		AT3G44610	AGC1-12			+					Kinase involved in phototropism and gravitropism. Phosphorylates PIN1	Auxin signaling
Potri.017G083000		AT5G15230	GASA4			+					Encodes GA-regulated protein GASA4. Promotes GA responses and exhibits redox activity.	GA signaling
Potri.006G117200		AT2G36570	PXC1			+					Leucine-rich repeat protein kinase family protein	Xylogenesis and SW formation
Potri.001G057800		AT1G67310				–					Calmodulin-binding TF	Ca^{2+}-related signaling

(Continued)

TABLE 1 | Continued

First neighbors	Poplar name	Best BLAST AGI codes	Ath-names	Baits							Ath short description	Pathway/process
				MD126 (Potri.006G110000)	MD94 (Potri.010G213200)	MD98 (Potri.001G405500)	MD88 (Potri.002G242700)	MD129 (Potri.008G105500)	MD137 (Potri.010G090800)	MD110 (Potri.001G467000)		
Potri.001G126100		AT5G61480	PXY				+				PHLOEM INTERCALATED WITH XYLEM -a LRR-RLK, receptor of TDIF regulating xylem cell fate	Xylogenesis and SW formation
Potri.006G114400		AT1G79620	VRLK1				+				VASCULAR-RELATED RLK1 - a LRR kinase regulating onset of secondary cell wall thickening.	Xylogenesis and SW formation
Potri.009G053900	MYB021	AT5G12870	MYB46					+			Master secondary wall TF MYB46	Xylogenesis and SW formation
Potri.001G018900		AT1G51220	WIP5					+	+		WIP domain 5. Target of WRKY53, involved cell fate determination in response to auxin via MP.	Auxin signaling
Potri.008G105600		AT4G24972	TPD1					+			TAPETUM DETERMINANT 1, peptide hormone perceived by EMS1-SERK1	P signaling and regulation
Potri.001G267300	MYB3	AT3G08500	MYB83					+			Master secondary wall TF MYB83	Xylogenesis and SW formation
Potri.016G104400		AT5G02010	ROPGEF7						+		ROP (RHO OF PLANTS) GUANINE NUCLEOTIDE EXCHANGE FACTOR 7	*Cr*RLK1L -mediated signaling
Potri.005G135500		AT2G15790	SQN						–		SQUINT - homolog of cyclophilin 40, involved in miRNA regulation	miRNA regulation
Potri.004G005900		AT4G22120	CSC1						+		CALCIUM PERMEABLE STRESS-GATED CATION CHANNEL 1- stretch activated cation channel.	Ca^{2+}-related signaling
Potri.005G051700		AT5G28300	GT2L					–			GT-2LIKE PROTEIN - a CaM-binding protein involved in cold stress signaling	Transcriptional regulation
Potri.001G295100		AT3G19590	BUB3.1					–			BUDDING UNINHIBITED BY BENZYMIDAZOL 3.1. - spindle assembly.	Cell division
Potri.001G394200		AT4G20010	PTAC9					–			PLASTID TRANSCRIPTIONALLY ACTIVE 9- a single-stranded DNA binding protein.	Cell division
Potri.013G079600		AT5G16750	TOZ					–			TORMOZ -rRNA processing required for cell division	Cell division
Potri.015G048000		AT5G08130	BIM1							+	BES1-INTERACTING MYC-LIKE 1-a BHLH TF involved in brassinosteroid signaling	BR signaling

All genes from network analyses are listed in ***Supplementary Tables 8, 9****.*

The network of *PtMD94* -the clade XII member related to *AtHERK1* and *AtCVY1* -included a homolog of *AtRALFL31* (**Figure 8A**, **Table 1** and **Supplementary Table 8**). *RALF* genes encode hormone peptides that signal developmental processes and stress responses by interacting with *Cr*RLK1Ls. *At*RALFL31 belongs to subfamily IIIA which includes as yet uncharacterized members, but both *At*RALFL31 and Potri.017G059500 have the conserved YISY motif essential for interaction with *At*FER (Campbell and Turner, 2017). Thus, *Potri.017G059500* could potentially encode a peptide hormone recognized by *Pt*MD94. The *PtMD94* network also included other candidates for signaling. For example, there was a homolog of *PLANT U-BOX 13* (*AtPUB13)*, which encodes an E3 ligase involved in signal-activated ubiquitination and subsequent degradation of different receptors including ABA INSENSITIVE 1 (*At*ABI1) (Kong et al., 2015), BRASSINOSTEROID INSENSITIVE 1 (*At*BRI1) (Zhou et al., 2018), LYSM-CONTAINING RECEPTOR-LIKE KINASE 5 (*At*LYK5) (Liao et al., 2017), and FLAGELLIN-SENSITIVE 2 (*At*FLS2) (Liu et al., 2012; Antignani et al., 2015). The ubiquitination of flg22-bound *At*FLS2 by *At*PUB13 depends on its interactor protein RAB GTPASE HOMOLOG A 4B (*At*RABA4B) (Antignani et al., 2015). Interestingly, a homolog to another *PtMD94* network member encodes ROOT HAIR DEFECTIVE 4 (*At*RHD4) which mediates polar localization of *At*RABA4B (Thole et al., 2008). Consequently, it seems likely that these *PtMD94* network members are indeed functionally linked within the same network.

Two other *PtMD* genes expressed during early secondary wall biosynthesis, *PtMD88* and *PtMD145*, formed small networks, which included important regulatory genes in xylem cell differentiation (**Figure 8A**, **Table 1** and **Supplementary Table 8**). One of them was the homolog of the master spatial regulator of vascular differentiation, *PHLOEM INTERCALATED WITH XYLEM* (*AtPXY*), encoding an LRR-RLK that promotes cell division in the cambium upon binding the small CLE peptide *At*TDIF, which is essential for xylem differentiation (Fisher and Turner, 2007). The other was a homolog of *VASCULAR-RELATED RECEPTOR-LIKE KINASE 1* (*AtVRLK1*) (Huang et al., 2018) which is probably responsible for the switch between xylem cell expansion and secondary wall deposition.

The late secondary wall-expressed baits formed five networks (**Figure 8B**, **Table 1** and **Supplementary Table 9**). The largest of these was associated with two *PtMD* genes, *PtMD129*, a clade XII member related to *AtANX1* and *AtANX2*, and *PtMD137*, which encodes an LRR-RLK, from clade XIII. Orthologs of key signaling-related genes were included within this network. One of them was *CALCIUM PERMEABLE STRESS-GATED CATION CHANNEL 1 (AtCSC1*). Stretch-activated Ca^{2+} channels have been predicted to be important players in CWI (Engelsdorf and Hamann, 2014). *At*CSC1 belongs to a newly characterized family of stretch-activated Ca^{2+} channels conserved in eukaryotes (Hou et al., 2014; Liu et al., 2018). In addition, we found *Potri.015G108700/AT5G61820*, encoding an uncharacterized NOD19-like protein, which has been implicated in responses to cold stress downstream of mechanosensitive Ca^{2+} channels (Mori et al., 2018). The aspen homolog of *AtCSC1* is thus a promising candidate for a secondary wall damage sensor. Another important signaling-related homolog is *TAPETUM DETERMINANT 1* (*AtTPD1*), which encodes a small peptide hormone that is recognized by an RLK complex consisting of *At*EMS1 and *At*SERK1/2 to activate transcription factors of the BES1 family (Chen et al., 2019). Moreover, a homolog of *Arabidopsis ROP (RHO OF PLANTS) GUANINE NUCLEOTIDE EXCHANGE FACTOR 7* (*AtROPGEF7*) was among the hits for *PtMD137*. *At*ROPGEF7 interacts with the kinase domain of *At*FER, mediating downstream NADPH oxidase-dependent ROS signaling which is needed for polarized cell growth (Duan et al., 2010). Finally, we identified a homolog of *Arabidopsis GT-2LIKE PROTEIN* (*AtGT2L*), which encodes a Ca^{2+}-dependent calmodulin (CaM)-binding trihelix transcription factor involved in plant abiotic stress signaling (Xi et al., 2012). In addition to signaling-related genes, the *PtMD129-PtMD137* network included some key cell fate regulator proteins (**Figure 8B**, **Table 1** and **Supplementary Table 9**). One of these was the homolog of *WIP DOMAIN PROTEIN 5* (*AtWIP5*), which encodes a zinc-finger protein involved in root patterning downstream of auxin (Crawford et al., 2015) and ROS signaling (Miao et al., 2004). Another was a homolog of *Arabidopsis SQUINT* (*AtSQN*), which encodes a cyclophilin 40-like protein that promotes the accumulation of miRNAs miR156 and miR172, targeting master regulatory genes in organ development (Smith et al., 2009; Prunet et al., 2015). The network also included orthologs of two genes encoding master transcriptional regulators, *At*MYB46 and *At*MYB83, which activate the secondary wall program (Zhong and Ye, 2012). Both these genes showed positive correlation with *PtMD129*. In contrast, orthologs of three genes with roles in cell division were negatively correlated with *PtMD129* (**Table 1**). This supports the hypothesis that secondary wall integrity signaling results in coordination between cell division and secondary wall formation activities in developing wood (Ratke et al., 2018).

The network for *PtMD110*, which together with *PtMD111* forms a pair orthologous to *AtHERK2*, included a homolog of the *Arabidopsis* gene encoding the transcription factor BES1-INTERACTING MYC-LIKE1 (*At*BIM1) (**Figure 8B**, **Table 1** and **Supplementary Table 9**), which mediates brassinosteroid signaling (Chandler et al., 2009). Several other genes discussed above can be linked to BR-dependent or BES-related BR-independent signaling (**Table 1**). Intriguingly, a secondary wall xylan defect induced transcriptomic changes suggesting stimulation of BR signaling in aspen (Ratke et al., 2018), supporting the involvement of the *AtBIM1* homolog in sensing secondary wall integrity.

CONCLUSION

Malectin and malectin-like domains (MD/MLD) are lectin-like motifs found in proteins (MD proteins) of pro- and eukaryotes; they are particularly abundant in plants, where they carry out essential signaling functions in defense and development (Bellande et al., 2017; Franck et al., 2018). This has been shown by studies on *MD* genes from herbaceous plants such as *Arabidopsis* (Bellande et al., 2017; Sultana et al., 2020), strawberry (Zhang et al., 2016) and rice (Jing et al., 2020). However, no such

comprehensive study has been available for *MD* genes in trees. Here we carried out a census of *MD* genes in the model woody species *P. trichocarpa* (**Supplementary Table 1**) and expanded the set for *A. thaliana* (**Supplementary Table 2**).

In total, 146 *MD* genes were found in *P. trichocarpa* and they were assigned to fourteen clades based on sequence similarity, and to five superclades based on predicted protein domain organization and intron-exon structures (**Figures 1**, **2**). The variety of MD protein structures reflects their range of different functions in plants.

Additional genome-wide analysis by using available sequence data from different woody species revealed, that certain *MD* genes appeared to be specific either to trees or to the *Populus* lineage and absent from *Arabidopsis* (**Supplementary Figure 3**). The prevalence of tandem duplications within the *MD* gene family, which apparently led to family expansion, may have created conditions conducive to gene neofunctionalization and rapid evolution (Schaper and Anisimova, 2015; Choi et al., 2016).

The majority of the poplar *MD* genes were found to be highly expressed in mature leaves, particularly those subjected to biotic and abiotic stress conditions (**Figure 6**), supporting their role in stress signaling. Detailed analysis of expression in wood forming tissues revealed subsets upregulated in xylem cells during secondary wall deposition (**Figure 7**). These genes, not unexpectedly, include candidates for the sensing of cell wall integrity. We identified their co-expression networks revealing potential molecular pathways in which these *MD* genes might participate to ensure the coordination of secondary wall formation (**Table 1**).

The current study provides an extensive analysis of *Populus MD* genes and opens the possibility to better understand their role in essential physiological pathways related to stress signaling and the regulation of wood formation in trees.

DATA AVAILABILITY STATEMENT

The datasets presented in this study can be found in online repositories. The names of the repository/repositories and accession number(s) can be found in the article/ **Supplementary Material**.

AUTHOR CONTRIBUTIONS

VK identified *MD* genes and their chromosomal clustering, and wrote the first draft. VK and FB identified protein domains and the main clades of *MD* genes. VK and SK analyzed exon-intron structures. ED analyzed gene expression in leaves and wood. VK and ED analyzed *in silico* gene expression in different organs. ED, JU, and VK analyzed conserved regions in MD and MLD of poplar. VK and FB analyzed co-expression networks. VK and CM analyzed the phylogeny across the tree species. EM conceived and coordinated the project, and finalized the manuscript with contributions from all authors. All authors contributed to the article and approved the submitted version.

FUNDING

This work was supported by Swedish Research Council, the Kempe Foundation, the Knut and Alice Wallenberg Foundation, and the SSF program ValueTree RBP14-0011.

ACKNOWLEDGMENTS

We thank Dr. Nicolas Delhomme and the Bioinformatics Facility at UPSC for allowing us to use their server during the work. This manuscript has been released as a pre-print at Research Square, Kumar et al. (2020).

SUPPLEMENTARY MATERIAL

The Supplementary Material for this article can be found online at: https://www.frontiersin.org/articles/10.3389/fpls.2020.588846/full#supplementary-material

REFERENCES

Adebali, O., Ortega, D. R., and Zhulin, I. B. (2015). CDvist: a webserver for identification and visualization of conserved domains in protein sequences. *Bioinformatics* 31, 1475–1477. doi: 10.1093/bioinformatics/btu836

Altschul, S. F., Gish, W., Miller, W., Myers, E. W., and Lipman, D. J. (1990). Basic local alignment search tool. *J. Mol. Biol.* 215, 403–410. doi: 10.1016/S0022-2836(05)80360-2

Antignani, V., Klocko, A. L., Bak, G., Chandrasekaran, S. D., Dunivin, T., and Nielsen, E. (2015). Recruitment of PLANT U-BOX13 and the PI4Kβ1/β2 phosphatidylinositol-4 kinases by the small GTPase RabA4B plays important roles during salicylic acid-mediated plant defense signaling in *Arabidopsis*. *Plant Cell* 27, 243–261. doi: 10.1105/tpc.114.134262

Armenteros, A. J. J., Sønderby, C. K., Sønderby, S. K., Nielsen, H., and Winther, O. (2017). DeepLoc: prediction of protein subcellular localization using deep learning. *Bioinformatics* 33, 3387–3395. doi: 10.1093/bioinformatics/btx431

Asai, T., Tena, G., Plotnikova, J., Willmann, M. R., Chiu, W.-L., Gomez-Gomez, L., et al. (2002). MAP kinase signalling cascade in *Arabidopsis* innate immunity. *Nature* 415, 977–983. doi: 10.1038/415977a

Bella, J., Hindle, K. L., McEwan, P. A., and Lovell, S. C. (2008). The leucine-rich repeat structure. *Cell. Mol. Life Sci.* 65, 2307–2333. doi: 10.1007/s00018-008-8019-0

Bellande, K., Bono, J.-J., Savelli, B., Jamet, E., and Canut, H. (2017). Plant lectins and lectin receptor-like kinases: how do they sense the outside? *Intern. J. Mol. Sci.* 18:1164. doi: 10.3390/ijms18061164

Bi, G., Zhou, Z., Wang, W., Li, L., Rao, S., Wu, Y., et al. (2018). Receptor-like cytoplasmic kinases directly link diverse pattern recognition receptors to the activation of mitogen-activated protein kinase cascades in *Arabidopsis*. *Plant Cell* 30, 1543–1561. doi: 10.1105/tpc.17.00981

Boisson-Dernier, A., Franck, C. M., Lituiev, D. S., and Grossniklaus, U. (2015). Receptor-like cytoplasmic kinase MARIS functions downstream of *Cr*RLK1L-dependent signaling during tip growth. *Proc. Natl. Acad. Sci. U.S.A.* 112, 12211–12216. doi: 10.1073/pnas.1512375112

Boisson-Dernier, A., Lituiev, D. S., Nestorova, A., Franck, C. M., Thirugnanarajah, S., and Grossniklaus, U. (2013). ANXUR receptor-like kinases coordinate cell wall integrity with growth at the pollen tube tip via NADPH oxidases. *PLoS Biol.* 11:e1001719. doi: 10.1371/journal.pbio.1001719

Bray, N. L., Pimentel, H., Melsted, P., and Pachter, L. (2016). Near-optimal probabilistic RNA-seq quantification. *Nat. Biotechnol.* 34, 525–527. doi: 10.1038/nbt.3519

Buchfink, B., Xie, C., and Huson, D. H. (2015). Fast and sensitive protein alignment using DIAMOND. *Nat. Methods* 12, 59–60. doi: 10.1038/nmeth.3176

Campbell, L., and Turner, S. R. (2017). A comprehensive analysis of RALF proteins in green plants suggests there are two distinct functional groups. *Front. Plant Sci.* 8:37. doi: 10.3389/fpls.2017.00037

Chandler, J. W., Cole, M., Flier, A., and Werr, W. (2009). BIM1, a bHLH protein involved in brassinosteroid signalling, controls *Arabidopsis* embryonic patterning via interaction with DORNRÖSCHEN and DORNRÖSCHEN-LIKE. *Plant Mol. Biol.* 69, 57–68. doi: 10.1007/s11103-008-9405-6

Chen, W., Lv, M., Wang, Y., Wang, P.-A., Cui, Y., Li, M., et al. (2019). BES1 is activated by EMS1-TPD1-SERK1/2-mediated signaling to control tapetum development in *Arabidopsis thaliana*. *Nat. Commun.* 10:4164. doi: 10.1038/s41467-019-12118-4

Choi, K., Reinhard, C., Serra, H., Ziolkowski, P. A., Underwood, C. J., Zhao, X., et al. (2016). Recombination rate heterogeneity within *Arabidopsis* disease resistance genes. *PLoS Genet.* 12:e1006179. doi: 10.1371/journal.pgen.1006179

Crawford, B. C. W., Sewell, J., Golembeski, G., Roshan, C., Long, J. A., and Yanofsky, M. F. (2015). Genetic control of distal stem cell fate within root and embryonic meristems. *Science* 347, 655–659. doi: 10.1126/science.aaa0196

Crooks, G. E., Hon, G., Chandonia, J.-M., and Brenner, S. E. (2004). WebLogo: a sequence logo generator. *Genome Res.* 14, 1188–1190. doi: 10.1101/gr.849004

Denness, L., McKenna, J. F., Segonzac, C., Wormit, A., Madhou, P., Bennett, M., et al. (2011). Cell wall damage-induced lignin biosynthesis is regulated by a reactive oxygen species- and jasmonic acid-dependent process in *Arabidopsis*. *Plant Physiol.* 156, 1364–1374. doi: 10.1104/pp.111.175737

Draeger, C., Ndinyanka Fabrice, T., Gineau, E., Mouille, G., Kuhn, B. M., Moller, I., et al. (2015). *Arabidopsis* leucine-rich repeat extensin (LRX) proteins modify cell wall composition and influence plant growth. *BMC Plant Biol.* 15:155. doi: 10.1186/s12870-015-0548-8

Du, C., Li, X., Chen, J., Chen, W., Li, B., Li, C., et al. (2016). Receptor kinase complex transmits RALF peptide signal to inhibit root growth in *Arabidopsis*. *Proc. Natl. Acad. Sci. U.S.A.* 113, E8326–E8334. doi: 10.1073/pnas.1609626113

Du, S., Qu, L.-J., and Xiao, J. (2018). Crystal structures of the extracellular domains of the *Cr*RLK1L receptor-like kinases ANXUR1 and ANXUR2. *Protein Sci.* 27, 886–892. doi: 10.1002/pro.3381

Duan, Q., Kita, D., Li, C., Cheung, A. Y., and Wu, H.-M. (2010). FERONIA receptor-like kinase regulates RHO GTPase signaling of root hair development. *Proc. Natl. Acad. Sci. U.S.A.* 107, 17821–17826. doi: 10.1073/pnas.1005366107

Dünser, K., Gupta, S., Herger, A., Feraru, M. I., Ringli, C., and Kleine-Vehn, J. (2019). Extracellular matrix sensing by FERONIA and leucine-rich repeat extensins controls vacuolar expansion during cellular elongation in *Arabidopsis thaliana*. *EMBO J.* 38:e100353. doi: 10.15252/embj.2018100353

El-Gebali, S., Mistry, J., Bateman, A., Eddy, S. R., Luciani, A., Potter, S. C., et al. (2019). The Pfam protein families database in 2019. *Nucleic Acids Res.* 47, D427–D432. doi: 10.1093/nar/gky995

Engelsdorf, T., and Hamann, T. (2014). An update on receptor-like kinase involvement in the maintenance of plant cell wall integrity. *Ann. Bot.* 114, 1339–1347. doi: 10.1093/aob/mcu043

Escobar-Restrepo, J.-M., Huck, N., Kessler, S., Gagliardini, V., Gheyselinck, J., Yang, W.-C., et al. (2007). The FERONIA receptor-like kinase mediates male-female interactions during pollen tube reception. *Science* 317, 656–660. doi: 10.1126/science.1143562

Feng, W., Kita, D., Peaucelle, A., Cartwright, H. N., Doan, V., Duan, Q., et al. (2018). The FERONIA receptor kinase maintains cell-wall integrity during salt stress through Ca^{2+} signaling. *Curr. Biol.* 28, 666–675.e665. doi: 10.1016/j.cub.2018.01.023

Fisher, K., and Turner, S. (2007). PXY, a receptor-like kinase essential for maintaining polarity during plant vascular-tissue development. *Curr. Biol.* 17, 1061–1066. doi: 10.1016/j.cub.2007.05.049

Foreman, J., Demidchik, V., Bothwell, J. H. F., Mylona, P., Miedema, H., Torres, M. A., et al. (2003). Reactive oxygen species produced by NADPH oxidase regulate plant cell growth. *Nature* 422, 442–446. doi: 10.1038/nature01485

Franck, C. M., Westermann, J., and Boisson-Dernier, A. (2018). Plant malectin-like receptor kinases: from cell wall integrity to immunity and beyond. *Ann. Rev. Plant Biol.* 69, 301–328. doi: 10.1146/annurev-arplant-042817-40557

Galindo-Trigo, S., Grand, T. M., Voigt, C. A., and Smith, L. M. (2020). A malectin domain kinesin functions in pollen and seed development in *Arabidopsis*. *J. Exper. Bot.* 71, 1828–1841. doi: 10.1093/jxb/eraa023

Galindo-Trigo, S., Gray, J. E., and Smith, L. M. (2016). Conserved roles of *Cr*RLK1L receptor-like kinases in cell expansion and reproduction from algae to angiosperms. *Front. Plant Sci.* 7:1269. doi: 10.3389/fpls.2016.01269

Gatz, C. (2013). From pioneers to team players: TGA transcription factors provide a molecular link between different stress pathways. *Mol. Plant Microb. Interact.* 26, 151–159. doi: 10.1094/mpmi-04-12-0078-ia

Ge, Z., Bergonci, T., Zhao, Y., Zou, Y., Du, S., Liu, M.-C., et al. (2017). *Arabidopsis* pollen tube integrity and sperm release are regulated by RALF-mediated signaling. *Science* 358, 1596–1600. doi: 10.1126/science.aao3642

Gentleman, R. C., Carey, V. J., Bates, D. M., Bolstad, B., Dettling, M., Dudoit, S., et al. (2004). Bioconductor: open software development for computational biology and bioinformatics. *Genome Biol.* 5:R80. doi: 10.1186/gb-2004-5-10-r80

Gish, L. A., and Clark, S. E. (2011). The RLK/Pelle family of kinases. *Plant J.* 66, 117–127. doi: 10.1111/j.1365-313X.2011.04518.x

Gonneau, M., Desprez, T., Martin, M., Doblas, V. G., Bacete, L., Miart, F., et al. (2018). Receptor kinase THESEUS1 is a rapid alkalinization factor 34 receptor in *Arabidopsis*. *Curr. Biol.* 28, 2452–2458.e2454. doi: 10.1016/j.cub.2018.05.075

Gu, Z., Eils, R., and Schlesner, M. (2016). Complex heatmaps reveal patterns and correlations in multidimensional genomic data. *Bioinformatics* 32, 2847–2849. doi: 10.1093/bioinformatics/btw313

Haga, K., Frank, L., Kimura, T., Schwechheimer, C., and Sakai, T. (2018). Roles of AGCVIII kinases in the hypocotyl phototropism of *Arabidopsis* seedlings. *Plant Cell Physiol.* 59, 1060–1071. doi: 10.1093/pcp/pcy048

Hamann, T. (2015). The plant cell wall integrity maintenance mechanism - A case study of a cell wall plasma membrane signaling network. *Phytochemistry* 112, 100–109. doi: 10.1016/j.phytochem.2014.09.019

Haruta, M., Sabat, G., Stecker, K., Minkoff, B. B., and Sussman, M. R. (2014). A peptide hormone and its receptor protein kinase regulate plant cell expansion. *Science* 343, 408–411. doi: 10.1126/science.1244454

Hématy, K., Sado, P.-E., Van Tuinen, A., Rochange, S., Desnos, T., Balzergue, S., et al. (2007). A receptor-like kinase mediates the response of *Arabidopsis* cells to the inhibition of cellulose synthesis. *Curr. Biol.* 17, 922–931. doi: 10.1016/j.cub.2007.05.018

Holub, E. B. (2001). The arms race is ancient history in *Arabidopsis*, the wildflower. *Nat. Rev. Genet.* 2, 516–527. doi: 10.1038/35080508

Hou, C., Tian, W., Kleist, T., He, K., Garcia, V., Bai, F., et al. (2014). DUF221 proteins are a family of osmosensitive calcium-permeable cation channels conserved across eukaryotes. *Cell Res.* 24, 632–635. doi: 10.1038/cr.2014.14

Huang, C., Zhang, R., Gui, J., Zhong, Y., and Li, L. (2018). The receptor-like kinase *At*VRLK1 regulates secondary cell wall thickening. *Plant Physiol.* 177, 671–683. doi: 10.1104/pp.17.01279

Immanen, J., Nieminen, K., Smolander, O.-P., Kojima, M., Alonso Serra, J., Koskinen, P., et al. (2016). Cytokinin and auxin display distinct but interconnected distribution and signaling profiles to stimulate cambial activity. *Curr. Biol.* 26, 1990–1997. doi: 10.1016/j.cub.2016.05.053

Jing, X.-Q., Shalmani, A., Zhou, M.-R., Shi, P.-T., Muhammad, I., Shi, Y., et al. (2020). Genome-wide identification of malectin/malectin-like domain containing protein family genes in rice and their expression regulation under various hormones, abiotic stresses, and heavy metal treatments. *J. Plant Growth Regul.* 39, 492–506. doi: 10.1007/s00344-019-09997-8

Katoh, K., Kuma, K.-I., Toh, H., and Miyata, T. (2005). MAFFT version 5: improvement in accuracy of multiple sequence alignment. *Nucleic Acids Res.* 33, 511–518. doi: 10.1093/nar/gki198

Kessler, S. A., Shimosato-Asano, H., Keinath, N. F., Wuest, S. E., Ingram, G., Panstruga, R., et al. (2010). Conserved molecular components for pollen tube reception and fungal invasion. *Science* 330, 968–971. doi: 10.1126/science.1195211

Khan, M., Ragni, L., Tabb, P., Salasini, B. C., Chatfield, S., Datla, R., et al. (2015). Repression of lateral organ boundary genes by PENNYWISE and POUND-FOOLISH is essential for meristem maintenance and flowering in *Arabidopsis*. *Plant Physiol.* 169, 2166–2186. doi: 10.1104/pp.15.00915

Kong, L., Cheng, J., Zhu, Y., Ding, Y., Meng, J., Chen, Z., et al. (2015). Degradation of the ABA co-receptor ABI1 by PUB12/13 U-box E3 ligases. *Nat. Commun.* 6:8630. doi: 10.1038/ncomms9630

Kopylova, E., Noé, L., and Touzet, H. (2012). SortMeRNA: fast and accurate filtering of ribosomal RNAs in metatranscriptomic data. *Bioinformatics* 28, 3211–3217. doi: 10.1093/bioinformatics/bts611

Kumar, S., Stecher, G., and Tamura, K. (2016). MEGA7: molecular evolutionary genetics analysis version 7.0 for bigger datasets. *Mol. Biol. Evol.* 33, 1870–1874. doi: 10.1093/molbev/msw054

Kumar, V., Barbut, F., Kushwah, S., Donev, E. N., Urbancsok, J., and Mellerowicz, E. J. (2020). Genome-wide identification of poplar malectin/malectin-like domain-containing proteins and *in-silico* expression analyses find novel candidates for signaling and regulation of wood development. *Research Square* [Preprint], doi: 10.21203/rs.3.rs-28356/v1

Kumar, V., Hainaut, M., Delhomme, N., Mannapperuma, C., Immerzeel, P., Street, N. R., et al. (2019). Poplar carbohydrate-active enzymes: whole-genome annotation and functional analyses based on RNA expression data. *Plant J.* 99, 589–609. doi: 10.1111/tpj.14417

Le, M. H., Cao, Y., Zhang, X.-C., and Stacey, G. (2014). LIK1, a CERK1-interacting kinase, regulates plant immune responses in *Arabidopsis*. *PLoS One* 9:e102245. doi: 10.1371/journal.pone.0102245

Lemoine, F., Correia, D., Lefort, V., Doppelt-Azeroual, O., Mareuil, F., Cohen-Boulakia, S., et al. (2019). NGPhylogeny.fr: new generation phylogenetic services for non-specialists. *Nucleic Acids Res.* 47, W260–W265. doi: 10.1093/nar/gkz303

Li, C., Wu, H.-M., and Cheung, A. Y. (2016). FERONIA and her pals: functions and mechanisms. *Plant Physiol.* 171, 2379–2392. doi: 10.1104/pp.16.00667

Li, N., Muthreich, M., Huang, L.-J., Thurow, C., Sun, T., Zhang, Y., et al. (2019). TGACG-BINDING FACTORs (TGAs) and TGA-interacting CC-type glutaredoxins modulate hyponastic growth in *Arabidopsis thaliana*. *New Phytol.* 221, 1906–1918. doi: 10.1111/nph.15496

Liao, D., Cao, Y., Sun, X., Espinoza, C., Nguyen, C. T., Liang, Y., et al. (2017). *Arabidopsis* E3 ubiquitin ligase PLANT U-BOX13 (PUB13) regulates chitin receptor LYSIN MOTIF RECEPTOR KINASE5 (LYK5) protein abundance. *New Phytol.* 214, 1646–1656. doi: 10.1111/nph.14472

Liebsch, D., Sunaryo, W., Holmlund, M., Norberg, M., Zhang, J., Hall, H. C., et al. (2014). Class I KNOX transcription factors promote differentiation of cambial derivatives into xylem fibers in the *Arabidopsis* hypocotyl. *Development* 141, 4311–4319. doi: 10.1242/dev.111369

Liu, H.-H., Xiong, F., Duan, C.-Y., Wu, Y.-N., Zhang, Y., and Li, S. (2019). Importin β4 mediates nuclear import of GRF-interacting factors to control ovule development in *Arabidopsis*. *Plant Physiol.* 179, 1080–1092. doi: 10.1104/pp.18.01135

Liu, J., Li, W., Ning, Y., Shirsekar, G., Cai, Y., Wang, X., et al. (2012). The U-Box E3 ligase SPL11/PUB13 is a convergence point of defense and flowering signaling in plants. *Plant Physiol.* 160, 28–37. doi: 10.1104/pp.112.199430

Liu, J., Rice, J. H., Chen, N., Baum, T. J., and Hewezi, T. (2014). Synchronization of developmental processes and defense signaling by growth regulating transcription factors. *PLoS One* 9:e98477. doi: 10.1371/journal.pone.0098477

Liu, X., Wang, J., and Sun, L. (2018). Structure of the hyperosmolality-gated calcium-permeable channel OSCA1.2. *Nat. Commun.* 9:5060. doi: 10.1038/s41467-018-07564-5

Lohse, M., Bolger, A. M., Nagel, A., Fernie, A. R., Lunn, J. E., Stitt, M., et al. (2012). RobiNA: a user-friendly, integrated software solution for RNA-Seq-based transcriptomics. *Nucleic Acids Res.* 40, W622–W627. doi: 10.1093/nar/gks540

Love, M. I., Huber, W., and Anders, S. (2014). Moderated estimation of fold change and dispersion for RNA-seq data with DESeq2. *Genome Biol.* 15:550. doi: 10.1186/s13059-014-0550-8

Mang, H., Feng, B., Hu, Z., Boisson-Dernier, A., Franck, C. M., Meng, X., et al. (2017). Differential regulation of two-tiered plant immunity and sexual reproduction by ANXUR receptor-like kinases. *Plant Cell* 29, 3140–3156. doi: 10.1105/tpc.17.00464

Mayfield, J. D., Folta, K. M., Paul, A.-L., and Ferl, R. J. (2007). The 14-3-3 proteins μ and υ influence transition to flowering and early phytochrome response. *Plant Physiol.* 145, 1692–1702. doi: 10.1104/pp.107.108654

Meng, J.-G., Liang, L., Jia, P.-F., Wang, Y.-C., Li, H.-J., and Yang, W.-C. (2020). Integration of ovular signals and exocytosis of a Ca^{2+} channel by MLOs in pollen tube guidance. *Nat. Plants* 6, 143–153. doi: 10.1038/s41477-020-0599-1

Merz, D., Richter, J., Gonneau, M., Sanchez-Rodriguez, C., Eder, T., Sormani, R., et al. (2017). T-DNA alleles of the receptor kinase THESEUS1 with opposing effects on cell wall integrity signaling. *J. Exper. Bot.* 68, 4583–4593. doi: 10.1093/jxb/erx263

Miao, Y., Laun, T., Zimmermann, P., and Zentgraf, U. (2004). Targets of the WRKY53 transcription factor and its role during leaf senescence in *Arabidopsis*. *Plant Mol. Biol.* 55, 853–867. doi: 10.1007/s11103-004-2142-6

Mineev, K. S., Bocharov, E. V., Pustovalova, Y. E., Bocharova, O. V., Chupin, V. V., and Arseniev, A. S. (2010). Spatial structure of the transmembrane domain heterodimer of ErbB1 and ErbB2 receptor tyrosine kinases. *J. Mol. Biol.* 400, 231–243. doi: 10.1016/j.jmb.2010.05.016

Mori, K., Renhu, N., Naito, M., Nakamura, A., Shiba, H., Yamamoto, T., et al. (2018). Ca^{2+}-permeable mechanosensitive channels MCA1 and MCA2 mediate cold-induced cytosolic Ca^{2+} increase and cold tolerance in *Arabidopsis*. *Sci. Rep.* 8:550. doi: 10.1038/s41598-017-17483-y

Moussu, S., Augustin, S., Roman, A. O., Broyart, C., and Santiago, J. (2018). Crystal structures of two tandem malectin-like receptor kinases involved in plant reproduction. *Acta Crystallogr.* 74(Pt 7), 671–680. doi: 10.1107/s205979831800774x

Omidbakhshfard, M. A., Fujikura, U., Olas, J. J., Xue, G.-P., Balazadeh, S., and Mueller-Roeber, B. (2018). GROWTH-REGULATING FACTOR 9 negatively regulates *Arabidopsis* leaf growth by controlling *ORG3* and restricting cell proliferation in leaf primordia. *PLoS Genet.* 14:e1007484. doi: 10.1371/journal.pgen.1007484

Pagnussat, G. C., Yu, H.-J., Ngo, Q. A., Rajani, S., Mayalagu, S., Johnson, C. S., et al. (2005). Genetic and molecular identification of genes required for female gametophyte development and function in *Arabidopsis*. *Development* 132, 603–614. doi: 10.1242/dev.01595

Petersen, T. N., Brunak, S., von Heijne, G., and Nielsen, H. (2011). SignalP 4.0: discriminating signal peptides from transmembrane regions. *Nat. Methods* 8, 785–786. doi: 10.1038/nmeth.1701

Pinard, D., Mizrachi, E., Hefer, C. A., Kersting, A. R., Joubert, F., Douglas, C. J., et al. (2015). Comparative analysis of plant carbohydrate active enZymes and their role in xylogenesis. *BMC Genom.* 16:402. doi: 10.1186/s12864-015-1571-8

Prunet, N., Morel, P., Champelovier, P., Thierry, A.-M., Negrutiu, I., Jack, T., et al. (2015). SQUINT promotes stem cell homeostasis and floral meristem termination in *Arabidopsis* through APETALA2 and CLAVATA signalling. *J. Exper. Bot.* 66, 6905–6916. doi: 10.1093/jxb/erv394

R Core Team (2014). *R: A Language and Environment for Statistical Computing*. Vienna: R Foundation for Statistical Computing.

Rao, S., Zhou, Z., Miao, P., Bi, G., Hu, M., Wu, Y., et al. (2018). Roles of receptor-like cytoplasmic kinase VII members in pattern-triggered immune signaling. *Plant Physiol.* 177, 1679–1690. doi: 10.1104/pp.18.00486

Ratke, C., Terebieniec, B. K., Winestrand, S., Derba-Maceluch, M., Grahn, T., Schiffthaler, B., et al. (2018). Downregulating aspen xylan biosynthetic GT43 genes in developing wood stimulates growth via reprograming of the transcriptome. *New Phytol.* 219, 230–245. doi: 10.1111/nph.15160

Rubinovich, L., and Weiss, D. (2010). The *Arabidopsis* cysteine-rich protein GASA4 promotes GA responses and exhibits redox activity in bacteria and in planta. *Plant J.* 64, 1018–1027. doi: 10.1111/j.1365-313X.2010.04390.x

Rui, Y., and Dinneny, J. R. (2020). A wall with integrity: surveillance and maintenance of the plant cell wall under stress. *New Phytol.* 225, 1428–1439. doi: 10.1111/nph.16166

Schallus, T., Fehér, K., Sternberg, U., Rybin, V., and Muhle-Goll, C. (2010). Analysis of the specific interactions between the lectin domain of malectin and diglucosides. *Glycobiology* 20, 1010–1020. doi: 10.1093/glycob/cwq059

Schallus, T., Jaeckh, C., Fehér, K., Palma, A. S., Liu, Y., Simpson, J. C., et al. (2008). Malectin: a novel carbohydrate-binding protein of the endoplasmic reticulum and a candidate player in the early steps of protein *N*-glycosylation. *Mol. Biol. Cell* 19, 3404–3414. doi: 10.1091/mbc.e08-04-0354

Schaper, E., and Anisimova, M. (2015). The evolution and function of protein tandem repeats in plants. *New Phytol.* 206, 397–410. doi: 10.1111/nph.13184

Shannon, P., Markiel, A., Ozier, O., Baliga, N. S., Wang, J. T., Ramage, D., et al. (2003). Cytoscape: a software environment for integrated models of biomolecular interaction networks. *Genome Res.* 13, 2498–2504. doi: 10.1101/gr.1239303

Shiu, S.-H., and Bleecker, A. B. (2001). Receptor-like kinases from *Arabidopsis* form a monophyletic gene family related to animal receptor kinases. *Proc. Natl. Acad. Sci. U.S.A.* 98, 10763–10768. doi: 10.1073/pnas.181141598

Shiu, S.-H., and Bleecker, A. B. (2003). Expansion of the receptor-like kinase/Pelle gene family and receptor-like proteins in *Arabidopsis*. *Plant Physiol.* 132, 530–543. doi: 10.1104/pp.103.021964

Smith, M. R., Willmann, M. R., Wu, G., Berardini, T. Z., Möller, B., Weijers, D., et al. (2009). Cyclophilin 40 is required for microRNA activity in *Arabidopsis*. *Proc. Natl. Acad. Sci. U.S.A.* 106, 5424–5429. doi: 10.1073/pnas.0812729106

Song, H., Guo, Z., Chen, T., Sun, J., and Yang, G. (2018). Genome-wide identification of LRR-containing sequences and the response of these sequences to nematode infection in *Arachis duranensis*. *BMC Plant Biol.* 18:279. doi: 10.1186/s12870-018-1508-x

Stegmann, M., Monaghan, J., Smakowska-Luzan, E., Rovenich, H., Lehner, A., Holton, N., et al. (2017). The receptor kinase FER is a RALF-regulated scaffold controlling plant immune signaling. *Science* 355, 287–289. doi: 10.1126/science.aal2541

Sultana, M. M., Hachiya, T., Dutta, A. K., Nishimura, K., Suzuki, T., Tanaka, A., et al. (2020). Expression analysis of genes encoding malectin-like domain (MLD)- and leucine-rich repeat (LRR)- containing proteins in *Arabidopsis thaliana*. *Biosci. Biotechnol. Biochem.* 84, 154–158. doi: 10.1080/09168451.2019.1661769

Sundell, D., Mannapperuma, C., Netotea, S., Delhomme, N., Lin, Y.-C., Sjödin, A., et al. (2015). The plant genome integrative explorer resource: plantGenIE.org. *New Phytol.* 208, 1149–1156. doi: 10.1111/nph.13557

Sundell, D., Street, N. R., Kumar, M., Mellerowicz, E. J., Kucukoglu, M., Johnsson, C., et al. (2017). AspWood: high-spatial-resolution transcriptome profiles reveal uncharacterized modularity of wood formation in *Populus tremula*. *Plant Cell* 29, 1585–1604. doi: 10.1105/tpc.17.00153

Swarup, K., Benková, E., Swarup, R., Casimiro, I., Péret, B., Yang, Y., et al. (2008). The auxin influx carrier LAX3 promotes lateral root emergence. *Nat. Cell Biol.* 10, 946–954. doi: 10.1038/ncb1754

Thole, J. M., Vermeer, J. E. M., Zhang, Y., Gadella, T. W. J., and Nielsen, E. (2008). ROOT HAIR DEFECTIVE4 encodes a phosphatidylinositol-4-phosphate phosphatase required for proper root hair development in *Arabidopsis thaliana*. *Plant Cell* 20, 381–395. doi: 10.1105/tpc.107.054304

Voxeur, A., and Höfte, H. (2016). Cell wall integrity signaling in plants: "To grow or not to grow that's the question". *Glycobiology* 26, 950–960. doi: 10.1093/glycob/cww029

Wang, G., Ellendorff, U., Kemp, B., Mansfield, J. W., Forsyth, A., Mitchell, K., et al. (2008). A genome-wide functional investigation into the roles of receptor-like proteins in *Arabidopsis*. *Plant Physiol.* 147, 503–517. doi: 10.1104/pp.108.119487

Wang, J., Kucukoglu, M., Zhang, L., Chen, P., Decker, D., Nilsson, O., et al. (2013). The *Arabidopsis* LRR-RLK, PXC1, is a regulator of secondary wall formation correlated with the TDIF-PXY/TDR-WOX4 signaling pathway. *BMC Plant Biol.* 13:94. doi: 10.1186/1471-2229-13-94

Wang, Y., Salasini, B. C., Khan, M., Devi, B., Bush, M., Subramaniam, R., et al. (2019). Clade I TGACG-motif binding basic leucine zipper transcription factors mediate BLADE-ON-PETIOLE-dependent regulation of development. *Plant Physiol.* 180, 937–951. doi: 10.1104/pp.18.00805

Wang, J., Hu, T., Wang, W., Hu, H., Wei, Q., and Bao, C. (2019). Investigation of evolutionary and expressional relationships in the function of the leucine-rich repeat receptor-like protein kinase gene family (LRR-RLK) in the radish (*Raphanus sativus* L.). *Sci. Rep.* 9:6937. doi: 10.1038/s41598-019-43516-9

Waterhouse, A. M., Procter, J. B., Martin, D. M. A., Clamp, M., and Barton, G. J. (2009). Jalview Version 2 - a multiple sequence alignment editor and analysis workbench. *Bioinformatics* 25, 1189–1191. doi: 10.1093/bioinformatics/btp033

Wolf, S. (2017). Plant cell wall signalling and receptor-like kinases. *Biochem. J.* 474, 471–492. doi: 10.1042/bcj20160238

Wolf, S., and Höfte, H. (2014). Growth control: a saga of cell walls, ROS, and peptide receptors. *Plant Cell* 26, 1848–1856. doi: 10.1105/tpc.114.125518

Won, S.-K., Lee, Y.-J., Lee, H.-Y., Heo, Y.-K., Cho, M., and Cho, H.-T. (2009). cis-Element- and transcriptome-based screening of root hair-specific genes and their functional characterization in *Arabidopsis*. *Plant Physiol.* 150, 1459–1473. doi: 10.1104/pp.109.140905

Xi, J., Qiu, Y., Du, L., and Poovaiah, B. W. (2012). Plant-specific trihelix transcription factor *AtGT2L* interacts with calcium/calmodulin and responds to cold and salt stresses. *Plant Sci.* 185–186, 274–280. doi: 10.1016/j.plantsci.2011.11.013

Xi, L., Wu, X. N., Gilbert, M., and Schulze, W. X. (2019). Classification and interactions of LRR receptors and co-receptors within the *Arabidopsis* plasma membrane - an overview. *Front. Plant Sci.* 10:472. doi: 10.3389/fpls.2019.00472

Xiao, Y., Stegmann, M., Han, Z., DeFalco, T. A., Parys, K., Xu, L., et al. (2019). Mechanisms of RALF peptide perception by a heterotypic receptor complex. *Nature* 572, 270–274. doi: 10.1038/s41586-019-1409-7

Yanai, I., Benjamin, H., Shmoish, M., Chalifa-Caspi, V., Shklar, M., Ophir, R., et al. (2005). Genome-wide midrange transcription profiles reveal expression level relationships in human tissue specification. *Bioinformatics* 21, 650–659. doi: 10.1093/bioinformatics/bti042

Yang, Y., Labbé, J., Muchero, W., Yang, X., Jawdy, S. S., Kennedy, M., et al. (2016). Genome-wide analysis of lectin receptor-like kinases in *Populus*. *BMC Genom.* 17:699. doi: 10.1186/s12864-016-3026-2

Yeh, Y.-H., Panzeri, D., Kadota, Y., Huang, Y.-C., Huang, P.-Y., Tao, C.-N., et al. (2016). The *Arabidopsis* malectin-like/LRR-RLK IOS1 is critical for BAK1-dependent and BAK1-independent pattern-triggered immunity. *Plant Cell* 28, 1701–1721. doi: 10.1105/tpc.16.00313

Yuan, N., Yuan, S., Li, Z., Zhou, M., Wu, P., Hu, Q., et al. (2018). STRESS INDUCED FACTOR 2, a leucine-rich repeat kinase regulates basal plant pathogen defense. *Plant Physiol.* 176, 3062–3080. doi: 10.1104/pp.17.01266

Zan, Y., Ji, Y., Zhang, Y., Yang, S., Song, Y., and Wang, J. (2013). Genome-wide identification, characterization and expression analysis of *Populus* leucine-rich repeat receptor-like protein kinase genes. *BMC Genom.* 14:318. doi: 10.1186/1471-2164-14-318

Zhang, Q., Jia, M., Xing, Y., Qin, L., Li, B., and Jia, W. (2016). Genome-wide identification and expression analysis of *MRLK* family genes associated with strawberry (*Fragaria vesca*) fruit ripening and abiotic stress responses. *PLoS One* 11:e0163647. doi: 10.1371/journal.pone.0163647

Zhong, R., and Ye, Z.-H. (2012). MYB46 and MYB83 bind to the SMRE sites and directly activate a suite of transcription factors and secondary wall biosynthetic genes. *Plant Cell Physiol.* 53, 368–380. doi: 10.1093/pcp/pcr185

Zhou, J., Liu, D., Wang, P., Ma, X., Lin, W., Chen, S., et al. (2018). Regulation of *Arabidopsis* brassinosteroid receptor BRI1 endocytosis and degradation by plant U-box PUB12/PUB13-mediated ubiquitination. *Proc. Natl. Acad. Sci. U.S.A.* 115, E1906–E1915. doi: 10.1073/pnas.1712251115

Zulawski, M., Schulze, G., Braginets, R., Hartmann, S., and Schulze, W. X. (2014). The *Arabidopsis* kinome: phylogeny and evolutionary insights into functional diversification. *BMC Genom.* 15:548. doi: 10.1186/1471-2164-15-548

Conflict of Interest: The authors declare that the research was conducted in the absence of any commercial or financial relationships that could be construed as a potential conflict of interest.

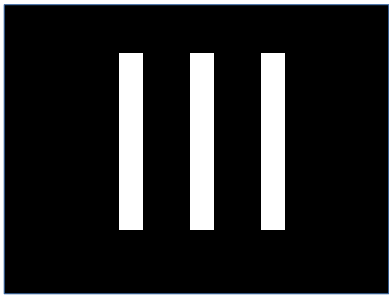

frontiers in Plant Science

ORIGINAL RESEARCH
published: 25 May 2020
doi: 10.3389/fpls.2020.00651

Cell Wall Acetylation in Hybrid Aspen Affects Field Performance, Foliar Phenolic Composition and Resistance to Biological Stress Factors in a Construct-Dependent Fashion

*Marta Derba-Maceluch[1], Fariba Amini[2,3], Evgeniy N. Donev[1], Prashant Mohan-Anupama Pawar[1†], Lisa Michaud[2], Ulf Johansson[4], Benedicte R. Albrectsen[2] and Ewa J. Mellerowicz[1]**

[1] Department of Forest Genetics and Plant Physiology, Umeå Plant Science Centre, Swedish University of Agricultural Sciences, Umeå, Sweden, [2] Department of Plant Physiology, Umeå Plant Science Centre, Umeå University, Umeå, Sweden, [3] Biology Department, Faculty of Science, Arak University, Arak, Iran, [4] Tönnersjöheden Experimental Forest, Swedish University of Agricultural Sciences, Simlångsdalen, Sweden

The production of biofuels and "green" chemicals from the lignocellulose of fast-growing hardwood species is hampered by extensive acetylation of xylan. Different strategies have been implemented to reduce xylan acetylation, resulting in transgenic plants that show good growth in the greenhouse, improved saccharification and fermentation, but the field performance of such plants has not yet been reported. The aim of this study was to evaluate the impact of reduced acetylation on field productivity and identify the best strategies for decreasing acetylation. Growth and biological stress data were evaluated for 18 hybrid aspen lines with 10–20% reductions in the cell wall acetyl content from a five year field experiment in Southern Sweden. The reduction in acetyl content was achieved either by suppressing the process of acetylation in the Golgi by reducing expression of *REDUCED WALL ACETYLATION* (*RWA*) genes, or by post-synthetic acetyl removal by fungal acetyl xylan esterases (AXEs) from two different families, CE1 and CE5, targeting them to cell walls. Transgene expression was regulated by either a constitutive promoter (*35S*) or a wood-specific promoter (*WP*). For the majority of transgenic lines, growth was either similar to that in WT and transgenic control (*WP:GUS*) plants, or slightly reduced. The slight reduction was observed in the AXE-expressing lines regulated by the *35S* promoter, not those with the *WP* promoter which limits expression to cells developing secondary walls. Expressing AXEs regulated by the *35S* promoter resulted in increased foliar arthropod chewing, and altered condensed tannins and salicinoid phenolic glucosides (SPGs) profiles. Greater growth inhibition was observed in the case of CE5 than with CE1 AXE, and it was associated with increased foliar necrosis and distinct SPG profiles, suggesting that CE5 AXE could

OPEN ACCESS

Edited by:
Zeng-Yu Wang,
Qingdao Agricultural University, China

Reviewed by:
Ajaya K. Biswal,
University of Georgia, United States
R. Glen Uhrig,
University of Alberta, Canada

***Correspondence:**
Ewa J. Mellerowicz
ewa.mellerowicz@slu.se

†Present address:
Prashant Mohan-Anupama Pawar,
Regional Centre for Biotechnology, NCR Biotech Science Cluster, Haryana, India

Specialty section:
This article was submitted to Plant Biotechnology, a section of the journal Frontiers in Plant Science

Received: *21 February 2020*
Accepted: *27 April 2020*
Published: *25 May 2020*

Citation:
Derba-Maceluch M, Amini F, Donev EN, Pawar PM-A, Michaud L, Johansson U, Albrectsen BR and Mellerowicz EJ (2020) Cell Wall Acetylation in Hybrid Aspen Affects Field Performance, Foliar Phenolic Composition and Resistance to Biological Stress Factors in a Construct-Dependent Fashion. Front. Plant Sci. 11:651. doi: 10.3389/fpls.2020.00651

be recognized by the pathogen-associated molecular pattern system. For each of three different constructs, there was a line with dwarfism and growth abnormalities, suggesting random genetic/epigenetic changes. This high frequency of dwarfism (17%) is suggestive of a link between acetyl metabolism and chromatin function. These data represent the first evaluation of acetyl-reduced plants from the field, indicating some possible pitfalls, and identifying the best strategies, when developing highly productive acetyl-reduced feedstocks.

Keywords: *Populus tremula* × *tremuloides*, transgenic trees, field trial, biotic resistance, salicinoid phenolic glucosides, condensed tannins, *HjAXE*, *AnAXE1*

INTRODUCTION

Plant cell walls (lignocellulose) constitute by far the most abundant carbon source on Earth available for the sustainable production of advanced biofuels and "green" chemicals (Bar-On et al., 2018). These products are made through saccharification which converts lignocellulose to fermentable sugars. The industrial saccharification and fermentation processes are challenged by, among other factors, the abundance of acetylation substituents (Jönsson and Martín, 2016) present in most cell wall polymers (Gille and Pauly, 2012; Donev et al., 2018). Dicotyledonous plants, including broadleaf trees (hardwoods), are particularly rich in *O*-acetyl substituents, the majority of which are associated with xylan (Pawar et al., 2013; Pauly and Ramírez, 2018). Biological role of xylan acetylation is not fully understood, but it is known to affect xylan solubility (Gröndahl et al., 2003), susceptibility to enzymatic degradation (Biely et al., 2016), interaction with cellulose (Grantham et al., 2017) and lignin (Giummarella and Lawoko, 2016). On the other hand, there is a considerable variation among different groups of plants in xylan acetylation, and some of them, like conifers, have no acetyl xylan substitution (Pawar et al., 2013). Several attempts have therefore been made to reduce acetyl content in dicotyledon species (Pogorelko et al., 2011; Xiong et al., 2015; Pawar et al., 2016) including hardwoods (Ratke et al., 2015; Pawar et al., 2017a,b; Wang et al., 2020). Based on the performance of greenhouse-grown plants, reductions in *O*-acetylation were found to be well tolerated by plants when the degree of xylan substitution was reduced by 30% or less (Pogorelko et al., 2011; Xiong et al., 2015; Pawar et al., 2016). Moreover, reducing acetylation was found to be one of the most promising strategies for improving plant cell walls for the purposes of saccharification and fermentation (Donev et al., 2018). These results were encouraging, but the performance of such acetylation-reduced lines also needs to be tested in the field.

Field conditions impose both biotic and abiotic stresses on plants, and therefore field performance may be very different from growth observed in the greenhouse (Strauss, 2003). Acetylation-challenged plants in particular could perform differently between these two sets of conditions, since such plants have been shown to react differently to both biotic and abiotic stresses. For example, *Arabidopsis* plants with a mutation in the *TRICHOME BIREFRINGENCY-LIKE 29 (TBL29)* gene encoding a key acetyl transferase involved in secondary wall xylan acetylation (Urbanowicz et al., 2014) were reported to be highly resistant to water deficit and freezing stress, and were thus named *eskimo1 (esk1)* (Xin and Browse, 1998; Xin et al., 2007; Lefebvre et al., 2011; Xu et al., 2014). Plants mutated in *TBL44/PMR5* from the same family are known to be resistant to powdery mildew (Vogel et al., 2004). Similarly, an acetylation deficit caused by mutations in *REDUCED WALL ACETYLATION* (*RWA*) genes that affect acetylation of all cell wall polysaccharides resulted in biotic resistance to biotrophic and necrotrophic fungi in *Arabidopsis* (Manabe et al., 2011; Pawar et al., 2016). Post-synthetic removal of acetic groups from the xylan backbone by transgenic expression of fungal acetyl xylan esterases (AXEs) has been shown to increase resistance to certain pathogenic fungi (Pogorelko et al., 2013; Pawar et al., 2016). Thus deacetylation of xylan appears to lead to better plant resistance to biotic and abiotic stresses. Naturally occurring deacetylation of pectin by the enzyme encoded by *PECTIN ACETYLESTERASE 9* (*AtPAE9*) has been shown to be required for proper basal levels of innate immunity and resistance to aphids (Kloth et al., 2019). A knock out *pae9* mutant with increased rhamnogalacturonan I (RGI) and homogalacturonan acetylation compared to wild-type plants (De Souza et al., 2014) exhibited decreased concentrations of JA, SA, ABA, and IAA, and initial facilitation of cell wall penetration by aphids (Kloth et al., 2019). Although the mechanism by which the cell wall acetylation level is communicated to the plant cell protoplast is at present not known (reviewed by Bacete et al., 2018), it is clear that modifying acetylation can impact plant biotic and abiotic resistance, which are key parameters affecting the field performance of plants.

To assess the field performance of acetylation-reduced plants we tested transgenic hybrid aspen (*Populus tremula* L. × *tremuloides* Michx.) lines in which the acetyl content was reduced by different means. These lines, in which xylan acetylation was post-synthetically reduced, included ones expressing AXEs of fungal origin from two Carbohydrate Esterase families, CE1 and CE5, *Aspergillus niger* AXE1 (*An*AXE1) and *Hypocrea jecorina* AXE (*Hj*AXE), respectively (Ratke et al., 2015; Pawar et al., 2017b; Wang et al., 2020).

Abbreviations: *35S*, Cauliflower mosaic virus *35S* promoter; ABA, abscisic acid; *An*AXE1, *Aspergillus niger* ACETYL XYLAN ESTERASE 1; CT, Condensed Tannin; *Hj*AXE, *Hypocrea jecorina* ACETYL XYLAN ESTERASE; IAA, indole-3-acetic acid; JA, jasmonic acid; PAE9, PECTATE ACETYLESTERASE 9; RGI, rhamnogalacturonan I; RWA, REDUCED WALL ACETYLATION; SA, salicylic acid; SPGs, salicinoid phenolic glucosides; TBL, TRICHOME BIREFRINGENCY-LIKE; *WP*, Wood Promoter.

AnAXE1 and *HjAXE* expressing lines grown in a greenhouse environment developed as well as wild type, and had superior saccharification properties. The lines in which acetyl content was reduced due to deficiencies in the biosynthetic acetylation machinery were those with reduced expression of native *REDUCED WALL ACETYLATION* (*RWA*) genes (Pawar et al., 2017a). The latter lines exhibited similar reductions in acetylation and improved saccharification properties, with good growth in the greenhouse, as the lines in which the xylan was post-synthetically deacetylated. Using these lines we were able to compare the impacts of reducing acetylation during the biosynthesis of xylan in the Golgi by suppressing *RWA* genes with those where the reduction was achieved post-synthetically in cell walls by expressing the fungal enzymes *An*AXE1 and *Hj*AXE targeted to the apoplast. We also addressed the question of the promoter to be used for genetic engineering. We compared the effects of the same transgenes expressed from either constitutive *35S* or wood-specific *WP* (Ratke et al., 2015) promoters. Finally, we compared the effects of two fungal enzymes belonging to the different CE families. We monitored growth over five years, and determined foliar biotic damage and foliar concentrations of phenylpropanoid compounds, which are indicators of stress induction and stress resistance (Dixon and Paiva, 1995; Papazian et al., 2019). In *Populus* spp., biotic stress has commonly been associated with levels of condensed tannins (CTs) (Bandau et al., 2015; Lindroth and Madritch, 2015; Lindroth et al., 2015) and salicinoid phenolic glucosides (SPGs) (Albrectsen et al., 2010; Robinson et al., 2012; Lindroth and St. Clair, 2013; Lindroth and Madritch, 2015), and these phenylpropanoid compounds are often related to environmental stress responses and performance (Lindroth et al., 2011; Robinson et al., 2012; Keefover-Ring et al., 2014; Bandau et al., 2015; Decker et al., 2016). We therefore measured foliar concentrations of these compounds in acetylation-compromised aspen lines. This is the first analysis of the field performance of plants with reduced acetylation.

MATERIALS AND METHODS

Biological Material

Hybrid aspen (*Populus tremula* L. × *tremuloides* Michx.) clone T89 was used as wild-type and all transgenic lines were made in this genetic background. Transgenic lines initially tested in the greenhouse included those expressing *35S:An*AXE1 (Pawar et al., 2017b), *35S:HjAXE* and *WP:Hj*AXE (Ratke et al., 2015; Wang et al., 2020), as well as lines with RNAi constructs targeting hybrid aspen *RWA-C* and *RWA-D* genes, denoted *35S:RWA-CD* (previously called *35S::CD-RWA RNAi*), and all four *RWA* genes, denoted *WP:RWA-ABCD* (previously called *pGT43B::RWA-ABCD RNAi*) (Pawar et al., 2017a). Two lines expressing a β-glucuronidase (GUS) gene under the control of the *WP* promoter (Ratke et al., 2015) were used as transgenic controls. Additional lines were generated that expressed *WP:AnAXE1* using the *pK-pGT34B-GW* destination vector (Ratke et al., 2015) and the *AnAXE1* cDNA as previously described (Pawar et al., 2017b). Each construct was represented by two to four lines selected from among approx. 20 independent lines, as described previously, based on the strength of transgene expression and superiority of greenhouse performance with regard to growth and saccharification properties (as described by Ratke et al., 2015; Pawar et al., 2017a,b; Wang et al., 2020), with the exception of *WP:AnAXE1*. The *WP:AnAXE1* lines were selected based on the strength of transgene expression in plants cultivated *in vitro*, as determined by RT-PCR analysis (**Supplementary Figure S1**). A list of the lines and constructs is given in **Table 1**.

TABLE 1 | Lines included in the field trial analysis.

Construct	Lines	References
35S:RWA-CD	10, 21, 22	Pawar et al., 2017a
WP:RWA-ABCD	11, 15	Pawar et al., 2017a
35S:AnAXE1	4, 8, 17	Pawar et al., 2017b
WP:AnAXE1	1, 5, 8, 10	This paper, **Supplementary Figure S1**
35S:HjAXE	9, 13, 22	Ratke et al., 2015; Wang et al., 2020
WP:HjAXE	11, 14B, 14C	Ratke et al., 2015; Wang et al., 2020
WP:GUS	25, 27	Ratke et al., 2015

Field Trial Establishment and Experimental Design

Transgenic trees were propagated *in vitro* at the Umeå Plant Science Centre transformation facility in Umeå, Sweden (Nilsson et al., 1992) and transplanted into soil for one month of acclimatization in the greenhouse in early spring 2014. Then, with permission from the Swedish Board of Agriculture (DNR. 4.6.18-761/14), the trees were moved to sheltered outdoor premises in Umeå for a two-week hardening period, before translocation to the field site (ca 1000 km south of Umeå) in Våxtorp, Laholm community, Sweden (56.42°N, 13.07°E). Between August 4 and 8, 2014, the trees were planted in the field, with a 3 m spacing, on abandoned farm land fenced according to the requirements for genetically modified plants. In total, 636 trees included in the current analysis, along with other trees not analyzed here, were arranged in a 14 block design, with two trees of each transgenic line randomly distributed within each block along with four wild-type (WT) trees (**Supplementary Figure S2**). For weed control, the field was harrowed twice a year during the first two years following planting and grass was mowed twice a year during subsequent years. All biosecurity and safety procedures for field trials with transgenic plants required by the Swedish Board of Agriculture have been adhered to.

Histochemical Analysis of GUS Expression

The stability of GUS gene expression was investigated in July of year four (2017) during the period of active cambial growth. The basal part of a two-year-old branch was hand sectioned and the sections were prefixed in acetone for 30 min, washed with water, placed in the reaction solution (1 mM X-GlcA (5-bromo-4-chloro-3-indolyl β-D-glucuronide), 50 mM Na-phosphate buffer pH 7, 0.1% (v/v) Triton, 1 mM $K_3[Fe(CN)_6]$, 1 mM $K_4[Fe(CN)_6]$), and incubated for 3 days in the dark at room temperature. Sections were then fixed in FAA (50% ethanol, 5% formaldehyde, 10% acetic acid, all v/v) overnight followed by clearing and dehydration in an ethanol series. Samples were

rehydrated, mounted in 50% (v/v) glycerol, and imaged with a Zeiss Axioplan 2 microscope using a 40× objective. Micrographs were taken with an Axiocam HRc camera and Axiovision V 4.8.2 Software (Carl Zeiss Light Microscopy, Göttingen, Germany). Images were combined into panoramas covering the section from bark to pith using the program Adobe Photoshop CS6.

Periodic Growth and General Damage Assessment

Growth parameters (plant height and root collar diameter) were assessed at the end of each growth season. Final tree height and diameter were also measured in June 2018, before harvesting. The height was assessed with a measuring stick and the stem diameter with a caliper (3 cm above ground level). Stem volume was calculated as: $V = 1/3\pi R^2 H$, where R – stem radius, H – stem height.

Standard assessments (Nilsson and Örlander, 1999) of damage were conducted four times a year; they included cause of damage (fungi, frost, drought, waterlogging, rodents, herbivores, insects, vegetation, unknown) and severity on a six-level scale (0 = undamaged, 1 = slight damage, 2 = uncertain or moderate damage, 3 = severe damage, 4 = life-threatening damage, and 5 = dead).

Detailed Biotic Stress Assessment and Leaf Collection

A detailed assessment of leaf damage was performed in July 2017 during the fourth growing season, according to previous methodology (Albrectsen et al., 2010; Robinson et al., 2012). Chewing damage by arthropods (chewing) was assessed as percentage of chewed leaves in the canopy. Evidence of other types of damage was scored in terms of presence (1) or absence (0). This was done for damage caused by arthropods including aphids, miners, gall-producing organisms, and pathogens including rust (*Melampsora spp.*) and venturia (*Venturia spp.*). Symptoms of chlorosis, necrosis, and hypersensitive response (HR) were recorded in the same way.

Assessment of Traits Related to Architecture and Leaf Chemical Profiling

Architectural traits, chlorophyll index, and leaf CT contents were assessed for a subsample consisting of 50% of trees having superior height selected from each transgenic line and wild type. The rationale for stratifying the samples by height rather than randomly selecting 50% of trees from each line was to avoid those trees that had been damaged by planting, field work or other types of random disturbance.

Architectural Traits

Branching was assessed according to Luquez et al. (2008). The apical dominance was scored on a scale from 0 to 8 as follows: clear leader (8)/good recovery after apex damage in 2017 (7)/good recovery after apex damage in 2016 (6)/good recovery after apex damage in 2015 (5)/main shoot lost in 2015 (4)/main shoot lost in 2016 (3)/main shoot lost in 2017 (2)/bushy growth (1)/dwarf (0).

Chlorophyll Content

Chlorophyll content was measured in fully developed leaves with no visible damage, collected from the upper part of the main stem between June 26 and 30, 2017, using a CCM-200 plus (Opti-Science, Huston, United States). A mean value from 18 measurements per tree was obtained (six leaves per tree and three measurements per leaf). The same leaves were collected for metabolite analyses and dry weight assessment. They were immediately frozen on dry ice and freeze-dried before being transported to Umeå for weighing, grinding and metabolic profiling.

Condensed Tannins

Six freeze-dried leaves per tree were ground together to a powder. Foliar CT contents were assessed based on the acid-butanol method of Porter et al. (1986). In short, 10.0 ± 2.0 mg leaf powder (exact weight) was extracted with 800 μl of a mix of acetone and 10 mM ascorbic acid solutions in a 70:30 (v:v) ratio, mixed by vortexing, sonicated, and centrifuged for 5 min at 3500 rpm on a bench top centrifuge. The absorbance of the extract (150 μl of supernatant) at 550 nm was measured with a spectrophotometer (Hitachi U-5100 UV/VIS, Hitachi High-Technologies, Tokyo, Japan). Results were compared to a standard curve of procyanidin B2 ($C_{30}H_{26}O_{12}$, Sigma-Aldrich®, St. Louis, MO, United States) and recalculated to give mg/g (d.w.) leaf powder.

Metabolite Analysis

Four trees per line were randomly selected from the set used for leaf CT determination. Ultra high performance liquid chromatography (UHPLC) with UV and electro-spray ionization time-of-flight mass spectrometry (ESI-TOF/MS) detectors was used as described by Abreu et al. (2011) and Keefover-Ring et al. (2014). In short, 10.00 ± 1.00 mg of ground leaf material was extracted in 1 ml of cold (4°C) methanol: chloroform: water, 60:20:20 (v:v:v), with deuterated SA as an internal standard. After centrifugation, 200 μl of the extract supernatant was dried in a speedvac. Before analysis, the samples were reconstituted with 20 μl of methanol and 20 μl of a 0.1% v/v aqueous formic acid solution. Compounds in the reconstituted plant extracts were separated on a C18 UPLC™ column (2.1 × 100 mm, 1.7 μm) and analyzed by an Acquity photodiode array detector coupled in line with a LCT Premier TOF/MS (all from Waters, Milford, MA, United States) as described by Abreu et al. (2011).

The MassLynx 4.1 software package (Waters Corp.) was used to extract single ion chromatograms (±0.15 exact mass unit) using the QuanLynx module to search for known and theoretical phenylpropanoids (using deprotonated ($[M-H]^-$) and formate adduct ($[M-H+FA]^-$) ions). QuanLynx software was used to obtain peak areas that were normalized with respect to internal standard peak area and sample weight; as described in Abreu et al. (2011) and Keefover-Ring et al. (2014). The phenylpropanoids salicortin, tremulacin, salicin, tremuloidin, salicyloylsalicin, HCH-salicortin, 2′-(E)-, and 2′-(Z)-cinnamoylsalicortin were determined using retention times and molecular weight information for purified standards. Other compounds

(2′-acetylsalicin, 2′-acetylsalicortin, acetyl tremulacin, HCH-2′-acetylsalicortin, HCH-tremulacin, and arachidonic acid) were tentatively identified based on LC-MS molecular weights and defragmentation patterns.

Statistical Analyses

All analyses were performed using the software package JMP 14.0.0 2018 (SAS Institute Inc.). The consequences of decreased acetylation for field performance were analyzed for a total of 19 growth related traits, 14 biotic stress related traits, and 23 foliar defense related chemicals (mainly phenylpropanoids). Effects of individual lines were tested by a one-way ANOVA with "line" used as fixed effect (**Supplementary Tables S1, S2**). Similarity of individual lines to WT was evaluated by a Dunnett's test, and consistent line effect within a construct were assessed by a contrast analysis (all lines for a given construct versus WT). These results were used to identify cases of reproducible construct effects among different transgenic lines.

A nested-ANOVA model design was used to answer questions about the impact of construct on phenotypic trait expression. "Line" nested in "construct" and block (random, considered when possible) effects were included (**Supplementary Tables S3, S4**). A multiple comparison Tukey test was used for cross-comparisons among different constructs.

Impacts of the promoter and the transgene (fixed effects) were analyzed by a two-way ANOVA with an interaction (**Supplementary Table S6**), and comparison of deacetylation strategy was carried out by a nested ANOVA model with "construct " nested in "pre- or post-synthetic strategy" and "line" nested within "construct" (**Supplementary Table S7**), all used as fixed effects.

RESULTS

Field Growth Analysis Identified Three Lines With Anomalies

Uniform growth and a stable survival rate of close to 100% (86–100%) characterized the majority of the transgenic lines throughout the period of testing at the field site (**Figure 1A** and **Supplementary Table S1**). However, three out of 20 transgenic lines for three different constructs (namely line 22 for construct *35S:RWA-CD*, line 15 for construct *WP:RWA-ABCD*, and line 11 for construct *WP:HjAXE*) exhibited distinct deviations from the general growth pattern. These lines were dwarf, reaching only 1, 26, and 2% of WT stem volume, respectively, and their apical dominance was reduced compared to that of WT and other lines with the same construct (**Figures 1B,C** and **Supplementary Table S1**). Line 11 of *WP:HjAXE* had significantly higher mortality than the other transgenic lines and WT (**Figure 1D**), and approx. 50% of trees of this line showed a striking variegated phenotype that suggested genomic instability (**Figures 1D,E**). None of these phenotypes were seen in greenhouse trials (Ratke et al., 2015; Pawar et al., 2017a,b; Wang et al., 2020). The three dwarf lines were also more affected by hare browsing and multiple injuries than the other lines or WT trees (**Supplementary Table S1**).

Since other lines with the *WP:HjAXE* and *35S:RWA-CD* constructs did not exhibit dwarf phenotypes, and moreover since line 11 of *WT:HjAXE* had lower transgene expression levels than the other lines carrying this construct (Wang et al., 2020), we do not consider these anomalies to have been caused by the respective transgenes. Rather these phenotypes should be attributed to mutations induced either by random transgene insertions in the genome or by somaclonal variation. However, the *WP:RWA-ABCD* construct was represented by only two lines that had very different phenotypes (**Figures 1B–D** and **Supplementary Table S1**). It was therefore not possible to infer any true construct effect from the data and both these lines were subsequently omitted from analyses testing construct effects. Thus, the subsequent analyses evaluate the effects of five constructs: *35S:RWA-CD*, *35S:AXE1*, *35S:HjAXE*, *WP:AnAXE1*, and *WP:HjAXE,* with the anomalous lines removed from analyses.

Effects of Constructs on Tree Growth and Development

Stem growth parameters (height and diameter) for the different constructs are shown in **Figure 2** and **Supplementary Tables S2, S3**. Trees expressing *WP:AXE1* and *WP:HjAXE* were slightly bigger than WT in the first year, but this advantage disappeared during the subsequent years. In contrast, those with two other constructs, *35S:AnAXE1* and *35S:HjAXE,* showed a small reduction in height and /or stem diameter after three and four years of growth (**Figures 2A,B**), resulting in a decrease in stem volume in the fourth year of 24 and 37%, respectively, as compared to WT (**Figure 2C**).

Shoot apical dominance and the branching pattern did not show any construct-related effects (**Supplementary Tables S2, S3**). Leaf dry weight and chlorophyll content were reduced in *35S:HjAXE* expressing trees as compared to WT, but their leaf morphology did not change (**Figure 3**). Interestingly, the chlorophyll content was slightly increased in *35S:RWA-CD* (**Figure 3**); this was not observed in any of the *WP:RWA-ABCD* lines (**Supplementary Table S1**). Unexpectedly, a small decrease in chlorophyll content was observed in *WP:GUS* lines.

To assess the suitability of the *35S* and *WP* promoters and the two *AXE* transgenes, *AnAXE1 and HjAXE* for transgenic expression, we analyzed the growth traits of a subset of transgenic lines (*35S:AXE1*, *35S:HjAXE*, *WP:AXE1*, *WP:HjAXE*) by a two-way ANOVA with promoter and transgene as fixed effects (**Supplementary Table S6**). This comparison revealed a positive effect of *WP*, compared to the *35S* promoter, on stem height, diameter, volume, and chlorophyll index (**Figures 2A–C**, **3B** and **Supplementary Table S6**). In contrast, there was hardly any effect of the transgene (*AnAXE1* vs. *HjAXE*) on growth, whereas the chlorophyll index was decreased in *HjAXE* compared with *AnAXE1* but only when combined with the *35S* promoter (**Figure 3B** and **Supplementary Table S6**).

Specificity of *WP* activity has been previously tested in greenhouse conditions (Ratke et al., 2015). We therefore investigated whether its activity and expression pattern are maintained in field conditions, using histochemical

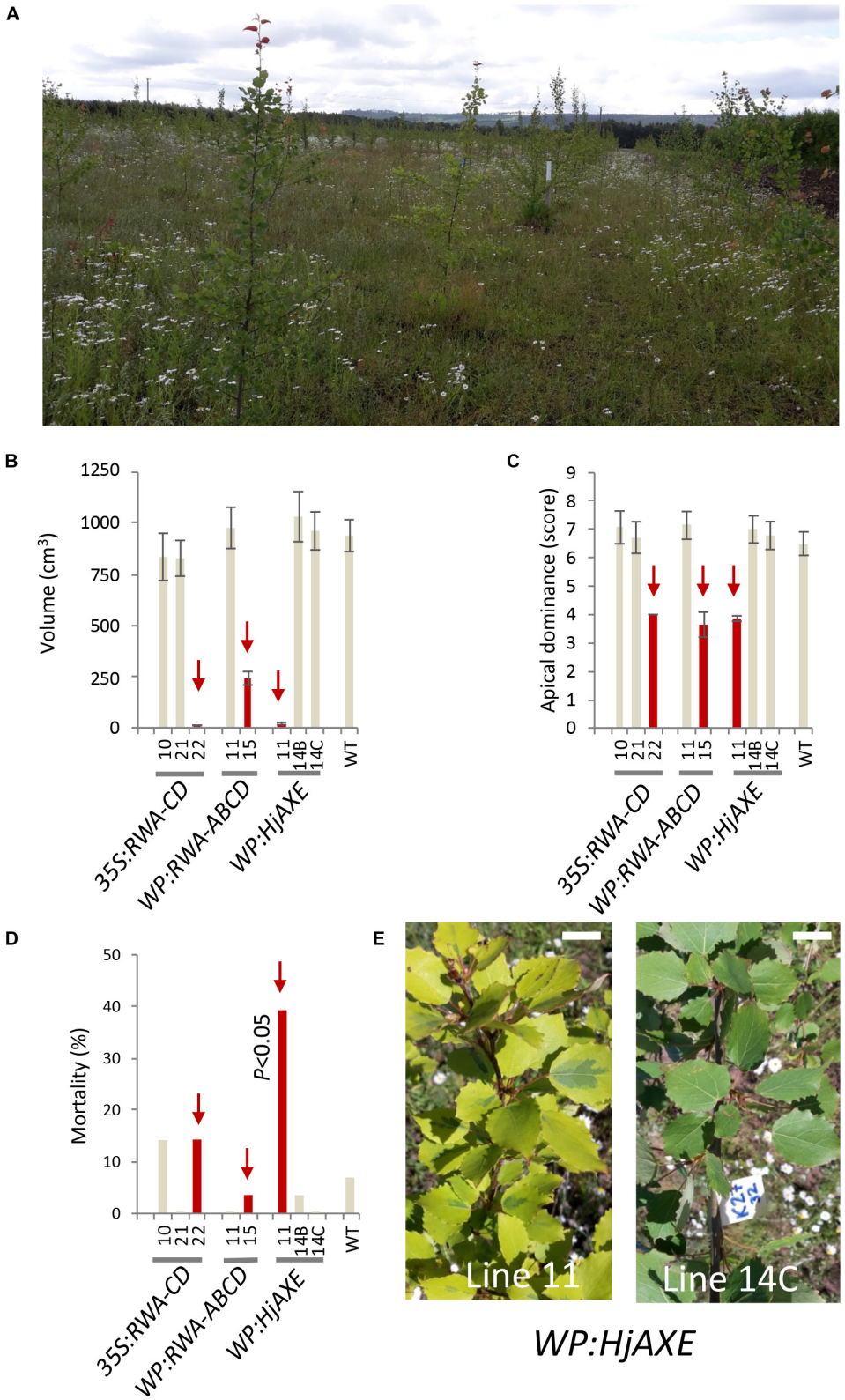

FIGURE 1 | Field testing revealed striking phenotypes in three out of 20 lines tested, effects which could not be related to transgenes. Overview of the field trial in July 2017 (fourth year) **(A)** and the corresponding data for anomalous lines: stem volume **(B)**, apical dominance **(C)** and mortality within the lines **(D)**. Lines marked in red showed aberrant morphology compared to other lines with the same construct and to WT. Line 11 with the *WP:HjAXE* construct had higher mortality than all other lines, and exhibited a variegated phenotype **(E)** not seen in other lines carrying this construct. Scale bar in E – 2 cm. Data in panels **(B)** and **(C)** are means ± SE.

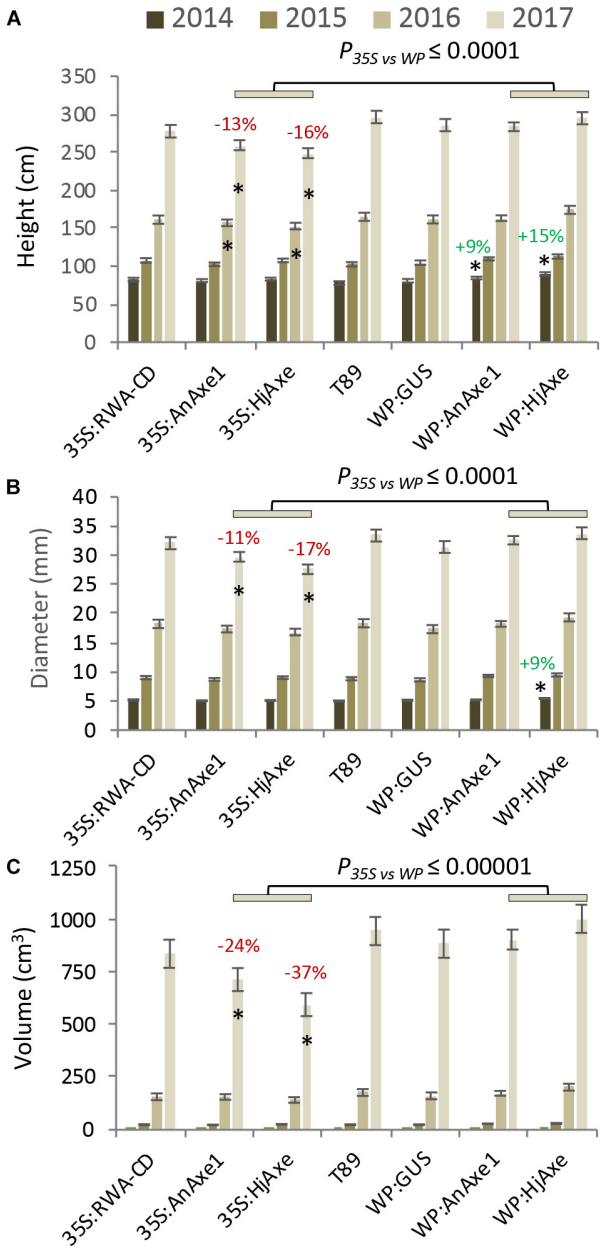

FIGURE 2 | Effects of different types of genetic modification on growth of transgenic lines during a four-year field trial. Height **(A)**, diameter **(B)**, and stem volume **(C)**. Means and SE, stars indicate means significantly different from WT, post-ANOVA contrast, $p \leq 0.05$). *P*-value indicates significance of the promoter effect based on a two-way ANOVA (**Supplementary Table S6**).

β-glucuronidase analysis of two *WP:GUS* lines during the fourth growing season. The test was carried out on branches with 1- and 2-year old cambia. In both samples and both lines, β-glucuronidase expression was detected in differentiating secondary xylem cells and secondary phloem fibers and sclereids depositing secondary walls (**Figure 4** and **Supplementary Figure S3**). This expression pattern was consistent with that previously observed in the same lines in the greenhouse (Ratke et al., 2015). We conclude that the activity and specificity of *WP* was not altered in the field.

We also investigated whether growth was differentially affected in plants in which xylan acetylation was modified during biosynthesis in the Golgi compared to plants in which post-synthetic xylan deacetylation was implemented (denoted *post-* vs. *synthetic* comparison). To answer this question, the lines with *RWA-CD* RNAi suppression driven by the *35S* promoter were compared with those where fungal *AXEs* were driven by *35S* using ANOVA (**Supplementary Table S7**). For these constructs, growth, assessed by stem height, diameter and volume, and leaf dry weight, was scarcely affected by the engineering strategy used; only the final height and diameter (measured in the middle of the fifth growing season) were slightly reduced in lines with the post-synthetic deacetylation strategy compared to those with synthetic reduction (**Supplementary Table S7**). This growth inhibition was preceded by a decrease in leaf dry weight and chlorophyll contents in the fourth year in lines with post-synthetic reduction (*35S:AnAXE1* and *35S:HjAXE*) (**Figure 3**).

Stress Response Traits

Stress-related responses were recorded regularly throughout the four-year field test period, and detailed mapping of necrosis, rust and chewing symptoms was additionally conducted in 2017 simultaneously with collection of leaf material for phenolic profiling. Some of these traits were related to construct identity and, in particular, to the choice of promoter (**Figure 5** and **Supplementary Tables S2, S3, S5–S7**). Necrosis was generally elevated for *35S:HjAXE* plants, potentially at the expense of rust symptoms (**Figure 5A**), which were generally reduced on plants belonging to the same construct. Moreover, both kinds of fungal AXE transgenes under the *35S* promoter (**Figure 5B**) suffered from an increase in the extent of chewing symptoms, with damage being increased by 187% (*35S:AnAXE1*) and 44% (*35S:HjAXE*) compared to wild type plants. Synthetic acetylation reduction (*35S:RWA-CD*), on the other hand, had no impact on chewing damage (**Figure 5B**).

Levels of phenolic compounds that are often associated with damage risk varied in a genotype-related way. For example, salicortin and HCH-acetyl-salicortin were elevated in *35S:RWA-CD* trees (**Table 2**). *35S:AnAXE1* and *35S:HjAXE* lines also expressed higher levels of certain SPGs, such as OH-tremuloidin, whereas acetyl-tremulacin and *p*-coumaric acid were greatly elevated in *35SAnAXE1*. Salicylic acid, on the other hand, was reduced in *35S:HjAXE* trees. Thus, use of the constitutive 35S promoter led to more alterations in concentrations of SPGs compared with transgenics created with the help of the *WP* promoter, which did not deviate significantly from the wildtype (WT, **Table 2**).

Catechin (the precursor of CTs) was elevated in *35S:AnAXE1*, which also had higher levels of CTs (**Figure 5C**). The elevated CT level characteristic of genotype *35S:AnAXE1* was accompanied by very much higher levels of damage caused by chewing herbivores, whereas a general decrease in CT levels for *35S:HjAXE* was also associated with elevated herbivory (by 44%). That the two fungal *35S* transformations were associated with varying responses in terms of CTs, but at the same time had similar susceptibility to

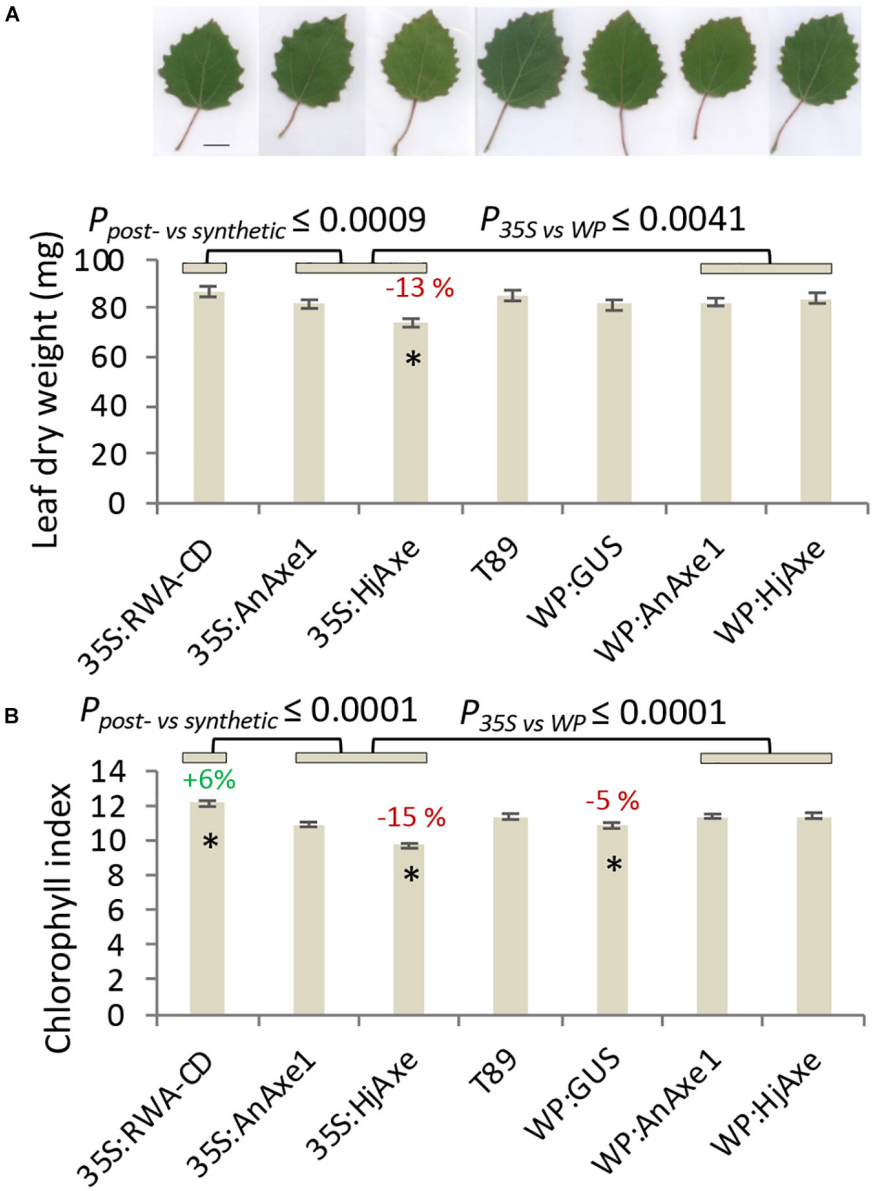

FIGURE 3 | Effects of different types of genetic modification on leaf traits. Leaf dry weight with representative images of leaves, size bar = 1 cm **(A)**. Leaf chlorophyll index **(B)**. Means and SE, stars indicate means significantly different from WT, post-ANOVA contrast, $p \leq 0.05$). *P*-value indicates significance of the promoter effect based on a two-way ANOVA (**Supplementary Table S6**) and synthetic vs. post-synthetic xylan modification (**Supplementary Table S7**).

herbivores, indicated a lack of any general relationship between CT levels and the risk of chewing damage.

In addition to SPGs, we monitored the foliar levels of arachidonic acid, a polyunsaturated fatty acid (20:4 Δ5,8,11,14) regulating different physiological and stress responses that is found in some plant species including poplars (Groenewald and van der Westhuizen, 1997). It has been shown to trigger different plant stress responses and induce resistance to fungal pathogens (Savchenko et al., 2010). Interestingly, the levels of arachidonic acid were decreased compared to WT in lines with all constructs except for those containing *AnAXE1* (**Table 2**). This suggests that the quality of lines carrying *AnAXE1* constructs is potentially superior compared to that of other transgenic lines with regard to biotic stress resistance.

DISCUSSION

Good Growth and Field Performance of Lines Carrying Constructs Targeting Acetylation

We have tested for the first time the field performance of trees with transgenically reduced cell wall acetyl content. We found

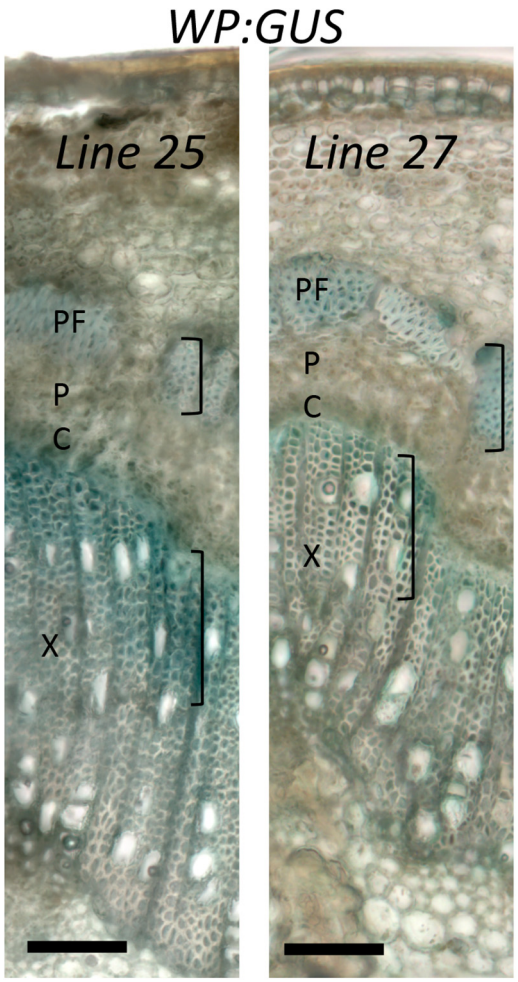

FIGURE 4 | Activity of wood-specific promoter (*WP*) in trees grown in the field. Histochemical β-glucuronidase analysis of a branch with one-year old cambium of *WP:GUS* trees (lines 25 and 27) in the fourth growing season in July, during the active wood production period. X – secondary xylem; P – secondary phloem, PF – phloem fibers; C-vascular cambium. Activity is seen in cells depositing secondary cell walls (marked with brackets). Scale bar = 100 μm.

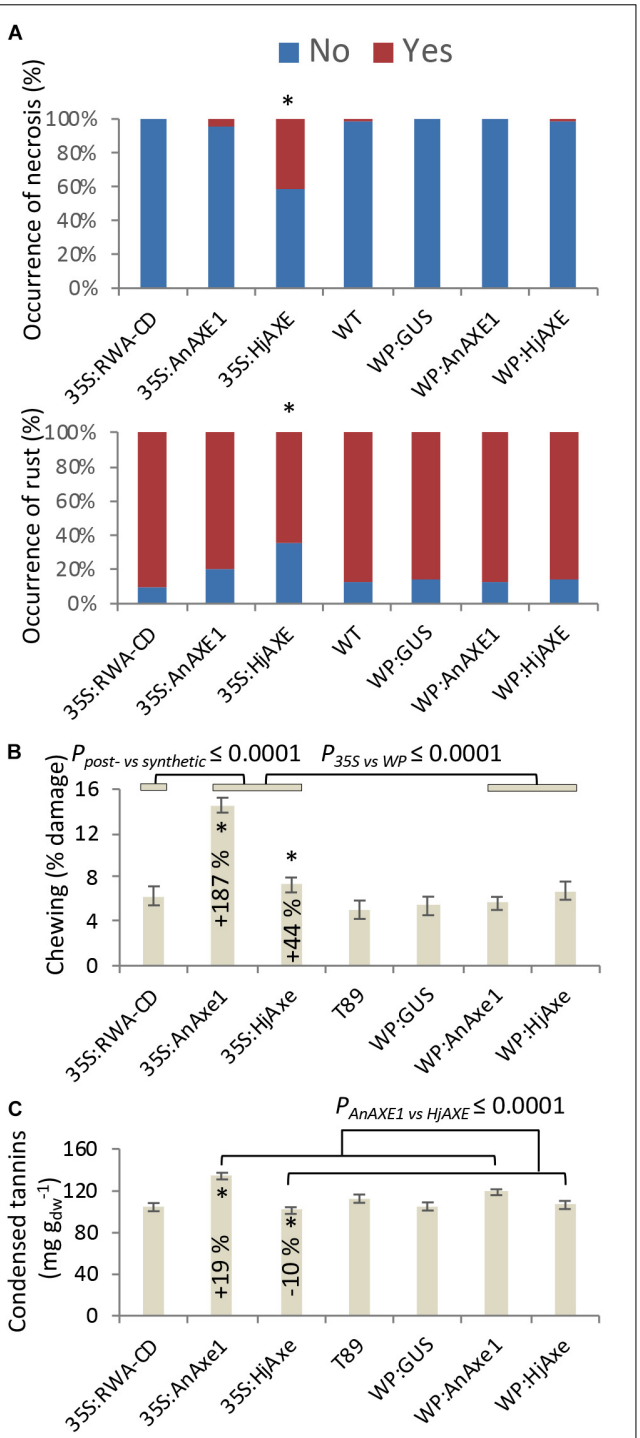

FIGURE 5 | Effects of different types of genetic modification on biotic stress responses. Instances of leaf damage recorded in the 2017 survey that showed significant effects of "construct." **(A)** Necrosis and rust. Constructs producing significantly different distributions are marked with *. Details of statistical analysis are provided in **Supplementary Table S5**. **(B)** Chewing damage. **(C)** Condensed tannin contents. Data in B and C are means and SE, stars indicate means significantly different from WT (post-ANOVA contrast, $p \leq 0.05$). *P*-value indicates significance of the transgene or promoter effect based on a two-way ANOVA (**Supplementary Table S6**) and synthetic vs. post-synthetic xylan modification strategy (**Supplementary Table S7**).

that, in general, apart from those lines with abnormal phenotypes, the reduction of acetylation in cell walls did not lead to either major detrimental effects or significant growth stimulation in the field (**Figures 2**, **3**). The level of reduction in acetyl content for the lines previously tested varied between 10 and 16% in *WP:HjAXE* (lines 11, 14B, 14C; Wang et al., 2020), and 13 and 16% in *35S:AnAXE1* (lines 4, 8, 17; Pawar et al., 2017a), and it was 20% in *35S:RWA-CD* (line 10; Pawar et al., 2017b). The reductions in acetyl content in *WP:AnAXE1* lines have not been analyzed, but based on previous comparisons between *35S* and *WP*-driven transgenes (Ratke et al., 2015), and the documented observation that the specific activity of the WP is stable (**Figure 4**), we expect a slightly stronger effect with *WP:AnAXE1* than with *35S:AnAXE1*. Thus, the mild reductions in cell wall acetylation levels (by 30% or less) are well supported by plants both, in the field (**Figure 2**), and

in the greenhouse conditions (discussed in Pawar et al., 2017b; Donev et al., 2018).

Better Field Performance of WP Compared to 35S Promoter

Analyses of growth and biotic stress responses in lines harboring *35S*- and *WP*-driven fungal AXEs point to a clear advantage offered by the specific transgene expression achieved with the *WP*. Both height and diameter growth were reduced in *35S* lines compared to *WP* lines, and the stem volume was reduced by as much as 21% and 41% in, respectively, *35S:AnAXE1* and *35S:HjAXE* compared to the corresponding *WP* constructs (**Figure 2**). These growth penalties in *35S* lines were seen only in the field; these lines did not exhibit growth defects in the greenhouse (Ratke et al., 2015; Pawar et al., 2017b; Wang et al., 2020). One factor which could have contributed to the growth penalty in the field is the alteration in interaction with herbivores as revealed by the more extensive foliar chewing damage (**Figure 5B**). The increase in susceptibility to herbivores is likely to be due to metabolic changes in the leaves in *35S* plants caused by AXE activity, changes which are largely avoided when *WP* targets the transgene expression to the developing wood. The fungal AXEs targeted to cell walls are expected to hydrolyze acetyl esters liberating acetic acid, thus changing the pH of the leaf, and since acetic acid can cross membranes in uncharged form, the reaction could contribute to the biosynthesis of acetyl-CoA. This compound is used in a variety of reactions, including the TCA cycle, glyoxylate cycle, lipid biosynthesis, mevalonate pathway, and it is considered an energy-status marker for a eukaryotic cell (Cai and Tu, 2011). It is therefore perhaps not surprising that ectopic manipulation of acetyl-CoA pools can have far-reaching consequences, and our results demonstrate that restricting the transgenic modification to specific tissues, such as developing wood, can prevent or attenuate such undesirable side-effects.

Synthetic Versus Post-synthetic Deacetylation Strategies

Assuming that the *RWA* genes encode Golgi-localized acetyl-CoA transporters (Gille and Pauly, 2012; Pauly and Ramírez, 2018), cytosolic accumulation of acetyl-CoA is expected when expression of these genes is suppressed. Apoplastic AXE expression which results in high acetic acid levels in the apoplast might eventually result in a similar outcome, assuming that acetic acid diffuses via membranes and is converted to acetyl-CoA by acetyl-CoA synthases. Even though the cytosolic accumulation of acetyl-CoA might be similar with the synthetic and the post-synthetic strategy, these two strategies might lead to differences in cell wall polymer structures. For example, increased glucuronosylation of xylan is expected when the xylan acetylation machinery is suppressed since the two processes apparently compete for the same substrate (Chong et al., 2014; Xiong et al., 2015; Grantham et al., 2017). Post-synthetic deacetylation might be also more specific toward a targeted polymer – xylan – in particular, *Hj*AXE, which was used in this study for the post-synthetic modification, has documented xylan specificity (Koutaniemi et al., 2013).

TABLE 2 | Metabolite (mostly phenylpropanoid) profiles affected by genetic transformation (construct) based on nested ANOVA.

	35S:RWA-CD	***35S:AnAXE1***	***35S:HjAXE***	**WT**	***WP:GUS***	***WP:AnAXE1***	***WP:HjAXE***
Acetyl-salicortin	458047*a* ± 27307	403962*ab* ± 22296	332471*b* ± 21540	387394*ab* ± 38618	419924*ab* ± 27307	408180*ab* ± 20098	442228*a* ± 27307
Acetyl-tremulacin	2182*b* ± 954	**109067*a*** ± 779	2293*b* ± 753	3158*b* ± 1349	2861*b* ± 954	3206*b* ± 702	2950*b* ± 954
Benzoic acid	9397*ab* ± 683	9340*a* ± 558	6842*b* ± 539	8803*ab* ± 966	7745*ab* ± 683	8337*ab* ± 503	7808*ab* ± 683
Catechin	18107820*b* ± 507156	**20517646*a*** ± 414091	19323366*ab* ± 400050	18648679*ab* ± 717226	18937764*ab* ± 507156	19594648*ab* ± 373256	18383082*b* ± 507156
Cinnamoyl-salicin	12097*ab* ± 987	11944*ab* ± 806	10358*b* ± 779	11808*ab* ± 1396	13966*a* ± 987	12987*ab* ± 727	14650*a* ± 987
HCH-Ac-salicortin	**30552*a*** ± 2279	15154*b* ± 1861	22385*ab* ± 1798	22058*ab* ± 3223	25912*a* ± 2279	23954*a* ± 1677	25120*a* ± 2279
HCH-salicortin	**2027209*a*** ± 117742	1941761*a* ± 96136	1590870*a* ± 92876	1819946*a* ± 166513	1814078*a* ± 117742	1891767*a* ± 86656	1690340*a* ± 117742
HCH-tremulacin	779420*ab* ± 54671	901451*a* ± 44639	702145*b* ± 43125	856067*ab* ± 77317	854546*ab* ± 54671	850986*ab* ± 40237	773174*ab* ± 54671
OH-tremuloidin	3083760*c* ± 22013	**379038*ab*** ± 17973	**404189*a*** ± 17364	295890*abc* ± 31131	295881*bc* ± 22013	312900*bc* ± 16201	285702*c* ± 22013
p-coumaric acid	72598*b* ± 5669	**117312*a*** ± 4628	69830*b* ± 4471	80959*b* ± 8017	83148*b* ± 5669	76046*b* ± 4172	81188*b* ± 5669
Salicoyl-tremuloidin	3393*ab* ± 536	3518*a* ± 438	1419*b* ± 423	2618*ab* ± 758	3566*a* ± 536	3503*a* ± 394	4019*a* ± 536
Salicortin	**31708303*** ± 1359824	27844354 ± 1110292	27399864 ± 1072644	26846382 ± 1923082	27934434 ± 1359824	30052206 ± 1000803	30601384 ± 1359824
Salicylic acid	1202017*a* ± 23487	1155301*ab* ± 19177	**1085672*b*** ± 18527	1179529*ab* ± 33216	1214922*a* ± 23487	1174446*a* ± 17286	1160759*ab* ± 23487
Arachidonic acid	**5687*b*** ± 252	6418*ab* ± 205	**5929*b*** ± 198	7235*a* ± 356	**6013*ab*** ± 252	6476*ab* ± 185	**6108*ab*** ± 252

Means ± SE and Tukey's test data (letters) are extracted from ***Supplementary Table S4****. Stars * and bold indicate means significantly different from WT (post-ANOVA contrast $P < 0.05$,* ***Supplementary Table S2****).*

Comparisons of the phenotypic effects of synthetic versus post-synthetic strategies (both using the *35S* promoter) revealed that some leaf-related traits were affected. Leaf weight, chlorophyll content, and chewing resistance appeared to be lower in the case of post-synthetic modification (**Figures 3**, **5**). Many SPGs were also affected by the deacetylation strategy (**Supplementary Table S7**). These foliar changes were not matched by stem growth during the first four years in the field, but in the final (fifth) year, both stem diameter and stem height were somewhat reduced by the post-synthetic modification strategy compared to the synthetic one (**Supplementary Table S7**). The lines available only allowed us to draw conclusions about the pre- vs. synthetic strategy in the case of ectopic modification using the *35S* promoter. It would be interesting to investigate whether the same conclusion applies to modification targeted specifically to developing wood.

Variability in Foliar Phenolics and Resistance Properties of the Transgenic Lines

Although the trees in this study were never exposed to an outbreak of severe attack by a particular herbivore or pathogen, the relatively low and variable relationships in the field between various kinds of biotic stressors and genotypes confirmed that the transgenic procedure in itself is unlikely to be associated with any systematic impact on surrounding organisms and *vice versa* (Strauss, 2003).

Leaf CTs of natural aspen populations are strongly tied to genotype (Lindroth et al., 2011; Robinson et al., 2012; Bandau et al., 2015; Decker et al., 2016), a feature that was also observed in our transformed genotypes. CTs are considered to be anti-oxidant phenolic polymers (Gourlay and Constable, 2019) that are expected to influence the presence and impact of plant-consuming microorganisms and herbivores (Mutikainen et al., 2000; Bailey et al., 2005; Barbehenn and Constabel, 2011), although they also express a high degree of plasticity in response to environmental factors such as nitrogen addition (Bandau et al., 2015) and they may be equally important and indicative of the extent of internal recovery and the mode of growth (Harding et al., 2013; Lindroth and Madritch, 2015; Decker et al., 2016). However, the two lines in this experiment that suffered from elevated chewing symptoms varied in tannin content, with *35S:HjAXE* giving lower and *35SAnAXE1* higher foliar CT concentrations when compared to WT (**Figures 5B,C**). No consistent relationship between CTs and chewing damage caused could therefore be deduced from this study, supporting the hypothesis that the potential defensive role of CTs in plants is indeed complex.

Salicinoid phenolic glucosides have often been investigated as suggested markers of innate resistance to herbivore damage in woody species (Mutikainen et al., 2000; Albrectsen et al., 2004; Philippe and Bohlmann, 2007; Witzell and Martin, 2008; Fabisch et al., 2019) and in particular as constitutive markers in aspen (Albrectsen et al., 2010; Robinson et al., 2012; Bernhardsson et al., 2013; Lindroth and St. Clair, 2013; Lindroth et al., 2015). The *35S*-driven transgenes appeared to be more affected with respect to their SPG profiles compared to the *WP*-driven transgenes, although the low number of lines per construct tested in the present experiment (between two and four) resulted in few significant changes in SPG contents among the constructs (**Table 2** and **Supplementary Tables S2, S4**). Despite this deficiency, the greater impact of the *35S* promoter compared to the *WP* promoter on SPG profiles was obvious. The synthesis of phenolic compounds belonging to the SPG group is still unresolved due to reticulate pathways with no apparent direct connection to the most simple salicinoid, salicin (Babst et al., 2010; Fellenberg et al., 2020), although it is increasingly accepted that the specialized metabolism of phenolic compounds is tightly linked to primary metabolism (Harding et al., 2013), and our study further suggests that cell wall acetylation may indeed alter, and determine levels of, phenolic compounds in aspen.

CE1 and CE5 AXEs Induce Distinct Foliar Phenotypes

The selection of enzymes appropriate for transgenic modification was addressed in this study by comparing two fungal enzymes, a CE1 representative, *An*AXE1 and a CE5 representative, *Hj*AXE, expressed from either *35S* or *WP* promoters, for their effects on several traits related to growth, biotic stress resistance and foliage characteristics. Stem growth and leaf weight were not affected by the enzyme used. In contrast, the occurrence of necrosis was associated with *HjAXE*, and there was a higher incidence of chewing with *AnAXE1*, although both transgenes induced more chewing than was seen in WT (**Figure 5** and **Supplementary Table S6**). CTs were more characteristic of *HjAXE* than *AnAXE1* expressing plants, and several SPGs accumulated differentially in the leaves of transgenic plants with the two transgenes (**Figure 5** and **Table 2**). These differences were primarily seen in the lines with *35S*-driven transgenes; effects were negligible in lines with the WP promoter. These data indicate that each transgene induced different susceptibilities to specific biotic stresses, associated with different patterns of accumulation of some stress-related SPGs and CTs. Previous greenhouse studies with *35S:AnAXE1* and *35S:HjAXE* expressing plants did not reveal any major morphological differences between plants with the two transgenes (Ratke et al., 2015; Pawar et al., 2017a), highlighting the importance of field testing.

The physiological background behind the contrasting phenotypes observed in *35SAnAXE1* and *35SHjAXE* expressing plants is not known, and it could encompass many factors. Beside the difference in enzymatic specificities and mode of action in the cell wall (discussed by Wang et al., 2020), the two proteins could be differentially perceived by the pathogen-associated molecular patterns (PAMP) recognition system (Bellincampi et al., 2014). The induction of necrosis by ectopically expressed *HjAXE* seen in our trial (**Figure 5**) is reminiscent of the effects of several fungal xylanases from family 11, including *Hypocrea jecorina* xylanase II, which induce ethylene and hypersensitive responses in plants, leading to necrosis (Noda et al., 2010). A conserved amino acid motif, TEIGSVTSDGS, has been identified as being involved in induction of necrosis. Amino

acid alignments of sequences used in the two constructs reveal that *Hj*AXE, but not *An*AXE1, includes a similar motif, 183-VGTCTTQG-190, and it would be interesting to test this for necrosis-inducing activity.

Imbalance in Cellular Acetyl Levels Could Lead to Genomic Instability

In this trial, three out of 18 transgenic lines with reduced acetylation exhibited dwarfism (**Figure 1B**) and growth abnormalities (**Figure 1C**), and one of them showed increased mortality (**Figure 1D**). These detrimental effects could not be associated with the transgenes introduced, and they are likely to have been caused by somaclonal variation or positional effects. Such a high (17%) incidence of dwarfism in acetylation-modified lines is, however, remarkable, and it was not predicted on the basis of the growth observed during greenhouse trials with the same transgenic lines. We also observed no dwarfism other than dwarfism related to transgenes among another set of 48 transgenic lines modified for other qualities that were grown in nearby transgenic fields. Reports from previous American field trials support the conclusion that somaclonal variations or detrimental positional effects are rare in transgenic poplars. For example, in a long-term trial with 948 lines engineered for sterility, not a single incident of detectable somaclonal variation was reported (Klocko et al., 2018); similarly, in a survey of field trial studies in United States covering a period of over 20 years and more than 100 transgenic poplar lines, only 0.1–1% dwarfism that could putatively be linked to positional effects or somaclonal variation was detected (Strauss et al., 2016).

The exceptionally high occurrence of random dwarfism and abnormalities among our transgenic lines with reduced acetyl content suggests a potential link between the acetylation status and genomic stability. Indeed, studies in other eucaryotes including mammals and yeasts showed that cellular levels of acetyl-CoA are directly associated with histone acetylation, which in turn regulates chromatin epigenetic state (Cai and Tu, 2011; Etchegaray and Mostoslavsky, 2016). In plants, epigenetic changes in chromatin state have been linked to the activation of transposable elements under stress conditions, thus contributing to somaclonal variation (Kaeppler et al., 2000). Moreover, in mammalian cells, the cellular ability to repair double strand breaks in DNA requires histone acetylation (Sivanand et al., 2017). These data support the hypothesis that the higher levels of acetyl-CoA expected to be induced by our engineering strategies could indeed lead to increased rates of mutation, especially when combined with stress. This hypothesis could be addressed by field testing and whole-genome sequencing of different acetyl-modified plants.

CONCLUDING REMARKS

The field growth of genetically modified plants is highly controversial in large parts of the World, but it is also warranted so that their potential can be carefully validated (Strauss, 2003; Viswanath et al., 2012; Strauss et al., 2016). On the one hand, genetic modifications promise to make it possible to tailor plants to perform better and produce higher quality products. On the other hand, genetic modification is a contentious topic among the public. The only way to assess the benefits and drawbacks of applying genetic modification techniques to crops, including forest trees, is to perform thorough characterization of transgenic lines. Here we present the results of the first field test of transgenic plants that target xylan-acetylation in cell walls, carried out to assess the consequences for growth, environmental stress resistance and biotic stress resistance in conditions similar to those used in short-rotation plantation forestry. Our data revealed novel plant phenotypes, not seen in the previous greenhouse experiments, as well as novel traits concerning the interaction of the genetically modified trees with their environment. The results highlight the need for early field testing in order to evaluate transgenic strategy and to assess the potential benefits and drawbacks expected when transgenic crops are used compared to their non-transgenic commercial counterparts.

DATA AVAILABILITY STATEMENT

All datasets generated for this study are included in the article/**Supplementary Material**.

AUTHOR CONTRIBUTIONS

MD-M, BA, and EM designed the research. MD-M, FA, ED, LM, UJ, BA, and EM carried out field the work and sample preparation. PP produced the transgenic lines. FA conducted the tannin analyses and prepared the leaves for metabolomics analyses. MD-M, ED, BA, and EM analyzed the data. BA and EM wrote the manuscript with contributions from all authors.

FUNDING

This work was supported by the Bio4Energy and the SSF program ValueTree RBP14-0011.

ACKNOWLEDGMENTS

We are grateful to Dr. Johanna Witzell, SLU, for help with conservation of field samples before transport to Umeå and the Swedish Metabolomic Centre for assistance with metabolomic analyses and to Erasmus student Kacper Dziewit for help with histochemical GUS analyses.

SUPPLEMENTARY MATERIAL

The Supplementary Material for this article can be found online at: https://www.frontiersin.org/articles/10.3389/fpls.2020.00651/full#supplementary-material

REFERENCES

Abreu, I. N., Ahnlund, M., Moritz, T., and Albrectsen, B. R. (2011). UHPLC-ESI/TOFMS determination of salicylate-like phenolic glycosides in *Populus tremula* leaves. *J. Chem. Ecol.* 37, 857–870. doi: 10.1007/s10886-011-9991-7

Albrectsen, B. R., Gardfjell, H., Orians, C. M., Murray, B., and Fritz, R. S. (2004). Slugs, willow seedlings and nutrient fertilization: intrinsic vigor inversely affects palatability. *Oikos* 105, 268–278. doi: 10.1111/j.0030-1299.2004.12892.x

Albrectsen, B. R., Witzell, J., Robinson, K. M., Wulff, S., Luquez, V. M. C., Ågren, R., et al. (2010). Large scale geographic clines of parasite damage to *Populus tremula L. Ecography* 33, 483–493.

Babst, B. A., Harding, S. A., and Tsai, C.-J. (2010). Biosynthesis of phenolic glycosides from phenylpropanoid and benzenoid precursors in *Populus*. *J. Chem. Ecol.* 36, 286–297. doi: 10.1007/s10886-010-9757-7

Bacete, L., Melida, H., Miedes, E., and Molina, A. (2018). Plant cell wall-mediated immunity: cell wall changes trigger disease resistance responses. *Plant J.* 93, 614–636. doi: 10.1111/tpj.13807

Bailey, J. K., Deckert, R., Schweitzer, J. A., Rehill, B. J., Lindroth, R. L., Gehring, C. A., et al. (2005). Host plant genetics affect hidden ecological players: links among *Populus,* condensed tannins, and fungal endophyte infection. *Can. J. Bot.* 83, 356–361. doi: 10.1139/b05-008

Bandau, F., Decker, V. H., Gundale, M. J., and Albrectsen, B. R. (2015). Genotypic tannin levels in *Populus tremula* impact the way nitrogen enrichment affects growth and allocation responses for some traits and not for others. *PLoS ONE* 10:e0140971. doi: 10.1371/journal.pone.0140971

Barbehenn, R. V., and Constabel, P. C. (2011). Tannins in plant-herbivore interactions. *Phytochemistry* 72, 1551–1565. doi: 10.1016/j.phytochem.2011.01.040

Bar-On, Y. M., Phillips, R., and Milo, R. (2018). The biomass distribution on Earth. *Proc. Natl. Acad. Sci. U.S.A.* 115, 6506–6511.

Bellincampi, D., Cervone, F., and Lionetti, V. (2014). Plant cell wall dynamics and wall-related susceptibility in plant–pathogen interactions. *Front. Plant Sci.* 5:228. doi: 10.3389/fpls.2014.00228

Bernhardsson, C., Robinson, K. M., Abreu, I. N., Jansson, S., Albrectsen, B. R., and Ingvarsson, P. K. (2013). Geographic structure in metabolome and herbivore community co-occurs with genetic structure in plant defence genes. *Ecol. Lett.* 16, 791–798. doi: 10.1111/ele.12114

Biely, P., Singh, S., and Puchart, V. (2016). Towards enzymatic breakdown of complex plant xylan structures: state of the art. *Biotechnol. Adv.* 34, 1260–1274. doi: 10.1016/j.biotechadv.2016.09.001

Cai, L., and Tu, B. P. (2011). On acetyl-CoA as a gauge of cellular metabolic state. *Cold. Spring Harb. Symp. Quant. Biol.* 76, 195–202. doi: 10.1101/sqb.2011.76.010769

Chong, S.-L., Virkki, L., Maaheimo, H., Juvonen, M., Derba-Maceluch, M., Koutaniemi, S., et al. (2014). *O*-acetylation of glucuronoxylan in *Arabidopsis thaliana* wild type and its change in xylan biosynthesis mutants. *Glycobiology* 24, 494–506. doi: 10.1093/glycob/cwu017

De Souza, A., Hull, P. A., Gille, S., and Pauly, M. (2014). Identification and functional characterization of the distinct plant pectin esterases PAE8 and PAE9 and their deletion mutants. *Planta* 240, 1123–1138. doi: 10.1007/s00425-014-2139-6

Decker, V. H. G., Bandau, F., Gundale, M. J., Cole, C., and Albrectsen, B. R. (2016). Aspen phenylpropanoid genes' expression levels correlate with genets' tannin richness and vary both in responses to soil nitrogen and associations with phenolic profiles. *Tree Physiol.* 37, 270–289.

Dixon, R. A., and Paiva, N. L. (1995). Stress-induced phenylpropanoid metabolism. *Plant Cell* 7, 1085–1097. doi: 10.1105/tpc.7.7.1085

Donev, E., Gandla, M. L., Jönsson, L. J., and Mellerowicz, E. J. (2018). Engineering non-cellulosic polysaccharides of wood for the biorefinery. *Front. Plant Sci.* 9:1537. doi: 10.3389/fpls.2018.01537

Etchegaray, J.-P., and Mostoslavsky, R. (2016). Interplay between metabolism and epigenetics: a nuclear adaptation to environmental changes. *Mol. Cell* 62, 695–711. doi: 10.1016/j.molcel.2016.05.029

Fabisch, T., Gershenzon, J., and Unsicher, S. (2019). Specificity of herbivore defense responses in a woody plant, black poplar (*Populus nigra*). *J. Chem. Ecol.* 45, 162–177. doi: 10.1007/s10886-019-01050-y

Fellenberg, C., Corea, O., Yan, L.-H., Archinuk, F., Piirtola, E.-M., Gordon, H., et al. (2020). Discovery of salicyl benzoate UDP-glycosyltransferase, a central enzyme in poplar salicinoid phenolic glycoside biosynthesis. *Plant J.* 102, 99–115. doi: 10.1111/tpj.14615

Gille, S., and Pauly, M. (2012). *O*-Acetylation of plant cell wall polysaccharides. *Front. Plant Sci.* 3:12. doi: 10.3389/fpls.2012.00012

Giummarella, N., and Lawoko, M. (2016). Structural basis for the formation and regulation of lignin–xylan bonds in birch. *ACS Sustain. Chem. Eng.* 4, 5319–5326. doi: 10.1021/acssuschemeng.6b00911

Gourlay, G., and Constable, C. P. (2019). Condensed tannins are inducible antioxidants and protect hybrid poplar against oxidative stress. *Tree Physiol.* 39, 345–355. doi: 10.1093/treephys/tpy143

Grantham, N. J., Wurman-Rodrich, J., Terrett, O. M., Lyczakowski, J. J., Stott, K., Iuga, D., et al. (2017). An even pattern of xylan substitution is critical for interaction with cellulose in plant cell walls. *Nat. Plants* 3, 859–865. doi: 10.1038/s41477-017-0030-8

Groenewald, E. G., and van der Westhuizen, A. J. (1997). Prostaglandins and Related Substances in Plants. *Bot. Rev.* 63, 199–220. doi: 10.1007/bf02857948

Gröndahl, M., Teleman, A., and Gatenholm, P. (2003). Effect of acetylation on the material properties of glucuronoxylan from aspen wood. *Carbohydr. Polym.* 52, 359–366. doi: 10.1016/s0144-8617(03)00014-6

Harding, S. A., Xue, L.-J., Du, L., Nyamdari, B., Lindroth, R. L., Sykes, R., et al. (2013). Condensed tannin biosynthesis and polymerization synergistically condition carbon use, defense, sink strength and growth in *Populus*. *Tree Physiol.* 34, 1240–1251. doi: 10.1093/treephys/tpt097

Jönsson, L. J., and Martín, C. (2016). Pretreatment of lignocellulose: formation of inhibitory by-products and strategies for minimizing their effects. *Bioresour. Technol.* 199, 103–112. doi: 10.1016/j.biortech.2015.10.009

Kaeppler, S. M., Kaeppler, H. F., and Rhee, Y. (2000). Epigenetic aspects of somaclonal variation in plants. *Plant Mol. Biol.* 43, 179–188.

Keefover-Ring, K., Ahnlund, M., Abreu, I. N., Jansson, S., Moritz, T., and Albrectsen, B. R. (2014). No evidence of geographical structure of salicinoid chemotypes within *Populus tremula*. *PLoS ONE* 9:e107189. doi: 10.1371/journal.pone.0107189

Klocko, A. L., Lu, H., Magnuson, A., Brunner, A. M., Ma, C., and Strauss, S. H. (2018). Phenotypic expression and stability in a large-scale field study of genetically engineered poplars containing sexual containment transgenes. *Front. Bioeng. Biotechnol.* 6:100. doi: 10.3389/fbioe.2018.00100

Kloth, K. J., Abreu, I. N., Delhomme, N., Petøík, I., Villard, C., Ström, C., et al. (2019). PECTIN ACETYLESTERASE9 affects the transcriptome and metabolome and delays aphid feeding. *Plant Physiol.* 181, 1704–1720. doi: 10.1104/pp.19.00635

Koutaniemi, S., van Gool, M. P., Juvonen, M., Jokela, J., Hinz, S. W., Schols, H. A., et al. (2013). Distinct roles of carbohydrate esterase family CE16 acetyl esterases and polymer-acting acetyl xylan esterases in xylan deacetylation. *J. Biotechnol.* 168, 684–692. doi: 10.1016/j.jbiotec.2013.10.009

Lefebvre, V., Fortabat, M.-N., Ducamp, A., North, H. M., Maia-Grondard, A., Trouverie, J., et al. (2011). *ESKIMO1* disruption in Arabidopsis alters vascular tissue and impairs water transport. *PLoS ONE* 6:e16645. doi: 10.1371/journal.pone.0016645

Lindroth, R. L., and Madritch, M. D. (2015). Condensed tannins increase nitrogen recovery by trees following insect defoliation. *New Phytol.* 208, 410–420. doi: 10.1111/nph.13444

Lindroth, R. L., Rubert-Nason, K. F., Couture, J. J., Major, I. T., and Constabel, C. P. (2015). Influence of genotype, environment, and gypsy moth herbivory on local and systemic chemical defenses in trembling aspen (*Populus tremuloides*). *J. Chem. Ecol.* 41, 651–661. doi: 10.1007/s10886-015-0600-z

Lindroth, R. L., Scioneaux, A. N., Schmidt, M. A., Moore, M. A., Wooley, S. C., and Hagerman, A. E. (2011). Qualitative variation in proanthocyanidin composition of *Populus* species and hybrids: genetics is the key. *J. Chem. Ecol.* 37, 57–70. doi: 10.1007/s10886-010-9887-y

Lindroth, R. L., and St. Clair, S. B. (2013). Adaptations of quaking aspen (*Populus tremuloides* Michx.) for defense against herbivores. *For. Ecol. Manage.* 299, 14–21. doi: 10.1016/j.foreco.2012.11.018

Luquez, V., Hall, D., Albrectsen, B. R., Karlsson, J., Ingvarsson, P., and Jansson, S. (2008). Natural phenological variation in aspen (*Populus tremula*): the

SwAsp collection. *Tree Genet. Genomes* 4, 279–292. doi: 10.1007/s11295-007-0108-y

Manabe, Y., Nafisi, M., Verhertbruggen, Y., Orfila, C., Gille, S., Rautengarten, C., et al. (2011). Loss-of-function mutation of *REDUCED WALL ACETYLATION2* in Arabidopsis leads to reduced cell wall acetylation and increased resistance to *Botrytis cinerea*. *Plant Physiol.* 155, 1068–1078. doi: 10.1104/pp.110.168989

Mutikainen, P., Walls, M., Ovaska, J., Keina, M., Julkunen-Tiitto, R., and Vapaavuori, E. (2000). Herbivore resistance in *Betula pendula*: effect of fertilization, defoliation, and plant genotype. *Ecology* 81, 49–65. doi: 10.1890/0012-9658(2000)081%5B0049:hribpe%5D2.0.co;2

Nilsson, O., Aldén, T., Sitbon, F., Little, C. H. A., Chalupa, V., Sandberg, G., et al. (1992). Spatial pattern of cauliflower mosaic virus *35S* promoter-luciferase expression in transgenic hybrid aspen trees monitored by enzymatic assay and non-destructive imaging. *Transgen. Res.* 1, 209–220. doi: 10.1007/bf02524751

Nilsson, U., and Örlander, G. (1999). Vegetation management on grass-dominated clearcuts planted with Norway spruce in southern Sweden. *Can. J. For. Res.* 29, 1015–1026. doi: 10.1139/x99-071

Noda, J., Brito, N., and Gonzalez, C. (2010). The *Botrytis cinerea* xylanase Xyn11A contributes to virulence with its necrotizing activity, not with its catalytic activity. *BMC Plant Biol.* 10:38. doi: 10.1186/1471-2229-10-38

Papazian, S., Girdwood, T., Wessels, B. A., Poelman, E. H., Dicke, M., Moritz, T., et al. (2019). Leaf metabolic signatures induced by real and simulated herbivory in black mustard (*Brassica nigra*). *Metabolomics* 15:130.

Pauly, M., and Ramírez, V. (2018). New insights into wall polysaccharide O-acetylation. *Front. Plant Sci.* 9:1210. doi: 10.3389/fpls.2018.01210

Pawar, P. M.-A., Ratke, C., Balasubramanian, V. B., Chong, S. L., Gandla, M. L., Adriasola, M., et al. (2017b). Downregulation of RWA genes in hybrid aspen affects xylan acetylation and wood processing properties. *New Phytol.* 214, 1491–1505. doi: 10.1111/nph.14489

Pawar, P. M.-A., Derba-Maceluch, M., Chong, S.-L., Gómez, L. D., Miedes, E., Banasiak, A., et al. (2016). Expression of fungal acetyl xylan esterase in Arabidopsis thaliana improves saccharification of stem lignocellulose. *Plant Biotechnol. J.* 14, 387–397. doi: 10.1111/pbi.12393

Pawar, P. M.-A., Koutaniemi, S., Tenkanen, M., and Mellerowicz, E. J. (2013). Acetylation of woody lignocellulose: significance and regulation. *Front. Plant Sci.* 4:118. doi: 10.3389/fpls.2013.00118

Pawar, P. M.-A., Derba-Maceluch, M., Chong, S. L., Gandla, M. L., Bashar, S. S., Sparrman, T., et al. (2017a). *In muro* deacetylation of xylan affects lignin properties and improves saccharification of aspen wood. *Biotechnol. Biofuels* 10:98. doi: 10.1186/s13068-017-0782-4

Philippe, R. N., and Bohlmann, J. (2007). Poplar defense against insect herbivores. *Can. J. Bot.* 85, 1111–1126.

Pogorelko, G., Fursova, O., Lin, M., Pyle, E., Jass, J., and Zabotina, O. A. (2011). Post-synthetic modification of plant cell walls by expression of microbial hydrolases in the apoplast. *Plant Mol. Biol.* 77, 433–435.

Pogorelko, G., Lionetti, V., Fursova, O., Sundaram, R. M., Qi, M., Whitham, S. A., et al. (2013). Arabidopsis and *Brachypodium distachyon* transgenic plants expressing *Aspergillus nidulans* acetylesterases have decreased degree of polysaccharide acetylation and increased resistance to pathogens. *Plant Physiol.* 162, 9–23. doi: 10.1104/pp.113.214460

Porter, L. J., Hrstich, L. N., and Chan, B. G. (1986). The conversion of procyanidins and prodelphinidins to cyanidin and delphinidin. *Phytochemistry* 25, 223–230. doi: 10.1016/s0031-9422(00)94533-3

Ratke, C., Pawar, P. M., Balasubramanian, V. K., Naumann, M., Duncranz, M. L., Derba-Maceluch, M., et al. (2015). Populus GT43 family members group into distinct sets required for primary and secondary wall xylan biosynthesis and include useful promoters for wood modification. *Plant Biotechnol. J.* 13, 26–37. doi: 10.1111/pbi.12232

Robinson, K. M., Ingvarsson, P. K., Jansson, S., and Albrectsen, B. R. (2012). Genetic variation in functional traits influences arthropod community composition in aspen (*Populus tremula* L.). *PLoS ONE* 7:e37679. doi: 10.1371/journal.pone.0037679

Savchenko, T., Walley, J. W., Chehab, E. W., Xiao, Y., Kaspi, R., Pye, M. F., et al. (2010). Arachidonic acid: an evolutionarily conserved signaling molecule modulates plant stress signaling networks. *Plant Cell* 22, 3193–3205. doi: 10.1105/tpc.110.073858

Sivanand, S., Rhoades, S., Jiang, Q., Lee, J. V., Benci, J., Zhang, J., et al. (2017). Nuclear acetyl-CoA production by ACLY promotes homologous recombination. *Mol. Cell* 67, 252–265.

Strauss, S. H. (2003). Genomics, genetic engineering, and domestication of crops. *Science* 300, 61–62. doi: 10.1126/science.1079514

Strauss, S. H., Ma, C., Ault, K., and Klocko, A. L. (2016). "Lessons from two decades of field trials with genetically modified trees in the USA: biology and regulatory compliance," in *Biosafety of Forest Transgenic Trees*, eds C. Vettori, F. Gallardo, H. Häggman, V. Kazana, F. Migliacci, G. Pilate, et al. (Dordrecht: Springer), 101–124. doi: 10.1007/978-94-017-7531-1_5

Urbanowicz, B. R., Pena, M. J., Moniz, H. A., Moremen, K. W., and York, W. S. (2014). Two *Arabidopsis* proteins synthesize acetylated xylan *in vitro*. *Plant J.* 80, 197–206. doi: 10.1111/tpj.12643

Viswanath, V., Albrectsen, B. R., and Strauss, S. H. (2012). Global regulatory burden for field testing of genetically modified trees. *Tree Genet. Genomes* 8, 221–226. doi: 10.1007/s11295-011-0445-8

Vogel, J. P., Raab, T. K., Somerville, C. R., and Somerville, S. C. (2004). Mutations in PMR5 result in powdery mildew resistance and altered cell wall composition. *Plant J.* 40, 968–978. doi: 10.1111/j.1365-313x.2004.02264.x

Wang, Z., Pawar, P. M.-A., Derba-Maceluch, M., Hedenström, M., Chong, S.-L., Tenkanen, M., et al. (2020). Hybrid aspen expressing a carbohydrate esterase family 5 acetyl xylan esterase under control of a wood-specific promoter shows improved saccharification. *Front. Plant Sci.* 11:380. doi: 10.3389/fpls.2020.00380

Witzell, J., and Martin, J. A. (2008). Phenolic metabolites in the resistance of northern forest trees to pathogens — past experiences and future prospects. *Can. J. For. Res.* 38, 2711–2727. doi: 10.1139/x08-112

Xin, Z., and Browse, J. (1998). *Eskimo1* mutants of *Arabidopsis* are constitutively freezing-tolerant. *Proc. Natl. Acad. Sci. U.S.A.* 95, 7799–7804. doi: 10.1073/pnas.95.13.7799

Xin, Z., Mandaokar, A., Chen, J., Last, R. L., and Browse, J. (2007). Arabidopsis *ESK1* encodes a novel regulator of freezing tolerance. *Plant J.* 49, 786–799. doi: 10.1111/j.1365-313x.2006.02994.x

Xiong, G., Dama, M., and Pauly, M. (2015). Glucuronic acid moieties on xylan are functionally equivalent to O-acetyl-substituents. *Mol. Plant* 8, 1119–1121. doi: 10.1016/j.molp.2015.02.013

Xu, F., Liu, Z., Xie, H., Zhu, J., Zhang, J., Kraus, J., et al. (2014). Increased drought tolerance through the suppression of *ESKMO1* gene and overexpression of CBF-related genes in *Arabidopsis*. *PLoS ONE* 9:e106509. doi: 10.1371/journal.pone.0106509

Conflict of Interest: The authors declare that the research was conducted in the absence of any commercial or financial relationships that could be construed as a potential conflict of interest.

IV

Full Paper

New Phytologist

Sucrose synthase determines carbon allocation in developing wood and alters carbon flow at the whole tree level in aspen

Pia Guadalupe Dominguez[1], Evgeniy Donev[1]*, Marta Derba-Maceluch[1]*, Anne Bünder[1], Mattias Hedenström[2], Ivana Tomášková[3], Ewa J. Mellerowicz[1] and Totte Niittylä[1]

[1]Umeå Plant Science Centre, Department of Forest Genetics and Plant Physiology, Swedish University of Agricultural Sciences, Umeå 90183, Sweden; [2]Department of Chemistry, Umeå University, Umeå 90187, Sweden; [3]Department of Genetics and Physiology of Forest Trees, Faculty of Forestry and Wood Sciences, Czech University of Life Sciences Prague, Prague 165 00, Czech Republic

Author for correspondence:
Totte Niittylä
Tel: +46 7868434
Email: totte.niittyla@slu.se

Received: *23 April 2020*
Accepted: *19 May 2020*

New Phytologist (2021) **229:** 186–198
doi: 10.1111/nph.16721

Key words: ^{13}C labelling, aspen, biomass, carbon allocation, *Populus*, sucrose synthase.

Summary

- Despite the ecological and industrial importance of biomass accumulation in wood, the control of carbon (C) allocation to this tissue and to other tree tissues remain poorly understood.
- We studied sucrose synthase (SUS) to clarify its role in biomass formation and C metabolism at the whole tree level in hybrid aspen (*Populus tremula* × *tremuloides*). To this end, we analysed source leaves, phloem, developing wood, and roots of *SUSRNAi* trees using a combination of metabolite profiling, $^{13}CO_2$ pulse labelling experiments, and long-term field experiments.
- The glasshouse grown *SUSRNAi* trees exhibited a mild stem phenotype together with a reduction in wood total C. The $^{13}CO_2$ pulse labelling experiments showed an alteration in the C flow in all the analysed tissues, indicating that SUS affects C metabolism at the whole tree level. This was confirmed when the *SUSRNAi* trees were grown in the field over a 5-yr period; their stem height, diameter and biomass were substantially reduced.
- These results establish that SUS influences C allocation to developing wood, and that it affects C metabolism at the whole tree level.

Introduction

Wood biomass is a valuable raw material for wood-based industries including pulp, paper, sawn timber, and biofuel production (Plomion *et al.*, 2001; Novaes *et al.*, 2009). Wood formation depends on carbon (C) allocation to developing wood. In several tree species, C is distributed predominantly as sucrose (Rennie & Turgeon, 2009). Phloem loading in source leaves of the model tree aspen (*Populus tremula* L.) occurs via a symplasmic route (Zhang *et al.*, 2014). Phloem unloading mechanism into developing wood is less well understood but is thought to include both symplasmic and apoplasmic steps (Van Bel, 1990; Chaffey & Barlow, 2001; Mahboubi *et al.*, 2013). Despite our increasing understanding of C transport routes in trees, the mechanism of C allocation and biomass accumulation in the different tissues remain poorly understood.

Biomass formation depends partly on the capacity of the wood tissue and other C competitor sink tissues such as shoot and root meristems to metabolize and incorporate C (Yu *et al.*, 2015). Primary metabolic reactions are especially important in this process because they are responsible for sucrose catabolism, energy production, and the synthesis of the precursors for cell wall polymers. Studies on biomass accumulation in trees commonly focus on hormonal factors and C allocation to cell wall polymers (Dubouzet *et al.*, 2013; Busov, 2018), while primary metabolism has received less attention (Mahboubi & Niittylä, 2018). The C availability for biomass production by sink tissues depends on the photosynthetic and sucrose export capacity of source leaves (Yu *et al.*, 2015); in recognition of this, efforts have been made to increase wood biomass by improving tree photosynthesis (Dubouzet *et al.*, 2013; Busov, 2018). However, C acquisition, allocation, and metabolism in the different tissues of a tree depend on the relationship between sink and source tissues, which should therefore be considered jointly (Sonnewald & Fernie, 2018).

The concept of sink strength refers to a sink tissue capacity to compete for photoassimilates. This is determined by the capacity of the tissue to import C from the leaves and to synthesize macromolecules (Yu *et al.*, 2015). The capacity for C import depends in part on enzymes that degrade sucrose. Two types of enzymes catalyse sucrose degradation in sink tissues: sucrose synthase (SUS) and invertase. SUS has been associated with C allocation, increased biomass, and sink strength (Stein & Granot, 2019). It is known to be the main sink strength determinant in potato tubers (Zrenner *et al.*, 1995), and to control C import in young tomato fruits (D'Aoust *et al.*, 1999). In tobacco plants, SUS overexpression increased height and biomass, indicating that it can also control C allocation in this species (Coleman *et al.*, 2006).

*These authors contributed equally to this work.

Conversely, evidence from rice and corn suggests that acid invertases are the main grain sink strength determinants in these species (Cheng *et al.*, 1996; Li *et al.*, 2013; Morey *et al.*, 2018). The relative impacts of SUS and invertase on C allocation thus appear to depend on the tissue, species, developmental stage, and season. Consequently, it is impossible to predict the contributions of these two enzymes to C metabolism a priori.

We previously observed decreased wood density in aspen trees with reduced SUS levels, which was accompanied by a decrease in cellulose, hemicellulose, and lignin content per unit volume of wood (Gerber *et al.*, 2014). The decrease in total polymer biomass per unit volume suggested reduced C incorporation into wood cell walls. Moreover, expression of a cotton SUS in aspen trees increased cell wall thickness and wood density (Coleman *et al.*, 2009), while aspen SUS expression in tobacco plants increased xylem cell wall thickness (Wei *et al.*, 2015). These observations support a central role for SUS in C allocation to wood, but they do not reveal the role of SUS in C allocation and metabolism, and biomass accumulation at the whole tree level. This prompted us to study the role of SUS at the whole tree level under glasshouse and field conditions using transgenic *SUSRNAi* lines. The assessment of the C metabolism was performed by combining total metabolite pool measurements and the tracking of a carbon-13 (^{13}C) flow among the central metabolites in leaves, phloem, developing wood and roots after $^{13}CO_2$ supply.

Materials and Methods

Plant material

Three *35S:SUSRNAi* transgenic lines (Gerber *et al.*, 2014) along with wild-type (WT) T89 hybrid aspens (*Populus tremula* × *tremuloides*) were grown in a glasshouse in commercial soil (Yrkes Plantjord; SW Horto, Hammenhög, Sweden) under an 18 h : 6 h, 20°C : 15°C, light : dark photoperiod. Trees were fertilized using 150 ml 1% Rika-S (nitrogen (N)–phosphorus (P)–potassium (K), 7 : 1 : 5; SW Horto) once a week, and were harvested when they were 2 months old. Wood samples were collected from 15 to 45 cm above the soil. In the field experiment, the same genotypes were grown for 5 yr in a field setting in Våxtorp, Laholm community, Sweden (56.42°N, 13.07°E). Trees were planted with a 3 m spacing in 2011. Four trees per each transgenic line and 32 WT trees were randomly distributed over the field area. The field was harrowed twice a year during the first 2 yr following planting and grass was mowed twice a year during subsequent years. Height and diameter (at the stem base) were measured at the end of each growing season and before harvest in the summer 2016.

Sample preparation

All samples were frozen on liquid nitrogen immediately after collection and stored at −80°C until preparation. Developing wood from both glasshouse and field trees was obtained by scrapping the surface of frozen debarked stems with a scalpel while maintaining the low temperature with liquid nitrogen. Phloem samples were obtained by scrapping the inner side of the barks. Fully expanded leaves number 14–16 (counting from the top) were sampled. The tips of the roots were cut, cleaned and immediately frozen. All the obtained frozen tissues were ground with a mortar and pestle. The ground material was kept at −80°C until use.

Sucrose synthase activity determination in glasshouse grown trees

The protocol was based on that of Gerber *et al.* (2014). Extracted samples (extraction buffer: 100 mM Tris-HCl pH 7.5, 2 mM EDTA, 5 mM DTT, a scoop of PVPP; Roche proteinase inhibitor, Roche, Basel, Switzerland) were incubated with 45 µl of reaction mix (100 mM Tris pH 7.5, 100 mM sucrose, 4 mM UDP (uridine diphosphate)) for 30 min at 25°C. A control for each sample was prepared simultaneously using 45 µl of reaction mix without UDP. The reaction product, UDP–glucose, was determined by incubating 25 µl (developing wood) or 100 µl (roots) of the reaction mix with 25 µl of the determination buffer (100 mM Tris pH 7.5, 2 mM NAD^+, 0.02 u UGDH) at 340 nm. The absorbances were interpolated into a UDP–glucose standard curve. Total protein contents were determined by using the DC Protein Assay (Bio-Rad, Hercules, CA, USA).

Quantitative polymerase chain reaction (qPCR) in glasshouse and field grown trees

Total mRNA was extracted with Trizol® (Gibco, Gaithersburg, MD, USA) according to the manufacturer's specifications. The cDNA was prepared using the MessageAmp Premier RNA Amplification Kit (Ambion, Austin, TX, USA). The reference gene was *Ubiquitin*, which was chosen based on its transcript stability. Quantitative polymerase chain reactions (qPCRs) were performed using SYBR® Green Master Mix (Bio-Rad) in a CFX96 Real Time System (Bio-Rad) with the following programme: 95°C for 5 min, then 50 cycles of 95°C for 30 s, 60°C for 15 s, and 72°C for 30 s. The employed primers are listed in Supporting Information Table S1. Primers were designed with PRIMER3 (Untergasser *et al.*, 2012). Ratios were calculated using the equation proposed by Pfaffl (2001): $\text{Ratio} = (E_{\text{target}})^{\Delta \text{Cp target(MEAN control} - \text{MEAN sample)}} / ((E_{\text{reference}})^{\Delta \text{Cp reference(MEAN control} - \text{MEAN sample)}})^{-1}$.

Dry weight and total C phenotype

Tissues from 2-month-old or 5-yr-old trees were dried for 1 wk at 80°C to measure the dry weight. Total C from tissues of glasshouse-grown trees was measured by elemental analyser-isotope ratio mass spectrometry (EA-IRMS; Thermo Fisher Scientific, Waltham, MA, USA). Furthermore, 5 mg of oven-dried sample were employed for each measurement. Measurements were performed with an elemental analyser (Flash EA 2000; Thermo Fisher Scientific) connected to a continuous flow isotope ratio mass spectrometer (DeltaV) (Thermo Fisher Scientific). Samples were analysed together with cyclohexanone, nicotinamide, and sucrose standards, which were standardized against standard reference materials. Data were corrected for drift and size.

Photosynthetic parameters in glasshouse grown trees

The leaf nitrogen balance index (NBI), chlorophyll index (CHL), flavonol index (FLV), and anthocyanin index (ANTH) were measured with a Force A Dualex Scientific+™ device on 10 independent plants at midday. Chlorophyll a fluorescence (ChlF) measurements were performed on 10 leaves per plant over five consecutive days from 09:00 h to 16:00 h using a FluorPen FP100max portable fluorometer (Photon Systems Instruments, Brno, Czech Republic). The kinetics of chlorophyll fluorescence induction were estimated based on the polyphasic rise of the ChlF transient (OJIP) curve using the calculations proposed by Stirbet & Govindjee (2011). The second employed protocol applied with the FluoPen fluorometer was the Light Curve protocol (protocol LC3) using the calculations proposed by Maxwell & Johnson (2000).

^{13}C labelling experiment in glasshouse grown trees

A Percival Scientific cabinet with a CO_2 system (model: PGC-7L2) was employed to supply $^{13}CO_2$ (> 99 atom%, > 99.98%; BOC UK & Ireland, Bluebell, Dublin, Ireland) to the trees. When the experiment started, $^{12}CO_2$ was removed from the air in the chamber using the chamber's in-built CO_2 scrubbing system, and $^{13}CO_2$ was quickly injected up to 400 ppm. The $^{13}CO_2$ was re-injected whenever its levels fell below 350 ppm. The CO_2 levels were measured with a WMA-4 CO_2 analyser (www.ppsystems.com). Groups of four plants were injected with $^{13}CO_2$ on each experimental run, and were sampled after 4, 6 and 8 h of treatment. Unlabelled controls for each genotype were injected with $^{12}CO_2$ in the same chamber, and sampled at 6, 8, 10 and 14 h after the start of the light period, covering the times of the day in which ^{13}C labelling was performed on the experimental plants. The generated labelled material was analysed by gas chromatography mass spectrometry (GC-MS) and/or two-dimensional nuclear magnetic resonance (2D-NMR) as described later. Only metabolites with slow labelling rates (data obtained from Szecowka *et al.*, 2013) were examined to minimize the influence of potential ^{12}C incorporation during sampling.

GC-MS measurements

All the labelled samples and controls were analysed by GC-MS. Frozen samples (10 mg) were extracted with 1 ml of a chloroform–methanol–water (20 : 60 : 20, v/v/v) solution containing two stable isotope reference compounds (7 ng μl^{-1} [$^{13}C_3$]-myristic acid and [$^{2}H_7$]-cholesterol). *N*-Methyl-*N*-(trimethylsilyl)trifluoroacetamide (MSTFA) was used as a reagent for silylation derivatization done according to Lindén *et al.* (2016). The GC-MS protocol was based on that of Gullberg *et al.* (2004). Thus, 1 µl of each derivatized sample was injected in splitless mode per run. The GC-MS system used electron impact (EI) ionization and consisted of a CTC PAL systems autosampler (CTC Analytics AG, Zwingen, Switzerland), an Agilent technologies 7890A GC system (Agilent Technologies, Atlanta, GA, USA), and a Pegasus HT GC high-throughput TOF-MS instrument (LECO Corp., St Joseph, MI, USA). The analysed fragments for the labelling calculations were selected based on Lindén *et al.* (2016) and Beshir *et al.* (2017). Corrections for the ^{13}C natural abundance and the presence of tetramethylsilane (TMS) groups, and computations of ^{13}C enrichment percentages for each identified metabolite were performed as described by Mahboubi *et al.* (2015) and Lindén *et al.* (2016).

2D-NMR analysis

The protocol was based on that of Hedenström *et al.*, 2009. Developing wood samples belonging to *SUSRNAi-1* and WT with no label (time 0) and labelled for 8 h (time 8) were analysed by 2D-NMR. Before analyses, soluble sugars and starch were removed from the samples as described in Smith & Zeeman (2006) to avoid signal interferences in the cell wall NMR measurements. Next, 20 mg of ground tissues were added to 600 µl of deuterated dimethyl sulfoxide (DMSO-d_6). The 2D ^{1}H-^{13}C heteronuclear single quantum coherence (HSQC) experiments were performed on a Bruker 600 MHz Avance III HD spectrometer equipped with a 5 mm BBO cryoprobe with z-gradients (Bruker Biospin, Rheinstetten, Germany). All measurements were performed at 25°C. In the pulse sequence, adiabatic ^{13}C-inversion and ^{13}C-refocusing pulses were used (Bruker pulse sequence hsqcetgpsisp.2). The sweep width was 10 ppm for the ^{1}H dimension and 165 ppm for the ^{13}C dimension. Processing and peak integration were performed using Topspin 3.6 (Bruker Biospin). The peak assignments were based on that of Kim *et al.* (2008).

Starch content measurement in glasshouse grown trees

Briefly, 10 mg of the tissues were extracted with 250 µl of 80% v/v ethanol and gelatinized according to Smith & Zeeman (2006). Next, 40 µl of the resuspension was treated with 6 U of alpha-amyloglucosidase and 0.5 U of alpha-amylase prepared in 50 mM acetate buffer. Negative controls were processed in the same way using 50 mM acetate buffer without the enzymes. The tubes were incubated at 37°C overnight. The treatment with the enzymes was done twice for phloem, developing wood and mature wood, and three times in the leaf samples to assure a complete starch degradation. Then, 50 µl of the samples or controls were then incubated with 75 µl of the determination buffer (HEPES pH 7.5 50 mM, NADP 0.4 mM, ATP 2 mM, G6P DHG 2 U ml^{-1}, HXK 2 U ml^{-1}, PGI 2 U ml^{-1}). The absorbances were interpolated into a glucose standard curve.

Acid invertase activity determination in glasshouse grown trees

The protocol was based on that of Hubbard *et al.* (1989). Developing wood samples (10 µl each) were incubated with 45 µl of reaction buffer (25 mM citrate phosphate buffer, pH 5, and 25 mM sucrose) for 1 h at 25°C. A control for each sample was prepared in parallel replacing the reaction buffer with 25 mM citrate phosphate buffer pH 5. Then, 50 µl of the reaction mix

was then incubated with 75 µl of the determination buffer (HEPES pH 7.5 50 mM, NADP 0.4 mM, ATP 2 mM, G6P DHG 2 U ml^{-1}, HXK 2 U ml^{-1}, PGI 2 U ml^{-1}). The absorbances measured at 340 nm were interpolated into a glucose standard curve.

Neutral invertase activity determination in glasshouse grown trees

The protocol was based on that of Rende *et al.* (2016). Briefly, 1 µl of each sample extract (extraction buffer: 50 mM HEPES pH 7, 10 mM $MgCl_2$, 1 mM EDTA, 0.25 mM DTT, 1% Triton X-100, 20% glycerol; Roche proteinase inhibitor) was incubated with 75 µl of the determination buffer (50 mM HEPES pH 7, 0.4 mM $NADP^+$, 2 mM ATP, 2 U ml^{-1} glucose-6-phosphate dehydrogenase, 2 U ml^{-1} hexokinase, 2 U ml^{-1} phosphoglucose isomerase). Then, 20 µl of 100 mM sucrose was added to each mixture to initiate the reactions. Controls for each sample were prepared in parallel replacing the 100 mM sucrose with HEPES pH 7. Absorbances measured at 340 nm were interpolated into a glucose standard curve.

Statistical analyses

All experiments were analysed statistically by analysis of variance (ANOVA), using Duncan's multiple range test (MRT) for multiple comparison. All analyses were performed with the Infostat software (v.2008; Infostat Universidad Nacional de Córdoba, Argentina). A significance threshold of $P < 0.05$ was applied. The three-dimensional (3D) principal component analysis (PCA) scatter plot was created with BioVinci software (BioTuring Inc., San Diego, CA, USA).

Results

SUSRNAi reduces SUS activity in developing wood and roots

The *Populus* genome contains seven *SUS* genes, named *SUS1*–*SUS7* (Zhang *et al.*, 2011). The *SUSRNAi* construct targets *SUS1* and *SUS2*, which are the most strongly expressed isoforms in developing wood (Zhang *et al.*, 2011; Gerber *et al.*, 2014). *SUS1* and *SUS2* transcripts are also found in leaves and roots (Zhang *et al.*, 2011), suggesting that the RNAi construct may also reduce the total SUS activity in these tissues. To clarify the *SUSRNAi* effects at the whole tree level, we measured SUS activity in developing wood, roots, and source leaves. In accordance with our previous results, SUS activity was reduced to near background levels in developing wood of the *SUSRNAi* lines (Fig. 1a), while in roots its activity was reduced to 40% of the WT level (Fig. 1b). The more modest reduction in roots is probably partly due to the expression of other SUS isoforms (Zhang *et al.*, 2011). The SUS activity in the source leaf extracts of WT trees was close to background levels. Therefore, to assess the *SUSRNAi* effects in source leaves, we quantified the mRNA levels of all the *SUS* isoforms using qPCR. Only *SUS1* and *SUS5* transcript levels in the three transgenic lines were reduced to *c.* 30% and 50%, respectively, of the WT levels (Fig. 1c). The reduction in *SUS5* mRNA levels is not a direct *SUSRNAi* effect, because the percentage of similarity between the nucleotide coding regions of *SUS1* and *SUS5* is *c.* 58% (Zhang *et al.*, 2011) and the *SUSRNAi* does not target *SUS5*.

Total C is reduced in developing wood of *SUSRNAi* lines

We performed detailed growth phenotyping of 2-month-old glasshouse grown *SUSRNAi* trees. The total stem fresh weight of the glasshouse-grown transgenic lines did not differ significantly from that of the WT (Fig. 2a). However, the stem dry weight of the transgenics was slightly reduced, being statistically significant in *SUSRNAi-3* (Fig. 2b). Moreover, the total C content in developing wood as measured by IRMS was significantly reduced in all the silenced lines (Fig. 2c), clearly indicating that the C allocation to this tissue was reduced. These observations are consistent with our previous results documenting reduced stem wood density and increased fibre wall shrinkage upon drying in the *SUSRNAi* lines (Gerber *et al.*, 2014). The total leaf fresh and dry weight were unchanged in the transgenic lines, except in *SUSRNAi-3* (Fig. 2d,e). The total root fresh and dry weight were unchanged in all lines (Fig. 2g,h), as was the total C content in leaves and roots (Fig. 2f,i). Therefore, the growth defect in the *SUSRNAi* lines is primarily associated with wood formation, and not with leaf and root growth.

Photosynthetic light-dependent reactions are not affected in the *SUSRNAi* source leaves

Alterations in sugar metabolism can cause alterations in photosynthesis (Sheen, 1990). To determine whether the photosynthetic performance of the source leaves in transgenic genotypes contributed to the reduction in the developing wood C content, we assayed leaf pigments and the photosynthesis light-dependent reactions. CHL, ANTH, FLV, and NBI (i.e. the ratio of the chlorophyll and flavonol indexes) showed no significant differences (Table S2). The photosynthesis light-dependent reactions can be evaluated by measuring the ChlF and computing different parameters like those of OJIP and LC (light curve) that provide information on the condition of the photosystem II and the electron transport in the thylakoid membrane. OJIP shows how the photochemical efficiency varies under different light conditions (Baker, 2008). The OJIP test equations were therefore used to calculate parameters including the PI_{abs}, the F_v/F_m ratio, and the specific fluxes for the reaction centres (Table S3). All the tested genotypes had PI_{abs} values of *c.* 4 and F_v/F_m values between 0.80 and 0.83, indicating that the primary photochemical reactions do not show changes. The specific energy fluxes values involving the reaction centres (ABS/RC and ETo/RC) were higher in the *SUSRNAi-1* line than in WT trees. However, the values of the other photosynthetic parameters in the *SUSRNAi-1* line and all the photosynthetic parameters in the other *SUSRNAi* lines were comparable to those in WT trees. The computed LC parameters, which relate the photosynthesis rate to the photon flux density,

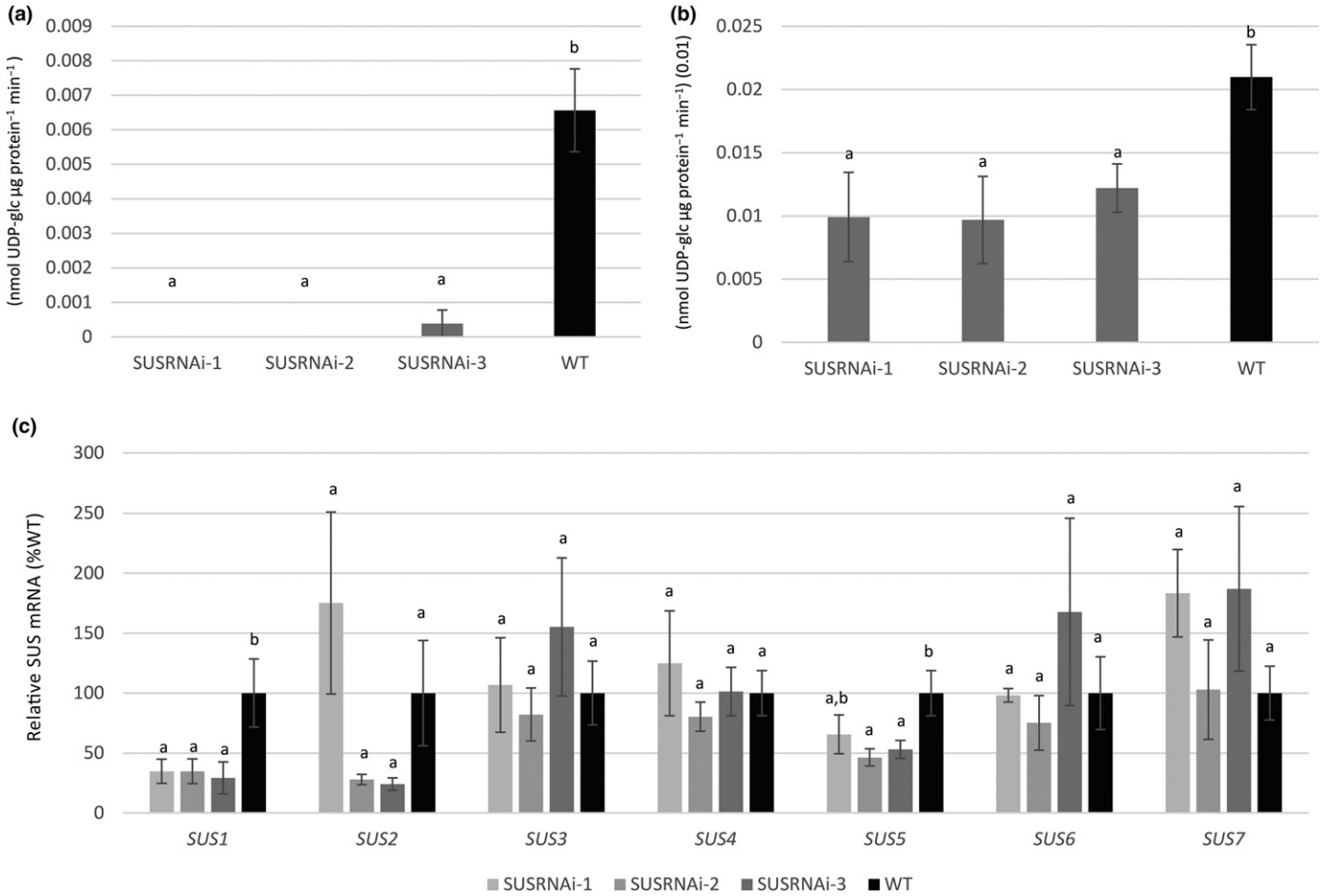

Fig. 1 SUS activity in 2-month-old wild-type (WT) and *SUSRNAi* hybrid aspen (*Populus tremula* × *tremuloides*) trees grown in the glasshouse and measured in (a) developing wood, and (b) in roots, (c) *SUS* mRNA abundance in source leaves measured by RT-qPCR. ANOVA, Duncan test, $n = 5$–4. Different letters indicate significant differences ($P < 0.05$). Bars indicate the average and error bars indicate the standard error.

included F_t, Q_y, F_0 and F_m (Table S4). No consistent differences were observed between WT and *SUSRNAi* lines, indicating that the photosynthesis is not affected by the light intensity in the transgenics. Based on these results, it can be concluded that *SUSRNAi* does not affect pigment levels or the photosynthetic performance in source leaves. Its effects on wood are thus not due to impaired photosynthesis light-dependent reactions but more likely due to changes at the leaf metabolic level, leaf-to-wood C transport, and/or developing wood metabolism.

^{13}C tracking in *SUSRNAi* lines revealed altered sucrose turnover and C flow at the whole tree level

To investigate C fluxes between organs and at the whole tree level, we developed a $^{13}CO_2$ labelling system based on a previously reported design (Mahboubi *et al.*, 2013, 2015) and used it to characterize the C fluxes in *SUSRNAi-1* and *SUSRNAi-3* during a $^{13}CO_2$ pulse. Mahboubi *et al.* (2013) showed that ^{13}C can be detected in developing wood after a 4-h exposure to $^{13}CO_2$. We therefore exposed 6-wk-old *SUSRNAi* and WT trees to a $^{13}CO_2$ pulse and collected samples 4, 6, and 8 h after the pulse start. The ^{13}C metabolic fate in leaves, roots, and developing wood was monitored using GC-MS. In parallel, we measured the total metabolite pools. While the total pool measurements provided a picture of the metabolic status of the tissues at fixed time points, the ^{13}C labelling experiments yielded insights into the movement of the ^{13}C among metabolites.

In leaves, during active photosynthesis sucrose is derived from the Calvin cycle (Fig. 3a). Sucrose showed decreased ^{13}C labelling at time 6 in both lines and at time 4 in *SUSRNAi-3*. Fructose and glucose did not show significant differences. The labelling of Krebs cycle metabolites was not altered, except for fumarate, which was increased at time 8. The ^{13}C-aspartate, ^{13}C-serine, ^{13}C-phenylalanine, and ^{13}C-glutamate were decreased in both lines at time 6. The ^{13}C-threonine was decreased at time 4 in both lines, while ^{13}C-glycerate was decreased in *SUSRNAi-1* at time 6. Total pools were unchanged, except for succinate and ketoglutarate in *SUSRNAi-1* (Table S5). Thus, the C flow changes in *SUSRNAi* leaves were primarily evident in the analysed amino acids.

The total sucrose levels in the phloem of the *SUSRNAi* lines were unchanged from those in the WT, but the ^{13}C

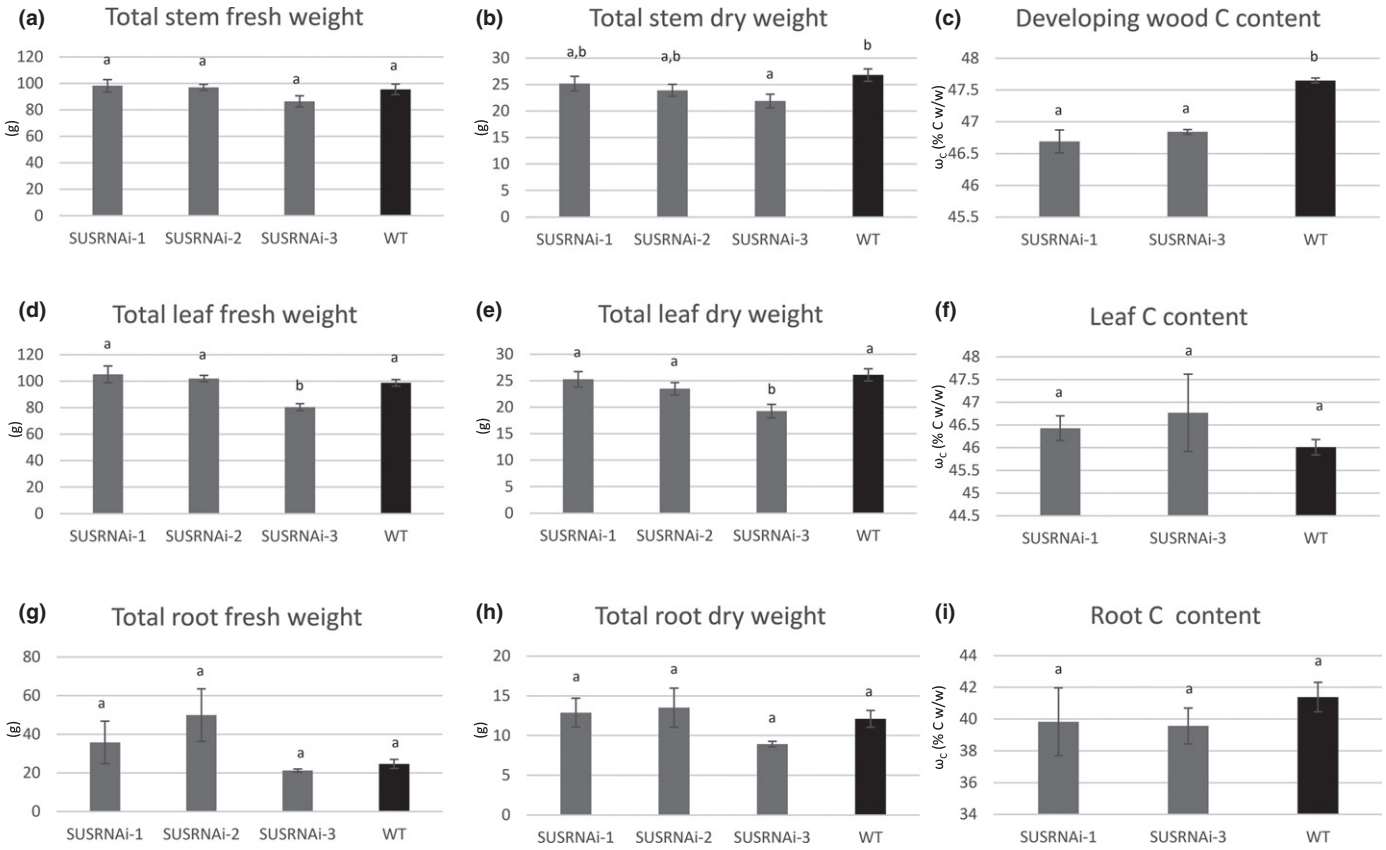

Fig. 2 Phenotype of 2-month-old wild-type (WT) and *SUSRNAi* hybrid aspen (*Populus tremula* × *tremuloides*) trees grown in the glasshouse. Top panels: total stem fresh weight (a), total stem dry weight (b), and C content of developing wood (c). Middle panels: total leaf fresh weight (d), dry weight (e), and C content (f). Bottom panels: root fresh weight (g), dry weight (h) and C content (i). Mass fraction of C was measured by IRMS. Bars indicate the average and error bars indicate the standard error. ANOVA, Duncan test, $n = 4$. Different letters indicate significant differences ($P < 0.05$).

incorporation rate into the phloem sucrose pool was reduced in both *SUSRNAi* lines at time 6 (Fig. 3b), suggesting that *SUSRNAi* reduced the phloem sucrose loading rates.

Carbon in roots is derived from sucrose imported via the phloem. Root ^{13}C-sucrose was only reduced in *SUSRNAi-1* at time 8 (Fig. 3c), while ^{13}C-fructose and ^{13}C-glucose did not show changes (Supporting Information Fig. S1). The same was observed for the Krebs cycle metabolites ^{13}C-citrate, ^{13}C-malate and ^{13}C-succinate. However, ^{13}C-ketoglutarate level was reduced in both lines at time 4 and time 6, and in *SUSRNAi-1* at time 8. The ^{13}C-glutamate, ^{13}C-aspartate, ^{13}C-phenylalanine and ^{13}C-serine did not show differences, but both lines showed decreased levels of ^{13}C-valine at time 8 and of ^{13}C-shikimate at time 6. Total pools for these metabolites did not differ significantly from WT (Fig. 3c; Table S6). Therefore, *SUSRNAi* changed the ^{13}C flow through some individual metabolite pools in the roots, but there was no overall change.

Sucrose import fuels the central metabolism also in developing wood (Fig. 4a). The ^{13}C-sucrose enrichment in developing wood of *SUSRNAi* lines was decreased in comparison to WT in both lines at time 6 and in *SUSRNAi-1* at time 8. The ^{13}C-glucose and ^{13}C-fructose, which can be produced from sucrose cleavage, were reduced in *SUSRNAi-1* at time 8 and in both lines at time 6 and 8, respectively. Apart from ^{13}C-malate, the Krebs cycle metabolites showed alterations as well: ^{13}C-citrate was reduced in *SUSRNAi-1* at time 6; ^{13}C-ketoglutarate was reduced in both lines at time 6 and 8; ^{13}C-succinate was reduced in *SUSRNAi-3* at times 4, 6 and 8; and ^{13}C-fumarate was reduced in both lines at time 8. The amino acids ^{13}C-serine and ^{13}C-phenylalanine showed decreased enrichment in both lines at times 6 and 8. The ^{13}C-glycine and ^{13}C-glycerate, which derive from ^{13}C-serine, were reduced in both lines at time 6 and reduced in *SUSRNAi-3* at time 8, respectively. The ^{13}C-aspartate was reduced in *SUSRNAi-1* at time 6 and 8. The ^{13}C-beta-alanine was reduced in *SUSRNAi-3* at time 4, while ^{13}C-asparagine was reduced in *SUSRNAi-3* at time 4 and in both lines at time 6. The ^{13}C-glutamate was reduced in *SUSRNAi-1* at time 6. The ^{13}C-GABA and ^{13}C-isoleucine did not show differences. Thus, there is an overall ^{13}C distribution decrease in the central metabolites of developing wood in the transgenic trees, which is linked to the reduction in ^{13}C-sucrose. Moreover, a PCA of these data clearly showed that the overall ^{13}C labelling profile of the metabolism in transgenic lines differs from the WT trees (Fig. 4b).

Total sucrose levels in the *SUSRNAi* developing wood did not differ significantly from those in WT trees between 6 and 14 h after the start of the light period (Fig. S2). Total pools of glucose and fructose in developing wood were also not significantly changed. However, all the three sugar levels exhibited increasing

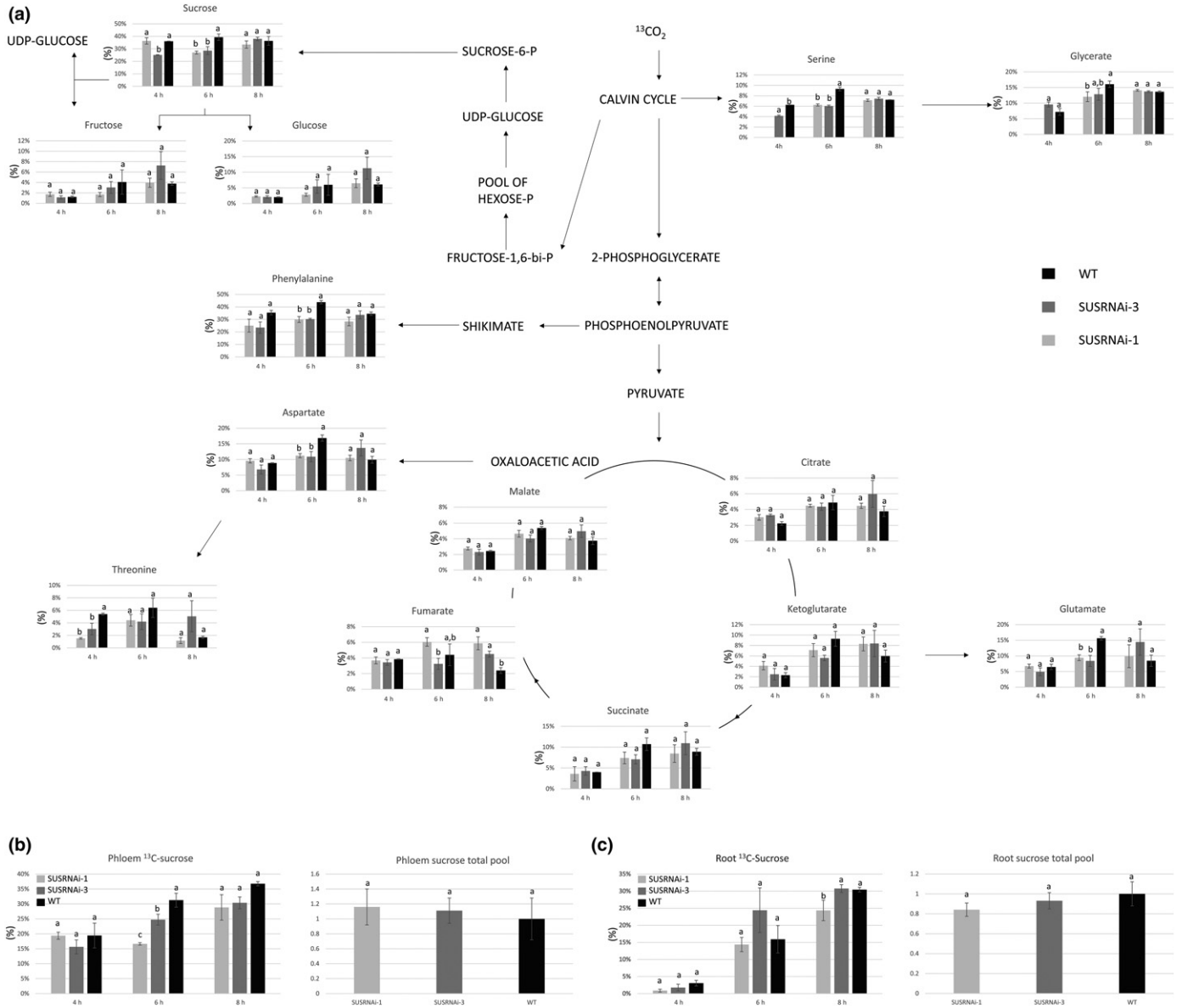

Fig. 3 Central metabolism in leaves (a) and sucrose metabolism in phloem (b) and roots (c) of 6-wk-old wild-type (WT) and *SUSRNAi* hybrid aspen (*Populus tremula* × *tremuloides*) trees grown in the glasshouse. Carbon-13 (^{13}C) enrichment of metabolites ((a) and left panels in (b) and (c)) and sucrose total pools (right panels in (b) and (c)) were measured by GC-MS. To obtain the ^{13}C enrichment of metabolites, trees were supplied with $^{13}CO_2$ for 4, 6 and 8 h. Total pool values in phloem and roots are relative to WT samples collected 6 h after the start of the light period. Bars indicate the average and error bars indicate the standard error. ANOVA, Duncan test, $n = 4$–3. Different letters indicate significant differences ($P < 0.05$).

trends at some time points. This is consistent with the results of Gerber *et al.* (2014), who observed a similar effect in the total pools of these sugars. The differences in significance between these two works may be due to the use of different analytical techniques and statistical methods. Most of the 14 other measured metabolites including aspartate, glycine and phenylalanine did not show differences between the *SUSRNAi* lines and the WT trees (Fig. S2). However, at one time point *SUSRNAi-3* contained increased levels of asparagine (8 h), glutamate (10 h) and serine (10 h), while for *SUSRNAi-1* increases were observed in beta-alanine (14 h) and isoleucine (10 h). The latter line also showed decreased levels in citrate (8 h), fumarate (6 h) and malate (6 h). Both lines showed decreased levels in ketoglutarate (6 h). Succinate and glycerate had decreased levels in *SUSRNAi-1* (6 h) and increased levels in *SUSRNAi-3* (10 h). These findings show that the transgenic trees had alterations in the steady-state levels of some metabolites in developing wood, which are indicative of rearranged central metabolism in response to the reduced SUS activity.

The decreased ^{13}C-sucrose and the overall decreased ^{13}C labelling of central metabolites in developing wood strongly suggest that the total C decrease in this tissue in the transgenic lines (Fig. 2c) is due to the decreased sucrose incorporation. The decreased C flow in wood would have an impact on the

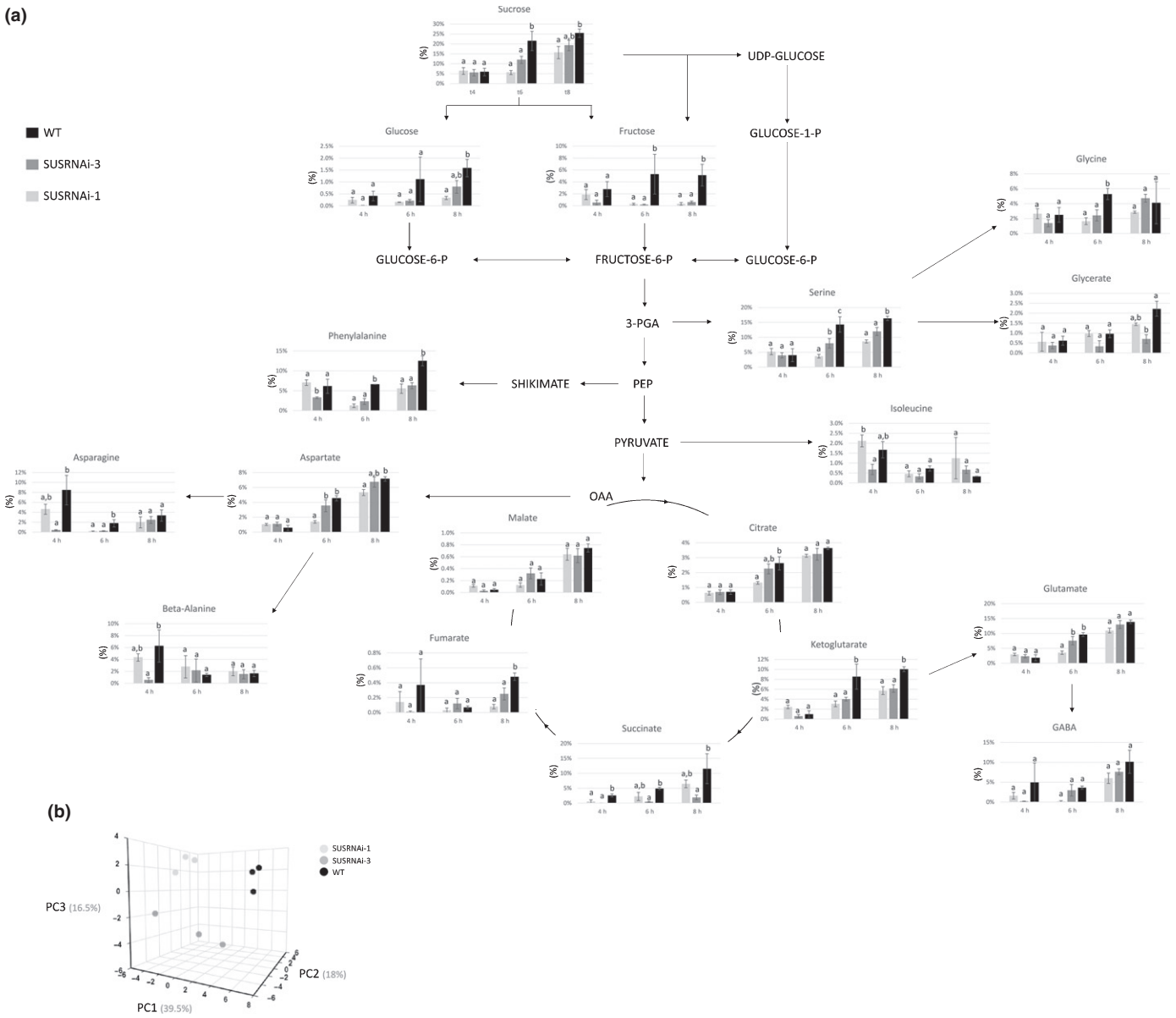

Fig. 4 Carbon-13 (^{13}C) labelling of metabolites of developing wood of 6-wk-old wild-type (WT) and *SUSRNAi* hybrid aspen (*Populus tremula* × *tremuloides*) trees grown in the glasshouse. Trees were supplied with $^{13}CO_2$ for 4, 6 and 8 h. (a) ^{13}C enrichment of central metabolites of developing wood measured by GC-MS. Columns indicate the average and error bars indicate the standard error. ANOVA, Duncan test, $n = 4$–3. Different letters indicate significant differences ($P < 0.05$). (b) Principal component analysis of the ^{13}C-metabolites shown in (a). The axes represent the first three principal components (PCs). The values between brackets indicate the variance of each PC. The data were standardized.

cell wall polymer biosynthesis. Indeed, the amounts of cellulose, lignin and hemicellulose per volume of wood were reduced in all the transgenic lines in comparison to WT (Gerber *et al.*, 2014). Thus, the alterations in the content of the polymers on a volume basis were due to an overall decrease in the C amount allocated to the cell walls. This conclusion was supported by NMR spectroscopy measurements comparing the ^{13}C content of *SUSRNAi-1* and WT cell wall polymers at times 0 and 8. The data point to a reduction in the ^{13}C levels in total cell wall (Fig. S3a), total G and S lignin (Fig. S3b) as well as in methoxy groups (Fig. S3c) and in individual structures related to lignin (Fig. S3d–g). With respect to cell wall carbohydrates, the effect was more subtle although some individual peaks seem to have reduced labelling (Fig. S3b,h).

SUSRNAi does not affect starch levels in glasshouse grown trees

Starch is an important C sink and storage reserve in some tree tissues (Dietze *et al.*, 2014). Therefore, we measured starch levels in developing wood, mature wood, phloem, and source leaves to assess the possible role of SUS in starch metabolism in glasshouse grown aspen. No statistically significant differences between the transgenic and WT trees were found in any of the tissues

(Fig. S4). Worth noting is that the developing wood starch content of WT trees was 0.7 nmol of glucose per milligram fresh weight, which is equivalent to 0.013% (w/w) of fresh developing wood. Unda *et al.* (2017) found that in 5-month-old glasshouse-grown hybrid poplar starch accounted for *c.* 2.5% of developing wood on a dry weight basis. These amounts are well below the cell wall polymer contribution to developing wood biomass, which is above 80% (w/w) (Gandla *et al.*, 2015; Wang *et al.*, 2018). Thus, we found no evidence of SUS involvement in starch metabolism during active growth, or that starch would constitute a significant C sink in aspen developing wood.

SUSRNAi causes strong growth reduction under field conditions

Aspen trees in natural stands undergo seasonal growth and are exposed to many environmental stresses. Therefore, to fully evaluate the *SUSRNAi* effects on tree growth, we grew the transgenic trees in a 5-yr field experiment. The stem height and diameter of the *SUSRNAi* aspen trees were initially identical to those of WT trees but began to show growth defects in subsequent years. We observed consistent reduced height from year 4 onwards, while stem diameter was reduced at year 5 (Fig. 5a,b). The growth defects were more pronounced in *SUSRNAi-3*. In the fifth year the trees were cut, and the total aboveground biomass measured. The fresh and dry stem weights of the transgenic lines were reduced by up to 80% compared to those for WT trees (Fig. 5c, d). To confirm that the *SUSRNAi* was still functional in the transgenics, *SUS2* expression was assessed by qPCR and shown to be reduced (Fig. S5). These data prove that SUS is critical for aspen growth and biomass accumulation under field conditions.

Acid invertase activity is increased in glasshouse *SUSRNAi* lines

Despite the metabolic changes in the *SUSRNAi* lines, stem biomass was only slightly reduced in the glasshouse-grown transgenic lines (Fig. 2). Since sucrose in the sink tissues is cleaved either by SUS or invertases, we hypothesized that invertases may compensate for SUS defects in the transgenics. Interestingly, the cytosolic neutral invertase activity in the developing wood of *SUSRNAi* lines was comparable to that of WT trees, but the acid invertase activity was increased (Fig. 6). This suggests that the acid invertase activity located in the apoplast and/or vacuoles can compensate for the lost SUS activity. However, the observed reduction in total C (Fig. 2c), and ^{13}C labelling over time (Fig. 4) in the developing wood of glasshouse-grown trees suggest that the acid invertase compensation was only partial. Moreover, field grown lines began to show a consistent reduction in stem height from year 4 and in stem diameter at year 5 (Fig. 5), suggesting that a partial compensation mechanism also operates under field conditions. Thus, the sustained reduction in SUS activity over multiple years under field conditions led to accumulative impairment of C incorporation to wood causing biomass reduction. Therefore, it can be concluded that SUS activity is a central determinant of wood formation and tree growth.

Discussion

Our results show that field grown *SUSRNAi* trees accumulate less stem biomass (Fig. 5), and the glasshouse grown transgenics contain less total C in developing wood (Fig. 2). Since stem biomass formation is dependent on the C derived from sucrose metabolism in sink tissues (Lemoine *et al.*, 2013; Ruan, 2014), we performed labelling experiments with $^{13}CO_2$ to investigate whether the reduced biomass and total C could be ascribed to altered ^{13}C-sucrose transport and/or metabolism in the transgenic lines. The reduced ^{13}C-sucrose in the developing wood of *SUSRNAi* trees suggested a reduction in sucrose import (Fig. 4a). The reduced ^{13}C-sucrose level in developing wood (Fig. 4) is also consistent with a reduction in *de novo* sucrose synthesis, however this process is not believed to contribute significantly to the C flux during wood formation (Roach *et al.*, 2017). The reduction in ^{13}C sucrose was reflected in the decreased ^{13}C labelling of many central metabolites (Fig. 4a); this trend was also observed for the ^{13}C accumulation in cell wall polymers (Fig. S3). Since also the cell wall polymer mass per volume unit is reduced in the transgenic lines (Gerber *et al.*, 2014), it can be concluded that C allocation to cell walls is decreased and the cause of the biomass loss (Fig. 5).

The mild phenotype of the glasshouse grown *SUSRNAi* trees (Fig. 2b) suggested the existence of an alternative compensatory sucrose cleavage mechanism involving invertases. We observed no significant changes in neutral invertase activity in the *SUSRNAi* lines, but the acid invertase activity was increased (Fig. 6). Compensation by acid invertases when SUS activity is reduced has also been reported in other species (Zrenner *et al.*, 1995; Baroja-Fernández *et al.*, 2009). The increased acid invertase activity also suggests that these invertases influence C allocation in developing wood. Cell wall acid invertases have coevolved with the vasculature and are believed to contribute to phloem unloading (Wan *et al.*, 2018). The tendency of increased glucose and fructose levels (Fig. S2) in *SUSRNAi* trees resembles that seen in potato tubers with reduced SUS, in which the hexose increase was attributed to a compensatory increase in invertase (Zrenner *et al.*, 1995). A similar compensation mechanism may also function in the developing wood of *SUSRNAi* trees. However, the observed phenotypes in the transgenics including the reduction in total C (Fig. 2c) and ^{13}C-metabolite labelling (Fig. 4) suggest that acid invertases only partially compensate for the SUS loss. This explanation is in line with the gradual growth reduction in the field grown *SUSRNAi* trees (Fig. 5). The seasonal changes and environmental effects under natural field conditions are likely to exacerbate this effect. Environmental stress conditions have been shown to exacerbate SUS defect phenotypes in other species (Ricard *et al.*, 1998; Wang *et al.*, 2014; Takehara *et al.*, 2018). Moreover, in aspen seasonal changes in SUS activity were observed in the outer trunk wood (Schrader & Sauter, 2002), suggesting that SUS may be involved in the activity–dormancy and dormancy–activity transitions.

SUS catalyses the sucrose degradation into fructose and UDP-glucose, the latter being the substrate for cellulose synthesis. Although it has often been hypothesized that SUS is essential for directly providing UDP-glucose to the cellulose synthase complex

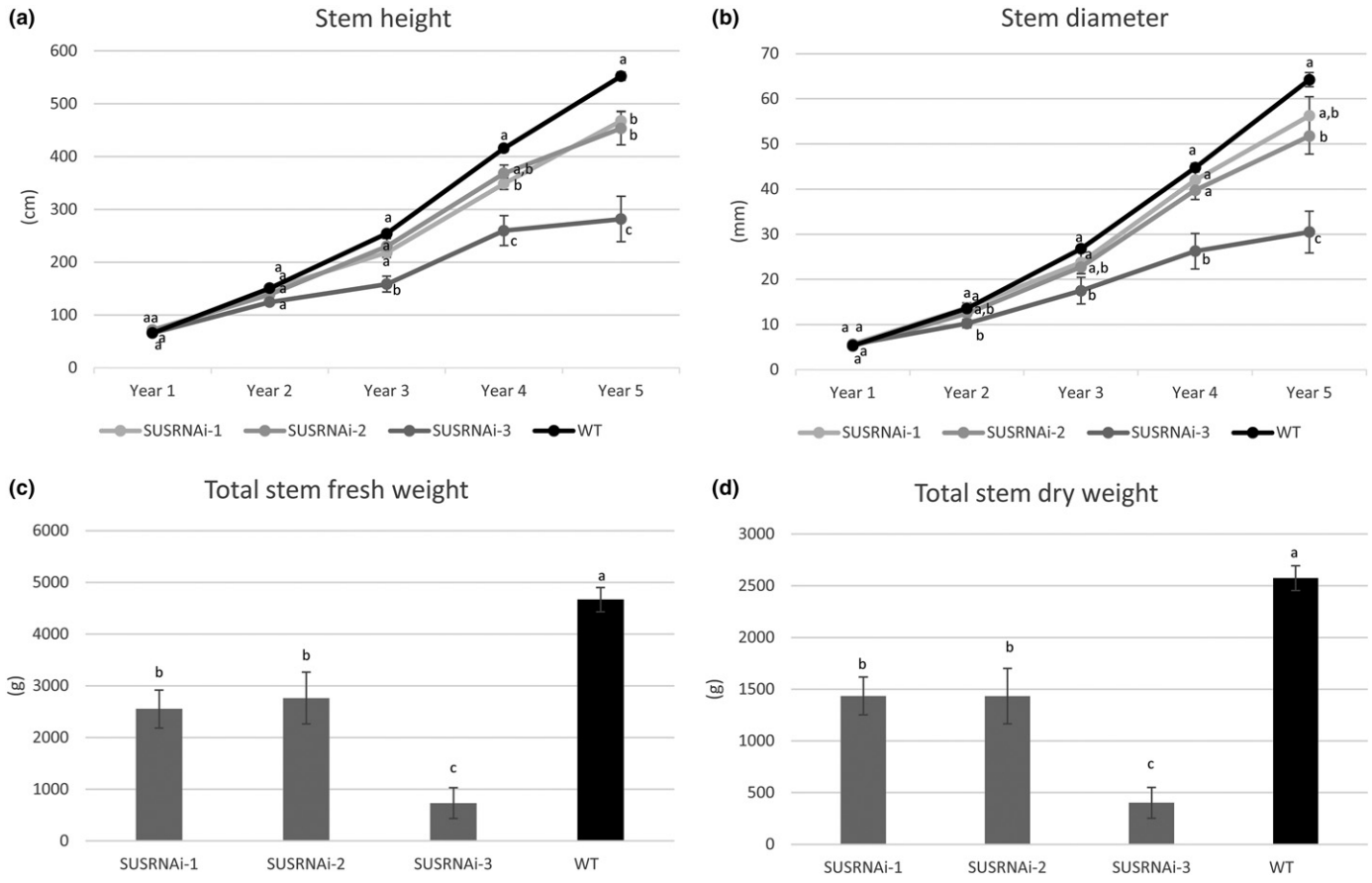

Fig. 5 Phenotype of wild-type (WT) and *SUSRNAi* hybrid aspen (*Populus tremula* × *tremuloides*) trees grown during 5 yr in the field. (a) Stem height and (b) stem diameter over time. (c) Total stem fresh weight, and (d) dry weight at harvest in the fifth year. Data points and bars indicate the average and error bars indicate the standard error. ANOVA, Duncan test, $n = 4$. Different letters indicate significant differences ($P < 0.05$).

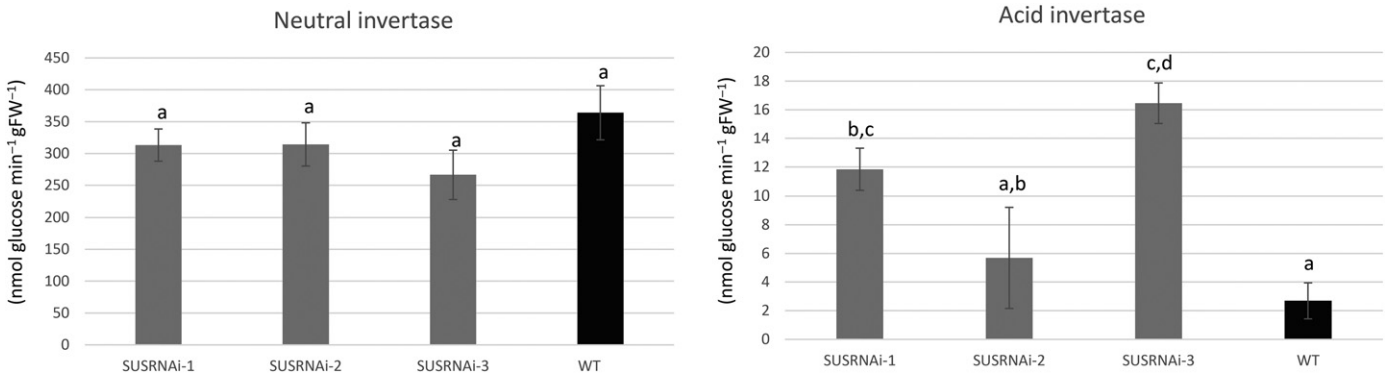

Fig. 6 Neutral and acid invertase activity in developing wood of 6-wk-old wild-type (WT) and *SUSRNAi* hybrid aspen (*Populus tremula* × *tremuloides*) trees grown in the glasshouse. Bars indicate the average and error bars indicate the standard error. ANOVA, Duncan test, $n = 5$–4. Different letters indicate significant differences ($P < 0.05$).

(Amor *et al.*, 1995; Haigler *et al.*, 2001; Stein & Granot, 2019), near complete silencing of SUS in aspen developing wood did not abolish cellulose biosynthesis (Gerber *et al.*, 2014). However, SUS overexpression in aspen can increase the cellulose content (Coleman *et al.*, 2009). Consequently, SUS can contribute to the UDP-glucose provision for cellulose synthesis in aspen trees but is not essential for this process. Instead, cytosolic invertase silencing significantly reduced cellulose levels in developing wood of aspen, suggesting that the cellulose biosynthesis pathway involves hexokinase and UDP-glucose pyrophosphorylase (Rende *et al.*, 2017), while SUS plays an essential role in controlling total C allocation.

When leaves transition from sink to source tissues, SUS levels fall significantly (Nguyen-Quoc *et al.*, 1990; Qiu *et al.*, 2007;

Zhu *et al.*, 2018). Consequently, SUS levels in mature leaves are low (Pavlinova *et al.*, 2002; Thirugnanasambandam *et al.*, 2019). In line with this, SUS activity in source leaves of glasshouse grown aspens was close to the background level. Leaf SUS is thought to be involved in sucrose degradation during the day (Rolland *et al.*, 2006). Hence, several mechanisms could be affecting the sucrose labelling in the SUS leaves (Fig. 3a), including reduced sucrose synthesis, or differential labelling kinetics of the different subcellular sucrose pools (Kruger *et al.*, 2007; Fernie & Morgan, 2013; Beshir *et al.*, 2017). Moreover, the alteration in ^{13}C labelling is not limited to sucrose in leaves, but several other central metabolites also show differences, especially amino acids (Fig. 3a). This may be considered a regulatory effect generated locally in the leaves or triggered by a sink-to-source signal from the developing wood in response to the reduced sucrose and C allocation (Ainsworth & Bush, 2011). However, the *SUSRNAi* source leaves do not show marked phenotypic (Fig. 2; Tables S3, S4) or metabolite pool alterations (Fig. S4d; Table S5), which suggests that SUS does not have an essential role in these leaves during active growth.

The role of SUS in aspen roots under glasshouse conditions seems even more limited. The fact that the roots of *SUSRNAi* lines show no phenotypic alterations (Fig. 2g–i) and that they have a few metabolites with altered ^{13}C labelling (Fig. S1) suggests that they can compensate for the reduced SUS activity. Similarly, no obvious role for SUS was observed in maize roots under aerobic conditions, but it was important under anaerobic condition such as caused by flooding (Ricard *et al.*, 1998). However, it is also possible that the limited effect of SUS silencing in aspen roots was due to residual SUS activity in this tissue.

Because all the analysed tissues had reduced SUS activity or reduced *SUS* mRNA levels, it is probable that the observed effects are initiated locally. This is especially true for developing wood, which has high SUS activity in WT and only residual SUS activity in the *SUSRNAi* lines (Fig. 1). However, systemic effects could be occurring simultaneously, including additive effects on the ^{13}C-sucrose transport across tissues. This is illustrated by the decreased ^{13}C-sucrose enrichment in the source to sink transport direction in the *SUSRNAi* lines (Figs 3, 4), especially from phloem towards developing wood. Since SUS has such low levels in source leaves (Fig. 1), it is not likely that the effect seen in developing wood is merely an effect generated in the leaves and then cascaded to the sink tissues. However, a feedback regulation produced by the reduced developing wood sink activity, which would impact the C metabolism in leaves, is possible (Ainsworth & Bush, 2011). Probing such a mechanism could be done through grafting experiments testing different combinations of WT and *SUSRNAi* scions and stocks. Indeed, the C flow alteration at the whole tree level together with the altered sucrose turnover in leaves, phloem and developing wood raises the interesting possibility that SUS could participate in a signal generation involved in the source–sink metabolic coordination.

To summarize, the decrease in SUS activity leads to decreased sucrose C incorporation in developing wood, which is subsequently reflected in the decreased C flow in the central metabolism. This determines a lower C allocation whose output is a reduced total C and reduced biomass in wood. This provides evidence that SUS is involved in determining C allocation in aspen developing wood and, thus, in affecting the biomass accumulation into this tissue. Likewise, SUS silencing affects the C metabolism at the whole tree level as shown through ^{13}C labelling. The alteration in C metabolism at the whole tree level suggests that SUS could participate in the sink–source metabolic coordination.

Acknowledgements

The authors thank the Swedish Metabolomics Centre (SMC) for technical support with the GC-MS runs, and Dr Ulf Johansson, Swedish University of Agricultural Sciences (SLU), for helping with field management and data acquisition. This work was supported by Bio4Energy (Swedish Programme for Renewable Energy), the Umeå Plant Science Centre, Berzelii Centre for Forest Biotechnology funded by Vinnova and the Swedish Research Council for Sustainable Development (Formas). Bio4Energy and the SSF project ValueTree are acknowledged for funding the field trials.

Author contributions

PGD planned and performed experiments and analysed data; TN planned experiments and analysed data; IT performed the chlorophyll fluorescence determinations and analysed data; AB performed experiments; MH performed the NMR measurements and analyses; ED, MD-M and EJM performed the field experiment and analysed field data; PGD and TN wrote the manuscript with contributions from all the authors. ED and MD-M contributed equally to this work.

ORCID

Pia Guadalupe Dominguez https://orcid.org/0000-0003-0413-2273
Evgeniy Donev https://orcid.org/0000-0002-7279-0481
Marta Derba-Maceluch https://orcid.org/0000-0002-8034-3630
Mattias Hedenström https://orcid.org/0000-0002-0903-6662
Ewa J. Mellerowicz https://orcid.org/0000-0001-6817-1031
Totte Niittylä https://orcid.org/0000-0001-8029-1503
Ivana Tomášková https://orcid.org/0000-0001-6219-5980

References

Ainsworth EA, Bush DR. 2011. Carbohydrate export from the leaf: a highly regulated process and target to enhance photosynthesis and productivity. *Plant Physiology* **155**: 64–69.

Amor Y, Haigler CH, Johnson S, Wainscott M, Delmer DP. 1995. A membrane-associated form of sucrose synthase and its potential role in synthesis of cellulose and callose in plants. *Proceedings of the National Academy of Sciences, USA* **92**: 9353–9357.

Baker NR. 2008. Chlorophyll fluorescence: a probe of photosynthesis *in vivo*. *Annual Review of Plant Biology* **59**: 89–113.

Baroja-Fernández E, Muñoz FJ, Montero M, Etxeberria E, Sesma MT, Ovecka M, Bahaji A, Ezquer I, Li J, Prat S *et al.* 2009. Enhancing sucrose synthase activity in transgenic potato (*Solanum tuberosum* L.) tubers results in increased levels of starch, ADPglucose and UDPglucose and total yield. *Plant & Cell Physiology* **50**: 1651–1662.

Beshir WF, Mbong VBM, Hertog MLATM, Geeraerd AH, Van Den Ende W, Nicolaï BM. 2017. Dynamic labeling reveals temporal changes in carbon re-allocation within the central metabolism of developing apple fruit. *Frontiers in Plant Science* **8**: 1–16.

Busov VB. 2018. Manipulation of growth and architectural characteristics in trees for increased woody biomass production. *Frontiers in Plant Science* **871**: 1–8.

Chaffey N, Barlow P. 2001. The cytoskeleton facilitates a three-dimensional symplasmic continuum in the long-lived ray and axial parenchyma cells of angiosperm trees. *Planta* **213**: 811–823.

Cheng WH, Taliercio EW, Chourey PS. 1996. The Miniature1 seed locus of maize encodes a cell wall invertase required for normal development of endosperm and maternal cells in the pedicel. *Plant Cell* **8**: 971–983.

Coleman HD, Ellis DD, Gilbert M, Mansfield SD. 2006. Up-regulation of sucrose synthase and UDP-glucose pyrophosphorylase impacts plant growth and metabolism. *Plant Biotechnology Journal* **4**: 87–101.

Coleman HD, Yan J, Mansfield SD. 2009. Sucrose synthase affects carbon partitioning to increase cellulose production and altered cell wall ultrastructure. *Proceedings of the National Academy of Sciences, USA* **106**: 13118–13123.

D'Aoust MA, Yelle S, Nguyen-Quoc B. 1999. Antisense inhibition of tomato fruit sucrose synthase decreases fruit setting and the sucrose unloading capacity of young fruit. *Plant Cell* **11**: 2407–2418.

Dietze MC, Sala A, Carbone MS, Czimczik CI, Mantooth JA, Richardson AD, Vargas R. 2014. Nonstructural carbon in woody plants. *Annual Review of Plant Biology* **65**: 667–687.

Dubouzet JG, Strabala TJ, Wagner A. 2013. Potential transgenic routes to increase tree biomass. *Plant Science* **212**: 72–101.

Fernie AR, Morgan JA. 2013. Analysis of metabolic flux using dynamic labelling and metabolic modelling. *Plant, Cell & Environment* **36**: 1738–1750.

Gandla ML, Derba-Maceluch M, Liu X, Gerber L, Master ER, Mellerowicz EJ, Jönsson LJ. 2015. Expression of a fungal glucuronoyl esterase in populus: effects on wood properties and saccharification efficiency. *Phytochemistry* **112**: 210–220.

Gerber L, Zhang B, Roach M, Rende U, Gorzsás A, Kumar M, Burgert I, Niittylä T, Sundberg B. 2014. Deficient sucrose synthase activity in developing wood does not specifically affect cellulose biosynthesis, but causes an overall decrease in cell wall polymers. *New Phytologist* **203**: 1220–1230.

Gullberg J, Jonsson P, Nordström A, Sjöström M, Moritz T. 2004. Design of experiments: an efficient strategy to identify factors influencing extraction and derivatization of *Arabidopsis thaliana* samples in metabolomic studies with gas chromatography/mass spectrometry. *Analytical Biochemistry* **331**: 283–295.

Haigler C, Ivanova-Datcheva M, Hogan P, Salnikov V, Hwang S, Martin K, Delmer D. 2001. Carbon partitioning to cellulose synthesis. *Plant Molecular Biology* **47**: 29–51.

Hedenström M, Wiklund-Lindström S, Öman T, Lu F, Gerber L, Schatz P, Sundberg B, Ralph J. 2009. Identification of lignin and polysaccharide modifications in populus wood by chemometric analysis of 2D NMR spectra from dissolved cell walls. *Molecular Plant* **2**: 933–942.

Hubbard NL, Huber SC, Pharr DM. 1989. Sucrose phosphate synthase and acid invertase as determinants of sucrose concentration in developing muskmelon (*Cucumis melo* L.) fruits. *Plant Physiology* **91**: 1527–1534.

Kim H, Ralph J, Akiyama T. 2008. Solution-state 2D NMR of ball-milled plant cell wall gels in DMSO-d6. *BioEnergy Research* **1**: 56–66.

Kruger N, Le Lay P, Ratcliffe R. 2007. Vacuolar compartmentation complicates the steady-state analysis of glucose metabolism and forces reappraisal of sucrose cycling in plants. *Phytochemistry* **68**: 2189–2196.

Lemoine R, La Camera S, Atanassova R, Dédaldéchamp F, Allario T, Pourtau N, Bonnemain JL, Laloi M, Coutos-Thévenot P, Maurousset L *et al.* 2013. Source-to-sink transport of sugar and regulation by environmental factors. *Frontiers in Plant Science* **4**: 1–21.

Li B, Liu H, Zhang Y, Kang T, Zhang L, Tong J, Xiao L, Zhang H. 2013. Constitutive expression of cell wall invertase genes increases grain yield and starch content in maize. *Plant Biotechnology Journal* **11**: 1080–1091.

Lindén P, Keech O, Stenlund H, Gardeström P, Moritz T. 2016. Reduced mitochondrial malate dehydrogenase activity has a strong effect on photorespiratory metabolism as revealed by ^{13}C labelling. *Journal of Experimental Botany* **67**: 3123–3135.

Mahboubi A, Linden P, Hedenström M, Moritz T, Niittylä T. 2015. ^{13}C tracking after $^{13}CO_2$ supply revealed diurnal patterns of wood formation in aspen. *Plant Physiology* **168**: 478–489.

Mahboubi A, Niittylä T. 2018. Sucrose transport and carbon fluxes during wood formation. *Physiologia Plantarum* **164**: 67–81.

Mahboubi A, Ratke C, Gorzsás A, Kumar M, Mellerowicz EJ, Niittylä T. 2013. Aspen SUCROSE TRANSPORTER3 allocates carbon into wood fibers. *Plant Physiology* **163**: 1729–1740.

Maxwell K, Johnson G. 2000. Chlorophyll fluorescence – a practical guide. *Journal of Experimental Botany* **51**: 659–668.

Morey SR, Hirose T, Hashida Y, Miyao A, Hirochika H, Ohsugi R, Yamagishi J, Aoki N. 2018. Genetic evidence for the role of a rice vacuolar invertase as a molecular sink strength determinant. *Rice* **11**: 6.

Nguyen-Quoc B, Krivitzky M, Huber SC, Lecharny A. 1990. Sucrose synthase in developing maize leaves: regulation of activity by protein level during the import to export transition. *Plant Physiology* **94**: 516–523.

Novaes E, Osorio L, Drost DR, Miles BL, Boaventura-Novaes CRD, Benedict C, Dervinis C, Yu Q, Sykes R, Davis M *et al.* 2009. Quantitative genetic analysis of biomass and wood chemistry of *Populus* under different nitrogen levels. *New Phytologist* **182**: 878–890.

Pavlinova OA, Balakhontsev EN, Prasolova MF, Turkina MV. 2002. Sucrose-phosphate synthase, sucrose synthase, and invertase in sugar beet leaves. *Russian Journal of Plant Physiology* **49**: 68–73.

Pfaffl MW. 2001. A new mathematical model for relative quantification in real-time RT-PCR. *Nucleic Acids Research* **29**: 45e–45.

Plomion C, Leprovost G, Stokes A. 2001. Wood formation in trees. *Plant Physiology* **127**: 1513–1523.

Qiu QS, Hardin SC, Mace J, Brutnell TP, Huber SC. 2007. Light and metabolic signals control the selective degradation of sucrose synthase in maize leaves during deetiolation. *Plant Physiology* **144**: 468–478.

Rende, U, Wang, W, Gandla, ML, Jönsson, LJ & Niittylä, T. 2016. Cytosolic invertase contributes to the supply of substrate for cellulose biosynthesis in developing wood. *New Phytologist* **214**: 796–807.

Rende U, Wang W, Gandla ML, Jönsson LJ, Niittylä T. 2017. Cytosolic invertase contributes to the supply of substrate for cellulose biosynthesis in developing wood. *New Phytologist* **214**: 796–807.

Rennie EA, Turgeon R. 2009. A comprehensive picture of phloem loading strategies. *Proceedings of the National Academy of Sciences, USA* **106**: 14162–14167.

Ricard B, VanToai T, Chourey P, Saglio P. 1998. Evidence for the critical role of sucrose synthase for anoxic tolerance of maize roots using a double mutant. *Plant Physiology* **116**: 1323–1331.

Roach M, Arrivault S, Mahboubi A, Krohn N, Sulpice R, Stitt M, Niittylä T. 2017. Spatially resolved metabolic analysis reveals a central role for transcriptional control in carbon allocation to wood. *Journal of Experimental Botany* **68**: 3529–3539.

Rolland F, Baena-Gonzalez E, Sheen J. 2006. Sugar sensing and signaling in plants: conserved and novel mechanisms. *Annual Review of Plant Biology* **57**: 675–709.

Ruan Y-L. 2014. Sucrose metabolism: gateway to diverse carbon use and sugar signaling. *Annual Review of Plant Biology* **65**: 33–67.

Schrader S, Sauter JJ. 2002. Seasonal changes of sucrose-phosphate synthase and sucrose synthase activities in poplar wood (*Populus x canadensis* Moench 'robusta') and their possible role in carbohydrate metabolism. *Journal of Plant Physiology* **159**: 833–843.

Sheen J. 1990. Metabolic repression of transcription in higher plants. *Plant Cell* **2**: 1027–1038.

Smith AM, Zeeman SC. 2006. Quantification of starch in plant tissues. *Nature Protocols* **1**: 1342–1345.

Sonnewald U, Fernie AR. 2018. Next-generation strategies for understanding and influencing source–sink relations in crop plants. *Current Opinion in Plant Biology* **43**: 63–70.

Stein O, Granot D. 2019. An overview of sucrose synthases in plants. *Frontiers in Plant Science* **10**: 1–14.

Stirbet A, Govindjee. 2011. On the relation between the Kautsky effect (chlorophyll a fluorescence induction) and Photosystem II: basics and applications of the OJIP fluorescence transient. *Journal of Photochemistry and Photobiology B: Biology* **104**: 236–257.

Szecowka M, Heise R, Tohge T, Nunes-Nesi A, Vosloh D, Huege J, Feil R, Lunn J, Nikoloski Z, Stitt M *et al.* 2013. Metabolic fluxes in an illuminated Arabidopsis rosette. *Plant Cell* **25**: 694–714.

Takehara K, Murata K, Yamaguchi T, Yamaguchi K, Chaya G, Kido S, Iwasaki Y, Ogiwara H, Ebitani T, Miura K. 2018. Thermo-responsive allele of sucrose synthase 3 (Sus3) provides high-temperature tolerance during the ripening stage in rice (*Oryza sativa* L.). *Breeding Science* **68**: 336–342.

Thirugnanasambandam PP, Mason PJ, Hoang NV, Furtado A, Botha FC, Henry RJ. 2019. Analysis of the diversity and tissue specificity of sucrose synthase genes in the long read transcriptome of sugarcane. *BMC Plant Biology* **19**: 1–14.

Unda F, Kim H, Hefer C, Ralph J, Mansfield SD. 2017. Altering carbon allocation in hybrid poplar (*Populus alba* × *grandidentata*) impacts cell wall growth and development. *Plant Biotechnology Journal* **15**: 865–878.

Untergasser A, Cutcutache I, Koressaar T, Ye J, Faircloth BC, Remm M, Rozen SG. 2012. Primer3 – new capabilities and interfaces. *Nucleic Acids Research* **40**: 1–12.

Van Bel AJE. 1990. Xylem-phloem exchange via the rays: the undervalued route of transport. *Journal of Experimental Botany* **41**: 631–644.

Wan H, Wu L, Yang Y, Zhou G, Ruan YL. 2018. Evolution of sucrose metabolism: the dichotomy of invertases and beyond. *Trends in Plant Science* **23**: 163–177.

Wang H, Sui X, Guo J, Wang Z, Cheng J, Ma S, Li X, Zhang Z. 2014. Antisense suppression of cucumber (*Cucumis sativus* L.) sucrose synthase 3 (CsSUS3) reduces hypoxic stress tolerance. *Plant, Cell & Environment* **37**: 795–810.

Wang Z, Winestrand S, Gillgren T, Jönsson LJ. 2018. Chemical and structural factors influencing enzymatic saccharification of wood from aspen, birch and spruce. *Biomass and Bioenergy* **109**: 125–134.

Wei Z, Qu Z, Zhang L, Zhao S, Bi Z, Ji X, Wang X, Wei H. 2015. Overexpression of poplar xylem sucrose synthase in tobacco leads to a thickened cell wall and increased height. *PLoS ONE* **10**: 1–20.

Yu SM, Lo SF, Ho THD. 2015. Source-sink communication: regulated by hormone, nutrient, and stress cross-signaling. *Trends in Plant Science* **20**: 844–857.

Zhang C, Han L, Slewinski TL, Sun J, Zhang J, Wang ZY, Turgeon R. 2014. Symplastic phloem loading in poplar. *Plant Physiology* **166**: 306–313.

Zhang D, Xu B, Yang X, Zhang Z, Li B. 2011. The sucrose synthase gene family in *Populus*: structure, expression, and evolution. *Tree Genetics and Genomes* **7**: 443–456.

Zhu J, Qi J, Fang Y, Xiao X, Li J, Lan J, Tang C. 2018. Characterization of sugar contents and sucrose metabolizing enzymes in developing leaves of *Hevea brasiliensis*. *Frontiers in Plant Science* **9**: 1–11.

Zrenner R, Salanoubat M, Willmitzer L, Sonnewald U. 1995. Evidence of the crucial role of sucrose synthase for sink strength using transgenic potato plants (*Solanum tuberosum* L.). *The Plant Journal* **7**: 97–107.

Supporting Information

Additional Supporting Information may be found online in the Supporting Information section at the end of the article.

Fig. S1 ^{13}C labelling of central metabolites of roots of 6-wk-old SUS trees.

Fig. S2 Metabolite total pool content measured in developing wood by GC-MS.

Fig. S3 ^{13}C labelling of cell wall monomers of developing wood of 6-wk-old SUS trees measured by 2D-NMR.

Fig. S4 Starch content in developing wood, mature wood, phloem and leaves of SUS trees measured by the enzymatic method.

Fig. S5 *SUS2* mRNA levels in developing wood of SUS trees grown in the field measured by RT-qPCR.

Table S1 Primer list used in the qPCRs.

Table S2 Nitrogen balance index (NBI), chlorophyll index (CHL), flavonol index (FLV) and anthocyanin index (ANTH).

Table S3 Polyphasic chlorophyll fluorescence induction curve (OJIP transient).

Table S4 Light curve parameters measured with a portable fluorometer FluorPen FP100max.

Table S5 Total metabolite pools in leaves of 6-wk-old trees measured by GC-MS.

Table S6 Total metabolite pools in roots of 6-wk-old trees measured by GC-MS.

Please note: Wiley-Blackwell are not responsible for the content or functionality of any supporting information supplied by the authors. Any queries (other than missing material) should be directed to the *New Phytologist* Central Office.

See also the Commentary on this article by Gessler, **229**: 8–10.